HELSINKI UNIVERSITY OF TECHNOLOGY
PUBLICATIONS OF THE LABORATORY OF HYDROLOGY
AND WATER RESOURCES ENGINEERING

1988/1

A MODEL FOR PREDICTING THE EFFECT OF DRAINAGE ON SOIL MOISTURE, SOIL TEMPERATURE AND CROP YIELD

Tuomo Karvonen

HELSINKI UNIVERSITY OF TECHNOLOGY
LABORATORY OF HYDROLOGY AND WATER RESOURCES ENGINEERING
RAKENTAJANAUKIO 4, SF-02150 ESPOO 15, FINLAND

HELSINKI UNIVERSITY OF TECHNOLOGY
FACULTY OF SURVEYING AND CIVIL ENGINEERING
DEPARTMENT OF TRANSPORTATION AND ENVIRONMENTAL ENGINEERING

A MODEL FOR PREDICTING THE EFFECT OF DRAINAGE ON SOIL MOISTURE, SOIL TEMPERATURE AND CROP YIELD

Tuomo Karvonen

Thesis for the degree of Doctor of Technology to be presented with due to permission for public examination and criticism in the Auditorium R4 at the Helsinki University of Technology (Otaniemi, Finland) on the 29th of January, 1988, at 12 o'clock noon.

OTANIEMI 1988

ISBN 951-754-319-0

LIST OF ILLUSTRATIONS

LIST OF TABLES

HELSINKI UNIVERSITY OF TECHNOLOGY
FACULTY OF SURVEYING AND CIVIL ENGINEERING
DEPARTMENT OF TRANSPORTATION AND ENVIRONMENTAL ENGINEERING

Abstract

A MODEL FOR PREDICTING THE EFFECT OF DRAINAGE ON SOIL MOISTURE, SOIL TEMPERATURE AND CROP YIELD

by Tuomo Karvonen

The primary objective of this study was to develop a methodology that combines climatological data, soil properties, crop drainage requirements and drainage theory into a design method called water management model. The aim of this type of approach is to characterize the effect of drainage on soil moisture, soil temperature and crop yield. The final result of the application of the methods presented in this study is a decision on optimum drainage parameters, i.e. drain spacing and depth, and drainage coefficient.

Determination of the soil water retention curve, the unsaturated hydraulic conductivity function and the soil thermal conductivity is discussed. Methods for describing the movement of water and heat in a seasonally frozen soil are presented. A model for estimating the effect of soil moisture on crop yield is described. When tested by comparisons with analytical solutions, laboratory data and field experiments, the results were favourable.

It was shown that the methods presented in this study can be used in estimating the proper drainage coefficient, i.e. the design flow that the pipe system must be capable of conveying. According to the results obtained, it seems realistic to decrease the design flow; this would reduce the total costs of the drainage system by 1 - 5%. Another practical result was obtained, indicating that the optimum drain spacing is not only dependent on the soil type and crop grown; the choice is also affected by the time period used in the economic analysis and by the overall maximum yield level, which is an indication of the efficiency of the cultivation techniques used on the farm.

ACKNOWLEDGEMENTS

I am greatly indebted to Prof. Pertti Vakkilainen and Mr. Jussi Saavalainen, Managing Director of the Finnish Field Drainage Centre. Without their efforts this study could not have been possible. Prof. Vakkilainen supervised this study, and his continous advice and support has been very valuable in all stages of the research. Sincere appreciation goes to Mr. Saavalainen for his encouragement and support and for providing me with the best possible working conditions and excellent computer facilities.

I am most grateful to Dr. Esko Elomaa and Dr. Kim Pingoud for reading the manuscript and for making many valuable comments and correction proposals. I expresses my gratitude to Dr. Nick Jarvis for commenting the manuscript.

Gratitude is due to the whole personel of the Finnish Field Drainage Centre for creating a pleasant working atmosphere.

I was also inspired by the scientific enthusiasm of Prof. (act.) Juhani Kettunen and other researchers of the Laboratory of Hydrology and Water Resources Engineering.

Appreciation goes to Mr. Lauri Haverinen for translating some Russian papers and to Mr. David Miller for revising the English language.

I wish to express my gratitude to my family for all patience and support throughout the work.

I gratefully remember the financial support of the Finnish Drainage Foundation and Sven Hallin Foundation.

Helsinki, November 1987

Tuomo Karvonen

CHAPTER 1 INTRODUCTION

Due to the short growing season in Finland, artificial drainage is needed mainly to provide trafficable conditions for seedbed preparation and planting in the spring, and to permit harvest in the fall. However, excessive drainage is undesirable as it increases the costs of a drainage project and reduces the soil water available to growing plants.

The primary objective of this study was to develop a methodology that combines climatological data, soil properties, crop drainage requirements and drainage theory into a design method called water management model. An illustration of this approach is given in Fig. 1-1.

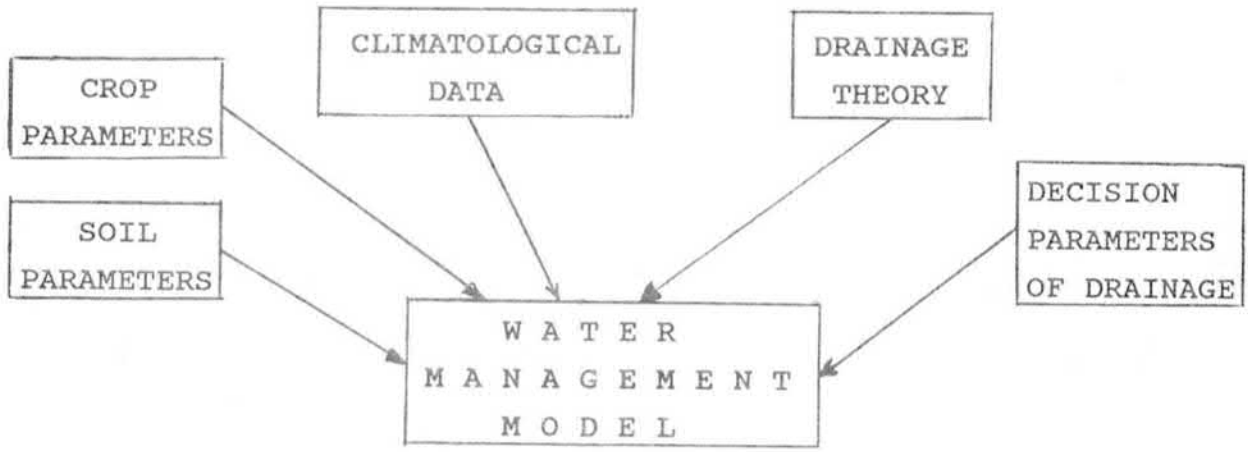

FIG. 1-1. An illustration of the components linked in a water management model.

The decision parameters regarding drainage are the only components in a water management model that can be affected by the planning of a drainage project. These parameters include drain spacing and depth, and drainage coefficient (the design flow that the pipe system must be capable of conveying when it is running full). The choice of drainage parameters affects the the soil moisture and soil temperature of a drained field. Soil moisture and soil temperature are related to each other by freezing and thawing phenomena. The effect of soil moisture and

soil temperature on crop yield must also be calculated. As a final step, the influence of the decision parameters on yield, cost and profit has to be estimated.

In the development stage of a water management model, measured field data are needed to verify the capability of the model to produce realistic results. In 1937 Pentti Kaitera proposed that an experimental field should be established to study the effects of different types of water management systems on the soil moisture regime of an agricultural field and to develop methods for the evaluation of the damage to crop yield caused by an excessively high water level and methods for the estimation of the effect of irrigation on crop yield. The Maasoja experimental field was built in 1938 and the measurement period was 30 years (1939-68). Almost at the same time as the Maasoja experiment, another experimental field was established at Backas, where the purpose was to study the effect of subsurface drainage on soil moisture, soil temperature and soil freezing. The main results obtained at the Maasoja experimental field have been described in detail by Wäre (1947) and Hooli (1971) and the measurements carried out at Backas have been presented in detail by Juusela (1945). Data collected at the Maasoja and Backas experimental fields are used in this study and the experimental fields are described briefly in Chapter 2.

Chapters 3 - 6 are devoted to a description of the submodels needed in the linking of the suggested methodology. It has been necessary to present methods for describing the movement of water and heat in a porous media, and to develop methods for the determination of the parameters of these calculations.

The application of the water management model to practical problems necessitates development of a number of auxiliary techniques to provide the parameter values for the models. Chapter 3 discusses the determination of the soil parameters - soil water retention curve, unsaturated hydraulic conductivity function and soil thermal conductivity. The extension of the theory originally presented by Sigvard Andersson (1969) for

calculating the unsaturated hydraulic conductivity function has been discussed.

At the time Juusela (1945) and Wäre (1947) published their results, an extrapolation technique called mathematical modeling was virtually unknown and even at the beginning of the 1970's when Hooli (1971) presented his results, the technique was not advanced enough to be used for solving actual field problems. Modeling efforts directed towards simulation of a water balance in a soil continuum have been presented e.g. by Neuman (1972), Nimah and Hanks (1973), Neuman et al. (1975) and Feddes et al. (1978). During the last few years the managements models aimed at quantifying the effects of drainage and irrigation on crop yield have been developed (Skaggs, 1980; van Wijk and Feddes, 1982, 1986; Skaggs and Nassehzadeh-Tabrizi, 1983; Zaradny, 1986).

When analyzing the data collected at the lysimeter field of the Helsinki University of Technology in Otaniemi, Vakkilainen (1982) started modeling of a soil-plant-atmosphere continuum in Finland. The experience gained by Vakkilainen has been available in the development of the proposed models and the present study can be considered a direct extension of the research carried out by Vakkilainen (1982).

Chapter 4 is devoted to the description of the selected models. The numerical solution of the saturated-unsaturated flow in seasonally frozen soil has been developed during this study by the author. The model for calculating the accumulation and melting of snow cover is a combination of the existing models of Jansson and Halldin (1980) and Kuusisto (1984).

The maximum possible crop production is dependent on many factors, e.g. the prevailing meteorological conditions, soil type, water status of the soil, nutrients, pesticides, herbicides, and the cultivation technique. The main objective of this study is to estimate field water use under conditions where water is the growth factor of special importance, i.e.

the crop yield is limited either by too wet or too dry soil.

Chapter 5 is devoted to the mathematical description of the crop growth model that accounts for the growth factor water and the potential growth rate. Methods for calculating the potential evapotranspiration rate are given in this Chapter. The model described in Chapter 5 is essentially the same as that presented by Feddes et al. (1978). The main contribution of the author is the inclusion of a method that combines the effective temperature sum (cumulative sum of air temperature values above 5 °C) with the calculation of the development stage of a plant.

The methodology developed is designed mainly for quantification of the effect of subsurface drainage on soil moisture, soil temperature and crop yield. The mathematical models of drainage are presented in Chapter 6. Programming of the strictly two-dimensional drainage model has been carried out by the author, whereas the coefficients have been given by Neuman et al. (1975). The quasi-two-dimensional solution of the drainage problem has been developed in this study.

The results obtained at the Maasoja and Backas experimental stations are applicable only to the local conditions where the measurements have been carried out. It is not possible to extrapolate the results directly for different crops, soils and meteorological conditions. The mathematical models developed in this study can be used as an extrapolation technique, provided the models have been carefully tested. Chapters 3-6 include test examples published in the recent literature, and Chapter 7 discusses the verification results of the Backas and Maasoja field experiments.

Finally, the objective of Chapter 8 is to discuss the possibilities for using the methodology presented in designing drainage systems in Finland. A comprehensive evaluation of the applicability of the methods developed is beyond the scope of this study and only a few practical examples are treated with the methodology suggested. Future development and research is the topic of Chapter 9.

2 EXPERIMENTAL FIELDS

2.1 Backas experimental field

The Backas experimental field was situated about 20 km north of Helsinki (24°58' E and 60°17' N). The measurements were started on June 1940 and the observation period was about two years. Juusela (1945) has described the measurement field in detail and published the results of the experiments. They are briefly reviewed here.

According to Juusela (1945), the primary objective of the field experiment was to study the effect of subsurface drainage on soil moisture, soil temperature and soil freezing. The tests concerned four different conditions and the observation points were situated midway between the drains as well as on their borders, at a distance of 1 meter from open ditches and subsurface drains, respectively. (see Fig. 2-1).

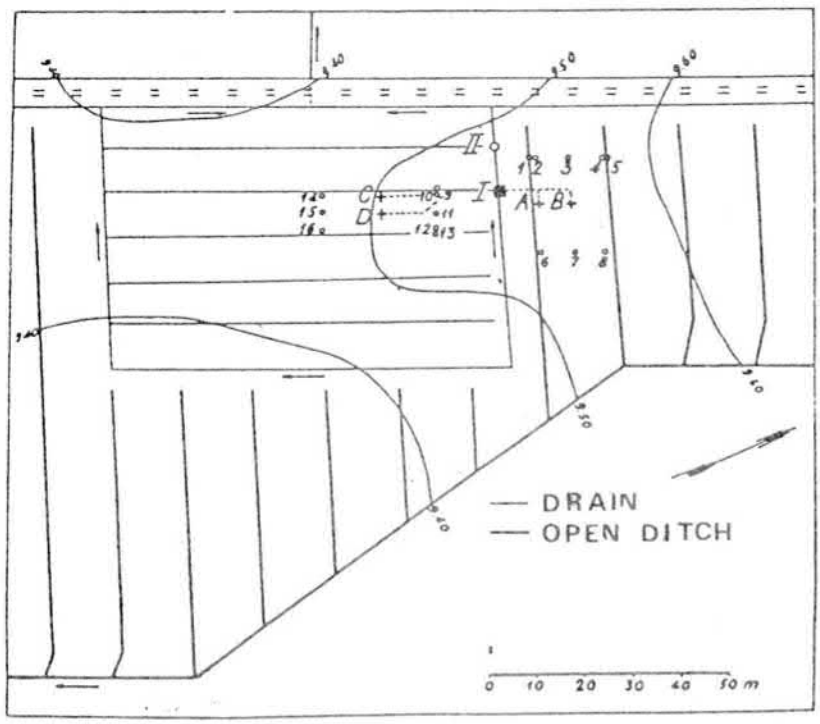

Fig. 2-1. The measurement field at Backas. I = Observation cabin, II = Rain gauge, A,B,C and D = Soil temperature measurement points and 1-16 = groundwater level measurement points

Monthly precipitation values at Tammisto (1.5 km from the Backas experimental field) are given in Table 2-1 (average values and for years 1940-1942). Air temperature values are shown in Table 2-2. The average depth of snow cover (16.3) has been 35 cm (Juusela 1945) and the maximum depth of ground frost 36 cm on average.

The soil at the experimental field was sticky clay with a clay content of 55 - 65% in the topsoil and about 75 - 85% in the subsoil. The saturated hydraulic conductivity was estimated with the method of Bloemen (1980), which is based on soil texture. For topsoil, a K_S-value of 0.1 $cm \cdot d^{-1}$ was obtained and for subsoil, the corresponding value was 0.07 $cm \cdot d^{-1}$.

Table 2-1. Montly precipitation (mm) at Tammisto (Juusela 1945).

Year	I	II	III	IV	V	VI	VII	VIII	IX	X	XI	XII	
Mean	35	25	27	36	48	56	61	88	72	74	66	38	623
1940	12	8	10	22	26	44	41	53	106	41	135	25	522
1941	4	22	15	7	13	12	15	98	44	34	21	22	306

Table 2-2. Air temperature at Tammisto (Juusela 1945).

Year	I	II	III	IV	V	VI
Mean	- 6.3	- 7.0	- 4.0	1.6	8.4	12.8
1940	-14.3	-15.9	- 9.5	0.6	10.7	14.8
1941	-15.1	- 9.6	- 5.3	-1.4	6.8	12.8

Year	VII	VIII	IX	X	XI	XII	Year
Mean	16.1	13.8	9.4	4.3	- 0.5	- 4.4	3.7
1940	17.3	14.1	9.3	4.9	1.6	- 5.3	2.4
1941	19.3	15.1	8.6	1.7	- 4.4	-11.3	1.4

In 1940-1942, soil temperature was measured at the following depths: 2.5, 5, 10, 15, 20, 30, 40, 50, 60, 80, 100 and 125 cm. Moreover, gravimetric moisture content measurements were made at five different depths (20, 40, 60, 80 and 100 cm) and groundwater level depth was measured at 16 observation points.

An example of soil temperature as a function of time and depth is given in Fig. 2-2. The thicker line in Fig. 2-2 indicates the measured depth of ground frost and it can be seen that soil is partly frozen even in May.

According to Juusela (1945) the main results from the Backas experimental station were as follows:

- groundwater level in spring was deeper in fields drained by subsurface drains
- the depth of ground frost was greater (15%) in the field drained by open ditches
- ground frost melted 7 to 10 days earlier in the field drained by subsurface drains
- soil temperature measurements showed that practically the same temperature prevailed at different observation points in the autumn
- during winter and spring the soil temperature was higher on the field with subsurface drains (see Fig. 2-3)

2.2 Maasoja experimental field

The Maasoja experimental station is situated about 60 km north-west from Helsinki (60°25' and 24°23'). The experimental field was established in 1938, and the main purpose of the experiments was to study the effect of sprinkler irrigation and subirrigation on crop yield.

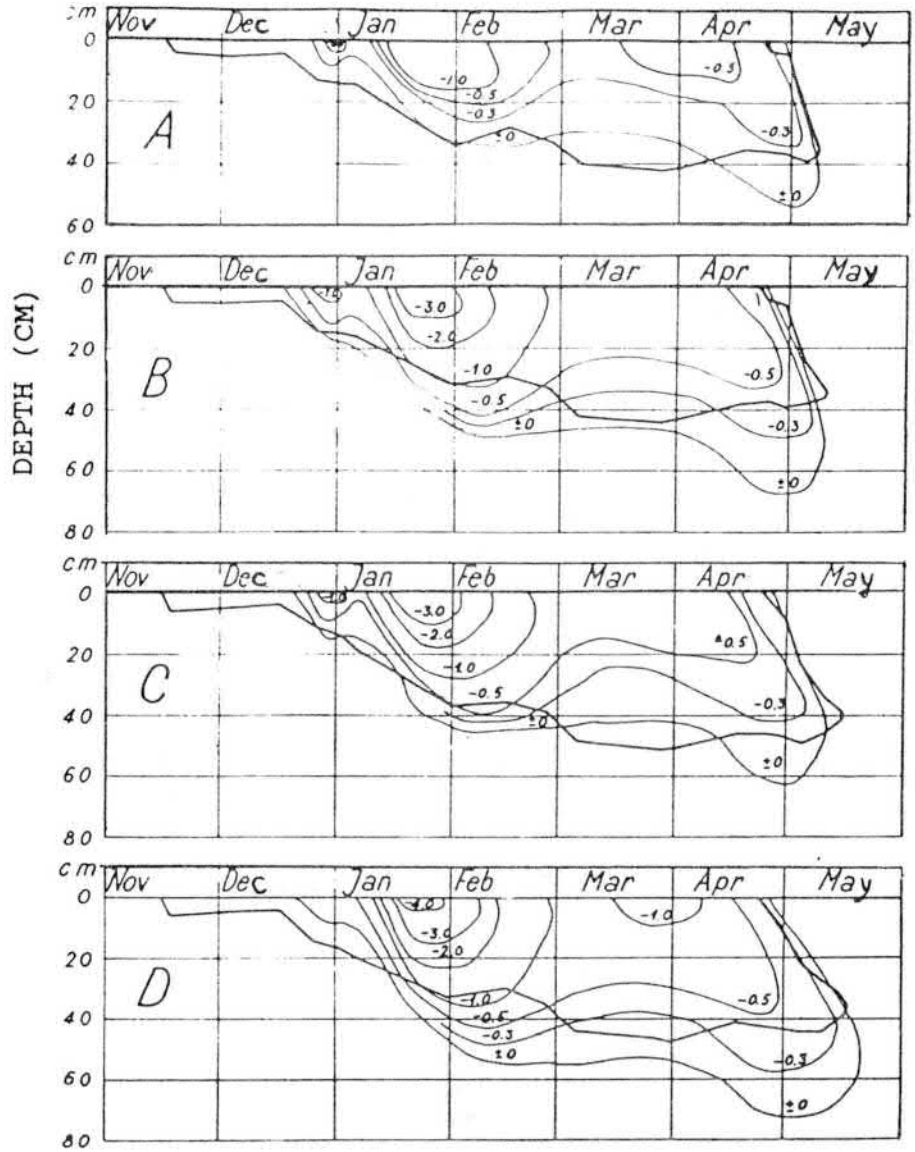

Fig. 2-2. Soil temperature at the Backas experimental station, 1940-1941. A = at a distance of 1 m from subsurface drain, B = midway between subsurface drains, C = at a distance of 1 m from open ditch, D = midway between open ditches.

The size of the experimental field is 3 ha and about 50% of it is on clay soil with a clay content of 25 - 40% in the layer between 30-100 cm and 40 - 80% below 100 cm. The rest of the experimental field is peat soil. The experimental field was divided into 34 test areas (20 in clay soil and 14 in peat soil) and the location of these areas is shown in Figs. 2-4 and 2-5. Test areas 10-12 (clay soil) and 24-26 (peat soil) have been drained by subsurface drains and the other test areas are surrounded by open ditches.

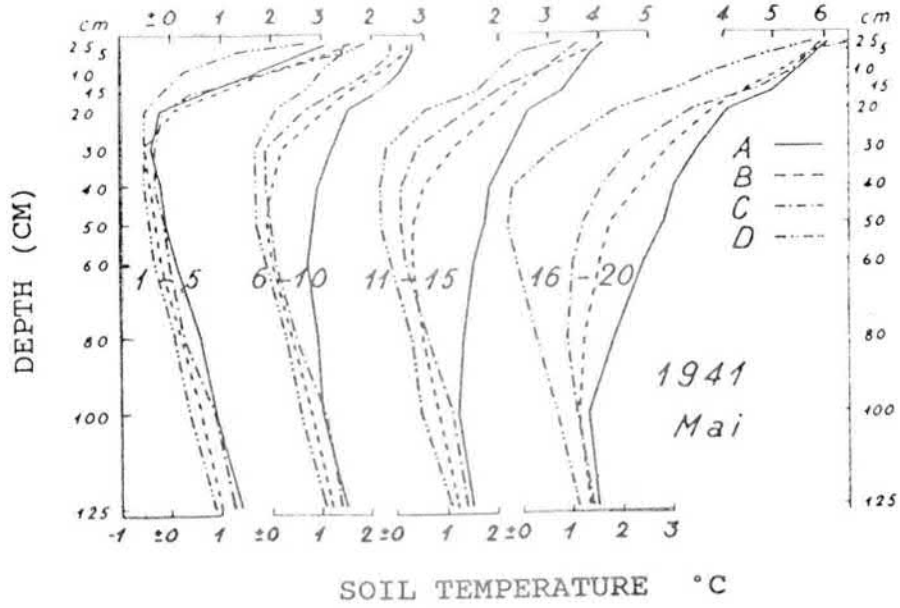

Fig. 2-3. Backas experimental station. Soil temperature during the melting period in May 1941. A = at a distance of 1 m from subsurface drain, B = midway between subsurface drains, C = at a distance of 1 m from open ditch, D = midway between open ditches.

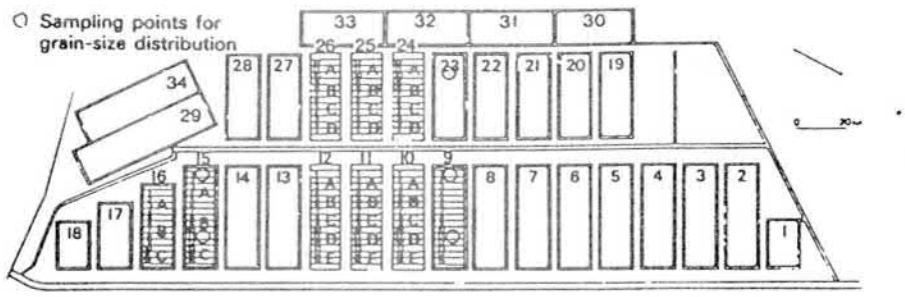

Fig. 2-4. Plots in the Maasoja test areas, 1939-1951. Sampling points for grain size distribution (Hooli, 1971).

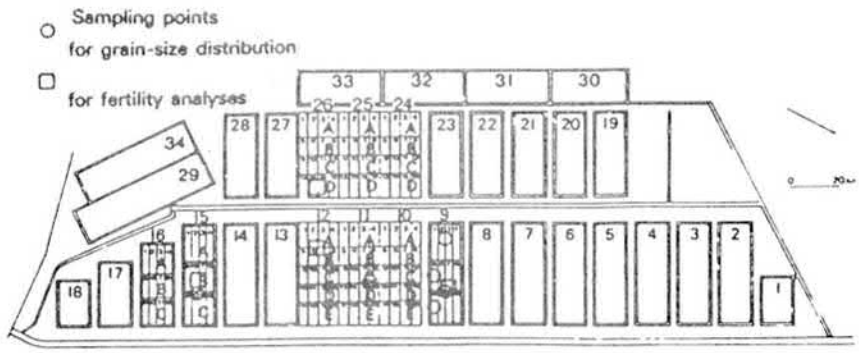

Fig. 2-5. Plots in the Maasoja test areas, 1952-1968. Sampling points for grain size distribution and fertility analyses (Hooli, 1971).

In 1939-1944 the most important experiments were the sub-irrigation experiments carried out in test areas 3-5. In test areas 4 and 5 the water level in the surrounding ditches was raised to 20 cm from the soil surface at the beginning of June, implying that the depth of the groundwater level was almost constant throughout the month. At the beginning of July the water level in the ditches surrounding test area 5 was lowered and at the same time raised in test area 3 to a depth of 20 cm from the soil surface. The groundwater level was lowered at the beginning of August in test areas 3 and 4. The results of these experiments have been described in detail by Wäre (1947) and briefly by Kaitera (1940 a, b). These experiments have been analyzed with the simulation models (see Chapter 7) and therefore the results are not reviewed here.

The objective of the Maasoja experimental station was also to study the effect of sprinkler irrigation on crop yield. The results from the measurement period between 1946 - 1968 have been published by Wäre (1955 and 1956), Maasilta (1961) and Hooli (1971).

Moreover, Hooli (1971) used the data obtained at the Maasoja experimental station to establish the dependence of yields on meteorological and soil factors. The procedures employed by Hooli were two-variable correlation analysis, linear regression analysis and bidirectional correlation analysis. An example of the correlation equations developed by Hooli (1971) is the formula for predicting the yield of oats at Maasoja experimental station (based on data from 1939 -1968).

$$Y_{OATS} = 1737.77 + 27.13 \cdot IL - 44.69 \cdot P_{SO-SP} + 36.13 \cdot P_{SP-HE} + 0.134 \cdot IL \cdot P_{HE-RI} + 0.496 \cdot P^2_{SO-SP} - 0.135 \cdot P^2_{SP-HE} \qquad (2\text{-}1)$$

where Y_{OATS} is the yield of oats at Maasoja on test area 9 (kg. ha^{-1}), IL is the ignition loss (%), P_{SO-SP} is precipitation between sowing and emergence, P_{SP-HE} is precipitation between emergence and flowering, P_{HE-RI} is precipitation from date of flowering to date of ripening. The multiple correlation

coefficient of equation (2-1) was 0.658 (Hooli 1971). Hooli had the following to say: "The biological growth of plants is a complex process that is difficult to treat statistically. Yield fluctuations are affected by numerous growth factors. Their correlations, both mutual and with growth, are very complicated." Hence, more advanced methods for the prediction of the effect of meteorological factors on biomass produced by plants and for evaluating the effect of drainage on crop yield are of great importance.

The field crops grown at the experimental station were oats, barley, spring wheat, potato, clover and timothy. Only the final yield was measured so that it is not possible to test the crop model within the growing season. In this study the harvested results from experiments with oats were used.

3 DETERMINATION OF THE PHYSICAL SOIL PROPERTIES

3.1 Introduction

Any application of the models describing flow in unsaturated media requires that the hydraulic functions are known, i.e. the water retention curve and the unsaturated hydraulic conductivity function. In section 3.2, the prospects for determining the water retention curve based on the grain size distribution curve are evaluated. In section 3.3, the various methods for estimating the conductivity function have been tested. A new contribution based on the work of Sigvard Andersson (1971) is presented. Finally, in section 3.4, a technique for the estimation of the saturated hydraulic conductivity or the soil thermal conductivity function is described. The method is based on a simplification of the Kalman filtering technique, and it can effectively use all the measured values of soil moisture, soil water potential and soil temperature.

3.2 Estimation of water retention curves from soil texture

3.2.1 The estimation procedure

It is preferable, of course, to measure the water retention curve for each application. However, it is not always possible to assess the relation between water content and capillary pressure in cases when the field experiments were carried out 20 or 30 years ago. This is the case in Finland. Detailed field experiments have been designed e.g. to find out the relationship between crop yield and various types of water management systems. These experiments are ideal for testing the soil water management models. Unfortunately, in most cases the water retention curves have not been measured at all. Instead, the grain size distribution curves have been determined. The main idea of this section is to discuss the prospects for predicting the water retention curve based on soil texture.

Andersson and Wiklert (1972) have published an extensive collection of water retention curves and grain size distribution curves . In total, 362 grain size distribution curves were stored in the computer memory, 91 from the topsoil (0 - 25 cm) and 271 from the subsoil (>25 cm). The grain size distribution of a known soil type is compared with the curves in the data base. The deviation between the measured grain size distribution curve and the curves in the data base is calculated. The curve with the minimum deviation in soil texture is selected and the corresponding water retention curve is considered to be the desired pF-curve.

It would be possible to use this curve as the approximation of the pF-curve. In many cases the saturated moisture content of the soil whose pF-curve should be estimated is known, but generally this value does not coincide with the saturated water content of the estimated curve. Hence, it is necessary to correct the curve due to the saturated water content. The simpliest way to accomplish this is to move the predicted curve so that measured and predicted saturated water contents are the same.

Based on the published data of Andersson and Wiklert, it is also possible to predict the water content at the wilting point (tension value equal to -15 000 cm). This type of analysis has been carried out for topsoil and subsoil. Simple regression formulas have been fitted to the data. The results of the regression analysis are shown in Fig. 3.1. Water content at the wilting point can be explained fairly reliably by the percentage of clay. For topsoil the equation is

$$w_w = 2.3 + 0.434 \cdot CLAY \qquad (3\text{-}1a)$$

and for subsoil

$$w_w = 4.0 + 0.423 \cdot CLAY \qquad (3\text{-}1b)$$

where w_w is water content (%) at the wilting point and CLAY is the percentage of clay (grain size smaller than 0.002 mm).

The procedure for predicting the water retention curve from soil texture can be summarized as follows:

1) A search is made for a curve with minimum deviation from the measured grain size distribution curve.
2) Water content at the wilting point is calculated from equations (3-1).
3) The curve selected in stage 1) is modified according to the known saturated water content and estimated water content at the wilting point.

The procedure described above is used to predict the water retention curves of the Maasoja and Backas experimental stations (see chapter 7). In these cases the saturated water content can be estimated from soil moisture measurements. Hence, the assumption of known saturated water content is used in the testing of the previously described procedure.

3.2.2 Testing of the prediction procedure

In the publication of Andersson and Wiklert (1972) the grain size distribution curve is composed of eight classes:

- < 0.002 mm
- 0.002 - 0.006 mm
- 0.006 - 0.020 mm
- 0.020 - 0.060 mm
- 0.060 - 0.200 mm
- 0.200 - 0.600 mm
- > 0.600 mm
- percentage of humus

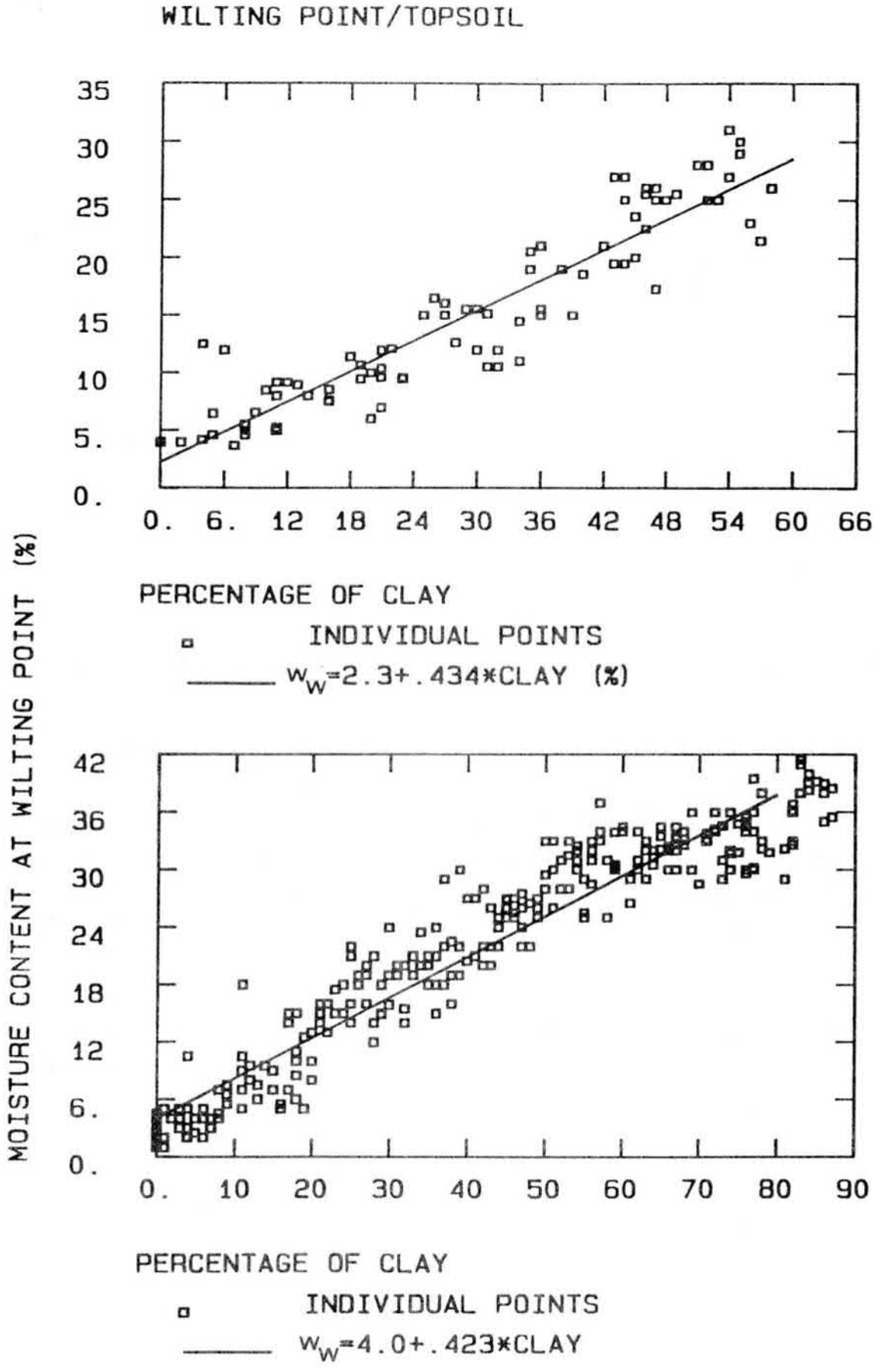

Fig. 3-1. The relationship between percentage of clay and water contents at the wilting point. a) topsoil, b) subsoil.

The testing of the procedure was carried out using 16 independent curves measured by Andersson (6 for topsoil and 10 for subsoil). In the testing the saturated water content was assumed to be known and the water content at the wilting point was estimated as a function of the clay percentage using equations (3-1). For topsoil the results from the testing are shown in Fig. 3-2 and for subsoil in Fig. 3-3.

According to Figs. 3-2 and 3-3 the prediction of water retention curve was satisfactory in most cases. Bearing in mind the fact that the determination of the pF-curve is not an error-free process, the deviation between the original and estimated retention curve is of reasonable magnitude with the exception of the curves in Fig. 3-2d, 3-2f , 3-3g, 3-3h and 3-3j (5 out of 16).

3.3 Estimation of the unsaturated hydraulic conductivity

3.3.1 Introduction

Unsaturated hydraulic conductivity is one of the most important hydraulic properties governing the transport of fluid and solutes in soil. Unfortunately, this parameter is time-consuming and expensive to measure in the field and laboratory. Prof. Sigvard Andersson from Uppsala University in Sweden has carried out an extensive research for 30 years on e.g. the theoretical relationships in capillary systems between tension, water content, pore size distribution and hydraulic conductivity.

Many methods have been developed to estimate the unsaturated hydraulic conductivity from empirical equations (Averjanov ,1950 ref. Mualem, 1976; Burdine, 1953; Millington and Quirk, 1961, ref. Al-Soufi, 1983; Brooks and Corey, 1964; Green and Corey, 1971), Jackson, 1972; Campbell, 1974; Mualem, 1976; Van Genuchten, 1978 and Bloemen, 1980). The prediction formulas can be divided into two main groups. The first is based on the

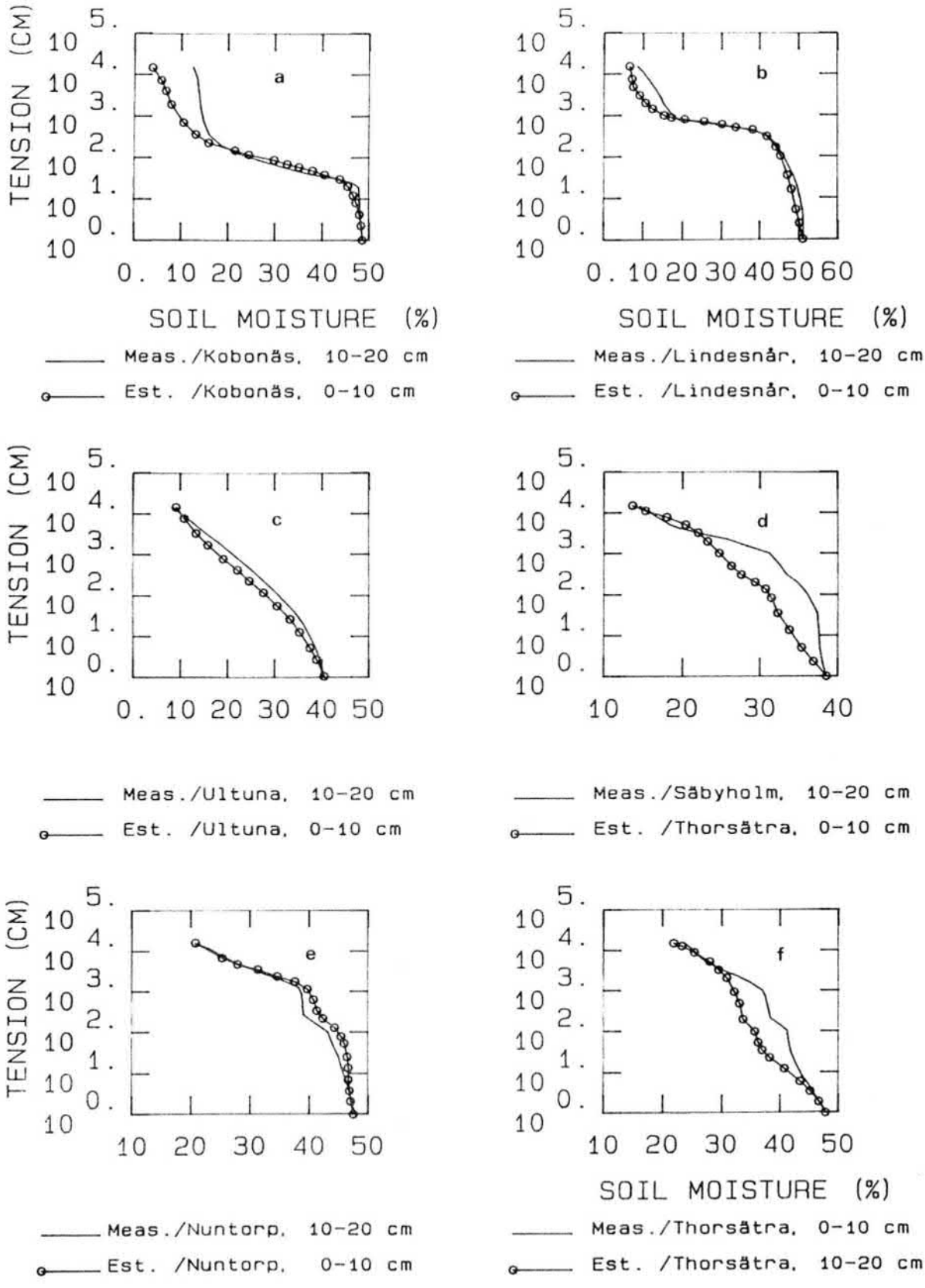

Fig. 3-2. Estimation of water retention curve from soil texture (topsoil).

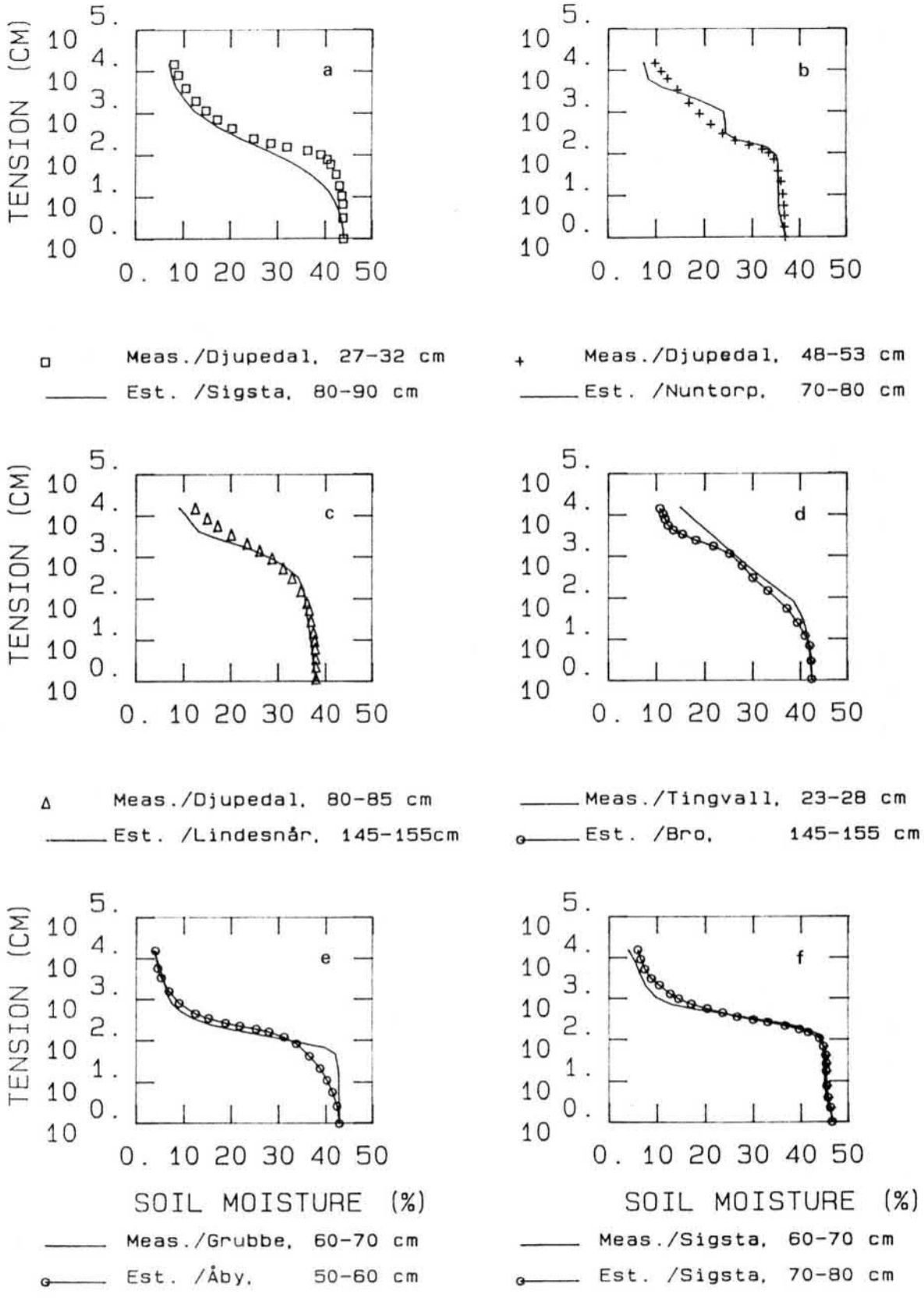

Fig. 3-3 a-f. Estimation of water retention curve from soil texture (subsoil).

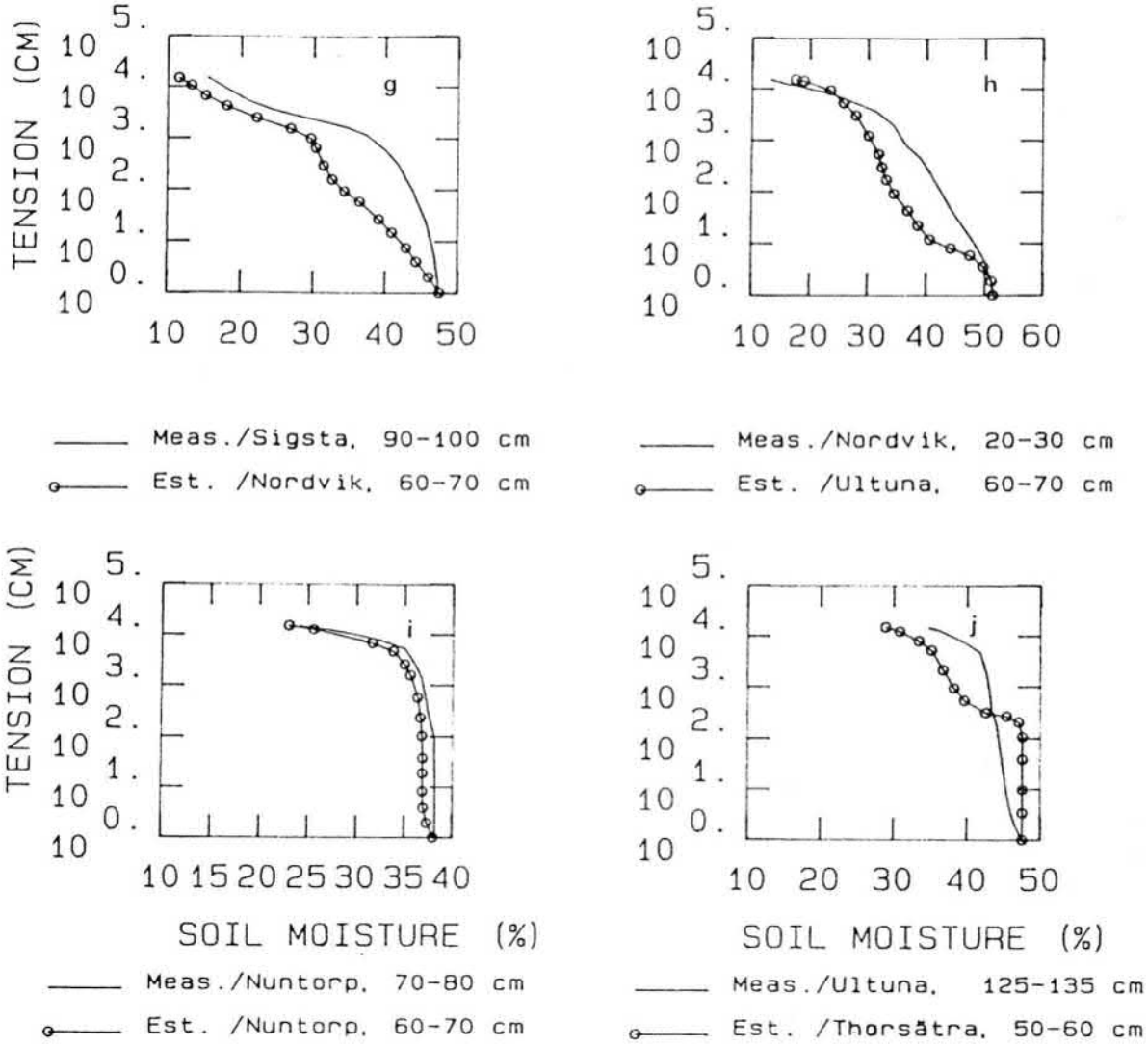

Fig. 3-3 g-j. Estimation of water retention curve from soil texture (topsoil).

effective saturation S_i according to which the relative hydraulic conductivity K_R can be calculated with equations:

$$K_R = K_i/K_S = S_i^e \quad (3\text{-}2)$$

$$S_i = (w_i - w_R)/(w_S - w_R) \quad (3\text{-}3)$$

where K_S is the hydraulic conductivity at saturation, K_i is the unsaturated conductivity, w_i is the actual water content, w_S and w_R are the saturated and the residual water content, respectively. The exponent e is a parameter whose value varies generally from 3 to 4. Averjanov proposed the value e = 3.5.

The second group of models make use of the measured pF-curve (soil moisture retention curve) to derive the hydraulic conductivity in the unsaturated state.

The purpose of this section is twofold. First, the theoretical model for calculating the unsaturated hydraulic conductivity is presented. This model was originally proposed by Andersson (1969). An extension of Andersson's model is formulated which is capable of predicting the unsaturated hydraulic conductivity function if the soil moisture retention curve (pF-curve) and the hydraulic conductivity at saturation are known. The improvements to the original model are the inclusion of a reduction factor due to tortuousity, inclusion of bubbling pressure to neglect some measured values from the pF-curve near saturation and determination of the residual water content with the method suggested by Mualem (1976). Second, the proposed new model was tested with data measured from 30 soils. The extension of Andersson's model was also tested against the existing models of Mualem (1976), Averjanov (1950), Van Genuchten (1978) and Brooks and Corey (1966).

3.3.2 The theoretical model proposed by Andersson

The theoretical model suggested by Andersson (1969) is based on the assumption that the negative pressure - water content curve w(h) is known and the phenomena of hysteresis is not taken into account. The pore volume of the soil sample is idealized to be composed of small pipes with different diameter. The cumulative pipe-size distribution curve y (%) is defined as follows:

$$y = (100/n) \cdot w \qquad (3\text{-}4)$$

where n is porosity and it is usually replaced by saturated water content) and w is the actual water content. The Laplace surface-tension equation is used to define the relationship between the soil water tension and the corresponding pipe diameter (Andersson, 1962).

$$h = 0.3/x \qquad (3\text{-}5)$$

where h is the negative pressure (cm) and x is the pipe diameter (cm). If the tension has a value h then the pipes with a diameter greater than x are empty (filled with air) and the pipes with a diameter smaller than x are filled with water.

The derivative of y with respect to x is

$$\emptyset(x)=dy/dx \qquad (3\text{-}6)$$

Consider a class of pipes where the lower limit of the pipe diameter is x-dx/2 and the upper limit is x+dx/2. The percentage of pipes from the total pipe-size distribution in this class is $dy=\emptyset(x)\cdot dx$. In a soil column with bottom area A and height L_h the total volume of pipes is $nAL_h/100$ and the total number of pipes in this class is dN

$$dN = \frac{nAL_h}{100^2} \frac{\emptyset(x)dx}{(\pi L_h x^2/4)} = \frac{4nA}{100^2\pi} \frac{\emptyset(x)dx}{x^2} \qquad (3\text{-}7)$$

where $\pi L_h x/4$ is the volume of a single pipe with diameter x and length L_h. According to the Hagen-Poiseuille law, the flow through a pipe with a diameter x is $(d_w \pi g I x^4)/(128\mu)$, where d_w is the density of water, g is the acceleration due to gravity, μ is the dynamic viscosity of water and I is the gradient causing the flow. All the pipes belonging to pipe class (x-dx/2,x+dx/2) can conduct an amount dq of water in a time unit:

$$dq = \frac{nA\, d_w\, g I}{32 \cdot 100^2 \mu} x^2 \cdot \emptyset(x)dx \qquad (3\text{-}8)$$

The total flow through completely saturated soil can be calculated as follows:

$$q = \int_{d_{min}}^{d_{max}} dq = \frac{nAd_w gI}{32 \cdot 100^2 \mu} \cdot \int_{d_{min}}^{d_{max}} x^2 \cdot \phi(x) dx \quad (3\text{-}9)$$

where d_{min} and d_{max} are the smallest and the largest pipe diameter taken into consideration, respectively. According to Darcy's law:

$$q = K_S \cdot A \cdot I \quad (3\text{-}10)$$

where K_S is the hydraulic conductivity at saturation. By equating (3-9) and (3-10) a formula for calculating the saturated hydraulic conductivity is obtained:

$$K_S = C_C \cdot \int_{d_{min}}^{d_{max}} x^2 \cdot \phi(x) dx \quad (3\text{-}11)$$

where

$$C_C = (nd_w g)/(32 \cdot 100^2 \mu) \quad (3\text{-}12)$$

The relative hydraulic conductivity K_R (= K/K_S) can be estimated from equation

$$K_R = \frac{\int_{d_{min}}^{d} x^2 \cdot \phi(x) dx}{\int_{d_{min}}^{d_{max}} x^2 \cdot \phi(x) dx} \quad (3\text{-}13)$$

where d implies the pipe diameter which is the upper limit in the integration of the numerator in (3-13). If the soil moisture retention curve is known, the pipe diameter d, water content w and negative pressure h can be related to each other using equation (3-5). Hence, the only unknown in (3-13) is the

derivative $\emptyset(x)$. The relative hydraulic conductivity can be calculated analytically if the functional form of $\emptyset(x)$ is known.

Consider that the pF-curve can be approximated with either a linear relationship

$$h = a + b \cdot w \qquad (3\text{-}14)$$

or an equation

$$^{10}\log(h) = a + b \cdot w \qquad (3\text{-}15)$$

where a and b are constants. In equation (3-14) h can be replaced by 0.3/x and w by $(n/100) \cdot y$. By making these substitutions the cumulative pipe-size curve y can be solved

$$y = \frac{100}{n}\left(\frac{0.3}{b\ x} - a\right) \qquad (3\text{-}16)$$

Hence the derivative $\emptyset(x)$ can be calculated from formula

$$\emptyset(x) = dy/dx = -\frac{30}{n \cdot b}\frac{1}{x^2} \qquad (3\text{-}17)$$

and the relative hydraulic conductivity can be calculated analytically from (3-13). If equation (3-15) is used the derivative $\emptyset(x)$ can be calculated from

$$\emptyset(x) = -\ 0.4343\ \frac{100}{n \cdot b}\frac{1}{x} \qquad (3\text{-}18)$$

The drawback in the formulation carried out by Andersson is the necessity to describe the total pF-curve with only one straight line (linear or log-linear). In section 3.3.3 the model is extended for use when the soil moisture retention curve is

defined in a tabular form (piecewise linear).

3.3.3 Formulation of the new model

3.3.3.1 Extension of the theoretical model of Andersson

Assume that the soil moisture retention curve can be presented in a tabular form composed of M (w_i ,h_i)-pairs, where i is the index of the measured point starting from the residual water content. Hence, the curve can be considered linear between two consecutive points. The original model for calculating the unsaturated hydraulic conductivity can be used independently for each interval in the curve. The starting point must be the smallest pipe diameter corresponding to the residual water content defined later on in the text. The effect of each interval (i.e. pipe class) is added to the cumulative sum of the previous classes. The limits between pipe classes are the pipe diameters obtained using the measured tension values in the pF-curve ($d_i = 0.3/h_i$). The relative hydraulic conductivity of each point in the pF-curve can be calculated from equation

$$K_{Ri} = \frac{\sum_{1}^{i} \int_{d_{i-1}}^{d_i} x^2 \cdot \Phi(x)\,dx}{\sum_{1}^{IB} \int_{d_{i-1}}^{d_i} x^2 \cdot \Phi(x)\,dx} \qquad (3\text{-}19)$$

where IB (< M) is the index of the bubbling pressure (air-entry-value) and M is the total number of measured points in the negative pressure - water content curve. The summation of the denominator cannot be carried out to point i=M since the tension h is zero and the corresponding pipe diameter is infinite. The index 1 in (3-19) refers to the pipe diameter at residual water content. The determination of the residual water content and the corresponding pipe diameter is discussed in section 3.3.3.2

In the integration of (3-19) d_i is replaced by a value $0.3/h_i$ and d_{i-1} by a value $0.3/h_{i-1}$. The soil moisture retention curve is approximated by piece-wise linear functions

$$h = a_i + b_i \cdot w \; ; \; w_{i-1} \leq w \leq w_i \qquad (3\text{-}20)$$

or

$$^{10}\log(h) = a_i + b_i \; w \; ; \; w_{i-1} \leq w \leq w_i \qquad (3\text{-}21)$$

For the linear model, coefficients a_i and b_i can be calculated using equations

$$a_i = h_{i-1} + (h_i - h_{i-1})/(w_i - w_{i-1}) \qquad (3\text{-}22)$$
$$b_i = - (h_i - h_{i-1})/(w_i - w_{i-1}) \qquad (3\text{-}23)$$

where h_i and w_i, i=1, 2, ..., M are the measured points of the pF-curve (suction and the corresponding actual water content, respectively). The coefficients of equation (3-21) can be obtained from (3-22) and (3-23) by replacing the suction values with their logarithmic values.

3.3.3.2 Estimation of the residual water content and the bubbling pressure

The residual water content is defined so that $dw/dh \rightarrow 0$ when $w \rightarrow w_R$. The assumption is that hydraulic conductivity is zero when $w=w_R$. By plotting the logarithm of effective saturation (equation (3-3)), S_i, versus the logarithm of negative pressure, h_i, a straight line with slope defined as λ is obtained. The parameter λ is the pore-size distribution index. To calculate S_i, the residual water content must be known. The determination of w_R is carried out with a method suggested by Mualem (1976). It is based on the idea that the soil moisture retention curve can be represented analytically with equation (3-24)

$$S_i = (h_i/h_b)^{-\lambda} \quad ; \; h_i \leq h_b \qquad (3\text{-}24)$$

where h_b is the bubbling pressure (air-entry value). The formula is supposed to be valid only up to an inflection point (see Fig. 3-4). Parameters w_R and λ are computed with the aid of a minimum square deviation procedure demanding that the dispersion of measured points, up to the inflection point around the analytical curve (3-24) should be minimum. In the computer program all values starting from 0.5% and continuing up to w_1 (the first measured point in the pF- curve) with interval 0.5% are tested. The residual water content w_R is chosen as the value which yields the minimum deviation between the analytical curve and the measured values.

The bubbling pressure is the intercept of the straight line described previously in this section (see also Fig. 3-4).

3.3.3.3 Effect of tortuousity on the relative hydraulic conductivity

In the theoretical model of Andersson the soil sample is said to be composed of small tubes with different diameters. However, not all the tubes are continuous and have connection with each other. Therefore, a new factor must be used to reduce the calculated conductivity values. In the proposed new model the reduction factor is S_i^2 . The exponent has been determined with the procedure suggested by Mualem (1976). Thirty soils for which w-h and K-w data are available were used for computation. Two different criteria were used to evaluate the goodness of fit. First, the mean square deviation between the logarithm of calculated and measured relative hydraulic conductivity was computed. The second criteria was based on the mean square deviation between the calculated and measured K_R-values. 20 different values of the exponent were used (1.1, 1.2,...,3.0). The results are shown in Fig. 3-5. According to the two criteria used, the best values were 1.7 and 2.3, respectively. The final value of the exponent was chosen to be 2.0.

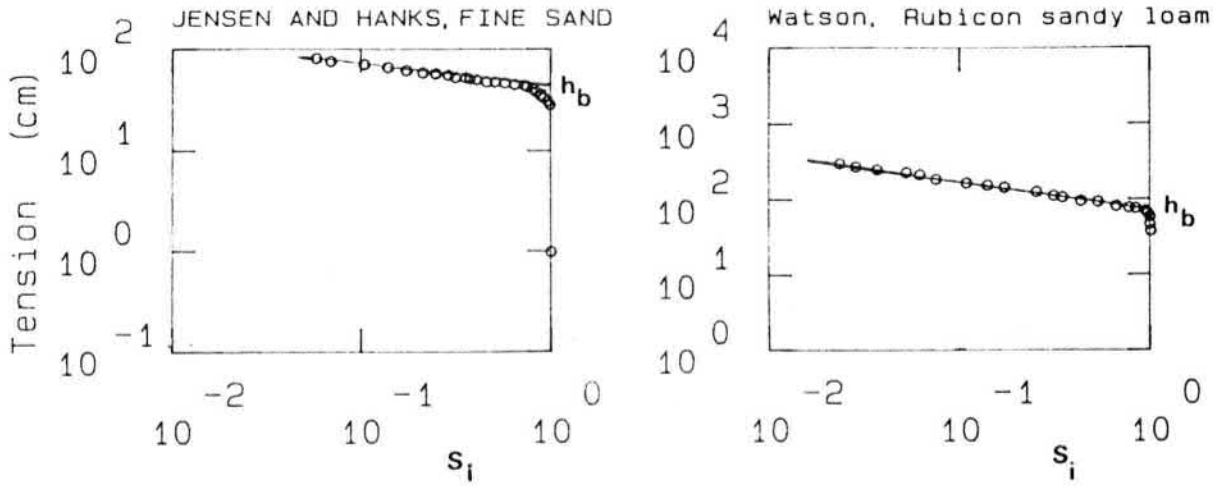

Fig. 3-4. Determination of the bubbling pressure with the measured soil moisture retention curve.

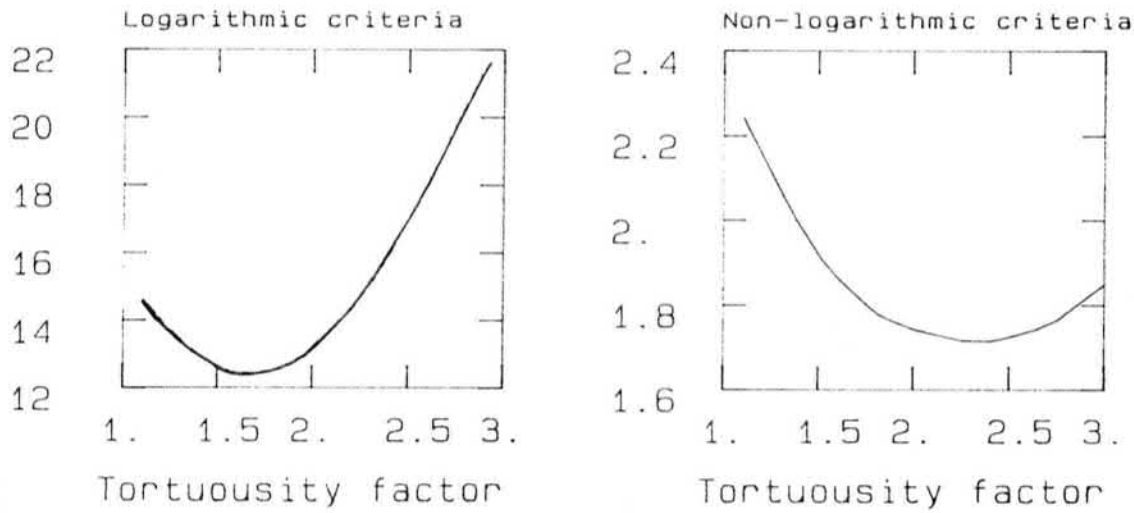

Fig. 3-5. The effect of the exponent e in the reduction factor (S_i^e) on the criteria of goodness of fit.

3.3.3.4 Summary of the proposed procedure

Fig. (3-6) illustrates a simplified flowchart of the proposed procedure. The algorithm is made up of the following steps.

0° Guess the initial value for the residual water content.

1° Calculate the effective saturation using the most recent

approximation for w_R and plot the logarithm of S_i and the logarithm of h_i. Determine the inflection point from this figure.

2° Determine the residual water content w_R with Mualem's method (described in section 3.3.3.2).

3° Determine the inflection point using the new estimate for the residual water content. If the new inflection point is different from the one chosen in 1° go back to 1°.

4° Calculate the bubbling pressure by solving h_b from equation (3-24) and substituting all the measured values of the pF-curve (S_i and h_i) up to the inflection point. The final bubbling pressure is the mean of the all h_b values calculated.

5° Compute the relative hydraulic conductivities from

$$K_{Ri} = \frac{\sum_{1}^{i} \int_{d_{i-1}}^{d_i} x^2 \cdot \emptyset(x) \cdot dx}{\sum_{1}^{IB} \int_{d_{i-1}}^{d_i} x^2 \cdot \emptyset(x) \cdot dx} \qquad (3\text{-}25)$$

Index IB is the point in the curve with the measured h_i nearest the value of the bubbling pressure, h_b. If needed, it is also possible to interpolate a point with tension value equal to the bubbling pressure.

The derivative $\emptyset(x)$ required in integrating (3-25) is calculated from equations (3-17) or (3-18) and (3-22)-(3-23).

3.3.4 Results and conclusions

Thirty soils with measured soil moisture retention curves and unsaturated hydraulic conductivities were used for testing the proposed extension of the model of Sigvard Andersson. Moreover, the new model is compared with the existing practical models of Mualem (1976), Averjanov (1950), Brooks and Corey (1966) and van Genuchten (1978). In the analytical model suggested by van

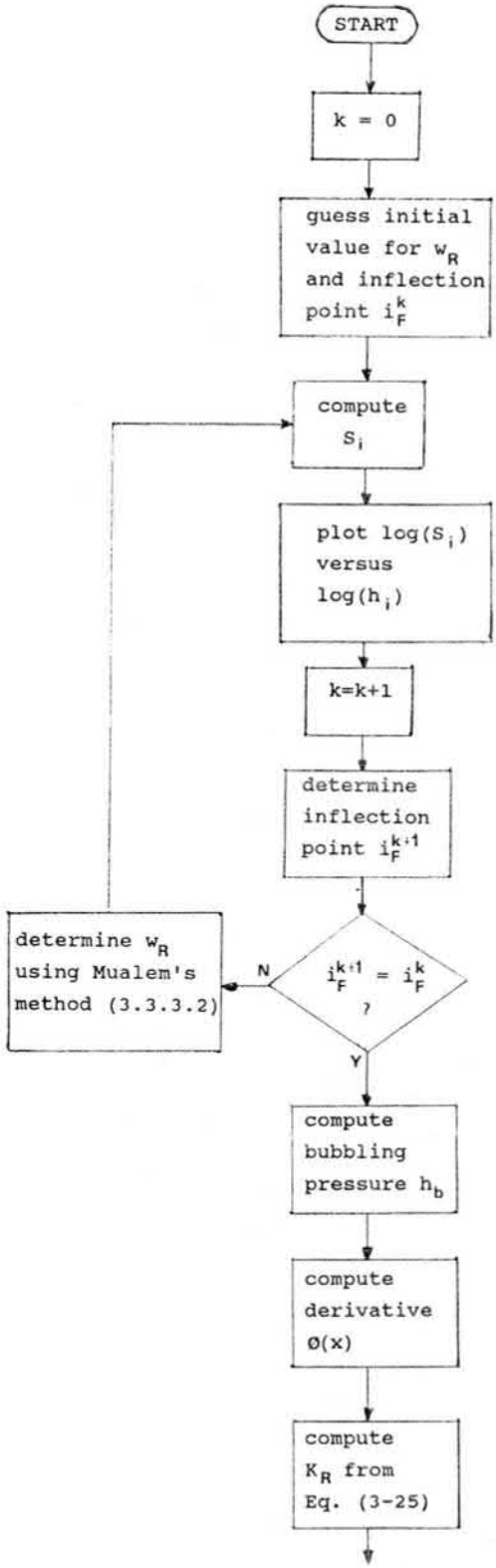

Fig. 3-6. Simplified flowchart of the algorithm CONDUC for estimation of unsaturated hydraulic conductivity function.

Genuchten, the soil moisture retention curve is approximated by a three-parameter non-linear function.

$$w_i = w_R + \frac{w_S - w_R}{(1+(\beta h)^{n_l})^{m_l}} \qquad (3\text{-}26)$$

where the values of the parameters w_R, n_l and β are optimized with the Marquardt-algorithm (ref. Box and Jenkins, 1970). The value of the parameter m_l is a function of n_l ($m_l = 1-1/n_l$).

The references of the soils tested are shown in table 3-1 and the characteristics of the soils are listed in table 3-2, including the saturated water content, the moisture content at the first measurement point, the calculated bubbling pressure, the pore-size distribution index, the residual water contents determined with two methods (Mualem and van Genuchten) and the parameters β and n_l of the van Genuchten model. The residual water content calculated with Mualem's method was generally different from the value determined with van Genuchten's approach. Unfortunately, the optimization routine of the parameters of van Genuchten's model yielded physically impossible results for some soils (negative residual water content). This is perhaps due to difficulties in the convergence of the Marquardt-algorithm. However, in most cases the non-linear function (3-26) predicted the measured pF-curve accurately (Fig. 3-7.)

Table 3-1. References of the soils used in testing.

Number	References
1	Fine sand (Jensen and Hanks, 1967)
2	Weld silty clay loam (Jensen and Hanks, 1967)
3	Touched silt loam (Jensen and Hanks, 1967)
4	River sand (screened) (Jensen and Hanks, 1967)
5	Volcanic sand (Jensen and Hanks, 1967)
6	Guelph loam (Elrick and Bowman, 1964)
7	Sand (Poulovassilis, 1970)
8	Aggregated glass beads (Topp and Miller, 1966)
9	Monodispersed glass beads (Topp and Miller, 1966)
10	Sand (Vachaud and Vauchlin, 1975)
11	Webster soil (Kunze, 1968)
12	Hygiene sandstone (Brooks and Corey, 1966)
13	Botany sand (Watson, 1967, ref. Hornberger and Remson, 1970)
14	Colo soil (Kunze, 1968)
15	Berea Sandstone (Brooks and Corey, 1966)
16	Amarillo silty clay loam (Brooks and Corey, 1966)
17	Poudre River sand (Brooks and Corey, 1966)
18	Plainfield sand (25-60 cm) (Black & al., 1969)
19	Wagram loamy sand (Wells and Skaggs, 1976)
20	Yolo light clay (ref. Jensen, 1983)
21	Rubicon sandy loam (Watson, 1974)
22	Adelaide dune sand (Talsma, 1970)
23	Molonglo River sand (Talsma, 1970)
24	Panoche soil (61 cm) (Skaggs and Tang, 1976)
25	Heavy clay (Al-Soufi, 1983)
26	Waukegan loam, 0-10 cm, sample 1 (Arya & al., 1975)
27	Waukegan loam, 0-10 cm, sample 2 (Arya & al., 1975)
28	Waukegan loam, 60-70 cm, sample 1 (Arya & al., 1975)
29	Waukegan loam, 60-70 cm, sample 2 (Arya & al., 1975)
30	Alfisol, 0-15 cm (Hundal and De Datta, 1984)

Table 3-2. Characteristics of the 30 soils.

No.	1	2	3	4	5	6	7
1	0.36/0.09	42	4.36	0.070	0.076	0.021	7.55
2	0.47/0.14	57	1.60	0.095	0.163	0.013	5.97
3	0.48/0.17	75	1.81	0.125	0.186	0.010	6.26
4	0.40/0.07	23	4.62	0.060	0.090	0.038	12.55
5	0.35/0.05	14	1.61	0.045	0.072	0.047	6.16
6	0.52/0.24	39	0.29	0.055	0.229	0.012	2.06
7	0.27/0.09	21	2.18	0.005	0.012	0.038	4.23
8	0.55/0.08	33	3.10	0.065	0.110	0.025	10.30
9	0.27/0.03	39	4.67	0.015	0.039	0.022	12.81
10	0.30/0.01	25	1.86	0.005	0.010	0.032	3.35
11	0.48/0.20	8	0.41	0.160	0.230	0.044	3.16
12	0.25/0.15	53	3.60	0.140	0.151	0.016	10.05
13	0.35/0.06	40	9.79	0.045	0.070	0.023	27.60
14	0.44/0.18	16	0.29	0.135	0.176	0.028	1.54
15	0.20/0.06	40	2.58	0.055	0.071	0.019	8.94
16	0.45/0.14	37	1.95	0.100	0.127	0.020	5.09
17	0.36/0.04	14	3.05	0.030	0.053	0.058	7.86
18	0.30/0.06	21	1.44	0.050	0.067	0.033	4.02
19	0.30/0.22	16	0.38	0.005	-0.020	0.023	2.14
20	0.50/0.14	31	0.41	0.125	0.125	0.025	1.43
21	0.38/0.17	70	2.60	0.160	0.174	0.011	6.66
22	0.32/0.10	66	2.82	0.005	-0.049	0.010	4.24
23	0.22/0.10	12	0.94	0.005	0.087	0.060	5.11
24	0.44/0.30	30	0.30	0.140	0.195	0.018	1.62
25	0.48/0.11	4900	0.55	0.005	-2.217	0.001	1.04
26	0.38/0.24	102	0.35	0.175	0.240	0.004	2.27
27	0.37/0.24	115	0.34	0.170	0.238	0.004	2.25
28	0.37/0.21	38	0.15	0.005	-0.735	0.011	1.05
29	0.37/0.19	38	0.16	0.005	-0.740	0.011	1.06
30	0.48/0.39	35	0.69	0.375	0.383	0.016	2.23

1=Saturated water content/measured water content at the 1st point, 2=Bubbling pressure, 3=Pore-size distribution index, 4=Residual water content determined with Mualem's method, 5=Residual water content according to van Genuchten's model, 6=Parameter ß in van Genuchten's model, 7 = Parameter n_1 in van Genuchten's model.

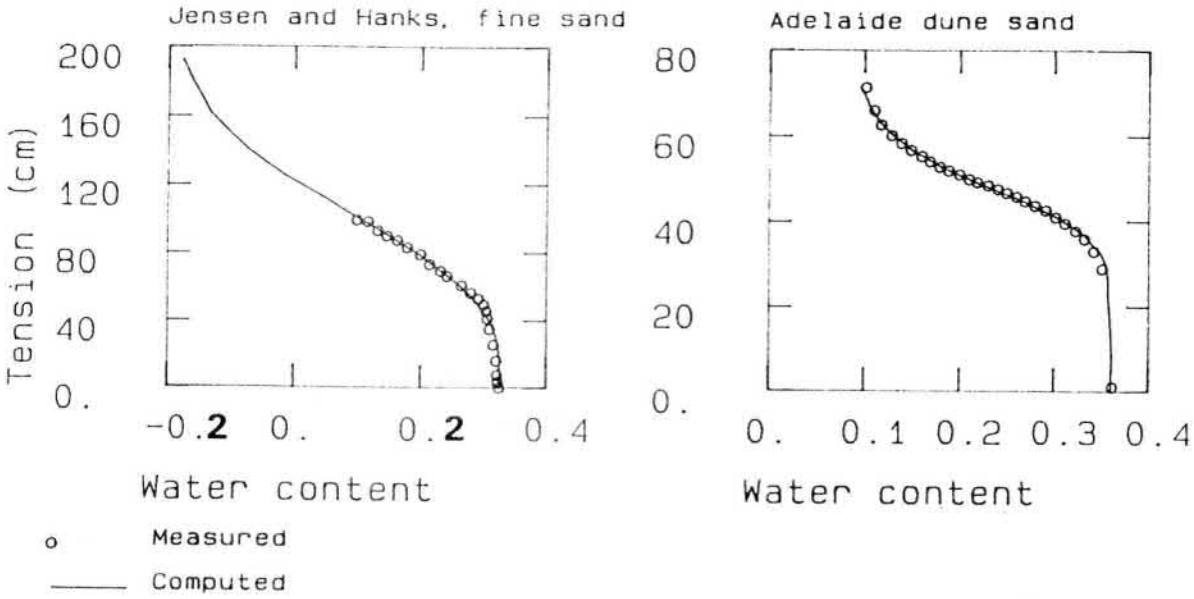

Fig. 3-7. Measured and computed (van Genuchten's model) soil moisture retention curves for two soils.

The results from calculations are shown in tables 3-3 and 3-4. In table 3-3 the logarithmic deviation between the measured and computed relative hydraulic conductivities is given for each of the 30 soils. The average logarithmic deviation, $\overline{D}$, is given in the last line. In table 3-4 the absolute deviation between the measured and computed relative hydraulic conductivity is given and the corresponding mean deviation, $\overline{D}$, in the last line. The logarithmic criteria (table 3-3) gives more weight to the conductivity values at low moisture content, whereas the use of the non-logarithmic criteria (table 3-4) favours proper estimation of conductivity near saturation.

Based on the results, the following conclusions can be drawn:
1° The proposed extensions of the theoretical model suggested originally by Andersson performed fairly well. The new model and Mualem's model gave better results than the other models used in testing (Averjanov, van Genuchten, Brooks and Corey).
2° The drawback of the proposed model is the calculation of the relative hydraulic conductivity at very low moisture content.

3° In some cases the negative values yielded by the method used in predicting the bubbling were too large. In these cases the proposed model overestimates the relative conductivity values near saturation.
4° The variations in the proposed model (logarithmic and linear) gave equally good results.
5° The drawback of Mualem's model is the exclusion of the bubbling pressure. Consequently, the calculated conductivity is generally too low near saturation.
6° The analytical version of Mualem's model (van Genuchten) gave the poorest fit. However, the comparison may not be completely valid for van Genuchten's model, since difficulties were encountered in the application of the analytical model.
7° The method of Brooks and Corey overestimates the relative hydraulic conductivity near saturation.
8° Averjanov's model fits sands very well, but fails to describe the conductivity of heavier soils accurately .
9° It is generally possible to describe the soil moisture retention curve accurately using the non-linear three-parameter model of van Genuchten. However, for five soils the optimization algorithm of Marquardt yielded a negative residual water content. The reason for these unrealistic results could be the non-convergence of the optimization algorithm.
10° None of the tested models proved to be superior in predicting the unsaturated hydraulic conductivity function and according to tables 3-3 and 3-4, the differences in the prediction capability are not pronounced.

However, the computations it is possible to recommend use of either the proposed model or Mualem's model in predicting the unsaturated hydraulic conductivity based on the measured hydraulic conductivity at saturation and the measured soil moisture retention curve.

The results of the predictions are also shown in Fig. 3.8a...h for those soils where the results were the poorest.

Table 3-3. Deviation between the measured and computed relative hydraulic conductivities (logarithmic criteria)

No.	1	2	3	4	5	6
1	0.44	0.44	0.51	0.27	0.49	0.21
2	0.22	0.22	0.42	0.65	0.77	0.22
3	0.40	0.40	0.15	0.46	1.02	0.38
4	0.93	0.94	1.09	1.19	1.64	1.09
5	0.29	0.29	0.46	0.46	0.80	0.70
6	0.22	0.22	0.37	2.06	0.94	0.25
7	0.23	0.23	0.31	0.23	0.37	0.48
8	0.49	0.49	0.21	0.42	1.64	1.30
9	0.25	0.25	0.08	0.30	0.61	0.30
10	0.91	0.91	0.82	0.71	0.88	1.23
11	0.22	0.21	0.27	2.60	3.42	0.88
12	0.11	0.10	0.19	0.09	0.22	0.08
13	0.14	0.14	0.12	0.35	0.38	0.19
14	1.15	1.14	1.00	5.63	2.21	1.52
15	0.18	0.18	0.37	0.25	0.31	0.22
16	0.13	0.13	0.12	0.12	0.09	0.18
17	0.15	0.15	0.20	0.16	0.30	0.13
18	0.37	0.37	0.17	0.47	0.64	0.37
19	0.22	0.23	0.50	0.27	0.18	0.36
20	1.47	1.51	2.17	1.14	2.67	1.71
21	0.35	0.35	0.15	0.21	0.73	0.48
22	0.47	0.47	1.38	0.67	0.43	0.62
23	0.40	0.41	0.40	0.14	0.55	0.60
24	0.93	0.96	0.45	1.89	0.36	0.69
25	0.56	0.56	1.20	0.41	1.37	1.13
26	0.40	0.41	0.32	1.38	1.04	0.44
27	0.50	0.52	0.39	1.58	1.30	0.53
28	0.43	0.41	0.74	2.31	3.47	0.84
29	0.91	0.89	0.42	2.91	1.13	1.07
30	1.46	1.47	1.33	0.45	1.97	1.75
$\bar{D}$	0.50	0.50	0.54	0.99	1.06	0.67

1 = Proposed logarithmic model, 2 = Proposed linear model
3= Mualem, 4 = Averjanov, 5 = van Genuchten, 6 = Brooks and Corey

Table 3-4. Deviation between the measured and computed relative hydraulic conductivities (non-logarithmic criteria)

No.	1	2	3	4	5	6
1	0.058	0.058	0.131	0.085	0.084	0.038
2	0.019	0.019	0.057	0.033	0.039	0.021
3	0.093	0.093	0.015	0.098	0.0469	0.079
4	0.126	0.126	0.218	0.170	0.160	0.154
5	0.041	0.041	0.069	0.029	0.038	0.110
6	0.051	0.051	0.056	0.175	0.064	0.060
7	0.066	0.067	0.044	0.033	0.067	0.140
8	0.016	0.016	0.025	0.020	0.042	0.239
9	0.027	0.027	0.032	0.020	0.033	0.047
10	0.084	0.084	0.045	0.055	0.052	0.130
11	0.010	0.010	0.007	0.049	0.123	0.199
12	0.018	0.018	0.044	0.036	0.087	0.035
13	0.014	0.014	0.014	0.041	0.055	0.032
14	0.019	0.018	0.018	0.088	0.156	0.064
15	0.020	0.020	0.036	0.024	0.070	0.050
16	0.043	0.043	0.052	0.022	0.038	0.082
17	0.038	0.038	0.062	0.054	0.114	0.050
18	0.083	0.083	0.039	0.067	0.022	0.093
19	0.136	0.136	0.180	0.164	0.069	0.183
20	0.109	0.109	0.076	0.122	0.200	0.145
21	0.033	0.033	0.024	0.014	0.067	0.054
22	0.132	0.132	0.450	0.206	0.190	0.129
23	0.048	0.048	0.051	0.034	0.122	0.077
24	0.160	0.162	0.069	0.267	0.072	0.173
25	0.081	0.081	0.165	0.145	0.260	0.140
26	0.021	0.020	0.024	0.164	0.170	0.044
27	0.016	0.016	0.019	0.156	0.157	0.033
28	0.091	0.089	0.067	0.328	0.247	0.121
29	0.176	0.174	0.024	0.396	0.176	0.206
30	0.046	0.046	0.017	0.059	0.097	0.064
$\bar{D}$	0.062	0.062	0.071	0.105	0.104	0.099

1 = Proposed logarithmic model, 2 = Proposed linear model
3= Mualem, 4 = Averjanov, 5 = van Genuchten, 6 = Brooks and Corey

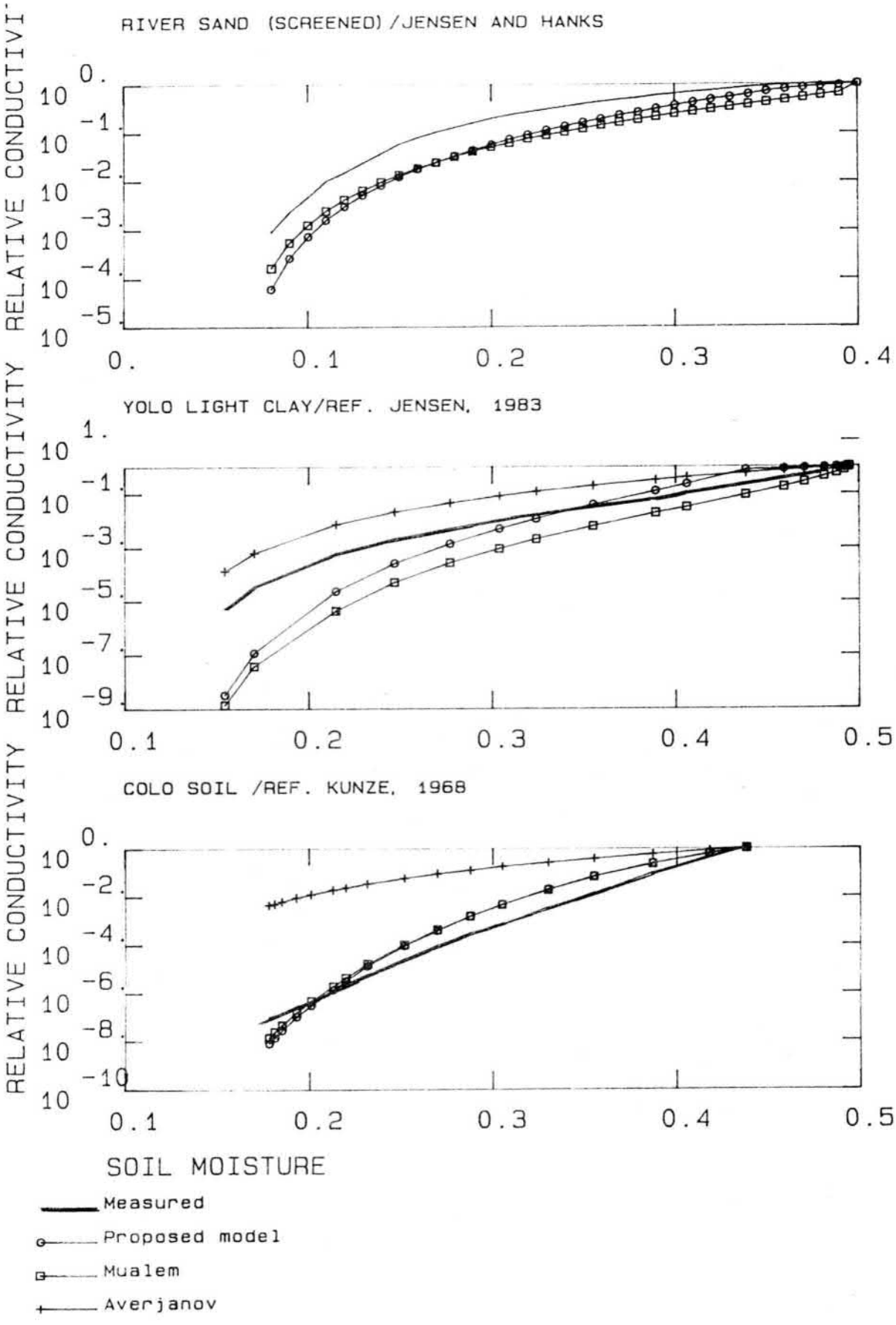

Fig. 3.8 a - c. Measured and calculated relative conductivity.

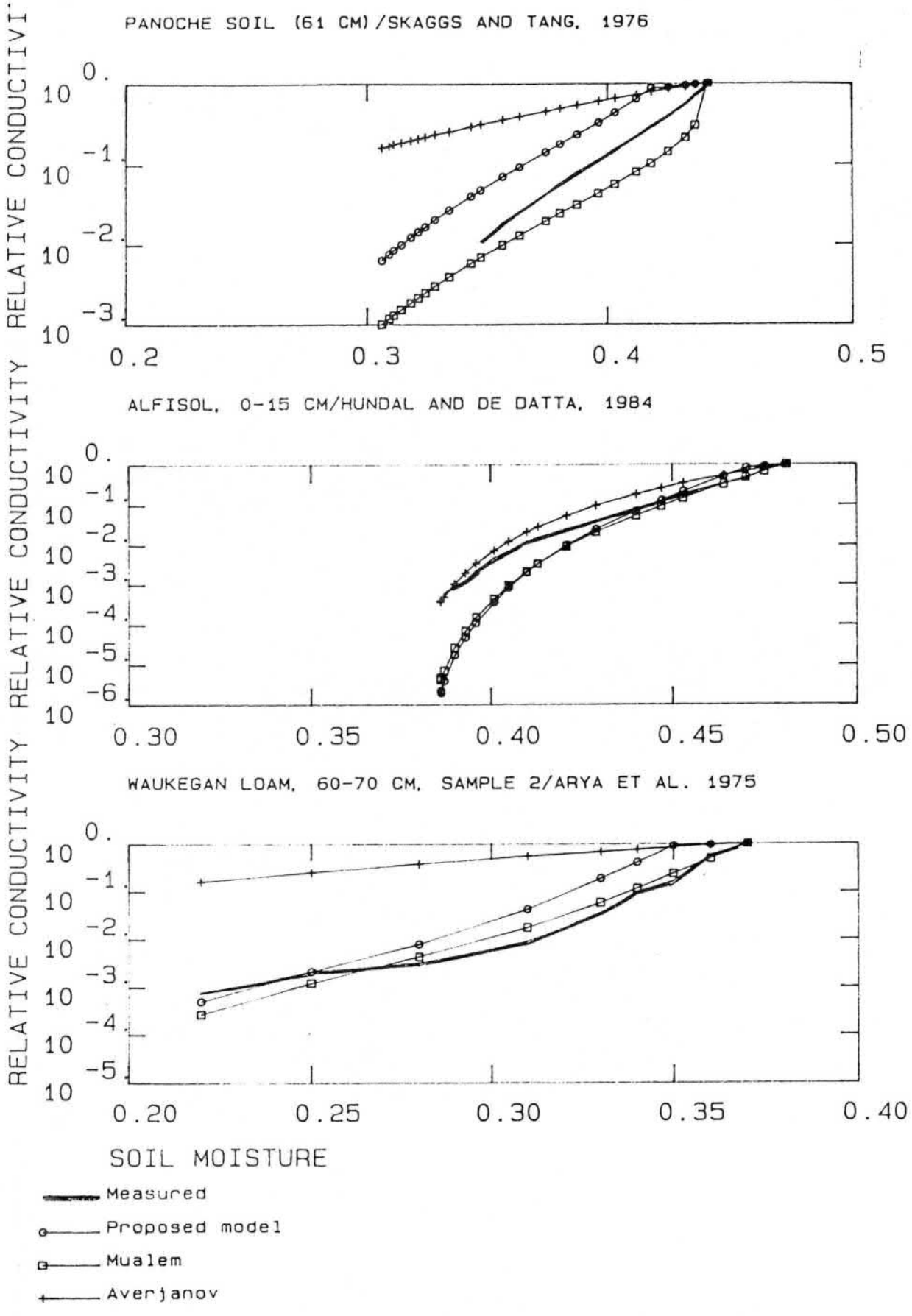

Fig. 3.8 d - f. Measured and calculated relative conductivity.

3.4 Estimation of soil properties with combined use of a mathematical model and a field experiment

It was shown in the previous section that in most cases the prediction of the unsaturated hydraulic conductivity function can be based on the soil moisture retention curve and the hydraulic conductivity at saturation. In some cases it is not possible to obtain a measured value for the saturated hydraulic conductivity and it is necessary to estimate it indirectly. Moreover, the horizontal hydraulic conductivity is generally not measured at all, and its value may be different from the vertical conductivity. Therefore, the indirect determination methods must be used based on the results of a field experiment. This type of problem is generally referred to as an inverse problem, i.e. the dependent state variables (soil water potential and/or soil moisture content) and input values are known and the parameters of the model have to be estimated.

A solution to the inverse problem of defining the unknown unsaturated hydraulic conductivity function was previously presented e.g. by Skaggs et al. (1971). Their method was based on the assumption that the conductivity function can be represented by the three parameter empirical equation presented by Gardner (1958). One of the parameters is saturated hydraulic conductivity K_S. Repeated solutions of the Richard's equation are used to define the parameters which will give the best prediction of the measured influx curve.

A new method for estimating the unknown soil properties is described in this section. These properties include saturated hydraulic conductivity in the vertical and horizontal directions and soil thermal conductivity as a function of soil moisture content. The method is based on a simplification of the Kalman filtering technique. The necessary data include input variables and measured soil moisture content or soil water potential and soil temperature at least at two different depths.

3.4.1 Simplification of the Kalman filtering technique

The Kalman filter is not in itself a model, but a technique used in conjunction with an analytical model which is an imperfect representation of some process. The model must be formulated within a framework of equations referred to as state-space representation. The state-space representation consists of the system equation - the model - and the measurement equation. The latter tells how the actual measurements and the system state variables are related to each other. A detailed description of the Kalman filtering technique can be found in Jazwinski (1970) and Maybeck (1979).

In the original Kalman filter the aim is to combine the measurements taken from the actual system with the information provided by the system model and statistical description of uncertainties, in order to obtain an optimal estimate of the system state. In the method presented in this section, the aim is somewhat controversial. A parameter combination that produces an acceptable state prediction is sought. From the original Kalman filter only a "measurement updating procedure" is used together with the system model, which in this case is the numerical solution of Richard's equation. The propagation of the covariance matrix is not calculated at all. Instead, a simple criteria is used to take into account the uncertainty involved in the measurements. A maximum allowed deviation from the observed value is given for each individual measurement point. The parameter calibration routine is stopped when the absolute deviation between the measured and calculated state variables is within the prescribed limits or the maximum number of iterations is exceeded.

Consider the case where the initial estimates of the unknown parameters are denoted by a n_p-dimensional vector $p[t_0]$. The system model is solved from time $t=t_0$ to time $t=t_1$, and the calculated state variables are defined by a n_x-dimensional vector $h[t_1]$. The measurement equation is of the form:

$$z[t_1] = H_M[t_1] \cdot h[t_1] \qquad (3\text{-}27)$$

where $z[t_1]$ is the n_m-dimensional measurement vector, $H_M[t_1]$ is a "measurement matrix" (n_m by n_x matrix). The latter is used to define the state variables which are measured. At time $t=t_1$ a new measurement vector $z[t_1]$ is obtained. The parameter vector has to be updated with the latest observations. According to the Kalman filter, the parameter vector can be updated by defining the Kalman gain $G[t_1]$ (e.g. Maybeck, 1979):

$$G[t_1]=P[t_1] \cdot H^T[t_1] \cdot \{H[t_1] \cdot P[t_1] \cdot H^T[t_1]+R[t_1]\}^{-1} \qquad (3\text{-}28)$$

where $P[t_1]$ and $R[t_1]$ are diagonal weighting matrices The numerical values for these matrices have to be determined by trial-and-error procedure. Once the Kalman gain has been calculated the parameter vector can be updated with the equation (Maybeck, 1979):

$$p[t_1]=p[t_0] + G[t_1] \cdot \{z[t_1] - H_M[t_1] \cdot h[t_1]\} \qquad (3\text{-}29)$$

In the traditional Kalman filtering technique, the next step would be integration of the state equation onward from time $t=t_1$ using the parameter vector $p[t_1]$. In the method described here, the solution method is different. If the measured and calculated values are not close enough to each other, the procedure is repeated from time $t=t_0$ and a substitution $p[t_0]=p[t_1]$ is carried out before the new solution of Richard's equation is obtained. After integration of the flow equation, a new parameter estimate is calculated with equations (3-28) and (3-29). The procedure is repeated until convergence is attained or the maximum number of iterations is exceeded.

A problem arises from the fact that the updating is fulfilled with repeated integration from time $t=t_0$ to $t=t_1$. Hence, the interpretation of the matrix $H[t_1]$ is not the same as in the original Kalman filter. In the present case $H[t_1]$ must include both the effect of time propagation and the traditional meaning of locating the state variables that are actually measured. The

solution of the problem of defining $H[t_1]$ is:

1° Integrate Richard's equation using the parameter vector $p[t_0]$ and store the calculated values of the state variables (nominal values).

2° Deviate each parameter component from its nominal value by a small amount (e.g. 0.1 - 1 %) and integrate the flow equation using this perturbated parameter vector. Only one parameter value at a time is perturbated. Hence, in the case of a three-parameter model the integration has to be performed three times. An estimate of the "sensitivity matrix" $S[t_1]$ can be calculated numerically from the equation:

$$S[t_1] = \{h[t_1,dp] - h[t_1]\}/dp \qquad (3\text{-}30)$$

where $h[t_1,dp]$ is the calculated state variable vector using the perturbated parameter vector and dp is the amount of perturbation.

3° Finally, the $H[t_1]$ matrix is obtained by taking into account the fact that only a few state variables are measured, i.e. $H[t_1] = H_M[t_1]\ S[t_1]$, where $H_M[t_1]$ is the original measurement matrix of the system.

The algorithm for estimating the unknown parameters can now be summarized as follows (see also Fig. 3-9):

a) Give an initial estimate for the unknown vector $p[t_0]$.

b) Solve Richard's equation starting from the known initial conditions from time $t=t_0$ to $t=t_1$. Store the values of the state variables.

c) Solve the $H[t_1]$ matrix using the procedure described previously in stages 1° - 3° (equation (3-30)).

d) Calculate the Kalman gain from equation (3-28) and update the parameter vector using equation (3-29).

e) Compare the measured and calculated values of the state variables. If the deviation is not within the prescribed limits and the number of iterations is smaller than some maximum value, substitute $p[t_0] = p[t_1]$ and go back to b).

f) Otherwise, the parameter vector is accepted and the procedure is repeated for the next time step (onward from time $t=t_1$) using

the latest parameter vector as an initial guess for the new time step.

Using the above described procedure a new parameter vector is obtained whenever the measurement updating is carried out. All the parameter vectors can be stored and they can be plotted e.g. as a function of time. If the parameter vector is not stabilized to a constant value, either the measurements are erroneous or the model is not a valid description of the system.

It is interesting to note that the procedure presented in this section is very similar to that proposed by Kettunen and Varis (1986). They derived their method from least squares estimates and their method is called a recursive Gauss-Newton algorithm.

The benefits of the simplified Kalman filtering technique compared with methods that use repeated solutions of the governing equation are the following:
1° It is possible to obtain a rough estimate for the uncertainty involved in the parameter estimate.
2° The dependence of the parameters on state variables can be revealed.
3° The method can be used to test whether the parameters are time invariant.
4° The sensitivity matrix $S[t_1]$ (equation (3-30)) can be used if a detailed sensitivity analysis is carried out (see e.g. Pingoud, 1984).
It should be noted that the proposed algorithm can be used in different types of mathematical models, i.e. it is not restricted to the models presented in Chapter 4.

The testing of the proposed estimation technique will be carried out in Chapters 4 (application to the estimation of soil thermal conductivity) and 6 (two-dimensional drainage problem).

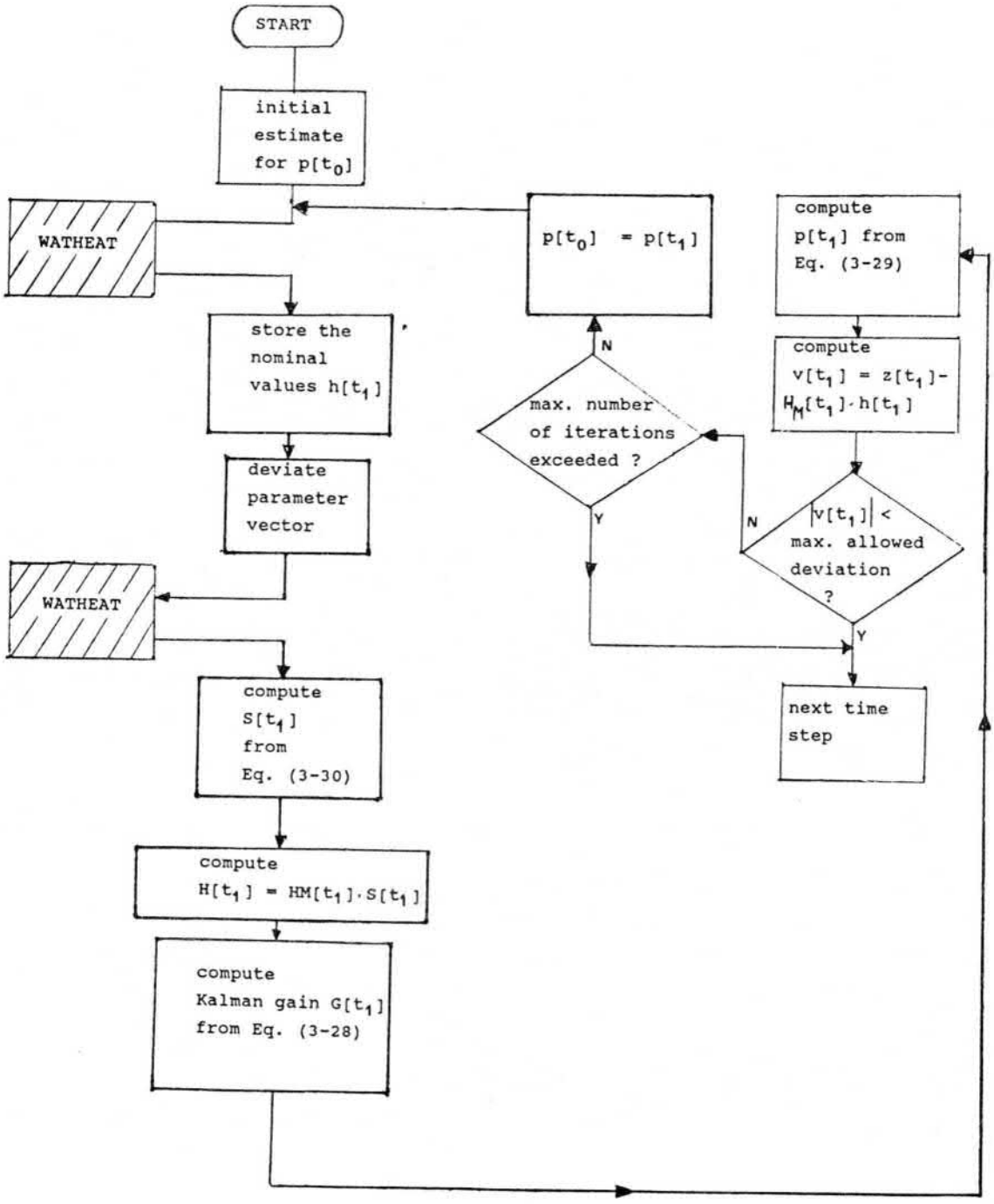

Fig. 3-9. Simplified flowchart of the algorithm KALMAN for estimation of unknown parameters.

CHAPTER 4. DESCRIPTION, SOLUTION AND TESTING OF THE SELECTED SOIL MODELS

4.1 Introduction

The mathematical models used in the quantification of the effects of drainage on soil moisture and soil temperature are presented in this chapter. The choice of the model to be used in evaluating the effects of water management systems is between low model complexity and high accuracy of results. Here the well-known equation chosen for calculation is the equation of conservation of mass in the 1-dimensional case (for 2-dimensional cases see Chapter 6). It is the so called Richards' equation. Richards derived the equation in 1931 but its nonlinear nature creates difficulties for solution of most problems. During the past two decades, however, numerical procedures utilizing high speed digital computers have been developed to solve the equation for many practical problems. Further refinement in computing hardware has made it possible to use this type of model in quantifying the effects of water management systems.

Section 4.2 presents a solution to the flow equation using the finite element method in saturated-unsaturated media. Special emphasis has been placed on evaluating the differential water capacity in order to produce a numerical solution with accurate water balance calculations.

A numerical solution of combined mass and heat transfer in unsaturated-saturated and seasonally frozen soil is desribed in section 4.3. A new technique for avoiding the numerical difficulties usually encountered in solving the equations in frozen soil is presented. The snowmodel needed in the simulation of winter period is described in section 4.4.

Special attention has been paid to testing the models. In this chapter the models have been verified with data presented in the literature. Both analytical solutions and actual field experiments are used in evaluating the capability of the proposed models.

4.2 One-dimensional Richards' equation

The Richards' equation for describing the flow in saturated-unsaturated soil-root system is

$$C(h)\frac{\partial h}{\partial t} = \frac{\partial}{\partial z}[K(h)\left(\frac{\partial h}{\partial z} - 1\right)] - S(h) \qquad (4\text{-}1)$$

where h is the soil water potential or negative pressure (m), K(h) is the hydraulic conductivity given as a function of the water potential ($m \cdot d^{-1}$), z is the position in the vertical dimension (positive downward from the surface) (m), t is time (d), C(h) is defined as the differential water capacity (derivative of the soil moisture retention curve) (m^{-1}), i.e. $C(h) = dw/dh$, where w is the volumetric water content. S(h) represents the volume of water taken up by the roots from the unit volume of soil ($m^3 m^{-3} d^{-1}$). Determination of this sink-term is discussed in Chapter 5.

Equation (4-1) forms the differential equation for liquid flow of water in the vertical direction in partly unsaturated soil. This equation is applicable under rather idealized conditions (for a more thorough review of the validity of Richards' equation, see e.g. Jensen, 1983). In the derivation the liquid flow is assumed to be the only component of significance contributing to the soil water flux; any contribution of the gas phase is neglected. The thermal effects on soil moisture flow are not taken into account, although they may affect the moisture flux (Ghali Sami Ghali, 1986). However, for the field systems to be considered in this study, the theory expressed in (4-1) is considered sufficiently valid for prediction of soil

water behaviour.

4.2.1 A numerical solution using the finite element method

An exact analytical solution of Richards' equation is virtually precluded, due to the non-linear nature of the equation. Numerical techniques are most commonly used for solving the flow problems in unsaturated media. Basically two numerical approaches are conceivable: finite element and finite difference techniques. Either one of these methods could have been chosen. Successful solutions have been reported in the literature using either the finite difference method or the finite element method, and both for h- based or w-based equations(e.g. Molz and Remson, 1970; Nimah and Hanks, 1973; Feddes et al., 1974; Feddes et al., 1978; Abbott et al., 1982; Jensen, 1983 and in Finland Pingoud and Orava, 1980; Pingoud, 1982 and Vakkilainen, 1982). In this study, the finite element method is used due to its ability to handle the various types of boundary conditions flexibly.

The finite element method is well-documented in standard textbooks (e.g. Pinder and Gray, 1977; Desai, 1979; Wang and Andersson, 1982) and the details of the solution are not described. Further information concerning the application of the Galerkin scheme, which is also used here, can be obtained e.g. from Neuman (1973) and Neuman et al. (1974). In the finite element method the solution domain is discretized into union of N_X rigid elements (maximum number in the present program version is 50). The state variables, i.e. the soil water potentials h are approximated within each element by:

$$h(z,t) = \sum_j N_j \cdot h_j \qquad ; j=1,2,\ldots,N_X \qquad (4\text{-}2)$$

where N_j is the shape function and h_j is the state variable at element nodal points. In the Galerkin scheme the shape functions are also the weighting functions used in the formulation.

By applying the Galerkin method for solving Richards' equation, one obtains a set of quasi-linear first-order differential equations:

$$[A]\cdot\{h\} + [C]\cdot\{dh/dt\}=\{Q\} + \{B\} + \{D\} \qquad (4\text{-}3)$$

where [A] is the conductance matrix, {h} is the vector composed of soil water potentials at each nodal point, [C] is the capacity matrix, {Q} is a vector including the boundary conditions, vector {B} accounts for the gravity term and vector {D} represents the sink term. The coefficients of the equation (4-3) can be obtained by applying the Galerkin method individually for each element and summing up the effects of these elements. The element-wise coefficients as follows:

$$[A]_e = \frac{K_1^e + K_2^e}{2\cdot L^e} \begin{bmatrix} 1 & -1 \\ -1 & 1 \end{bmatrix} \qquad (4\text{-}4)$$

$$[C]_e = \frac{L^e}{2} \begin{bmatrix} C_1^e & 0 \\ 0 & C_2^e \end{bmatrix} \qquad (4\text{-}5)$$

$$\{B\}_e = \frac{K_1^e + K_2^e}{2} \begin{bmatrix} -1 \\ 1 \end{bmatrix} \qquad (4\text{-}6)$$

$$\{D\}_e = -\frac{L^e}{2} \begin{bmatrix} S_1^e \\ S_2^e \end{bmatrix} \qquad (4\text{-}7)$$

where L^e is the length of the element e, K_1^e and K_2^e the hydraulic conductivities at the element nodal points 1 and 2 (linear elements), respectively, C_1^e and C_2^e are the values of the differential moisture capacities at element nodal points and S_1^e and S_2^e the calculated sink-terms. The {Q} -vector accounts for the fluxes into the system through the lower or the upper boundary (positive or negative).

It is important to note here that according to the method proposed by Neuman (1973) the capacity matrix $[C]_e$ was must be a diagonal matrix. Moreover, theoretically the elements of the elementwise $[C]_e$-matrix should read:

$$[C]_e = \frac{L^e}{6} \begin{vmatrix} 2C_1^e + C_2^e & 0 \\ 0 & C_1^e + 2C_2^e \end{vmatrix} \qquad (4\text{-}8)$$

However, it was decided to select the form shown in (4-5) because the local mass balance is better maintained with equation (4-5). This is of special importance in the combined solution of mass and heat transfer in a frozen soil.

Each element can be handled independently and therefore it is easy to take into account the inhomogeneity of the soil profile if the hydraulic functions of the materials are known (soil water retention curve and hydraulic conductivity).

Once the coefficient matrices of the equation (4-3) have been derived by taking the summation over all the elements, the first-order differential equation has to be integrated. The time domain is discretized into a sequence of finite intervals and the time derivatives are replaced by finite differences.

$$[A]_{t+\frac{1}{2}} \cdot \frac{\{h\}_{t+1} + \{h\}_t}{2} + [C]_{t+\frac{1}{2}} \cdot \frac{\{h\}_{t+1} - \{h\}_t}{\Delta t}$$

$$= \{Q\}_{t+\frac{1}{2}} + \{B\}_{t+\frac{1}{2}} + \{D\}_{t+\frac{1}{2}} \qquad (4\text{-}9)$$

where $t+\frac{1}{2}$ implies that the coefficients are evaluated at half the time step to reduce unwanted oscillations (Neuman, 1973; Neuman et al. 1974). Vector $\{h\}_{t+1}$ includes the unknown soil water potentials which should be solved when it is assumed that the pressure head values at time t (= $\{h\}_t$) are known. An initial guess for the unknown $\{h\}_{t+1}$ -vector must be given at the beginning of each time step. Here the initial guess is the

known vector at time t. The resulting set of equations is then solved, and due to the nonlinear nature of the equations, the results must be improved by an iterative process. The iteration is stopped when two consecutive iterations differ from each other by less than a selected covergence criterion (e.g. 1 cm). Two or three iterations have generally proved to be enough to attain sufficient accuracy. The coefficient matrix of the system is of tri-diagonal form, and the solution can be achieved efficiently using the Thomas algorithm (e.g. Remson et al. 1971).

4.2.2 Approximation of the differential moisture capacity

In solving the governing equation, the coefficients C_1^e and C_2^e of equation (4-5) have to be evaluated. Tests with numerical solution methods have shown that non-linear changes in C tend to produce mass conservation errors, whereas the non-linear changes in hydraulic conductivity mainly affect the internal water distribution (Jensen, 1983).

Three basic approximation methods have been used in the numerical solutions published in the literature:

$$C_{t+\frac{1}{2}} = C[h_t] \qquad (4\text{-}10a)$$

$$C_{t+\frac{1}{2}} = C[(h_{t+1} + h_t)/2] \qquad (4\text{-}10b)$$

$$C_{t+\frac{1}{2}} = C[h_{t+1}]/2 + C[h_t]/2 \qquad (4\text{-}10c)$$

where $t+\frac{1}{2}$ implies a mean value during one time step. The first approximation is purely an explicit one;the others are Crank-Nicolson approximations. Consider the case, when the soil moisture retention curve is given by:

$$w = 0.124 + \frac{274.2}{739.0 + [\ln(-h)]^4} \qquad (4\text{-}11)$$

Equation (4-11) is the water retention curve of Yolo light clay (Jensen, 1983). The differential moisture capacity can be calculated analytically from:

$$C(h) = dw/dh = - \frac{4 \cdot 274.2 \, [\ln(-h)]^3}{h \cdot [739.0 + (\ln(-h))^4]^2} \qquad (4\text{-}12)$$

Assume that the soil moisture potential of a soil layer at time t=0 is initially -150 cm, the thickness of the layer is 5 cm and the inflow to the layer is 0.1 $cm \cdot d^{-1}$, the outflow being equal to zero. What is the soil water potential at time t = 2 d ? The volumetric increase in the water content of the soil layer is 0.02 (from 0.32424 to 0.34424) and the new soil water potential should be -114.755 cm.

Using an explicit approximation (4-10a), the calculated soil water potential is -109.23 cm and the calculated increase in the moisture content 0.02379, i.e. 18% greater than the exact value. No iterations were needed in this explicit case. Approximation (4-10b) gave much better results. After four iterations the calculated value was -114.589 cm and the corresponding increase in the water content 0.02011, i.e. the error is 0.5%. The calculated values were -115.09 cm and 1.1% when approximation (4-10c) was used.

However, the most accurate approximation for $C_{t+\frac{1}{2}}$ would be:

$$C_{t+1} = \frac{w_{t+1} - w_t}{h_{t+1} - h_t} \qquad (4\text{-}13)$$

In fact C_{t+1} calculated with equation (4-13) is exactly the true value which should be used when the change in soil moisture potential is $h_{t+1} - h_t$ and the corresponding change $w_{t+1} - w_t$ should be calculated. How can an approximation of the form (4-13) be applied in the numerical solution? The solution method adopted here can be summarized as follows:

1° At the beginning of each time step an explicit approximation of the change in water content is calculated for each nodal point. An estimate of the soil moisture content of each nodal point can be obtained, denoted by w°_{t+1}

2° Approximation of soil water potential for each nodal point can be calculated using new water content values estimated in stage 1° (h°_{t+1} as a function of w°_{t+1})

3° Differential moisture capacities can now be estimated from (4-13), where w_{t+1} is replaced by w°_{t+1} and h_{t+1} by h°_{t+1} .

4° New pressure head values can be calculated by solving equation (4-9). If convergence is not attained, a new iteration is necessary and within this new cycle stages 1° through 3° are fulfilled again. At the end of the iteration procedure h°_{t+1} is equal to h_{t+1} .

The main merit of the procedure described above is the accurate calculation of mass balances. Hence, it is possible to use longer time steps and still maintain reliable water balance calculations. The validity of the proposed approximation method is verified using the following test example:

- the number of soil layers is four and the depth of each layer is 10 cm
- the inflow to the uppermost layer is 2 $cm \cdot d^{-1}$ and the outflow from the lowest storage is zero
- the period of two days will be calculated
- the water retention curve is the one shown in (4-11) and the hydraulic conductivity curve is:

$$K(h) = \frac{218.6}{124.6 + (-h)^{1.77}} \quad (cm \cdot d^{-1}) \qquad (4\text{-}14$$

In this case the exact distribution of the soil moisture potentials is not known. However, the numerical solution should preserve the water balance since the net increase in the total amount of water in the system is known (= 4 cm). Four different types of approximation of C_{t+1} were tested, (4-10a..c) and (4-13). The numerical solution in this example was fulfilled

using the finite difference method and the linearized equation was actually solved with the relatively inefficient Gauss-Seidel iteration. The period of two days was calculated and the effect of different time-steps on the accuracy of the mass balance was tested. The main results are shown in table 4-1.

Table 4-1. The effect of time step and approximation method on the accuracy of mass balance computations and on the number of iterations needed.

Time step	Approximation method			
	4-10a	4-10b	4-10c	4-13
0.01	1.2 %/400			
0.02	2.5 %/234	<0.01%/223	0.1 %/224	<0.01 %/219
0.05	6.5 %/134	0.2 %/133	0.3 %/137	<0.01 %/123
0.10	15.5 %/111	0.7 %/105	1.2 %/128	<0.01 %/71
0.167	-	2.1 %/123	3.6 %/311	<0.01 %/52
0.250	-	-	-	<0.01 %/87

According to table 4-1 the error in the water balance was always less than 0.01 % when approximation (4-13) was used. Moreover, the total number of iterations needed was considerably smaller compared with those for other approximation methods. The explicit approximation in particular produced a large error in the mass balance even with a relatively short time step (0.05 d corresponding to a maximum change <0.01 $m^3 \cdot m^{-3}$ during one time step). It should benoted that for approximations (4-10b..c) and (4-13) the total number of iterations was not the smallest when the longest time-step was used. Use of e.g. (4-13) does not violate the mass balance with a time step equal to 0.25 d. However, the total number of iterations needed is 87 as opposed to 52 when the time step was 1/6 d. This is because the convergence is more difficult to attain if the changes in the water content are too pronounced during one time step.

This single example shows the difficulties in choosing the optimal length of the time step. It is not possible to know in advance the effect of the time step used on the error in the water balance when e.g. approximation (4-10b) or (4-10c) is used. An automatic time step selection method could be used to restrict the maximum change during one time step. A method of this type has been used e.g. in SWATR (Feddes et al. 1978) and SWATRE (Belmans et al. 1983). An automatic time step selection method is not used here. Instead, it is assumed that the time step is a function of the precipitation. The greater the precipitation, the smaller the time step. In the computer program four different time steps can be chosen depending on the amount of precipitation. The limits are the following: 1) $P < 5$ mm d^{-1}, 2) $5 \leq P < 10$ mm d^{-1}, 3) $10 \leq P < 20$ mm d^{-1} and 4) $P \geq 20$ mm d^{-1}, where P is the measured daily precipitation.

4.2.3 Initial and boundary conditions

To obtain a solution for the one-dimensional vertical flow equation, the appropriate initial and boundary conditions must be defined. At the beginning of the calculation, either the soil water potential or the soil water content must be known at each nodal point. The upper and lower boundary conditions must be defined as a function of time.

4.2.3.1 Upper boundary condition

The flux at the upper boundary is governed by meteorological conditions. Thus, the exact boundary condition to be assigned at the soil surface is not known a priori, and a solution must be sought by maximizing the absolute value of the flux (Hanks et al. 1969; Feddes et al. 1978). The finite element method is very well suited for cases of these types. According to Feddes et al. (1978) it can be assumed that under all circumstances

$$h_{min} \leq h_{1n} \leq h_{max} \qquad (4\text{-}15)$$

where h_{min} and h_{max} are the minimum and maximum value for soil water potential h_{1n} at nodal point 1 , i.e. at the soil surface. Assuming that the pressure head at the soil surface is at equilibrium with the atmosphere, then h_{min} can be calculated from

$$h_{min} = R \cdot T \cdot \ln(F)/(M \cdot g) \qquad (4\text{-}16)$$

where R is the universal gas constant ($J \cdot mole^{-1} \cdot K^{-1}$), T is the absolute temperature (K), g is acceleration due to gravity ($m \cdot s^{-1}$), M is the molecular weight of water ($kg \cdot mole^{-1}$) and F is the relative humidity of the air (fraction). Here it is assumed that $h_{max}=0$, indicating that the possible effect of ponding is neglected. The actual solution can be obtained if the potential flux at the soil surface is known. The potential flux through the soil surface consists of the following components:

$$q_{pot} = P - E_i - E_s \qquad (4\text{-}17)$$

where q_{pot} is the potential flux through the soil surface, P is rainfall, E_i is interception rate and E_s is soil evaporation rate. The determination of E_i and E_s is discussed in Chapter 5.

During the first iteration, the surface node is treated as a prescibed flux boundary and the corresponding soil pressure heads are calculated. If the computed h_{1n} satisfies eq. (4-15), the iteration is continued and the upper boundary condition is continuously a flux boundary. However, if h_{1n} lies outside the limits specified in (4-15) then, during the subsequent iteration, the surface node is treated as a prescribed pressure head node with $h_{1n}=h_{max}$ for infiltration and $h_{1n}=h_{min}$ for soil evaporation. In the case of a prescribed soil water potential node, the actual flux can be calculated explicitly from (4-9). If the calculated flux exceeds the potential flux at any stage of computation, the surface node is again treated as a flux boundary.

4.2.3.2 Lower boundary condition

For the lower boundary either the flux or the soil water potential can be used as a boundary condition. The latter refers to the case, where recorded water table fluctuations are known a priori and the flux at the bottom of the system is calculated. However, in many water management models the flux through the lower boundary can be calculated and the elevation of the ground water table must be computed.

Consider the case where the elevation of the water table is given. At the water table pressure head h is zero. Since the nodepoints have fixed positions, it is most likely that none of them will coincide with the water table. For this reason the presribed pressure head node must be the one which is immediately beneath the water table. The positive pressure head value used for this node is the depth of this nodal point below the water table. This way of defining the position of the water table is not strictly correct for large fluxes across the water table, since the pressure head distribution within the saturated zone will not be hydrostatic under these circumstances. It can be assumed that the error introduced using this approximation is negligible (Jensen, 1983).

The flux at the bottom of the system can be given directly as input. In water management models the flux originates from subsurface flow to ditches and possibly to deep aquifers. The bottom flux q_d can be calculated with either the Hooghoudt equation (see Skaggs 1980) or the Ernst equation (see Belmans et al. 1983). The idea is based on the assumption that lateral movement occurs mainly in the saturated region. The effective horizontal saturated hydraulic conductivity is used and the flux is evaluated in terms of water table elevation midway between the drains and the water level in the drains.

The flux to the drains is calculated as a function of the average water table elevation during one time step. Since the new location of the water table is unknown at the beginning of the time step, the first guess will be that the groundwater remains unchanged during the time step. At the end of each time step the location of the water table is defined as a point where the pressure head is equal to zero.

The procedure described above can be considered a quasi two-dimensional solution to the drainage problem. The flow in the vertical direction is calculated with Richards' equation and the flow in the horizontal direction with either the Hooghoudt or the Ernst equation. These two systems are linked to each other via the boundary condition of the one-dimensional vertical flow model. In Chapter 6, a two-dimensional solution to the drainage problem is described and the results of these two approaches are compared.

4.3 A numerical solution for combined mass and heat flow in seasonally frozen soil

4.3.1 Introduction

The possibility of numerical modeling of the complex processes which occur in simultaneous heat and soil moisture transport in a freezing soil has received much attention during the past decade (e.g. Harlan, 1973; Guymon and Luthin, 1974; Taylor and Luthin, 1978; Guymon et al., 1980; Jansson and Halldin, 1980; Gilpin, 1980; Hromadka et al., 1981; O'Neill and Miller, 1982). Special attention has been devoted by Motovilov (1977, 1978, 1979) and Engelmark (1984, 1986) to the calculation of infiltration into a frozen soil.

In section 4.3.2, the equations describing the flow of mass and heat in partly unsaturated and seasonally frozen soil have been presented. Section 4.3.3 is devoted to the estimation of freezing point depression based on the soil moisture retention curve. In section 4.3.4, a new method for solving the problem

of dividing the total moisture content in a frozen soil into liquid and ice is presented. In section 4.3.5, the numerical solution of combined heat and mass transfer in partly unfrozen zone is described. The solution method adopted is based on the finite element method (Galerkin's scheme).

4.3.2 Combined heat and mass transfer

The equations describing the combined heat and water flow are given by (4-18) and (4-19):

$$C_s \frac{\partial T}{\partial t} - d_{ice} \cdot L_f \frac{\partial I}{\partial t} = \frac{\partial}{\partial z}\left(K_T(w) \frac{\partial T}{\partial z}\right) - c_w q_w \frac{\partial T}{\partial z} \qquad (4\text{-}18)$$

$$C(h) \frac{\partial h}{\partial t} + \frac{d_{ice}}{d_w} \frac{\partial I}{\partial t} = \frac{\partial}{\partial z}\left[K(h) \frac{\partial h}{\partial z} - K(h)\right] - S(h) \qquad (4\text{-}19)$$

where z is a space coordinate (m), t is time (d), T is temperature (°C), $K_T(w)$ is the soil thermal conductivity ($W \cdot m^{-1} \cdot °C^{-1}$) as a function of water content w, L_f is latent heat of fusion of water ($J \cdot kg^{-1}$), C_s is volumetric specific heat of soil ($J \cdot m^{-1} \cdot °C^{-1}$), d_{ice} and d_w are density of ice and water ($kg \cdot m^{-1}$), respectively, c_w is specific heat of water ($J \cdot kg^{-1} \cdot °C^{-1}$), q_w is flow of water ($m \cdot d^{-1}$), I is volumetric ice content, h is soil water potential, C(h) is differential moisture capacity (m^{-1}) and K(h) is unsaturated hydraulic conductivity of the soil matrix ($m \cdot d^{-1}$) and S(h) the sink term representing the volume of water taken up by the roots (the calculation of the sink term is described in Chapter 5.

A difficulty in the numerical solution of (4-18) and (4-19) is the inclusion of the ice term, since it generally dominates the solution (e.g. Guymon et al. 1980). To avoid excessive numerical difficulties, it is often assumed that there is a unique relationship between the unfrozen water content w and the soil temperature T in a frozen soil.

$$w = w(T) \quad ; \quad T < 0°C \qquad (4\text{-}20)$$

This implies that not all the water in soil will freeze at zero temperatures. The lower the temperature the smaller the amount of unfrozen water. Since it is very difficult to measure the form of this function, it is necessary to be able to predict it from other data that can be measured more easily. An assumption used in this study is that the functional form of (4-20) can be estimated from a known pF-curve. The validity of this estimate should be examined more carefully, but in this study it can unfortunately be verified only by comparing simulated and measured soil temperatures (see section 4.5 and chapter 5).

4.3.3 Freezing point depression in unsaturated soil

The formula expressing freezing point depression can be obtained thermodynamically from the generalized Clausius-Clapeyron equation (e.g. Miller, 1978):

$$u_w/d_w - u_i/d_{ice} = (L_f/K)\cdot T \qquad (4\text{-}21)$$

where u_w and u_i are pore water and pore ice pressure, respectively ($N\cdot m^{-1}$), K and T are temperature in Kelvin and Celsius degrees, L_f is latent heat of fusion and d_{ice} and d_w are density of ice and water, respectively. It can be assumed (e.g. Kinosita and Ishizaki, 1980) that ice pressure in unsaturated soil is zero. Then the freezing point depression is given by equation (4-22) where u_w is expressed in metres. Thus u_w is equal to soil water potential h (m). By replacing the variables of (4-21) with their numerical values (d_w = 1000 $kg\cdot m^{-1}$, u_i=0, L_f = 333 $kJ\cdot kg^{-1}$, K = 273.15 °C) the following expression is obtained:

$$T = h/122 \qquad (4\text{-}22)$$

where T is in °C and potential h in m. If the pF-curve of the soil is known, a relationship between unfrozen water content and soil temperature (below °C) can be obtained from (4-22).

The freezing point depression curve calculated as a function of the soil water retention curve and based on equation (4-22) is shown in Fig. 4-1. For Bensby Silt the approximation is very good, but for Tomakomai Silt the estimated curve gives excessively low temperature values throughout most of the potential range. According to Kinosita and Ishizaki (1980), this is because some pressure acts on the soil-ice matrix owing to the adsorption of pore water to the surface of soil particles.

In section 4.5, an attempt is made to verify the assumption behind (4-22) using two laboratory experiments presented in the literature.

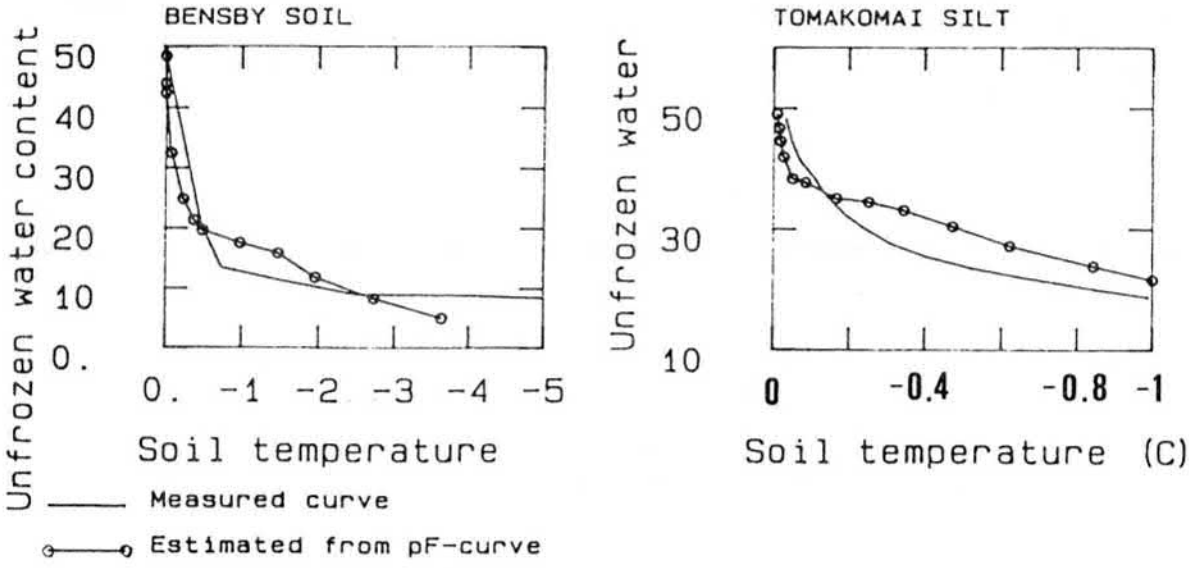

Fig. 4-1. Measured and estimated freezing point depression curves. (———) Measured. (⊶) Calculated based on equation (4-22) and the measured pF-curve. a) Bensby silt (Engelmark, 1984.) b) Tomakomai silt (Kinosita and Ishizaki, 1980).

4.3.4 Estimation of the amount of unfrozen and frozen water content and soil temperature

Two basic alternatives exist for solving the combined heat and mass transfer equations if a relationship between unfrozen water content and soil temperature is used. In the first version the derivative $\partial I / \partial t$ can be eliminated using the known $w = w(T)$ curve. This results in the "apparent heat capacity" C_a, defined by

$$C_a = C_s + L_f \partial w / \partial T \qquad (4\text{-}23)$$

As was shown by Hromadka et al. (1981) the equations (4-18) and (4-19) can be combined into a single equation in a frozen zone. Engelmark (1984, 1986) has also used this concept. However, according to Guymon et al. (1980) numerical methods employing this approach require exceedingly small time steps, and small space discretization. Instability problems may result in lengthy simulations, involving time spans of a week or more. According to Engelmark (1986), the maximum time step with a space discretization of 2.5 cm was 8 seconds. The total simulation time for a complete freezing-thawing cycle using this approach requires much computer time.

A new method based on the total energy concept is proposed. In this approach the total energy is divided into latent and sensible fractions using the known relationship between unfrozen water content and soil temperature. The energy concept was previously used by Jansson and Halldin (1980) (see also Halldin et al., 1980) in the SOIL model. The simplifying assumption in the SOIL model is that all water is frozen at the temperature:

$$T_f = - d_{f1} w_w \qquad (4\text{-}24)$$

where d_{f1} is a constant and w_w is the volumetric water content at a soil water potential of -15 000 cm. Moreover, another parameter is needed in the SOIL model to relate the pore-size distribution index and freezing point depression (see Jansson

and Halldin, 1980).

In the present model a different approach was selected. This approach uses the previously mentioned freezing characteristic curve (equation (4-20)) and the relationship between soil temperature and soil water potential in a frozen soil (equation (4-22)).

Consider the total energy needed to raise the temperature of a soil sample to 0°C from a negative temperature if the total water content is known, whereas both the amount of unfrozen and frozen water content and the soil temperature are not known. Then the energy E needed can be expressed as

$$E = - f_s \cdot c_s \cdot T - w \cdot c_w \cdot T - I \cdot c_i \cdot T + L_f \cdot I = FUN(w,T)$$
$$= - f_s \cdot c_s \cdot T - w \cdot c_w \cdot T - (W-w) \cdot c_i \cdot T + L_f \cdot (W-w) \quad (4-25)$$

where c_s, c_w and c_i are the specific heat of soil, water and ice, respectively, f_s is the volumetric fraction of soil, w is the unfrozen water content, I is the ice content, W is the total water content (water + ice). In equation (4-25) the amount of ice is expressed as the amount of frozen water (i.e. the volumetric amount of ice is about 9% greater).

Equation (4-25) can be used in the model for calculating the unknown unfrozen and frozen water content and soil temperature using known values of total water content W and energy state E. Equation (4-25) contains only two unknowns (w and T) and if the relationship w=w(T) is used, there exist two equations for solving the unknowns. The iterative solution is obtained by the Newton-Raphson method. The methods of obtaining the total water content W and the energy state E are described in Section 4.3.5. Simplified flowchart of the algorithm ENERGY for computation of unfrozen water content and soil temperature is given in Fig. 4-2.

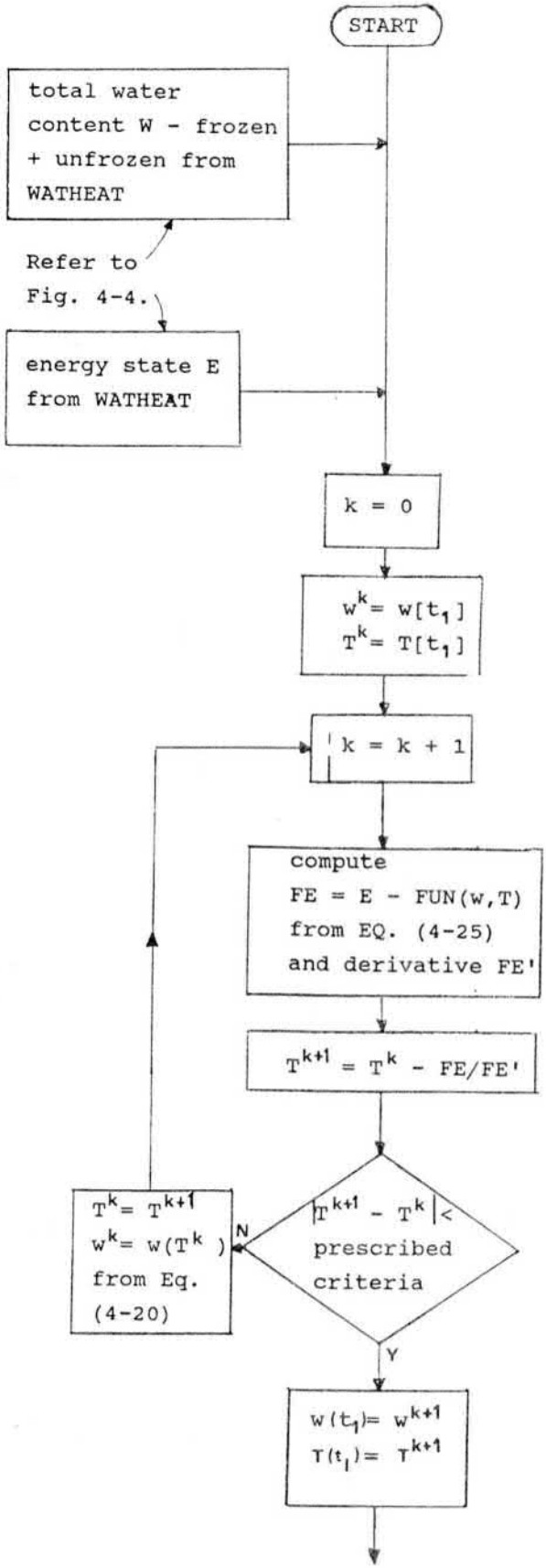

Fig. 4-2. Simplified flowchart of the algorithm ENERGY for computation of unfrozen water content and soil temperature.

4.3.5 Numerical solution method

The proposed model solves the mass and energy balances using the finite element method. The actual solution procedure is completely analogous to that described in section 4.2 in connection with the solution of Richards' equation. The only major difference is the inclusion of the ice accumulation term in the mass balance equation.

The actual solution proceeds through a three-stage process.
1) Solve the mass balance equation assuming no change in the ice content (the total amount of water W is thus obtained).
2) Solve the heat balance equation neglecting the latent part. By solving the new temperature profile the amount of energy lost from the system can be calculated (i.e. the energy state E can be calculated).
3) Solve the actual unfrozen water content w and ice content I as described in Section 4.3.3.

Two possibilities exist when iterating during one time step. In the first version stages 1) and 2) are solved and after that w and I are solved without further iterations. In the second version stages 1)-3) are repeated iteratively until convergence is attained. In calculating the energy state the amount of latent heat generated during the time step is taken into account. The first version can be considered explicit with respect to the calculation of the energy state of the system. It is preferable when the simulation of long time intervals is needed.

4.3.6 Initial and boundary conditions

The initial state of the system must be known at time t= 0. This implies that either the soil moisture content or total hydraulic head (e.g. steady-state situation) must be given for each nodal point for the solution of the mass balance equation. Moreover, it is necessary to define the initial temperature profile.

Different types of boundary conditions can be used, depending on the available data. At the upper and lower boundary the boundary conditions of the mass balance equation have been described in section 4.2.3. The upper boundary condition for the heat equation is the measured soil surface temperature, or if this is not measured then the air temperature measured at the level of e.g. 2 m can be used. In the heat flow equation, prescribed temperature or zero heat-flow can be used as the lower boundary condition.

4.4 Modeling snow accumulation and snowmelt

In order to be applicable to Finnish conditions, a soil water model should also be capable of simulating winter and spring periods. Treatment of soil frost has already been given in section 4.3 and therefore the computation of snow dynamics is the main topic of this section. Treatment of snow is based on a combination of snow models presented by Kuusisto (1984) in Finland and Jansson and Halldin (1980) in Sweden.

A snow model must include a precipitation submodel involving the estimation of the form of precipitation and a correction of measured precipitation. The thermal quality of precipitation, Q_{rain} is calculated from air temperature:

$$Q_{rain} = \begin{cases} 0 & ; T_{air} \geq T_{max} \\ [T_{max}-T_{air}]/[T_{max}-T_{min}] & ; T_{min} < T_{air} < T_{max} \\ 1 & ; T_{air} \leq T_{min} \end{cases} \quad (4\text{-}26)$$

This function assumes all precipitation to be rain for air temperatures above T_{max} and to be snow for T_{air} below T_{min}. Between these limits proportions vary linearly. The amount of rain, P_r and snow, P_s are calculated from equations:

$$P_r = C_{rain} \cdot [1-Q_{rain}] \cdot P_m \quad (4\text{-}27a)$$

$$P_s = C_{snow} Q_{rain} \cdot P_m \quad (4\text{-}27b)$$

where C_{rain} and C_{snow} are the correction factors for rain and

snow, respectively and P_m is recorded precipitation. For Finnish conditions, a rain correction of 7% and a snow correction of 30% can be used in Finland (Kuusisto, 1986).

Due to the complexity of the energy balance approach, simplified snowmelt equations have been widely used. According to Kuusisto (1984), the role of variables other than temperature is rather small in the climatic conditions prevailing in Finland. The daily amount of snow melt , M_d, can be calculated by the equation:

$$M_d = K_m \cdot [T_{air} - T_{ref}] \qquad (4\text{-}28)$$

where K_m is degree-day factor ($mm \cdot °C^{-1} d^{-1}$), T_{air} is air temperature (°C) and T_{ref} is threshold temperature (°C). For open fields the degree-day factor is correlated with snow density as follows (Kuusisto, 1984):

$$K_m = 0.0196 \cdot d_{snow} - 2.39 \qquad (4\text{-}29)$$

where d_{snow} is snow density ($kg \cdot m^{-1}$). According to Kuusisto, the equation is strictly applicable within the density range 200 - 400 $kg \cdot m^{-1}$. At the extremes of this range, K_m values are 1.5 and 5.5 $mm \cdot °C^{-1} \cdot d^{-1}$.

Free water, S_{liq} , in the snow pack can be calculated as:

$$S_{liq} = S_{old} + P_r + M_d - M_f \qquad (4\text{-}30)$$

where S_{old} is free water remaining from the previous day and M_f the amount of refreezing estimated as:

$$M_f = K_f \cdot T_{air} \qquad (4\text{-}31)$$

where K_f is the refreezing efficiency ($mm \cdot °C^{-1} \cdot d^{-1}$). If the free water in the snowpack exceeds a given retention threshold, it will be released as infiltration, q_{snow}:

$$q_{snow} = \max[0,\ S_{liq} - S_{l,max}] \qquad (4\text{-}32)$$

and the remaining water will be:

$$S_{old} = S_{liq} - q_{snow} \qquad (4\text{-}33)$$

The retention capacity, $S_{l,max}$, is assumed to be a fixed fraction, f_{ret}, of the snow water equivalent, W_{snow}, i.e.:

$$S_{l,max} = f_{ret} \cdot W_{snow} \qquad (4\text{-}34)$$

According to Kuusisto (1984), f_{ret} is about 11-15% by weight.

In the simulation of the winter period, the temperature at the soil surface is needed as an upper boundary condition for the heat balance equation. For periods with snow cover, the soil surface temperature is given by the presumption of steady state heat flow between the soil and the snow pack, which is assumed to be homogenous. The same approximation has been used in the SOIL-model (Jansson and Halldin 1980). To be able to estimate the temperature at the soil surface, the depth and density of snowcover has to be calculated.

Perfectly frozen precipitation is assumed to have a minimum density, d_{smin}, which is about 100 $kg \cdot m^{-1}$. For mixed precipitation, the density of precipitation, d_{prec}, depends on the thermal quality of the rain, Q_{rain} :

$$d_{prec} = d_{smin} + [d_w - d_{smin}]\ [1 - Q_{rain}] \qquad (4\text{-}35)$$

Depth of precipitation, Z_{prec}, follows from (4-35):

$$Z_{prec} = [P_r + P_s]/d_{prec} \qquad (4\text{-}36)$$

The weighted density of the snow pack, d_{snow}, is calculated from the equation:

$$d_{snow} = [d_{prec} \cdot Z_{prec} + d_{old} \cdot Z_{old}]/Z_{snow} \quad (4\text{-}37)$$

where d_{old} is the density of the old snow pack, Z_{old} is the depth of the snow pack in the previous day and Z_{snow} is the depth of the total snow pack ($=Z_{old} + Z_{prec}$). The density of the old snow pack increases with the relative amount of free water in the pack and with overburden pressure, i.e. with increasing water equivalent. The density of the old snowpack, d_{old}, is calculated as follows (Jansson and Halldin 1980):

$$d_{old} = d_{smin} + S_w \cdot [S_a / S_{l,max}] + S_a \cdot W_{old} \quad (4\text{-}38)$$

where S_w and S_a are parameter values, for which Jansson and Halldin have given values 200 ($kg \cdot m^{-3}$) and 0.5 (m^{-1}), respectively. W_{old} is the water equivalent of snow from the previous day. The depth of the old snow pack is given by definition as:

$$Z_{old} = W_{old} / d_{old} \quad (4\text{-}39)$$

When the depth of snow cover has been calculated, the the soil surface temperature can be estimated by equating two energy fluxes:

1° Steady state flux between the soil surface and air, i.e. through the snow pack

2° Steady state flux between the first nodal point below the soil surface and the soil surface.

$$K_{snow} \frac{T_{air} - T_{surf}}{Z_{snow}} = K_{soil} \frac{T_{surf} - T_{old}}{L_1} \quad (4\text{-}40)$$

where K_{snow} is the thermal conductivity of snow ($W \cdot m^{-1} \cdot °C^{-1}$), K_{soil} is the thermal conductivity of the soil, T_{surf} is the unknown soil surface temperature (°C), T_{old} is the calculated temperature of the second nodal point from the previous time step (explicit approximation) and L_1 is the length of the first element (the numbering is started from the soil surface). T_{surf}

is the temperature used as an upper boundary condition in the heat balance equation and T_{surf} can be solved from (4-40):

$$T_{surf} = \frac{T_{old} + w_{surf} \cdot T_{air}}{1 + w_{surf}} \qquad (4\text{-}41a)$$

$$w_{surf} = \frac{K_{snow} L_l}{K_{soil} \cdot Z_{snow}} \qquad (4\text{-}41b)$$

Thermal conductivity of snow is strongly dependent on density and the formula suggested is (Corps of Engineers 1956):

$$K_{snow} = S_K \cdot d_{snow} \qquad (4\text{-}42)$$

where parameter S_K has a value of 2.86E-06 $\cdot [W \cdot m^{-1} \cdot {}^{\circ}C^{-1} \cdot m^{-3} \cdot kg\ ]$.

Simplified flowchart of the algorithm SNOWMOD for computation of the snow accumulation, the snowmelt and the soil surface temperature is given in Fig. 4-3.

4.5 Testing of the proposed models

The purpose of this section is to present the main computer algorithm and evaluate the performance of the proposed models. This evaluation will be made by comparing the numerical solutions with solutions obtained either analytically (examples 1 and 4) or numerically with some carefully tested models (example 2). Moreover, the predictive capabilities of the model are examined by simulation of both laboratory and field experiments published in the literature (examples 3, 5, and 6). The applicability of the simplified Kalman filtering technique in the estimation of thermal conductivity has been tested in section 4.5.7.

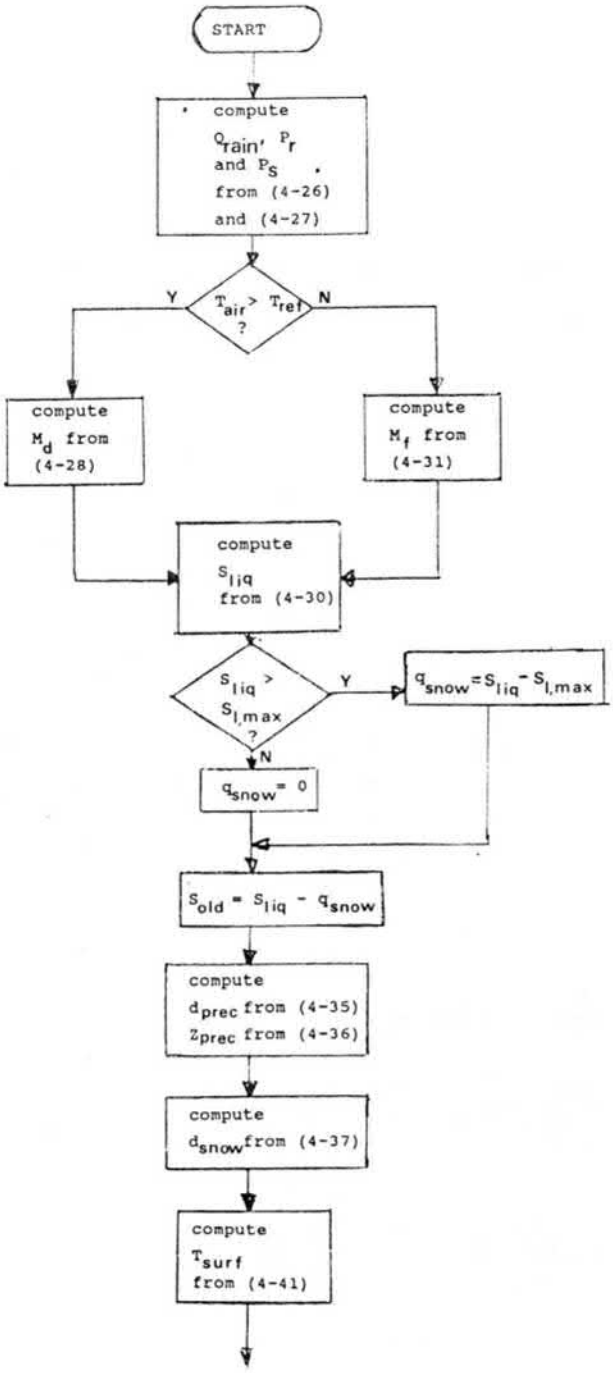

Fig. 4-3. Simplified flowchart of the algorithm SNOWMOD for computation of snow dynamics and upper boundary condition of the heat balance equation.

In evaluating the performance of the proposed models, the main criterion is the ability of the model to reproduce the measured values or results computed by another model. The test examples have been chosen so that the proposed models will be tested in different types of problems. However, the test examples presented in this section do not include the sink term (the determination of the sink term will be discussed in Chapter 5). The one-dimensional mass balance model is tested in examples 1, 2 and 3. The testing of the heat balance model is the topic of examples 4 and 5. The computation of combined mass and heat transfer in partly frozen soil is described in the sixth example.

4.5.1 The main computer algorithm and input data requirements

The numerical procedures developed in the previous sections are converted to computer codes in the form of the main algorithm WATHEAT and several auxiliary procedures. Fig. 4-4 illustrates a simplified flowchart of the algorithm WATHEAT. The auxiliary procedures used by the main algorithm are CONDUC, KALMAN, ENERGY, SNOWMOD, EVAPO and YIELD. CONDUC is used for the estimation of the unsaturated hydraulic conductivity function. KALMAN is the procedure utilizing the simplified Kalman filter for the determination of unknown parameters. ENERGY is the algorithm for the computation of the unfrozen water content and the soil temperature if the total water content W and the energy state E are known. SNOWMOD is responsible for the calculation of the snow dynamics and upper boundary condition of the heat balance equation. YIELD is the procedure for the computation of the daily actual and potential growth rate, and EVAPO is used in the computation of the potential transpiration and maximum possible soil evaporation rate. Algorithms EVAPO and YIELD are described in Chapter 5.

The mathematical models presented operate on the basis of the data listed below:

- rainfall and air temperature
- meteorological data needed for prediction of potential transpiration and soil evaporation rates

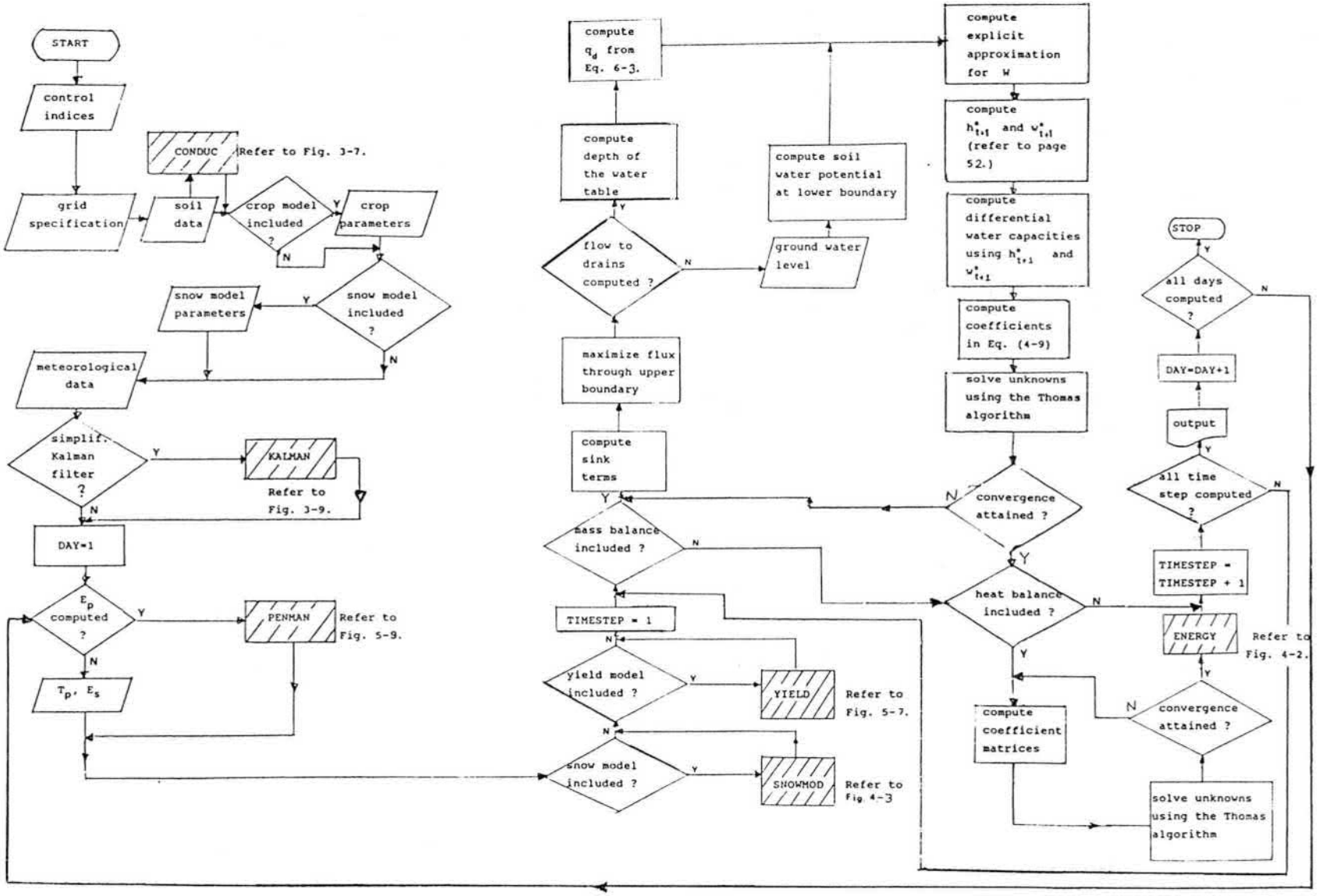

Fig. 4-4. A simplified flowchart of the main algorithm WATHEAT for computation of the combined mass and heat balance.

- soil layering
- soil properties for each soil layer (soil water retention curve, hydraulic conductivity function, thermal properties of the soil)
- the lower boundary condition for mass balance equation (prescribed variation in level of phreatic surface or parameters needed to calculate the flux through the bottom of the system) and for heat transfer equation

The following information can be obtained as output dat:
- infiltration and surface runoff
- soil moisture contents at specific depths
- soil-water pressure heads at specific depths
- flux through the bottom of the system (e.g. to drains)
- actual soil evaporation
- actual transpiration

In the one-dimensional case the mass and heat balance equations can be solved either together or separately. The latter implies that it is possible to solve only the mass balance equation assuming no change in the soil temperature or it is possible to calculate only the soil temperatures (soil moisture profile remains unchanged).

4.5.2 Test example 1 - Philip's quasi-analytical solution

One of the classical tests of the performance of a soil moisture flow model is for infiltration into a vertical semi-infinite column of Yolo light clay for which Philip (1957a and 1957b) has given a quasi-analytical solution. The problem represents a case where the initial moisture content is not very low. In the problem to be considered, the initial and boundary conditions are as follows:

$$t = 0,\ z > 0 \quad : w_0 = 0.2376,\quad h_0 = -600 \text{ cm}$$
$$t > 0,\ z = 0 \quad : w_{1n} = 0.4950 \ ,\quad h_{1n} = 0 \qquad (4\text{-}43)$$

where w_0 is the initial water content and h_0 the corresponding soil-water pressure head and w_{1n} is the boundary condition at the soil surface (prescribed pressure head node). (4-43) implies that the soil surface is assumed to remain saturated through the whole calculation period. The soil moisture retention curve and the hydraulic conductivity function can be given in a functional form (Jensen, 1983):

$$w(h) = \begin{cases} 0.124 + \dfrac{274.2}{739.0 + [\ln(-h)]^4}, & h < -1 \text{ cm} \\ 0.4950, & h \geq -1 \text{ cm} \end{cases} \qquad (4\text{-}44)$$

$$K(h) = \begin{cases} \dfrac{5.508}{124.6 + (-h)^{1.77}} \text{ cm} \cdot h^{-1}, & h < -1 \text{ cm} \\ 0.04428 \text{ cm} \cdot h^{-1}, & h \geq -1 \text{ cm} \end{cases} \qquad (4\text{-}45)$$

The finite element network is composed of a total of 30 elements so that the length of the first 10 elements (from the surface) is 1 cm, the length of the next 10 is 2 cm and the length of the last 10 is 3 cm. The numerical and quasi-analytical solutions are shown in Figs. 4-5 and 4-6 in terms of moisture contents versus depth and cumulative infiltration. The time step used in the calculations is 6 minutes.

The accordance between the numerical and quasi-analytical solution is very good. The calculation of infiltration is independent of the water balance computations. Hence it is possible to calculate the accuracy of the mass balance. Here the error is the difference between the change in total water content and the cumulative infiltration; according to the results this difference is less than 0.01%.

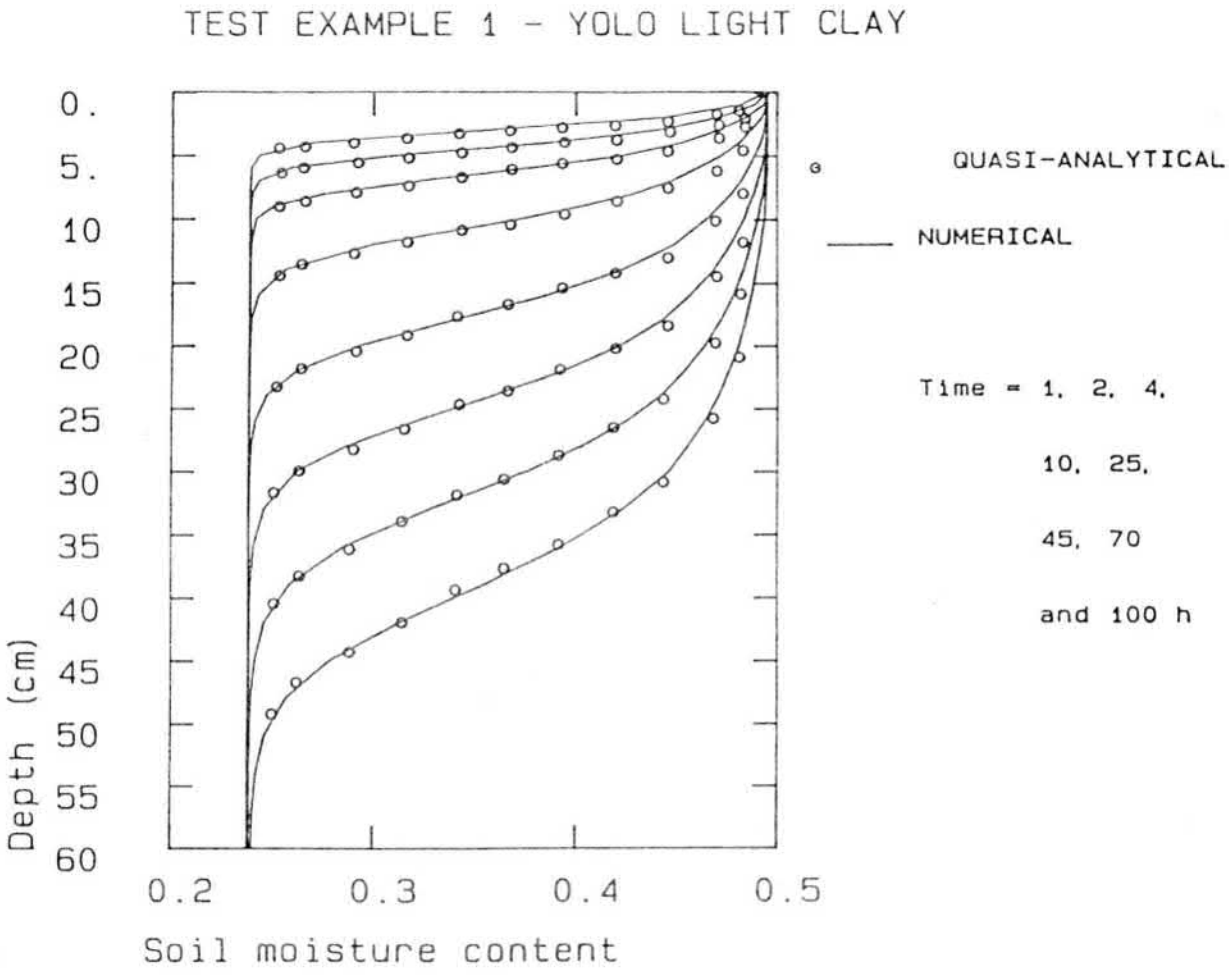

Fig. 4-5 Soil moisture profile in test example 1.

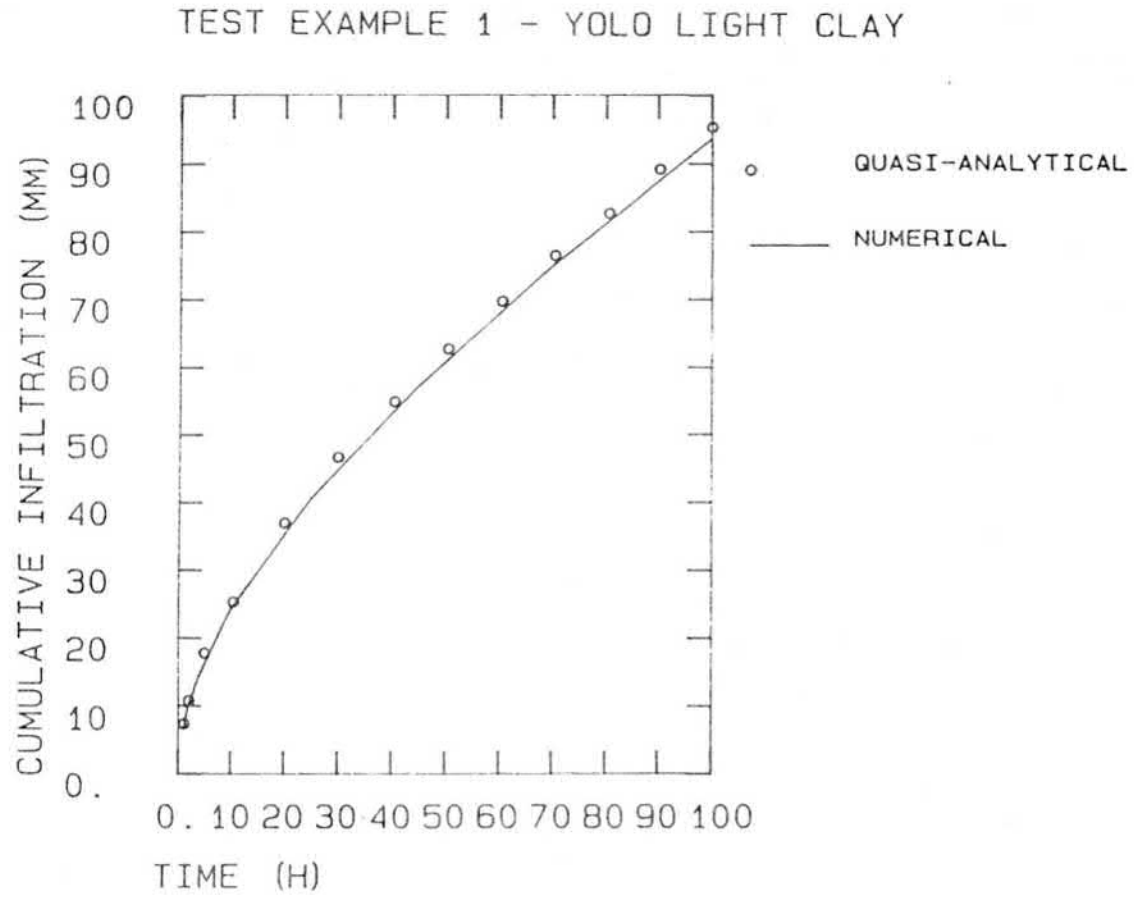

Fig. 4-6. Cumulative infiltration.

However, the space discretization used in the former test is very dense, and such a refinement is not appropriate in field applications because the computing time increases as the number of elements increases. Hence, to evaluate the effect of the size of the elements on the numerical solution, another space discretization is used. The length of each element is 5 cm with the exception of the first two elements (2 and 3 cm). In the second discretization the total number of nodal points is only 14 compared with 31 in the first discretization. According to the numerical solution (time step = 6 min) shown in Figs. 4-7 and 4-8, there is a discrepancy between the computed and Philip's solution at the beginning of the calculation. However, it appears that the numerical solution becomes progressively more accurate after some time, as the moisture front is not so abrupt as in the beginning.

In order to see the effect of uncertainty in the saturated hydraulic conductivity on the calculated moisture profile, the problem is solved using a K_S-value, which is 20% greater than the true one. The space discretization is the denser one and the time step in the computations is 6 minutes. According to the results presented in Fig. 4-9, the effect of the 20% deviation in the saturated conductivity value has a very pronounced effect on the estimated moisture content at different depths. The error of the numerical solution is negligible compared with the relatively small error in the saturated K_S-value.

4.5.3 Test example 2 - infiltration into a very dry soil

The purpose of test example 2 is twofold. First, it represents a case where the potential infiltration is known a priori, but must be calculated by maximizing the flow through the upper boundary. Second, it is a very good test example because the soil is initially very dry and the corresponding pressure head is extremely low. This is the situation usually encountered in the calculation of infiltration into a frozen soil. Moreover, test problem 2 is a very severe test to any soil water model.

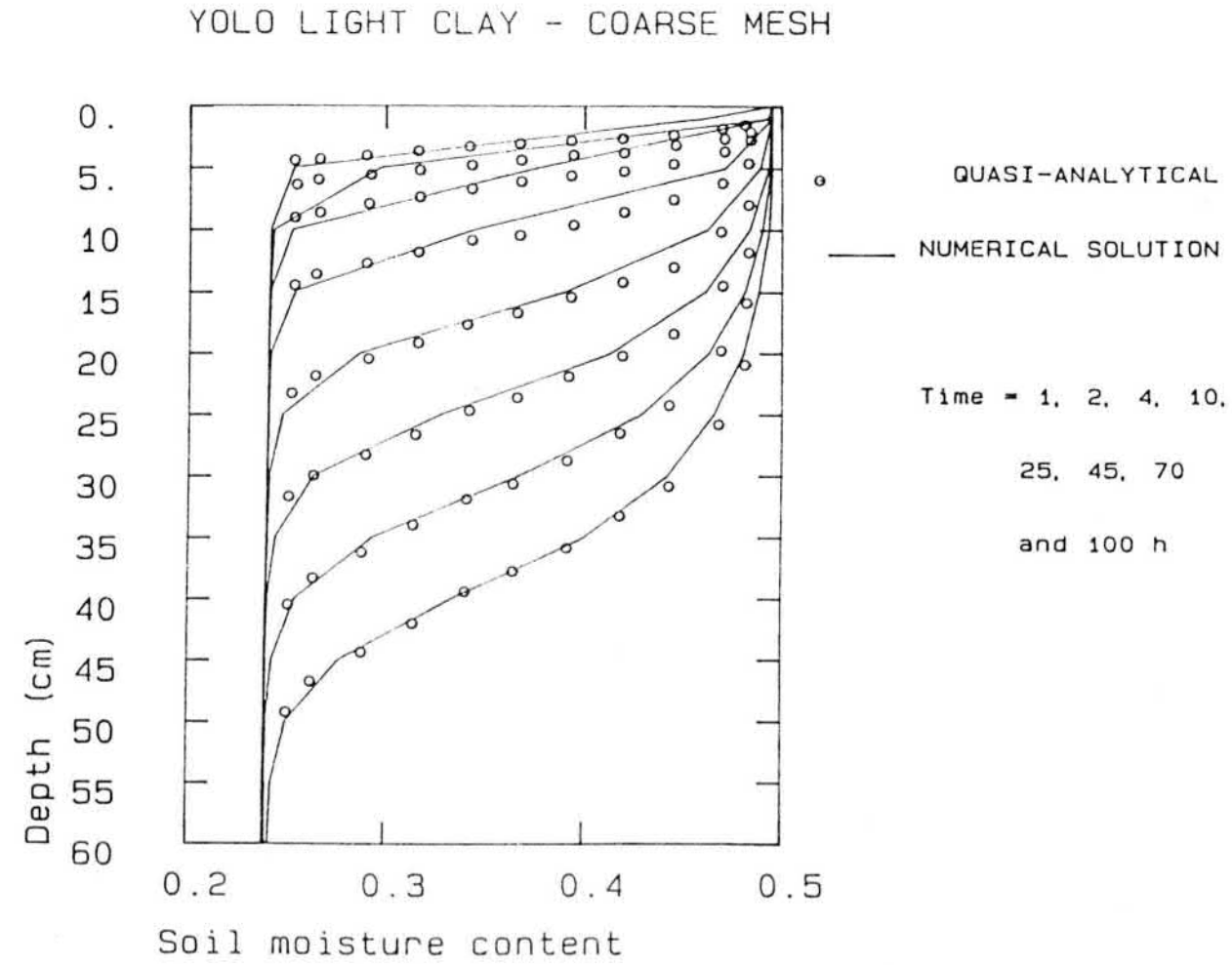

Fig. 4-7. Soil moisture profile (coarse mesh).

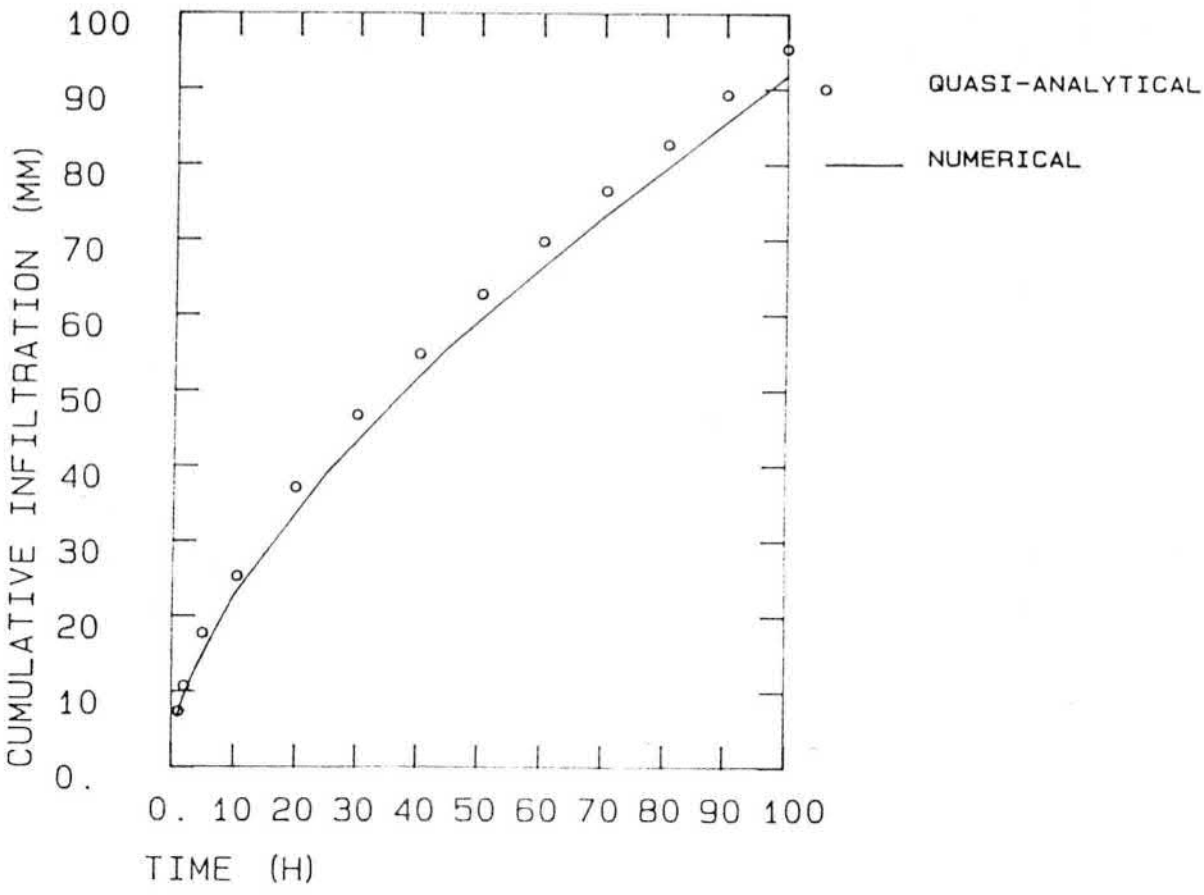

Fig. 4-8. Cumulative infiltration (coarse mesh).

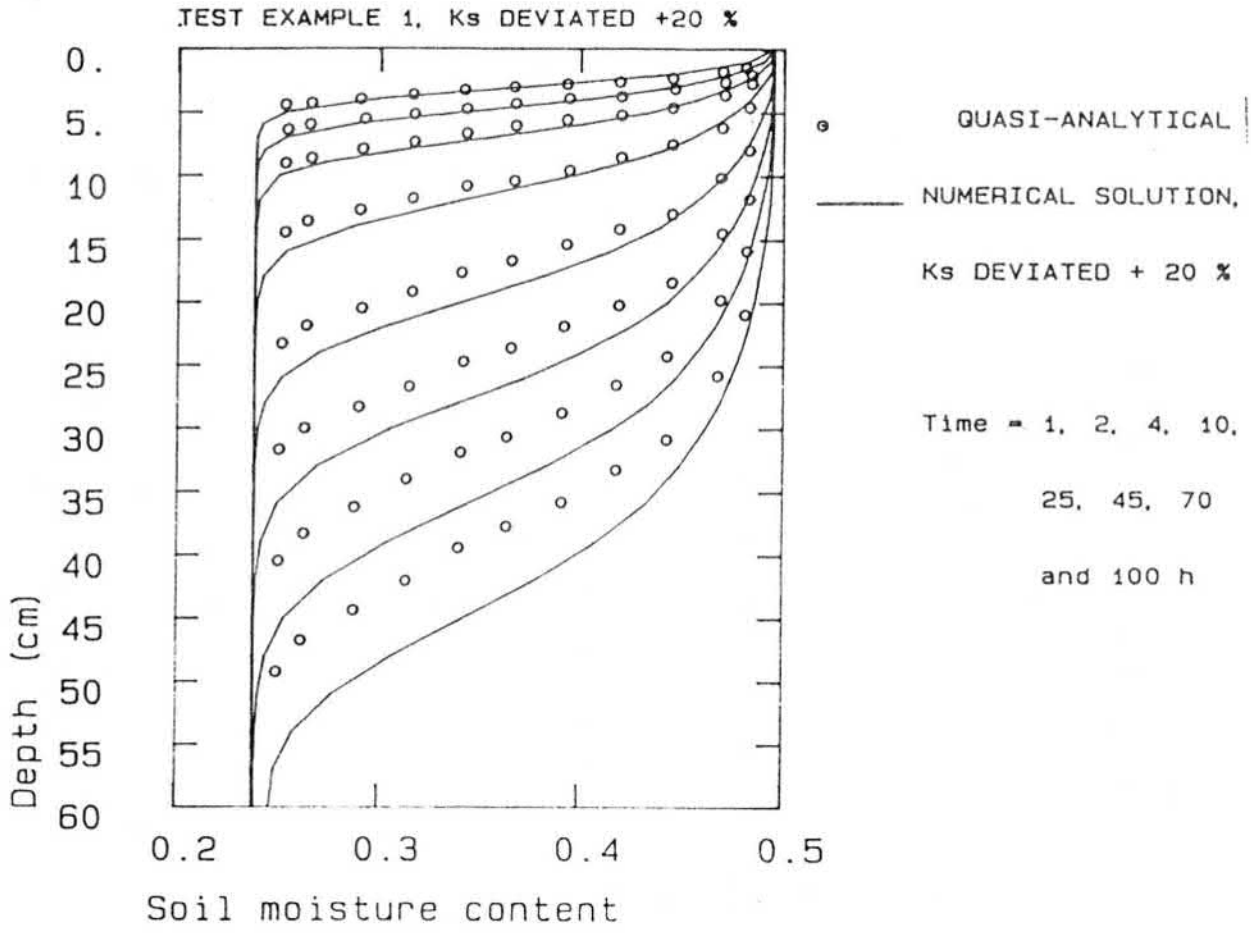

Fig. 4-9. Soil moisture profile in test example 1. Saturated hydraulic conductivity deviated 20 % from its true value.

The infiltration problem reported in the literature (Rubin and Steinhardt 1963; Neumann 1972, ref. Abbott et al. 1982) is the test example. The soil properties can be given the characteristic curve representation in the range of interest.

$$h = -(11.3+3.19/w-0.05\cdot\exp(15\cdot w)+\exp(16.3-575\cdot w) \quad \text{(cm)} \quad (4\text{-}46)$$

$$K(h) = 8400/[(-h)^5 + 14.45^5] \ \text{cm}\cdot\text{s}^{-1} \quad (4\text{-}47)$$

The values of w_s and K_s at saturation are w_s=0.397 and K_s=0.0133 $\text{cm}\cdot\text{s}^{-1}$. The initial moisture content is uniformly low and equal to w=0.005, corresponding to a pressure head value - 677 000 cm. Starting at time t=0, a constant rate of infiltration q_{pot}=0.0003528 $\text{cm}\cdot\text{s}^{-1}$ is imposed at the soil surface. The problem consists of predicting the wetting front advances and

how the moisture content varies with time at each point in the soil.

The numerical solution of the proposed model is compared with the solution presented by Neumann (1972). The finite element mesh is composed of 30 elements. Near the surface the length of the elements is 1 cm and at the bottom of the 100 cm profile the element length is 10 cm. The time step used in the calculations is 1 minute. The soil moisture profiles are shown in Fig. 4-10. The proposed model produces a considerable diffusion type numerical error at the leading edge. However, this is natural due to the initially very dry soil. In the calculations it was necessary to use a fully implicit approximation in order to produce a stable solution. Moreover, the coefficients had to be evaluated at half the time step to dampen unwanted oscillations (see Neuman et al. 1974), i.e. to under-relax the system.

The original paper by Neumann (1972) was not available, but according to Abbott et al. the numerical solution of Neuman is a very sophisticated one. It is probable that the test example represents a case in which the flow of water in vapour form has a significant effect on the moisture distribution. Moreover, as pointed out by Jensen (1983), deviations from the theory behind Richards' equation have been observed at low flow velocities where the flux increases more than proportionally with the gradient. Hence, the moisture profile calculated using the proposed model is somewhat too dry throughout the period.

4.5.4 Test example 3 - a gravity drainage problem

It is desirable to have a method for predicting transient flow of water in a porous medium that is partly saturated and partly unsaturated. Two theories exist that describe flow through saturated-unsaturated soil. One theory admits a fundamental difference between flow in the saturated zone and in the unsaturated zone. In this theory, the saturated-unsaturated interface constitutes an internal moving boundary. An alternate

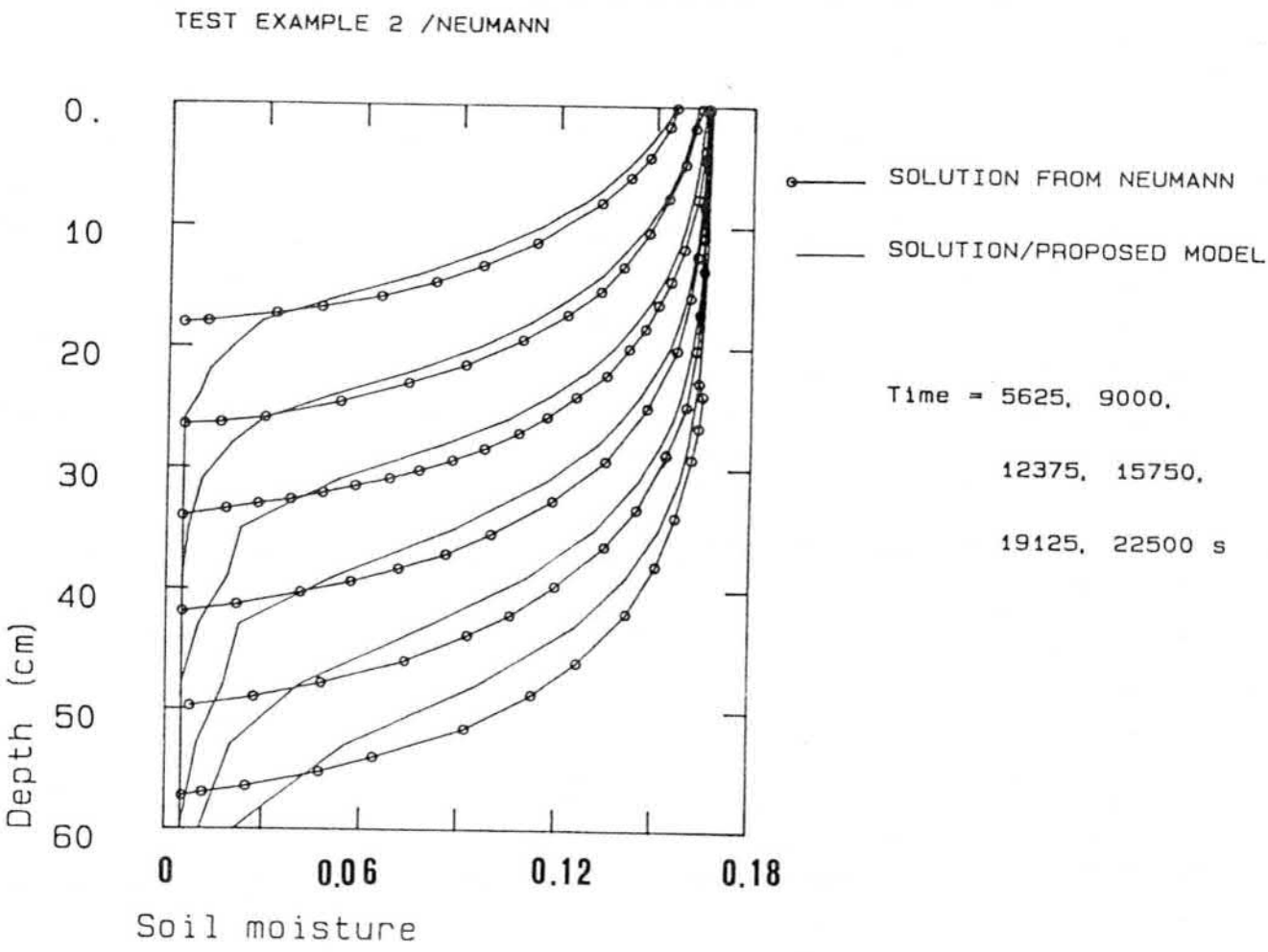

Fig. 4-10. Test example 2 - computed moisture content profiles.

theory proposes that the flow exhibit sufficient continuity so that it is mathematically unnecessary to differentiate between the saturated and unsaturated zone. In most of the models presented in the literature, the second of the theories given above has been accepted. As described earlier in section 4.2 the second theory has been used in the proposed model. A slight compressibility of the soil is allowed to prevent the case in which the coefficient of the time derivative in equation (4-1) would be equal to zero.

The main purpose of test example 3 is to discuss the capability of the model to predict the soil moisture profile in a case when the location of groundwater level is not given as an input, but must be calculated. The system used in the testing is gravity drainage of a vertical soil column (Watson 1967, ref. Hornberger and Remson 1970). The physical system consists of a vertical column of Botany sand, 57 cm long, which is initially saturated. The column is allowed to drain under the influence of gravity and the top of the column is assumed to be impermeable.

The relationship between water content w and pressure head h is given in Fig. 4-11 and between w and hydraulic conductivity K(w) as a function of water content w is given by:

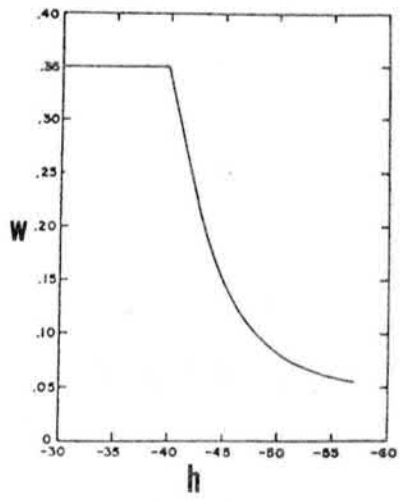

Fig. 4-11. The relationship between moisture content w and pressure head h (cm) for Botany sand (taken from Watson, 1967).

$$K(w) = 0.37 \cdot w^2 - 0.096 \cdot w + 0.00687 \ (cm \cdot s^{-1}) \quad (4\text{-}48)$$

Since the lower boundary is in direct contact with the atmosphere, the pressure head at the bottom of the system must be equal to zero, i.e. the prescribed pressure head is used as the lower boundary condition and the corresponding flux through the bottom of the system is calculated. The time step used in

the calculation is 30 s and the total time period computed is 20 minutes. Two different element mesh were tested (1 cm elements and 3 cm elements) and the results were almost the same (see Fig. 4-12). The computed results agree very well with the measured ones.

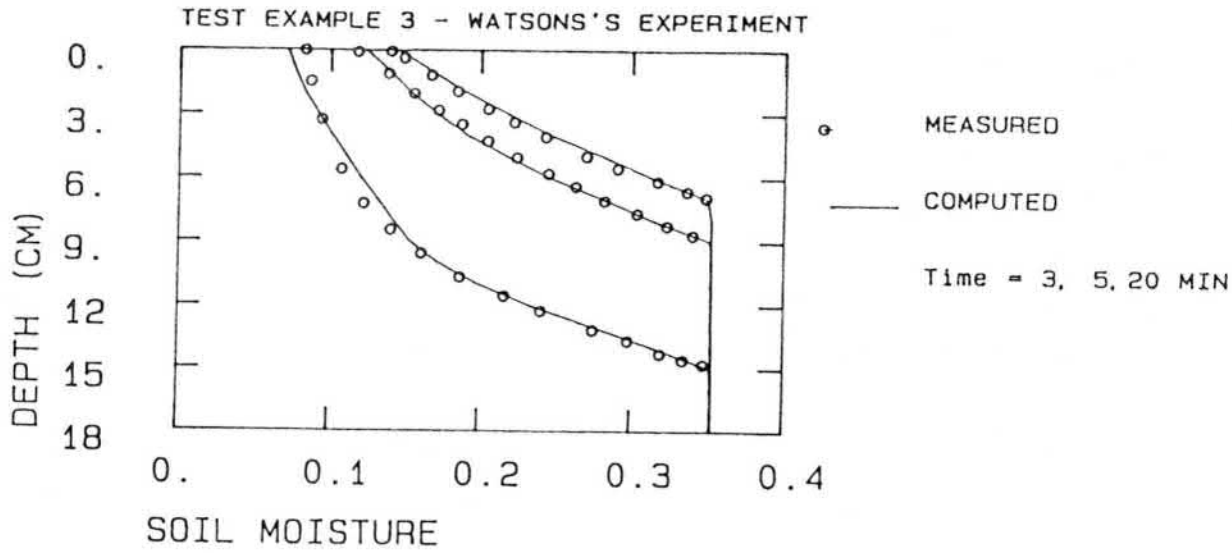

Fig. 4-12. Moisture content w versus depth below the top of the column as determined experimentally by Watson (1967) and as computed with the proposed model.

4.5.5 Test example 4 - comparison with an analytical solution for heat wave propagation

The purpose of this example is to compare the calculated soil temperature values with the results obtained from an analytical solution, assuming no change in the soil moisture content. A case is selected in which the average temperature in soil is 25 °C with oscillation aplitude of 20 °C on diurnal basis. The upper boundary condition is given by (e.g. Wierenga et al. 1969):

$$T_a = T_{av} + T_{amp} \cdot \sin(FII \cdot t) \qquad (4\text{-}49)$$

where T_a, T_{av} and T_{amp} are actual surface temperature, average soil temperature and amplitude of the temperature (°C), respectively and FII is the angular frequency (=2π /86400) for diurnal variations. With equation (4-49) as a boundary condition, an analytical solution can be derived to predict soil temperature at any depth (z) and time (t) (Carslaw and Jaeger 1959, ref. Wierenga et al. 1969):

$$T(z,t)=T_{av} + T_{amp}\cdot\exp(-z\sqrt{FII/2D_a})\ \sin(FII\cdot t- z\sqrt{FII/2D_a}) \quad (4\text{-}50)$$

where D_a is the apparent thermal diffusivity defined as a ratio $K_T(w)/C_s$ (thermal conductivity divided by volumetric heat capacity). In this case, D_a = 422 $cm\cdot d^{-1}$ and C_s = 1.072 $J\cdot cm^{-3}\cdot °C^{-1}$.

The comparison in Fig. 4-13 between the numerical and analytical solution at various depths indicates excellent agreement.

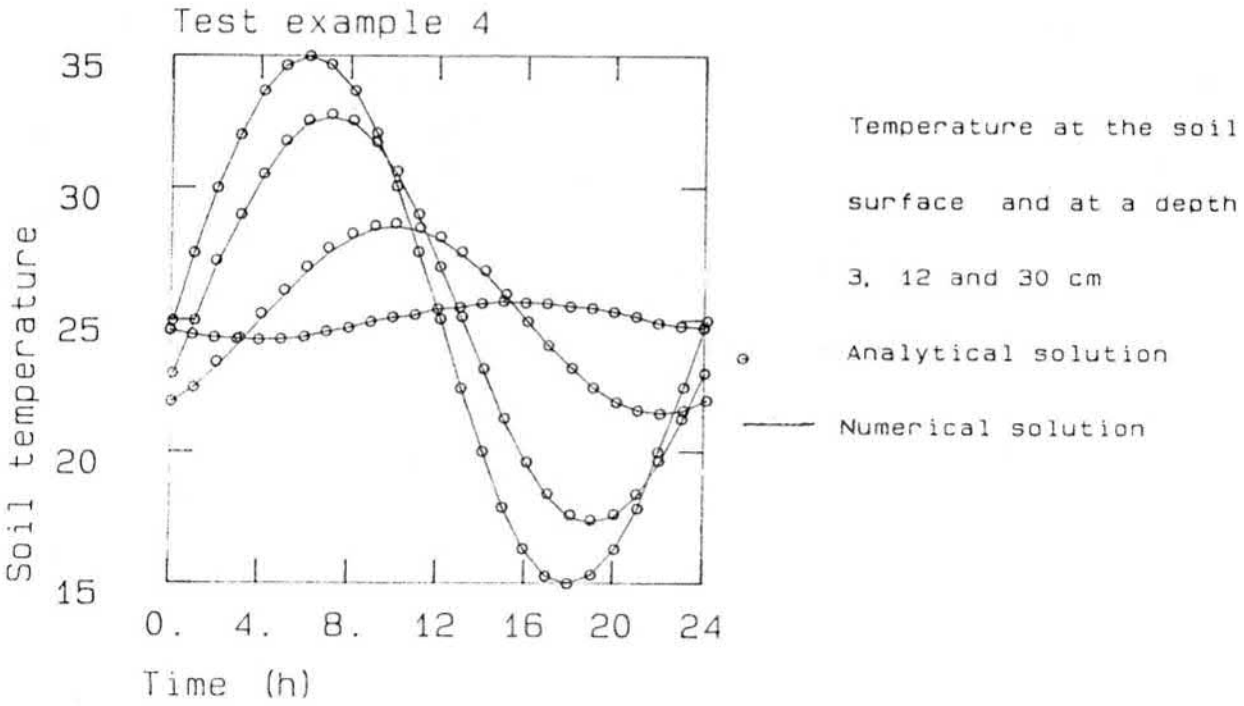

Fig. 4-13. Comparison between a numerical and analytical solution for test example 4.

4.5.6 Test example 5 - comparison with experimental data

In this example, the capability of the proposed heat balance model to produce a reliable prediction of soil temperature is tested using the field data of Hanks et al. (1972). In this problem the soil moisture content is again assumed to be constant and the soil thermal properties ($K_T(w)$ and C_s) are functions of moisture content according to equations (4-51) and (4-52) (Hanks et al. 1972):

$$C_s = 1.003 + 4.18 \cdot w \qquad (J \cdot cm^{-1} \cdot {}^{\circ}C^{-1}) \quad (4\text{-}51)$$

$$K_T(w) = 15.76 + 20.0\sqrt{w} \quad (J \cdot cm^{-1} \cdot h^{-1} \cdot {}^{\circ}C^{-1}) \quad (4\text{-}52)$$

In the original paper by Hanks et al. (1972) the thermal conductivity is given in a tabular form and equation (4-52) gives the best fit for the given data assuming that thermal conductivity can be represented with the simple equation shown in (4-52). This example will be analyzed in section 4.5.7 using the simplified Kalman filtering technique and therefore a functional form is chosen for the thermal conductivity. Temperature variations in the soil are given for a period of 24 hours, on an hourly basis. The measured soil temperature at a depth of 1 cm is used as the upper boundary condition and the temperature profile reported by Hanks et al. (1972) is used as the initial condition. The comparison is shown in Fig. 4-14, indicating a very good agreement between the measured and computed soil temperature.

4.5.7 Testing of the simplified Kalman filtering technique

In section 3.4 a new method for the determination of soil parameters using the simplified Kalman filtering algorithm was presented. In this section the aim is to find the soil thermal conductivity function of test example 5 using the method described in 3.4. Is is assumed that soil thermal conductivity is a function of soil moisture content and the functional form is as follows:

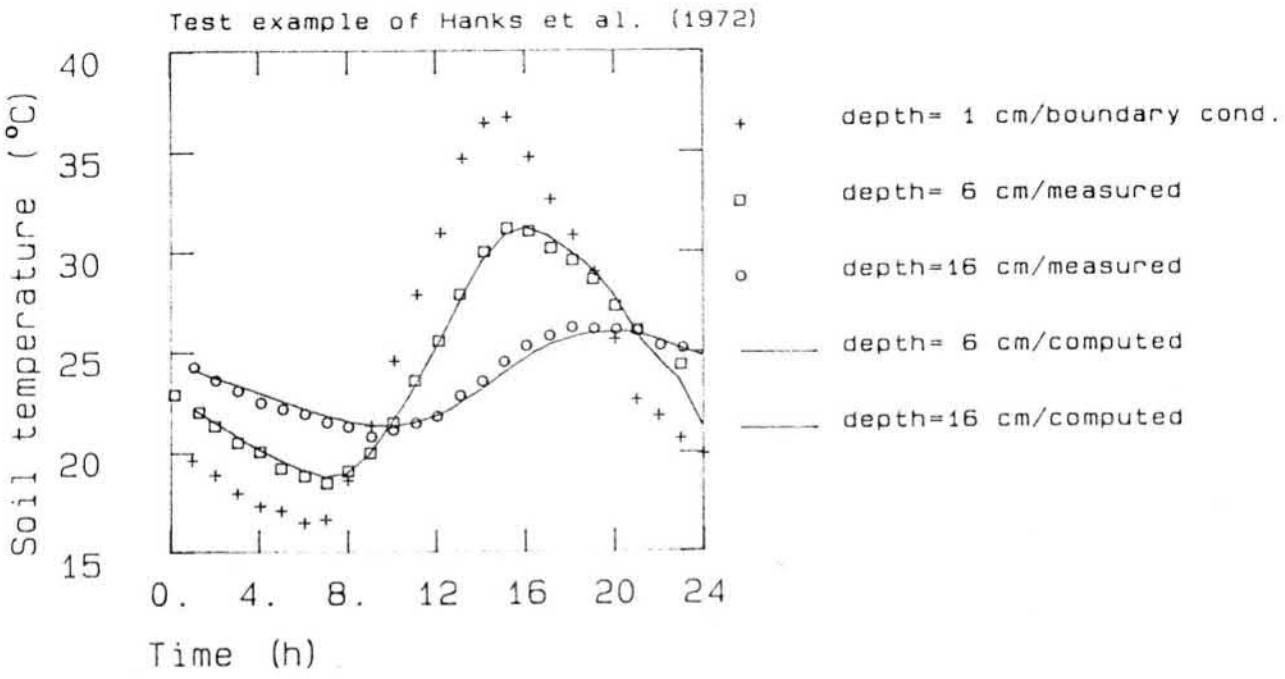

Fig. 4-14. Comparison of the computed soil temperature with the experimental data by Hanks et al. (1972).

$$K_T(w) = a_{T1} + a_{T3} \cdot \sqrt{w} \qquad (4\text{-}53)$$

where $K_T(w)$ is thermal conductivity, w is water content and a_{T1} and a_{T3} are the parameters to be estimated. Based on the measurements of Hanks et al. (1972), the "true values" are as follows: a_{T1}=15.76 and a_{T3}=20.0, when the unit is $J \cdot cm^{-1} \cdot h^{-1} \cdot °C^{-1}$.

The initial values for a_{T1} and a_{T3} were 10.0 and 10.0, respectively. Period of 24 hours was used in the estimation procedure and the measurements were given on an hourly basis. The maximum allowed deviation between the computed and measured soil temperature was 0.5 °C and the estimation procedure finds for all 24 time periods a parameter combination that produces acceptable soil temperature prediction. Hence, it would be possible to have 24 different curves for soil thermal conductivity. However, a single curve is needed and in the next stage the parameter combinations obtained in the estimation procedure were used to generate individual points from the $w\text{-}K_T(w)$ curve. Using a random number generator, four different

soil moisture values were used to calculate the soil thermal conductivity from each of the 24 parameter combinations. Hence, 96 points were obtained and they were plotted as a function of soil moisture content (Fig. 4-15). The final estimated $w\text{-}K_T(w)$-curve is the one which gives the best fit to the individual points. The final curve is:

$$K_T(w) = 16.72 + 27.12 \sqrt{w} \ (J \cdot cm^{-1} \cdot h^{-1} \cdot {}^{\circ}C^{-1}) \qquad (4\text{-}54)$$

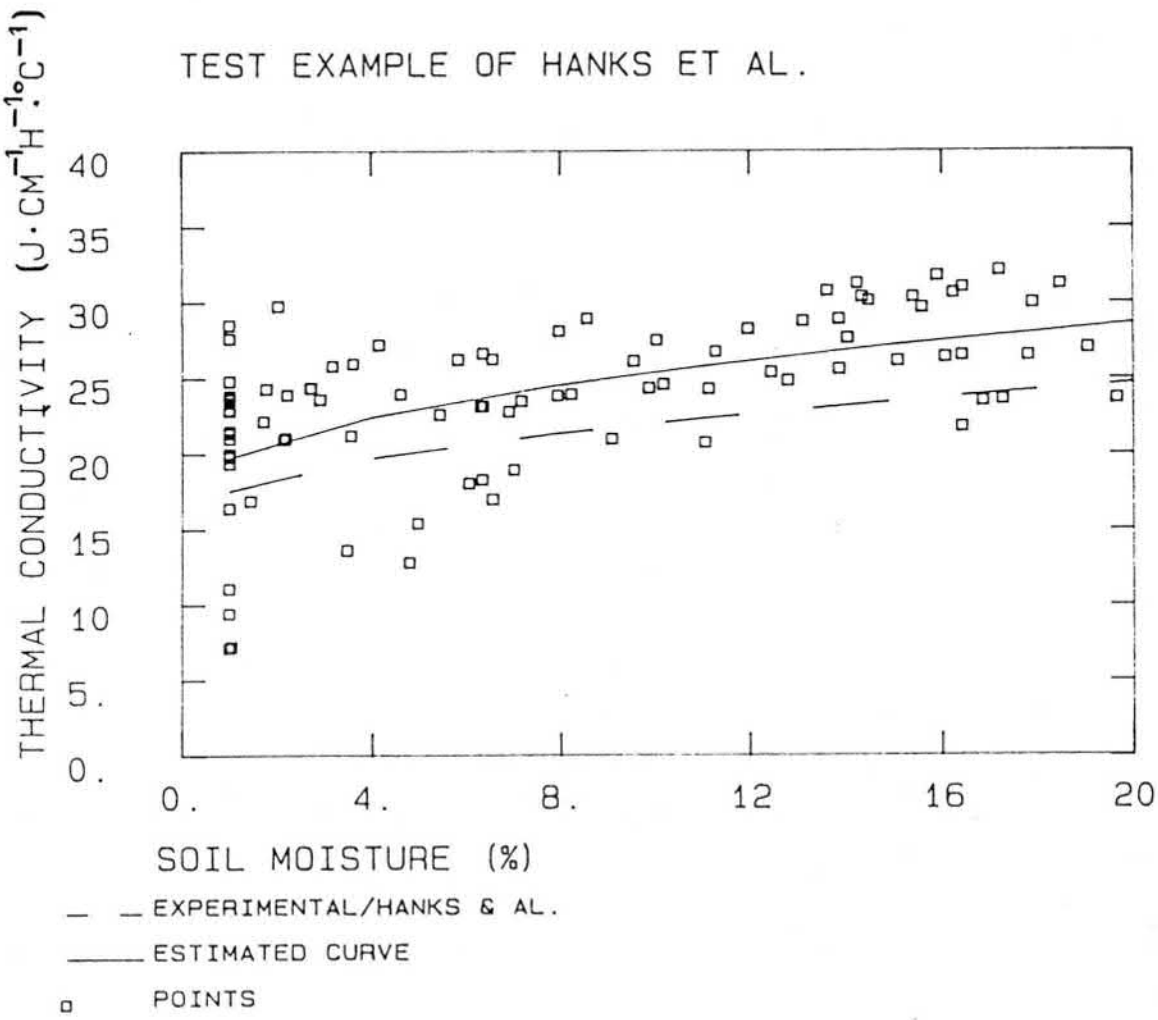

Fig. 4-15. Soil thermal conductivity as a function of soil moisture content.

where the moisture content w is given as a volumetric value. The estimated values are 6 - 13% greater than the curve measured by Hanks et al. (1972). However, using the estimated curve (4-54), the computed soil temperature is in slightly better agreement with the observations compared with the case when the original curve (4-52) was used (Fig. 4-16).

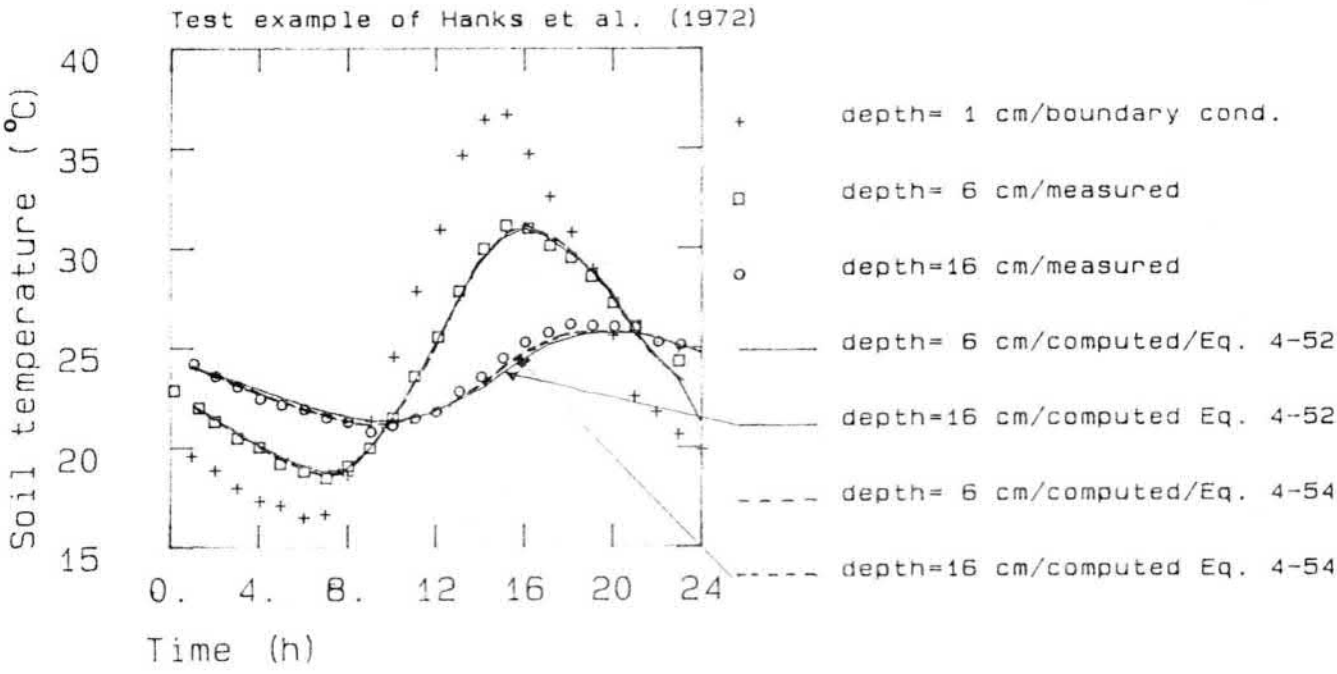

Fig. 4-16. Measured soil temperature (Hanks et al. 1972) and computed soil temperature using two different soil thermal conductivity functions.

4.5.8 Test example 6 - combined mass and heat transfer in partly frozen soil

The model is tested against the experiment carried out by Kalyuzhnyi et al. (1984). The column is 50 cm long and the measured temperature is given both as the upper and the lower boundary condition for the heat balance equation. For mass the balance equation, the upper boundary was a no-flow boundary. At the bottom of the system there was either a constant hydraulic head (case 1) or a zero- flux boundary condition (case 2). Changes in temperature and water content were measured during soil freezing. The soil moisture retention curve was estimated

from the measured steady state initial profile (average curve based on cases 1 and 2) and the extrapolation of the curve was carried out using the van Genuchten model (see equation (3-26)). The unsaturated hydraulic conductivity was estimated with the method described in section 3.3 (based on the theoretical model presented by Andersson (1971)). The thermal conductivity of the unfrozen soil was estimated with the method presented in section 3.4 and based on the soil temperature measurements during the first 48 hours (case 1). The effect of soil temperature on the hydraulic conductivity function must be taken into account if the soil is partly frozen or the temperature variations are pronounced. The hydraulic conductivity of a medium is directly proportional to the fluid density and inversely proportional to the viscosity of the percolating fluid. The variation in density of water with temperature is fairly small, while the temperature effect on viscosity is considerable (Ghali Sami Ghali, 1986). The following formulas can be used to quantify the effect of temperature on the hydraulic conductivity function (Ghali Sami Ghali, 1986):

$$K_{T,r} = K_{20} \frac{v_{20}}{v_T} \qquad (4\text{-}55a)$$

$$^{10}\log(v_T) = [1301/(998.333+8.1855\cdot(T-20)+ +.00585\cdot(T-20)^2] - 1.30233 \qquad (4\text{-}55b)$$

where $K_{T,r}$ and K_{20} are the relative conductivities at temperature T ($0<T<20$ °C) and at temperature 20 °C, respectively, v_T and v_{20} are the kinematic viscosity at temperatures T and 20 °C, respectively. Moreover, in the frozen zone the hydraulic conductivity must be reduced due to the presence of ice. According to e.g. Taylor and Luthin (1973) and Fukuda (1983), the unfrozen hydraulic conductivity had to be multiplied by a value from 0.001 to 0.01 in the frozen zone to produce reliable computations. A different approximation has been chosen in the presented model. The effect of ice on the hydraulic conductivity function is taken into account with the

formula proposed by Motovilov (1977, 1978 and 1979):

$$K_{I,r} = K_{0,r} \frac{1}{(1+c_k \cdot I)^2} \qquad (4\text{-}56)$$

where $K_{I,r}$ and $K_{0,r}$ are the relative conductivities at ice content I and in unfrozen soil, respectively, and c_k is a parameter with an average value equal to 8 according to Motovilov.

The objective of this test example is twofold. First, the applicability of the model to simulate soil freezing and freezing induced soil moisture redistribution is tested. Second, the sensitivity of the solution to small variations in the soil properties is evaluated.

In Fig. 4-17, the results from soil temperature and soil moisture calculations are shown for case 1 (Kalyuzhnyi et al. 1984). At the start, the temperature at the upper boundary was 5.6 °C. It was reduced to -4.3 °C in 48 hours, and then kept constant for 142 hours. It was then reduced to -8 °C over 24 hours and to -8.6 °C in 288 hours, after which it was lowered to -10.5 over 24 hours. The water content increased gradually in the layer between 6 and 16 cm during the first 190 hours, and later on at greater depths as well.

The measured and computed water content (ice + water) profiles at five times (48 h, 190 h, 214 h, 502 h and 526 h) are presented in Fig. 4-17. The measured and estimated initial profiles are also shown. The small deviation between the measured and predicted initial profile is due to the fact that the water retention curve had to be estimated from steady-state profiles. The computed and measured water contents are in good agreement with the exception of the last two times (502 h and 526 h) where the computed water content is greater in the layer between 25 and 35 cm. This is because the hydraulic

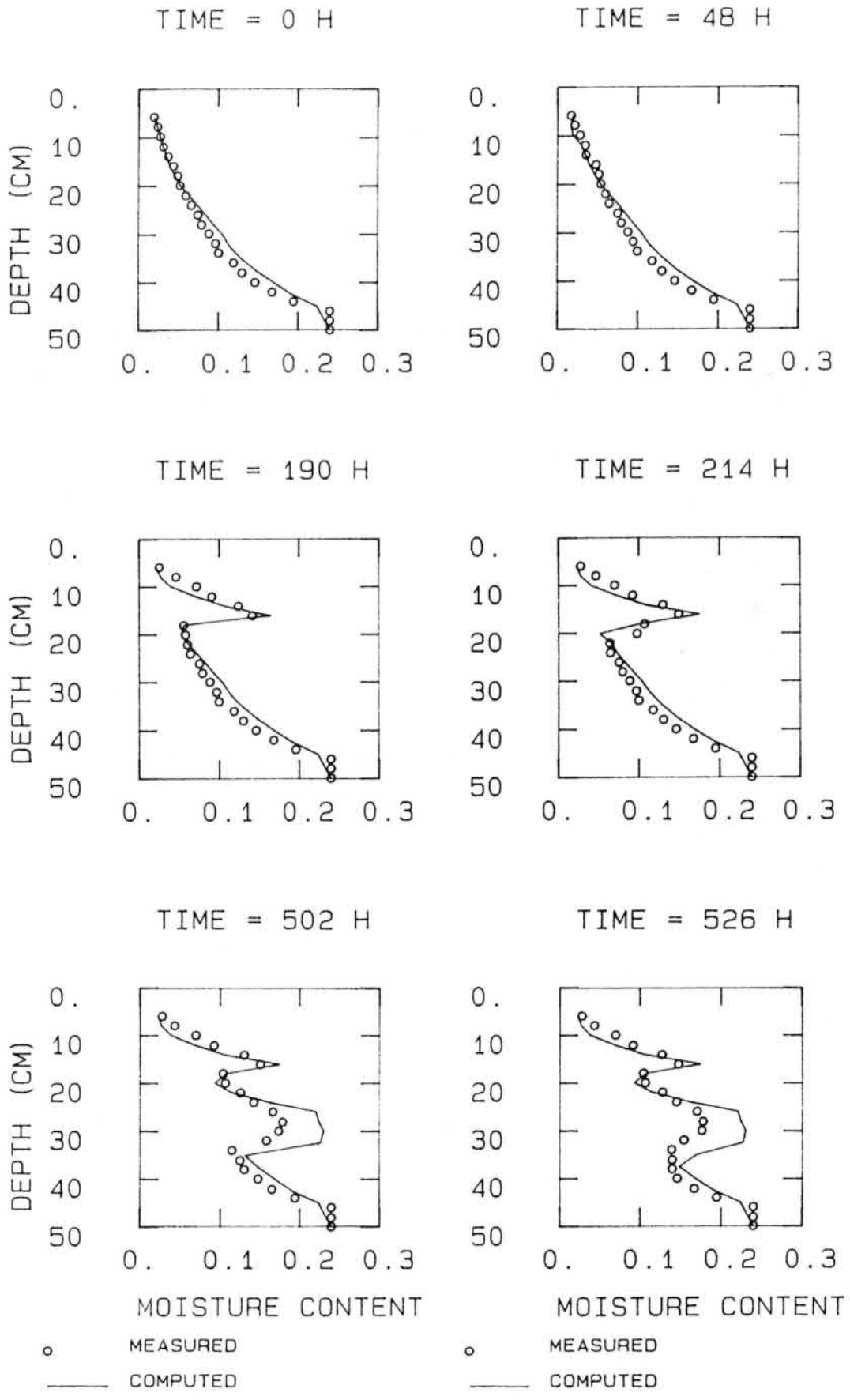

Fig. 4-17. Computed and measured water content profiles at discrete points of time (measured values taken from Kalyuzhnyi et al. 1984, computed by the model presented in section 4.3)

conductivity at pressure head values greater than -20 cm is overestimated as is the flow to the freezing zone. However, it is encouraging that the model is quite capable of predicting the overall shape of the water content profile.

Measured and computed soil temperature profiles are shown in Fig. 4-18. Especially at time t= 214 h and t= 526 h, the computed soil temperature is too low at a depth of 10 cm (about 1.2 and 1.6 °C too low). This is probably due to the fact that the unfrozen water content curve estimated from the soil water retention curve is not completely valid. The computed soil temperature at time t= 48 h is in very good agreement with the measured profile, indicating that the soil thermal conductivity function is accurate. The shape of this function was estimated with the simplified Kalman filtering technique (see section 3.4):

$$K_T(w) = 31.3 + 25.3 \cdot \sqrt{w} \ (J\ cm^{-1} \cdot h^{-1} \cdot {}^{\circ}C^{-1}) \qquad (4\text{-}57)$$

In frozen soil the soil thermal conductivity was assumed to be directly proportional to the ice content and since the thermal conductivity of ice is about four times greater than that of water, the thermal conductivity function K_{Tf} of frozen soil is in this case:

$$K_{Tf} = 31.3 + 25.3\sqrt{w} + 4 \cdot 25.3\sqrt{I} \ (J \cdot cm^{-1} \cdot h^{-1} \cdot {}^{\circ}C^{-1}) \qquad (4\text{-}58)$$

where w is the unfrozen water content and I is the frozen water content.

The sensitivity of the model to relatively small variations in the unsaturated hydraulic conductivity function was tested and the results are shown in Fig. 4-19. According to Fig. 4-19, a slight increase in the unsaturated hydraulic conductivity at low pressure head values has a very pronounced effect on the computed water content profile.

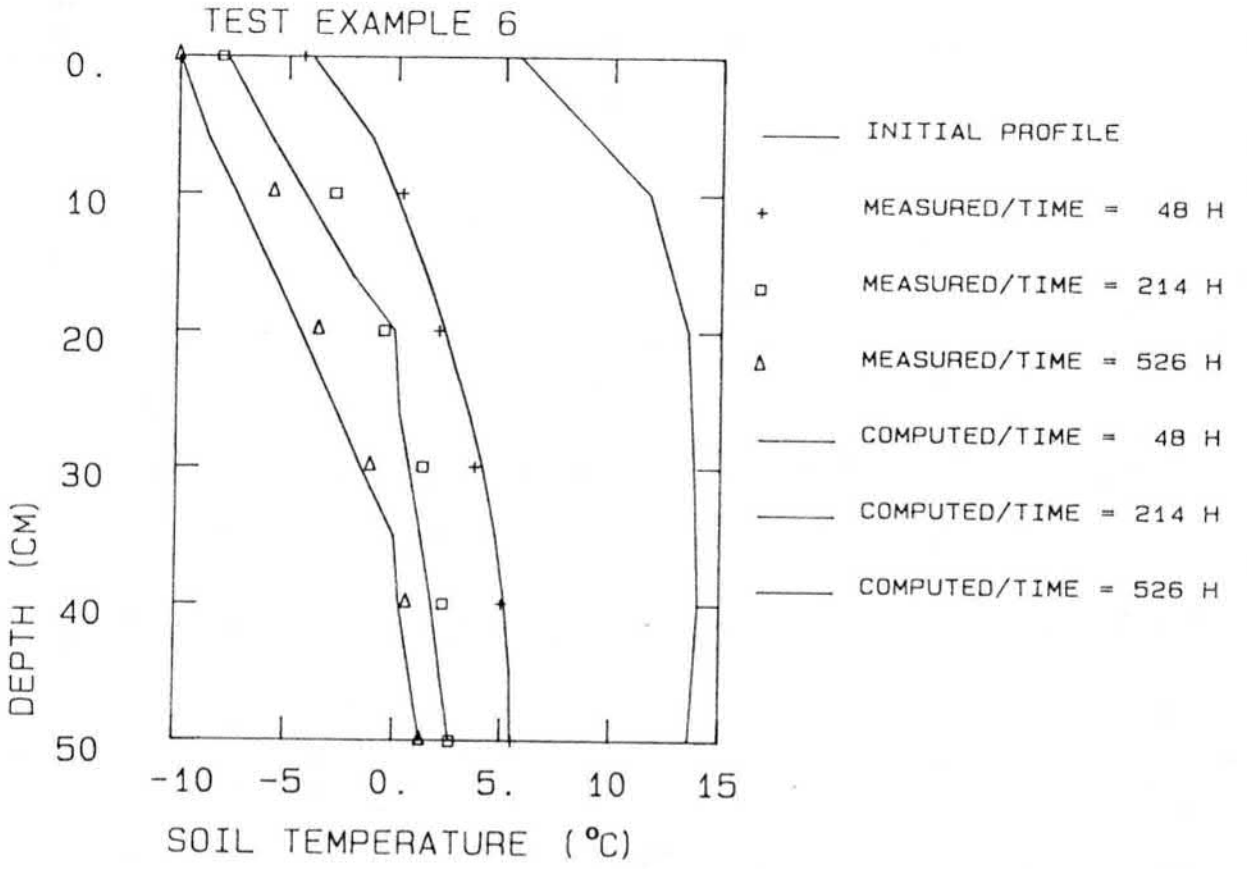

Fig. 4-18. Measured and computed soil temperature profile at discrete points of time(measured values taken from Kalyuzhnyi et al. 1984, computed by the model presented in section 4.3).

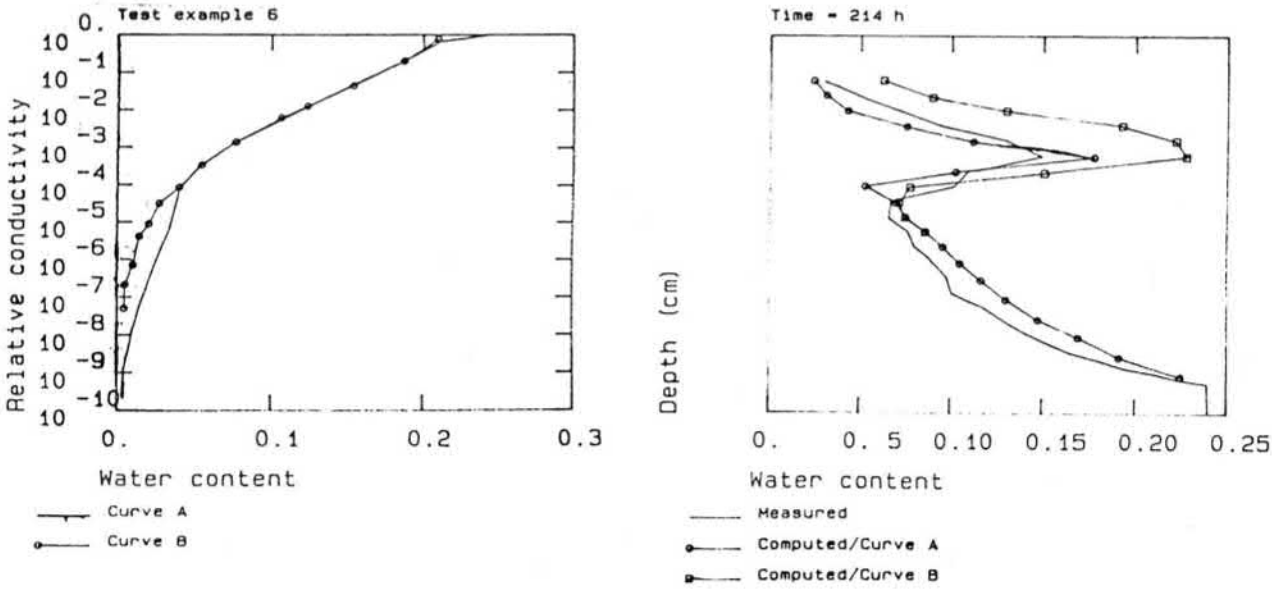

Fig. 4-19. Measured water content and computed water content using two different hydraulic conductivity curves (measured values taken from Kalyuzhnyi et al. 1984, computed by the model presented in section 4.3).

In case 2, the ground water level falls due to the fact that water is flowing to the freezing zone and the bottom of the system is a no-flow boundary. The results from the simulations are shown in Figs. 4-20. The soil temperature (Fig. 4-20b) profiles are in quite good agreement with the measured values but computed soil moisture values are too wet at the depth of 15-30 cm. This indicates that the unsaturated hydraulic conductivity curve is not accurate enough.

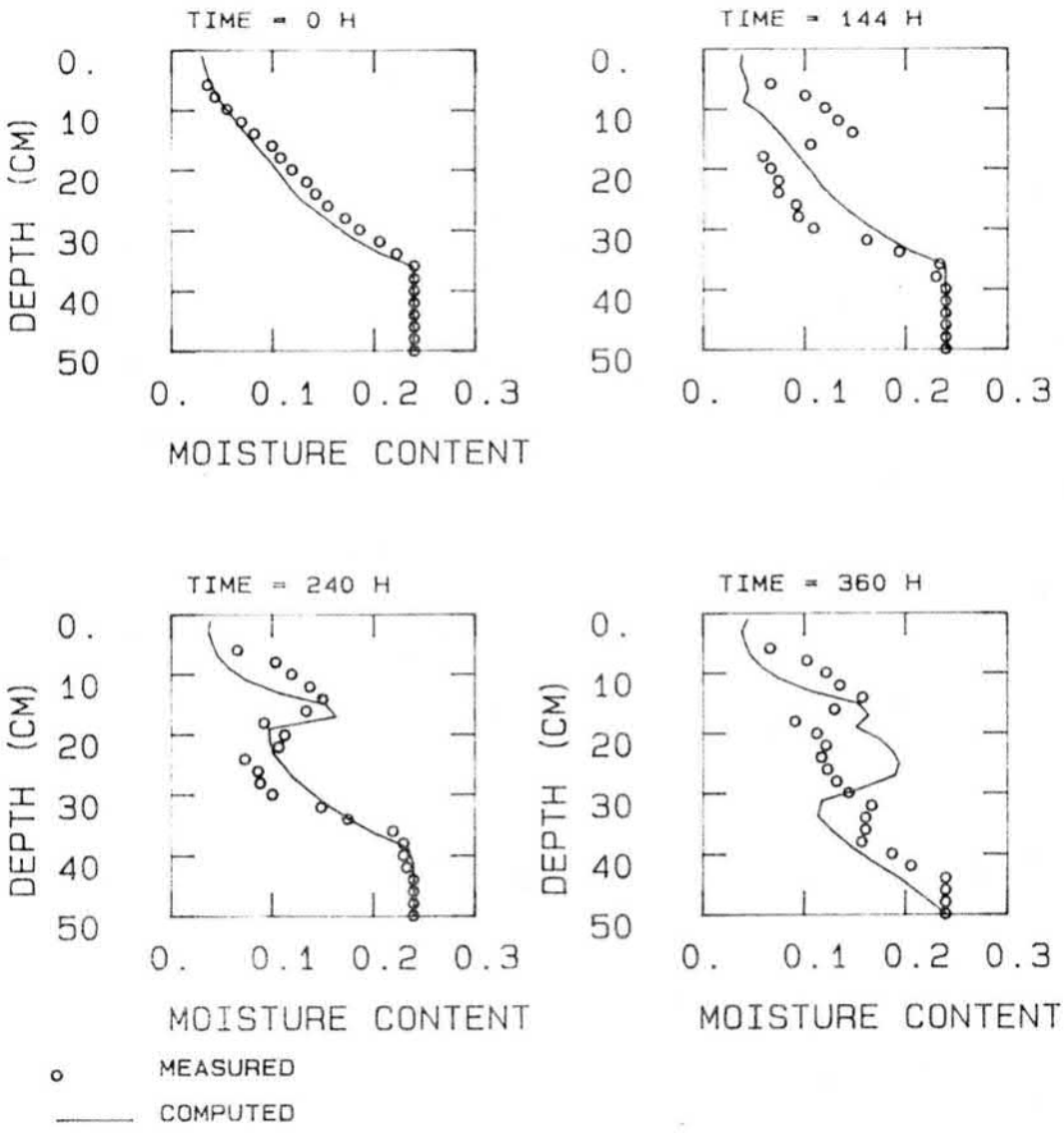

Fig. 4-20a. Computed and measured water content profile for the case when groundwater level is falling(measured values taken from Kalyuzhnyi et al. 1984, computed by the model presented in section 4.3).

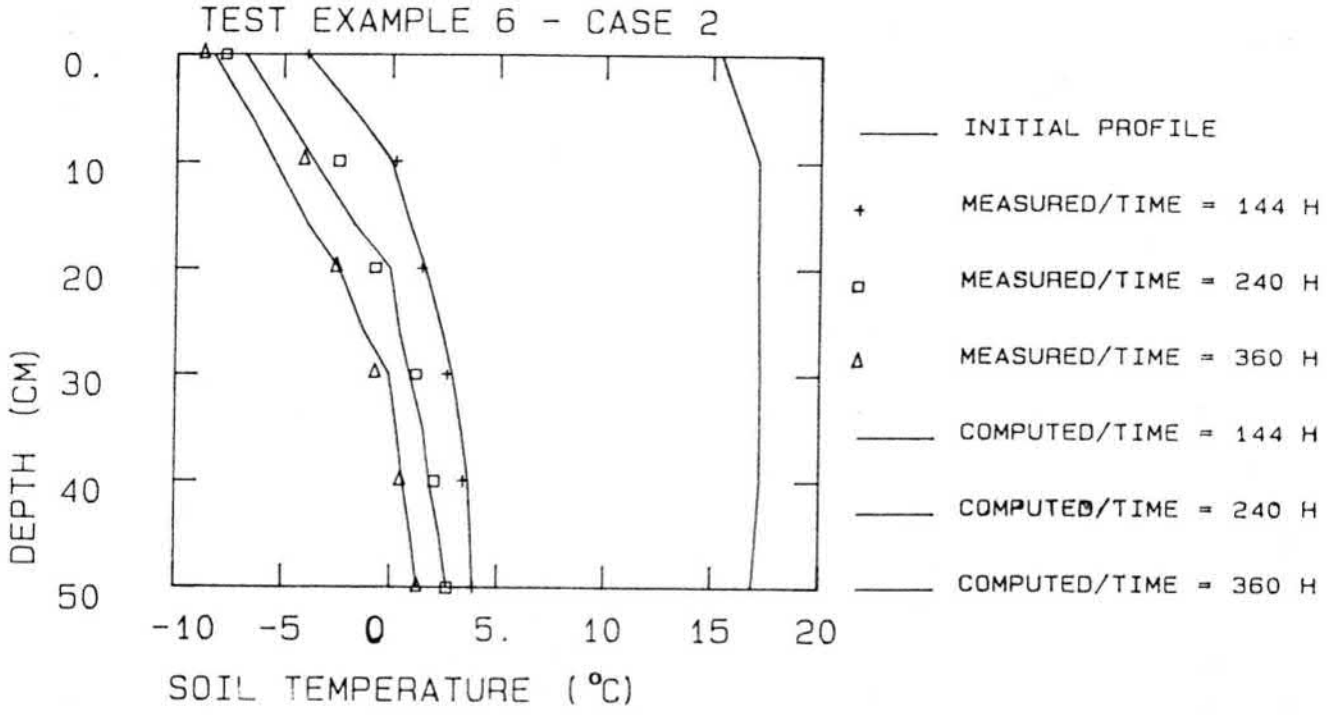

Fig. 4-20b. Computed and measured soil temperature profile (b) for the case when groundwater level is falling(measured values taken from Kalyuzhnyi et al. 1984, computed by the model presented in section 4.3).

CHAPTER 5. MODELS OF CROP YIELD, TRANSPIRATION AND ROOT WATER UPTAKE

5.1 Introduction

The calculation of potential crop production has been studied extensively and mathematical models have been developed for the continuous simulation of plant growth (e.g. de Wit, 1965; McKinion et. al., 1975; Curry et al.,1975; Thornley, 1976; de Wit et al., 1978;). The problem of actual crop yield limited by excessive or too low water content has been modelled e.g. by Feddes et al.(1978), Skaggs (1980), Kowalik and Sanesi (1980), Kowalik (1981), Aslyng and Hansen (1982), Hardjoamidjojo and Skaggs (1982), Busoni et al. (1983), van Wijk and Feddes (1982,1986) and Zaradny (1986). In Finland, Elomaa and Pulli (1985), Saarinen et al. (1986) and Ilola et al. (1986) have used a modified form of the WATCROS-model (Aslyng and Hansen, 1982) for the calculation of potential and actual crop production.

Crop production is generally determined by the prevailing environmental conditions, i.e. by the existing complex physical, chemical and biological factors. The amount of water available for transpiration has a great effect on dry matter production. Actual transpiration depends not only on the weather but also on the physical properties of the soil and factors related to the type of crop (Feddes et al., 1978). The drainage parameters used in planning affect the temperature and moisture conditions in a drained field. The optimal choice of drain spacing, drain depth and drainage coefficient has been studied very little in Finland.

This chapter presents a method for quantifying the effect of soil moisture on crop yield. By proper choice of drainage parameters the actual yield can be maximized. In section 5.2, the general relation between transpiration and net photosynthesis of leaves will be presented and the mathematical equations used in the calculation of actual and potential crop production. Section 5.3 is devoted to the estimation of the

maximum possible growth rate. Finally, in section 5.4, the methods for the calculation of actual and potential transpiration are given.

5.2 The relation between transpiration and photosynthesis

According to Penman and Schofield (1951, ref. Feddes, 1984) transpiration T_p and net photosynthesis P_n of leaves can be described in terms of molecular diffusion equations depending on a gradient and a resistance according to:

$$T_p = \frac{\epsilon d_a}{p_a} \frac{e^*_{leaf} - e_{air}}{r_s + r_a} \quad (kg \cdot m^{-2} \cdot s^{-1}) \qquad (5\text{-}1)$$

$$P_n = \frac{[CO_2]_{air} - [CO_2]_{leaf}}{r'_a + r'_s + r'_m} \quad (kg \cdot m^{-2} \cdot s^{-1}) \qquad (5\text{-}2)$$

where ϵ is the ratio of the molecular weight of water vapour and dry air, d_a is the density of moist air (kg m^{-1}), p_a is the atmospheric pressure (hPa), e^*_{leaf} the is saturated water vapour pressure inside the leaf (hPa) being a function of leaf temperature, e_{air} is the water vapour pressure in the air (hPa) being a function of the air temperature and relative humidity, r_s is stomatal resistance ($s \cdot m^{-1}$), and r_a the laminar boundary layer resistance for water vapour flow, $[CO_2]_{air}$ and $[CO_2]_{leaf}$ are carbon dioxide concentration in the air and inside the leaf, respectively ($kg \cdot m^{-1}$), and r'_a , r'_s and r'_m are the resistances of the boundary layer, the stomata and the mesophyll for carbon dioxide, respectively ($s \cdot m^{-1}$). Water use efficiency is the ratio P_n/T_p.

Bierhuizen and Slatyer (1965, ref. Feddes, 1984) approximated e^*_{leaf} in eq. (5-1) by e^*_{air} (saturated water vapour pressure in the air), when leaf temperature is equal to air temperature. Moreover, Bierhuizen and Slatyer showed that at natural light intensities in the field under conditions of not too severe

water stress the ratio $[r_a+r_s]/[r'_a+r'_s+r'_m]$ can be considered constant for any crop. At constant carbon dioxide concentration, and assuming that water use efficiency for dry matter production of a crop, Y/T_p, is proportional to the water use efficiency for net photosynthesis of individual leaves, P_n/T_p, the following relation can be given (Feddes, 1984):

$$Y = A \frac{T_p}{\Delta e} \qquad (5\text{-}3)$$

where A is the proportionality constant ($kg \cdot ha^{-1} \cdot mm^{-1} \cdot hPa^{-1}$) and Δe is the vapour pressure deficit (hPa) and transpiration T_p is expressed in $mm \cdot d^{-1}$. The slope A has to be determined from field experiments. Assuming that maximum yield, Y_{max}, is reached at maximum transpiration, T_{max}, it is possible to write:

$$\frac{Y_{max}}{T_{max}} = \frac{A'}{\Delta e} \qquad (5\text{-}4)$$

and if the slopes A and A' are the same, the following relationship can be obtained:

$$\frac{Y}{Y_{max}} = \frac{T}{T_{max}} \qquad (5\text{-}5)$$

which is also known as the model of Hanks (1974). This type of relation has been used e.g. in the WATCROS-model of Aslyng and Hansen (1982) and in a slightly modified form in the DRAINMOD-model (Skaggs and Nassehzadeh-Tabrizi, 1983) (e.g. the crop susceptibility factors are included in the DRAINMOD-model). The benefit of the equation (5-5) is that instead of slope A, the maximum yield Y_{max} has to be determined.

Feddes et al. (1978) and Feddes (1985) have given a mathematical derivation of the growth rate of a crop as a hyperbolic function of the growth factor water with the maximum growth rate as the upper limit and efficiency of utilization of

this factor as the initial slope of the hyperbola (see. Fig. 5-1). Daily actual growth rate q_a ($kg \cdot ha^{-1} \cdot d^{-1}$) can be calculated as:

$$\left(1 - \frac{q_a}{AT_p/\Delta e}\right)\left(1 - \frac{q_a}{q_m}\right) = p_\beta \qquad (5\text{-}6)$$

where q_m is the maximum possible growth rate (see section 5.3) and p_β is a mathematical parameter and according to Feddes et al. (1978) usually $p_\beta = 0.01$ is taken. Equation (5-6) can be solved explicitly for the actual dry matter growth rate q_a and actual transpiration rate T_a:

$$q_a = 0.5 \cdot A \left\{ - \frac{T_a}{\Delta e} + q_m - \left\{ \left[q_m + A \frac{T_a}{\Delta e} \right] - 4 \cdot q_m \cdot A \frac{T_a}{\Delta e} [1 - p_\beta] \right\}^{1/2} \right\} \qquad (5\text{-}7)$$

In a similar way it is possible to calculate potential growth rate q_p at potential transpiration rate T_p. It is possible to use the above described procedure for other limiting growth factors as well.

It was decided that in the water management model presented in this study either equation (5-5) or (5-7) can be used for estimating the daily actual growth rate, depending on the field data available for simulation purposes. On a daily basis, equation (5-5) is used in the form:

$$\frac{q_a}{q_p} = \frac{T_a}{T_p} \qquad (5\text{-}8)$$

Equation (5-8) has to be used if the slope A of equation (5-7) is not known. In both equations, the maximum possible growth rate q_m of a crop that is well supplied with water and nutrients has to be estimated.

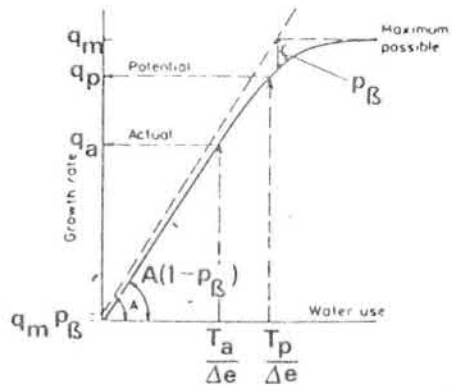

Fig. 5-1. Growth rate versus water use described as a non-rectangular hyperbola, bounded by two asymptotes. The left asymptote indicates the productivity of a crop for water that is well supplied with nutrients. The upper horizontal asymptote represents the production rate under conditions of adequate supply of water and limited supply of some other growth factor that represents weather conditions, especially solar radiation (adapted from Feddes, 1985).

5.3 Estimation of maximum possible growth rate

Gross potential photosynthesis of a crop canopy can be calculated according to the model of de Wit (1965) taking into account the latitude, the cloudiness of the sky, the canopy architecture and the photosynthesis function of the individual leaves and the day of the year. The main results for Finland (between the 60th and 70th Northern latitude) are given in Table 5-1.

From this table it is possible to estimate the photosynthetic rates on clear days P_c and on overcast days P_o for a standard canopy, which is defined as a canopy with a leaf area index LAI = 5 (5 ha of leaves over 1 ha of soil surface) that is fully supplied with water and nutrients. Table 5-1 implies that the light energy is considered the main factor in the production.

Table 5-1. Daily totals of photosynthetic production rates on clear days P_c and on overcast days P_o (kg carbohydrate·ha^{-1}·d^{-1}) for a standard crop (After de Wit, 1965, ref. Feddes et al. 1978)

North latitude		15 Apr.	15 May	15 June	15 July	15 Aug.	15 Sep.
60°	P_c	383	487	544	523	436	316
	P_o	187	245	276	265	216	148
70°	P_c	350	506	612	575	427	262
	P_o	158	241	291	273	200	112

The gross potential growth rate of the standard canopy (P_d) on an arbitrary day can be calculated from equation (Feddes et al., 1978):

$$P_d = f_c \cdot P_o + (1-f_c) \cdot P_c \qquad (5\text{-}9)$$

where f_c is the fraction of time the sky under actual conditions is overcast and P_o and P_c can be obtained from Table 5-1. Hence, the only meteorological data needed for calculating the gross potential growth rate is the cloudiness factor. The daily potential crop production is not as high as the values obtained from Table 5-1. The gross potential growth rate must be corrected for various reasons: respiration, air (or soil) temperature, and soil cover.

5.3.1 Respiration

Penning de Vries (1974) considers 5 types of respiration:
- photorespiration
- idle respiration
- transport respiration
- maintenance respiration
- growth respiration

The first two types of respiration can be neglected in the

model. As transport is associated with maintenance and with growth including storage growth, the two processes are considered to comprise transport respiration too. Thus the total respiration is the sum of maintenance and growth respiration.

The maintenance respiration is proportional to the existing total dry weight and it is a strong function of temperature. According to a literature review carried out by Aslyng and Hansen (1982) the following values for the maintenance respiration can be suggested: 1.0-1.5% d^{-1} of total dry weight for winter wheat and spring barley, 1.0% for potato and 0.8% for fodder beet at 25 °C and the temperature factor Q of 2 (i.e. a 10 °C increase in temperature doubles the maintenance respiration). The maintenance respiration can be calculated with the following expression:

$$R_m = m_r \cdot Y_{tot} \cdot 2^{[T_{air} - 25]/10} \qquad (5\text{-}10)$$

where m_r is the coefficient for maintenance respiration (the values suggested are listed above), Y_{tot} is the cumulative total dry matter weight (kg) and T_{air} is the air temperature (°C).

The growth respiration is only slightly dependent on the amount of biomass. It is about 20 to 50% of the gross potential production (see Feddes et al., 1978). The growth respiration can be expressed as a factor for efficiency in converting carbohydrate into structural plant material. According to e.g. Busoni et al. (1983) and Aslyng and Hansen (1982) the conversion factor, r_{conv}, for cereals is 0.70-0.75.

5.3.2 Temperature

Photosynthesis varies with temperature. An example of the effect of temperature on the reduction factor is shown in Fig. 5-2. Busoni et al. (1983) have used for winter wheat the values proposed by Sibma (1977): 0 % for 0°C, 80 % for 5°C and 100 % for 10°C or more. The effect of this reduction factor

r_{temp} can be very prominent. Unfortunately, the exact reduction factors are not known precisely.

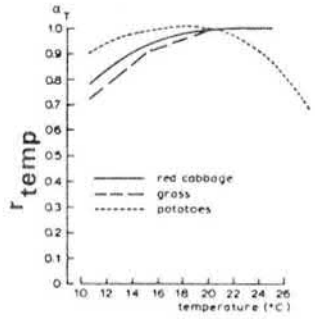

Fig. 5-2. Influence of temperature on phosynthesis of red cabbage (after Wiebe, 1975), of potatoes (after Winkler, 1961) and of grass (after Goudriaan, 1973) (From Feddes et al., 1978).

5.3.3 Correction due to incomplete soil cover

During the early stage of the growing season, photosynthesis is performed by the fractional area of the soil covered by plants. Correspondingly, the potential crop growth must be corrected. Two possibilities have been chosen for the estimation of the correction factor due to incomplete soil cover: 1) correction factor r_{sc} is equal to the fractional area of the soil covered by plants, S_c, and 2) r_{sc} is calculated as a function of the leaf area index, LAI, when this value is less than 5, i.e.:

$$\begin{cases} r_{sc} = S_c & (5\text{-}11a) \\ r_{sc} = \{1 - \exp[-K_e \cdot LAI]\} & (5\text{-}11b) \end{cases}$$

where K_e is the extinction coefficient and according to Aslyng and Hansen (1982) and Feddes (1984), K_e = 0.6-0.8.

The problem of how to determine either S_c or LAI as a function of time remains. The development of a crop varies from year to year depending on the environmental conditions. Therefore, a certain prescribed variation of soil cover or LAI is not possible, but the water management should be capable of

generating the crop development itself. Three different methods have been programmed and it is possible to choose one of them depending on the data available.

1) The first method is the same as that used by van Wijk and Feddes: time is made dimensionless by introducing the development stage D_s of the crop. In the formulation of van Wijk and Feddes, D_s is set 0 at emergence , t_{em} and 1 at harvest time, t_{ha} and any intermediate development stage is then defined according to:

$$D_s = [t - t_{em}]/[t_{ha} - t_{em}] \qquad (5\text{-}12)$$

According to van Wijk and Feddes (1986), the variation of soil cover S_c with D_s is constant over the years. An example of this type of interdependence is given in Fig. 5-3.

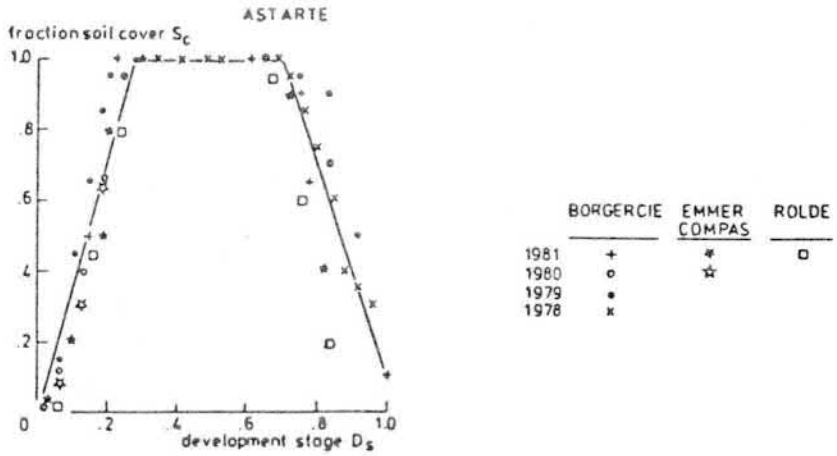

Fig. 5-3. Variation of S_c with development stage D_s for potatoes grown at different locations over a number of years (adapted from van Wijk and Feddes, 1986).

2) The date of emergence can be generated by the model itself but in order to be able to use equation (5-12) for calculating the development stage, the date of harvest has to be prescribed. Since it is possible to generate t_{ha} with the model, a slightly different type of development stage is introduced in the model. In the second method the growing season is divided into three

periods (Table 5-2). For each growing period the time is made dimensionless by introducing the concept of development stage in a way similar to that used by van Wijk and Feddes (1986). In the present model the development stage is -1 at planting, 0 at emergence, 1 at flowering and 2 at ripening (harvest).

Table 5-2. The division of growing season into three periods and the corresponding development stages.

Period	Development stage
From sowing/planting to emergence	-1...0
From emergence to flowering	0...1
From flowering to ripening	1...2

The intermediate values are calculated as a function of temperature sum in an analoguous way used by Feddes (1971) for predicting the date of emergence when the planting date is fixed. For the first growing period (from planting to emergence) the following equation is used:

$$F_e = \sum (T_{soil} - T_{mins}) \cdot t \qquad (5\text{-}13)$$

where T_{soil} is mean soil temperature , T_{mins} is the minimum temperature below which no germination occurs, F_e is the heat sum required for emergence (50 %) and t is the time needed for emergence. The minimum temperature and the heat sum required can be derived by plotting T_{soil} versus 1/t (Feddes, 1971). An example of the determination of F_e has been given in Fig. 5-4 where air temperature is used instead of soil temperature.
The determination of T_{mins} and temperature sum needed can be carried out for all of the three growing periods (see Chapter 7 for more details). It is possible to calculate the actual development stage when the planting date and mean soil (or air) temperature are known. The development of LAI must then be given as a function of the development stage.

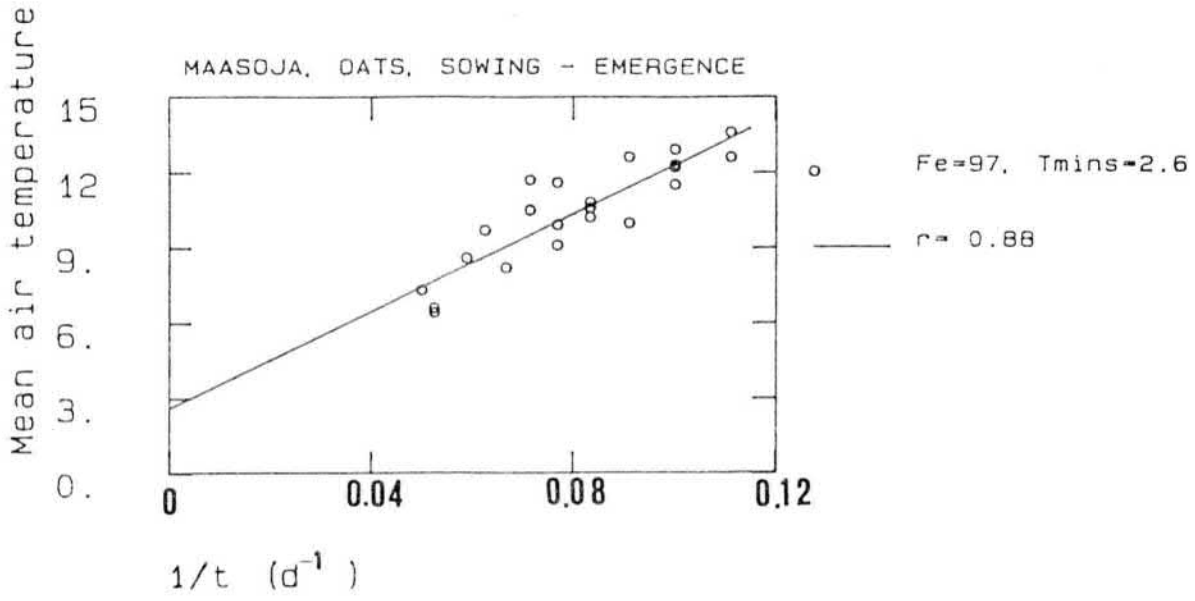

Fig. 5-4. Mean air temperature plotted versus the reciprocal of time for determining minimum temperature T_{mins} and heat sum F_e required from planting to emergence (Vihti, Maasoja, years 1939- 1968).

3) The third method used gives the simplest way to define the leaf area index LAI needed in the calculation of r_{sc} in equation (5-11b). The development of LAI is a function of the effective temperature sum ETS that is calculated as a function of daily mean air temperatures:

$$ETS = \sum(T_{air} - 5) \qquad (5\text{-}14)$$

This is the method used in the WATCROS model by Aslyng and Hansen (1982). Elomaa and Pulli (1985) and Ilola et al (1986) have presented the development of GAI (green area index) of spring barley at Jokioinen (in Southern Finland) (Fig. 5-5). It is assumed that LAI can be approximated by GAI. The advantage of this method is that the total growing period is implicitly included in the calculation of GAI, e.g. harvest time is reached when GAI is zero at the end of the summer (in Fig. 5-5 this corresponds to ETS-value 960 dd).

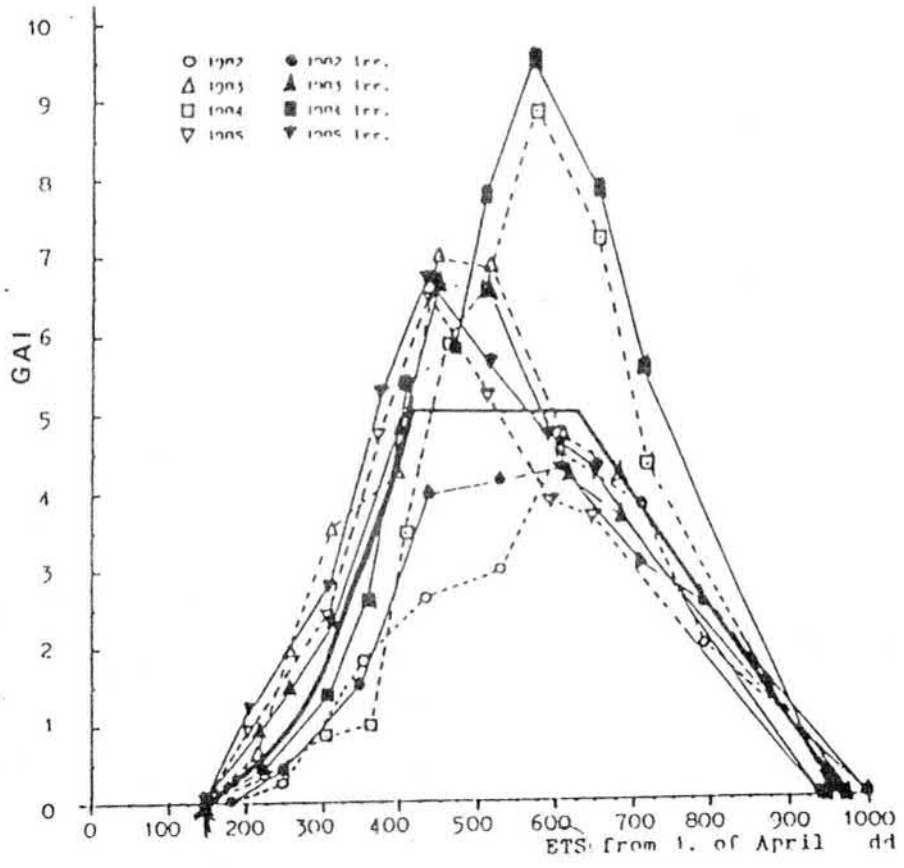

Fig. 5-5. The green area index for spring barley at Jokioinen, 1982 - 1985 (adapted from Ilola and Elomaa, 1986).

5.3.4 Harvested part

Gross potential production rates are calculated for the total dry matter, i.e. shoots plus roots. Generally we are interested in the harvested part and one has to apply a correction factor for the amounts of roots. The most appropriate way would be to define the distribution of dry matter production over the harvested and non-harvested part as a function of development stage (see e.g. Fig. 5-6). This is the first possibility to define the allocation of the total biomass produced during a particular period, i.e. as a tabulated function of the developments stage.

It is not always possible to determine this distribution function and an alternative method has to be used. It is based on a simple harvest index, i.e. the total calculated dry matter is multiplied by a harvest index r_{harv}. According to Ilola et al. (1986), the harvest index for spring barley was 0.49 on the average, but has varied yearly from 0.43 to 0.56.

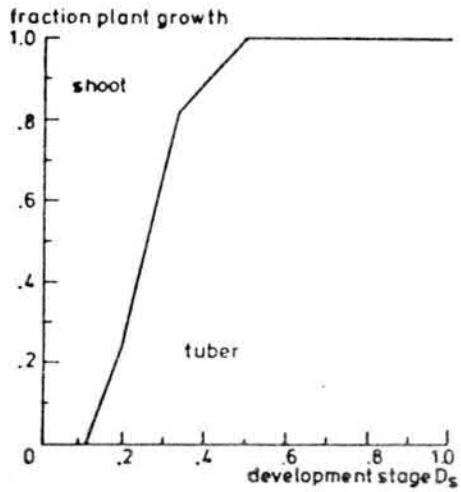

Fig. 5-6. Distribution of increase in total dry matter production over shoot and tubers of a potato crop (van Wijk and Feddes, 1986).

5.3.5 Calculation of the maximum growth rate

The estimation of the maximum potential (daily) growth rate q_m can now be carried out using expression :

$$q_m = [P_d \cdot r_{sc} \cdot r_{temp} - R_m] \cdot r_{conv} \qquad (5\text{-}15)$$

Simplified flowchart of the algorithm YIELD for computation of the daily actual and potential growth rate is given in Fig. 5-7.

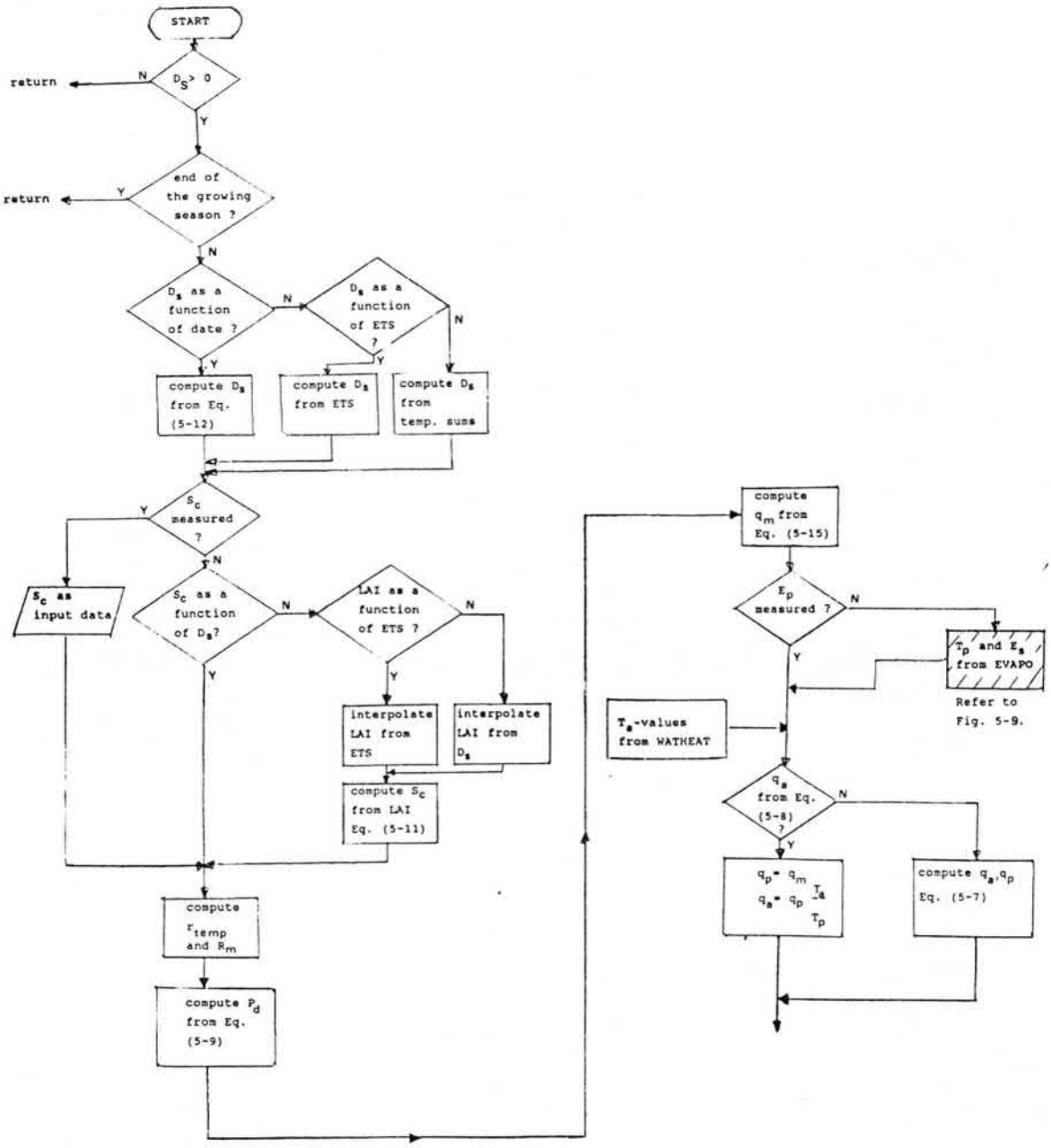

Fig. 5-7. Simplified flowchart of the algorithm YIELD for computation of the daily potential and actual growth rate.

5.4 Estimation of potential and actual transpiration and root water uptake

5.4.1 Calculation of potential evapotranspiration

The Penman-Monteith equation is used for the estimation of the potential evapotranspiration E_p:

$$L_V \cdot E_p = \frac{DEL \cdot R_{net} - c_p \cdot d_a \cdot \Delta e / r_a}{DEL + GAM\,[1 + r_{eff}/r_a]} \qquad (5\text{-}16)$$

where L_V is the latent heat of water vaporization ($J \cdot kg^{-1}$), DEL is the slope of saturated vapour pressure versus temperature curve, GAM is psychrometer constant ($hPa \cdot K^{-1}$), R_{net} is the net radiation ($W \cdot m^{-1}$), c_p is the specific heat of air ($J \cdot kg^{-1} \cdot K^{-1}$), d_a is the air density ($kg \cdot m^{-1}$), Δe is the vapour pressure deficit (hPA), r_a is the aerodynamic resistance ($s \cdot m^{-1}$) and r_{eff} is an effective surface resistance ($s \cdot m^{-1}$). Aerodynamic resistance is calculated with the equation (e.g. Jensen 1983):

$$r_a = \frac{\{\ln[z_r - d_c]/z_0\}^2}{k_k^2 \cdot u_z} \qquad (5\text{-}17a)$$

$$d_c = 0.75 \cdot H_c \qquad (5\text{-}17b)$$

$$z_0 = 0.1 \cdot H_c \qquad (5\text{-}17c)$$

where z_r is the reference height (m), d_c is the zero plane displacement (m), z_0 is the roughness length (m), k_k is von Karman's constant, u_z is the wind speed given at reference height ($m \cdot s^{-1}$) and H_c is the crop height (m).

In most cases direct measurements of net radiation are not available and R_{net} has to be estimated indirectly with empirical formulae. The following expression has been chosen (e.g. Feddes et al. 1978):

$$R_{net} = [1-r_{alb}]\cdot R_s - R_t \qquad (5\text{-}18)$$

where R_s is the flux of incident short-wave radiation ($W\cdot m^{-2}$), R_t is the flux of net outgoing thermal radiation ($W\cdot m^{-2}$) and r_{alb} is the surface reflection coefficient of short-wave radiation.

The following options are included for the estimation of R_s if it is not measured directly:

$$R_s = [a_{R1} + a_{R3}\cdot \frac{n_s}{N_s}]R_{top} \qquad (5\text{-}19a)$$

$$R_s = \{b_{R1} + b_{R3}\ [1-f_c]\}R_{top} \qquad (5\text{-}19b)$$

where n_s is the actual duration of bright sunshine in a day (min) , N_s is the maximum n_s can reach on completely clear days (min), R_{top} is the extra terrestial radiation flux at the top of the atmosphere ($W\cdot m^{-2}$), f_c is the mean fractional cloud cover and a_{R1} ...b_{R3} are the regression coefficients. The value of R_{top} and N_s depend on latitude and time of the year (Smithson. Meteor. Table, 1951). In Finland Mustonen (1964) has determined the coefficient a_{R1} and a_{R3} separately for different months and the results have been given in Table 5-3. In the same table, the results based on data from Ås (30 km South of Oslo, 59°40') (Heldal 1970) have been presented, as well. Coefficient a_{R0} in Table 5-3 refers to completely overcast days. According to Table 5-3, the results of Heldal differ in most cases less than 10 % from the results obtained by Mustonen. The equation used for thermal radiation R_t is the Brunt-type formula (Feddes et al. 1978):

$$R = 5.67\cdot 10^{-8}\ T_{air}^4\cdot[0.56-0.08\sqrt{e_{air}}\ ]\{0.10 + 0.90\frac{n_s}{N_s}\} \qquad (5\text{-}20)$$

where T_{air} is the air temperature (K) and e_{air} is the prevailing vapour pressure of air (hPa). If no n_s measurements are available, they have to be estimated from cloud cover measurements (e.g. Jansson and Halldin, 1980):

$$\frac{n_s}{N_s} = 1 - f_c \qquad (5\text{-}21)$$

Table 5-3. Values of constants a_{R0}, a_{RI}, a_{R3}, b_{RI} and b_{R3} used for calculation of solar radiation (Mustonen 1964; Heldal 1970).

	Mustonen (1964)			Heldal (1970)			
Month	a_{RI}	a_{R0}	a_{R3}	a_{RI}	a_{R3}	b_{RI}	b_{R3}
May	0.24	0.175	0.58	0.193	0.620	0.208	0.660
June	0.23	0.165	0.59	0.230	0.543	0.245	0.556
July	0.23	0.160	0.59	0.202	0.583	0.240	0.582
Aug.	0.23	0.155	0.56	0.232	0.536	0.247	0.554
Sept.	0.23	0.150	0.54	0.181	0.604	0.183	0.583

5.4.2 Partitioning transpiration and soil evaporation

The means to partition potential evapotranspiration, E_p, to potential transpiration, T_p, and potential soil evaporation, E_s are essentially the same as those used by Jensen (1983). The soil evaporation under a partly developed vegetation cover will not be the same as under bare soil because radiation, wind speed, and vapour pressure deficit are all reduced with increasing plant cover. The assumptions of Ritchie (1972) have been adopted here:

- the aerodynamic term in equation (5-16) is negligible compared with the radiation term

- the net radiation at the soil surface, $R_{net,s}$, can be estimated by the empirical relationship (based on net radiation above the canopy, R_{net} and leaf area index LAI):

$$R_{net,s} = R_{net} \cdot \exp(-0.4 \cdot LAI) \qquad (5\text{-}23)$$

The remaining part of the net radiation will be available for transpiration and evaporation from the interception storage. The potential soil evaporation E_s can be calculated from the following equation (e.g. Jensen 1983):

$$E_s = \frac{DEL}{L_V\,(DEL+GAM)}\, R_{net,s} \qquad (5\text{-}24)$$

For a soil with very sparse vegetation, or no crop cover at all, the assumptions of Ritchie are no longer valid, and the full Penman-Monteith equation (5-16) is used for predicting potential soil evaporation with surface resistance r_{eff} set equal to zero. The actual soil evaporation is calculated using the procedure already described in section 4.2.3.1.

The net radiation absorbed by the crop, $R_{net,c}$ is calculated according to (see equation (5-23):

$$R_{net,c} = R_{net} \cdot [1 - \exp(-0.4 \cdot LAI)] \qquad (5\text{-}25)$$

The potential transpiration can now be calculated by replacing net radiation, R_{net} in (5-16) by net radiation absorbed by the crop, $R_{net,c}$. The determination of the actual transpiration reduced by soil moisture conditions is discussed in section 5.4.3

A simple threshold formulation has been used to take into account the interception storage supplied by rainfall or irrigation and diminished by direct evaporation. Interception storage has a maximum limit, I_{max}, which is related to leaf area

index according to an expression proposed by Jensen (1983):

$$I_{max} = 0.5 \cdot LAI \qquad (5\text{-}25)$$

where I_{max} is in units mm. Evaporation from the interception storage is assumed to take place at a rate determined by (5-16) when surface resistance is set at zero. If the potential evaporation rate is greater than the amount of available water in the interception storage, the surplus is applied in the transpiration calculations.

5.4.3 Determination of root water uptake and actual transpiration

In Chapter 2, the Richards equation for solving the mass balance of a partly unsaturated soil-root system was given in equation (2-1). In this equation, S(h) represents the volume of water taken up by the soil roots. This function can be described by:

$$S(h) = a(h) \cdot a(T) \cdot S_{max} \qquad (5\text{-}26)$$

where a(h) is a dimensionless prescribed function of the pressure head h, a(T) is the reduction factor due to low soil temperature and S_{max} is the maximal possible water extraction by roots. Feddes (1986) has reviewed the possible ways to define S_{max} and the method proposed by Prasad (1986) has been selected:

$$S_{max} = \frac{2 \cdot T_p}{z_R} \left(1 - \frac{z}{z_R}\right) \qquad (5\text{-}27)$$

where z is the depth from the soil surface (m) and z_R is the rooting depth (m). Equation (5-27) implies that root water uptake is set equal to zero at the bottom of the root zone. This is in complete agreement with the observations presented by Salonen (1949). According to the measurements of Salonen, the root systems in the soils of Finland are to a large extent

situated in the furrow slice (e.g. 47 - 100% for spring cereals, and 62 - 99% for winter cereals) and the root biomass decreases with depth very rapidly. The rooting depth in the model is given as a function of the development stage. Moreover, the maximum depth has to be prescribed and these maximum values are taken from the measurements of Salonen (1949).

The reduction coefficient a(h) is taken from Feddes et al. (1978) (Fig. 5-8). Water uptake below $|h_1|$ (oxygen deficiency) and above $|h_4|$ is set equal to zero. Water uptake is maximal between $|h_2|$ and $|h_3|$. A linear variation is assumed between $|h_1|$ and $|h_2|$ and $|h_3|$ and $|h_4|$. The value of $|h_3|$ is dependent on the possible transpiration rate T_p (Zaradny 1986):

$$h_3 = -4.0 - 1.50\ [5 - T_p]\ ;\ 1.0 \leq T_p \leq 5\ \text{mm}\ d^{-1} \qquad (5\text{-}28)$$

where h_3 is in m and T_p in units $mm \cdot d^{-1}$.

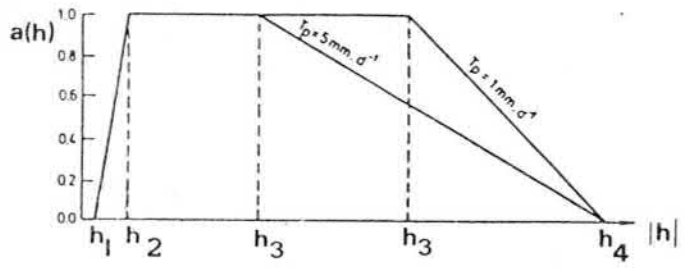

Fig. 5-8. Dimensionless reduction factor a(h) as a function of the absolute value of the soil water pressure head (adapted from Feddes et al. 1978).

Reduction due to low soil temperature acts primarily through a lower conductivity between root surface and xylem and is thus a function of soil temperature $T_{soil,z}$ at depth z (Axelsson and Ågren 1976, ref. Jansson and Halldin 1980):

$$a(T) = 1 - \exp[-0.02 \cdot \max(0, T_{soil,z})] \qquad (5\text{-}29)$$

where $\max(0,T_{soil,z})$ refers to the maximum of values 0 and $T_{soil,z}$. If $T_{soil,z}$ is greater than 15 °C, the effect of a(T) is negligible.

The simplified flowchart of the algorithm EVAPO for computation of potential and actual transpiration rate and for estimation of maximum possible soil evaporation rate is given in Fig. 5-9.

5.5 Testing of the crop growth model

5.5.1 The experimental field Geestmerambacht

A field experiment performed by Feddes in 1967 (ref. Feddes et al. 1978) in the Netherlands at the Geestmerambacht experimental field was taken as the test example since it includes both observed water balance components and measured crop yield as a function of time. Red cabbage was grown under optimum nutrient supply conditions on a heavy clay. The data and the parameter values used in the calculations were taken from Feddes et al. (1978) and they are not presented here. The purpose is to compare the numerical simulations of the proposed model with the measured values of Feddes et al. (1978).

5.5.2 Prediction of the water balance components.

The main results of computations are given in Figs. 5-10 and 5-11. In Fig. 5-10 the measured and computed cumulative evapotranspiration rates have been compared and the results show that there is a rather good agreement between computed and measured evapotranspiration, especially at the beginning and end of the period considered. The values computed with the proposed model are almost the same as the results of Feddes et al (1978). The small discrepancies are probably due to the different way of handling the interception storage.
The computed soil moisture profiles have been compared with the measured ones and the results are given in Fig. 5-11. The agreement with the measured values is rather good. Moreover, the computed values of the soil moisture content using two

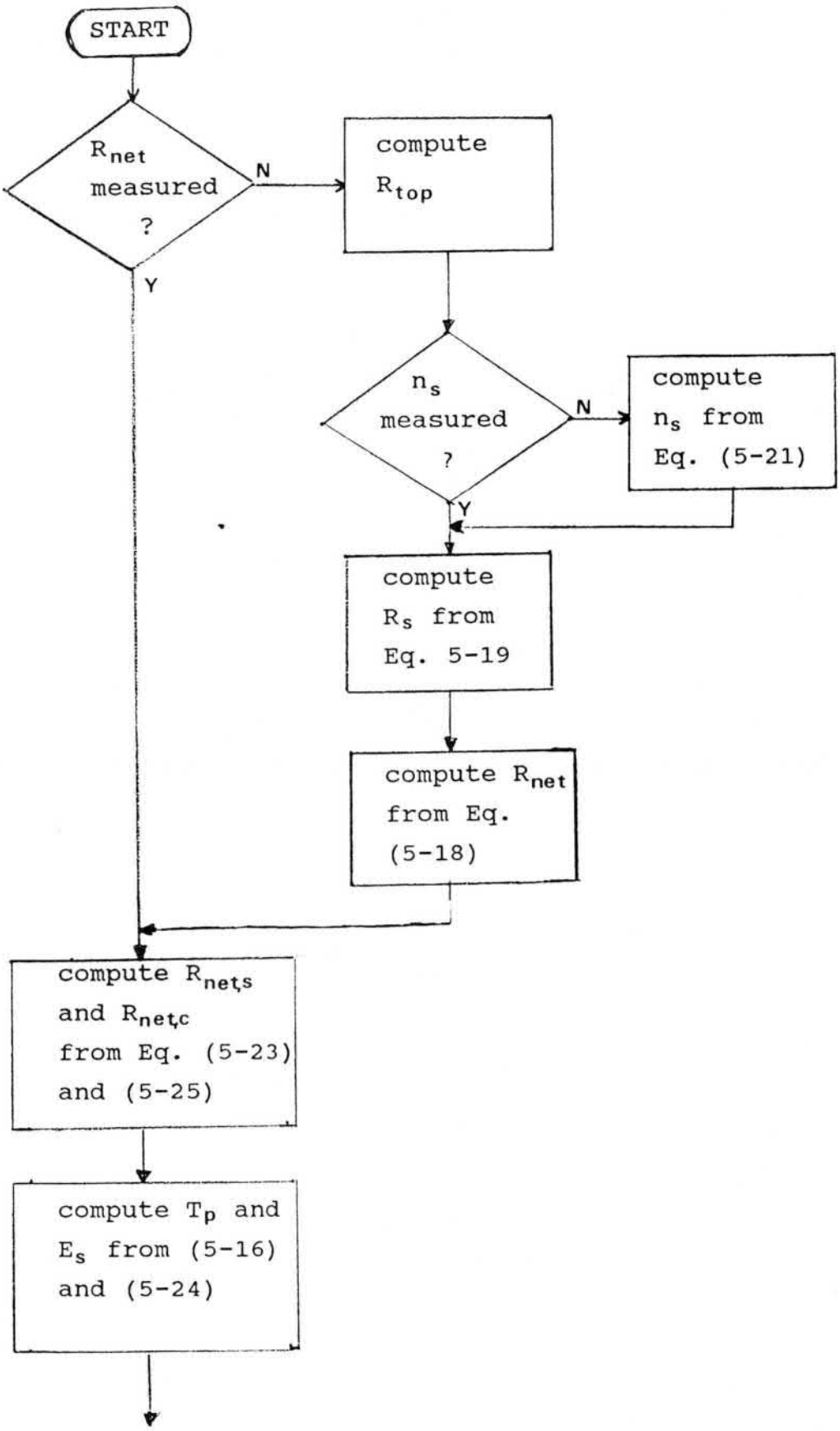

Fig. 5-9. Simplified flowchart of the algorithm EVAPO for computation of the potential and actual transpiration rate and maximum possible soil evaporation rate.

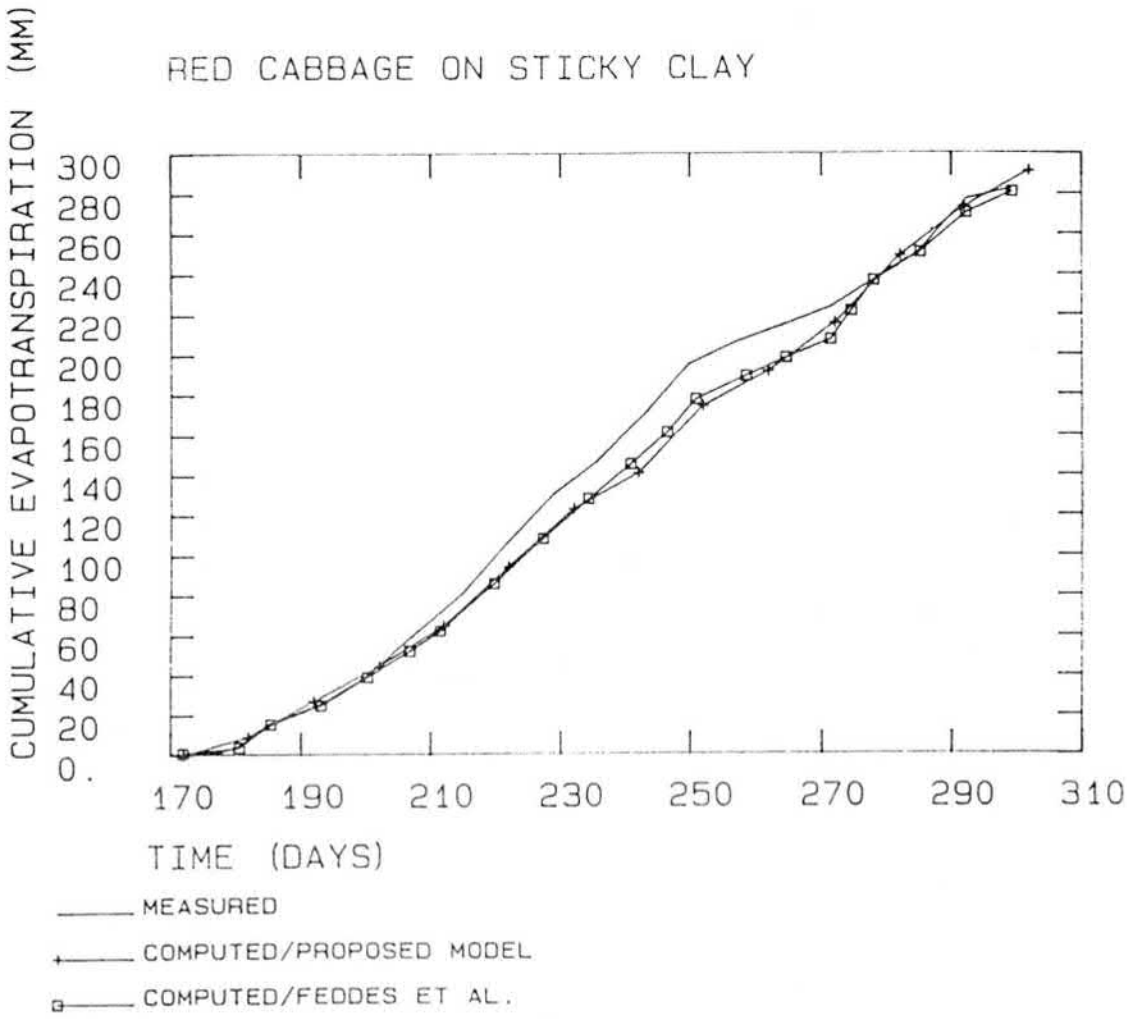

Fig. 5-10. Measured and computed cumulative evapotranspiration.

different numerical solution methods - the proposed model and the finite difference solution of Feddes et al (1978)- give almost the same results. Again, the small difference between the results can be caused by a different amounts of intercepted water.

The computed surface runoff during the growing period was 43 mm, which is almost the same value as that obtained by Feddes et al. 1978).

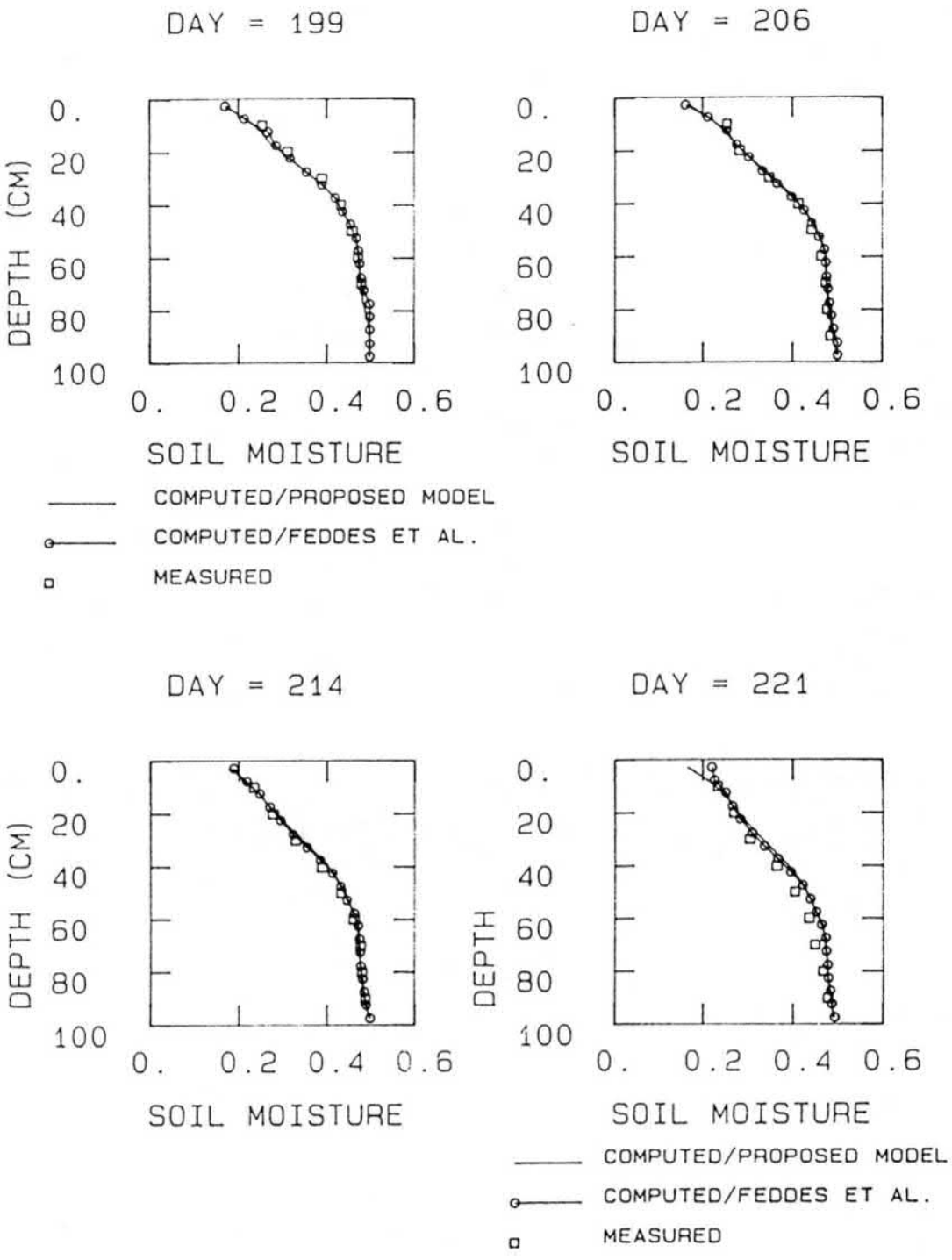

Fig. 5-11. Measured and computed soil moisture contents. a) t=199 d, b) t=206 d, c) t=214 d and d) t=221 d.

5.5.3 Prediction of crop yield

For the numerical predictions the computed potential and actual yield were compared with the calculated values of Feddes et al (1978) and with measured actual crop yield. The results are presented in Fig. 5-12.

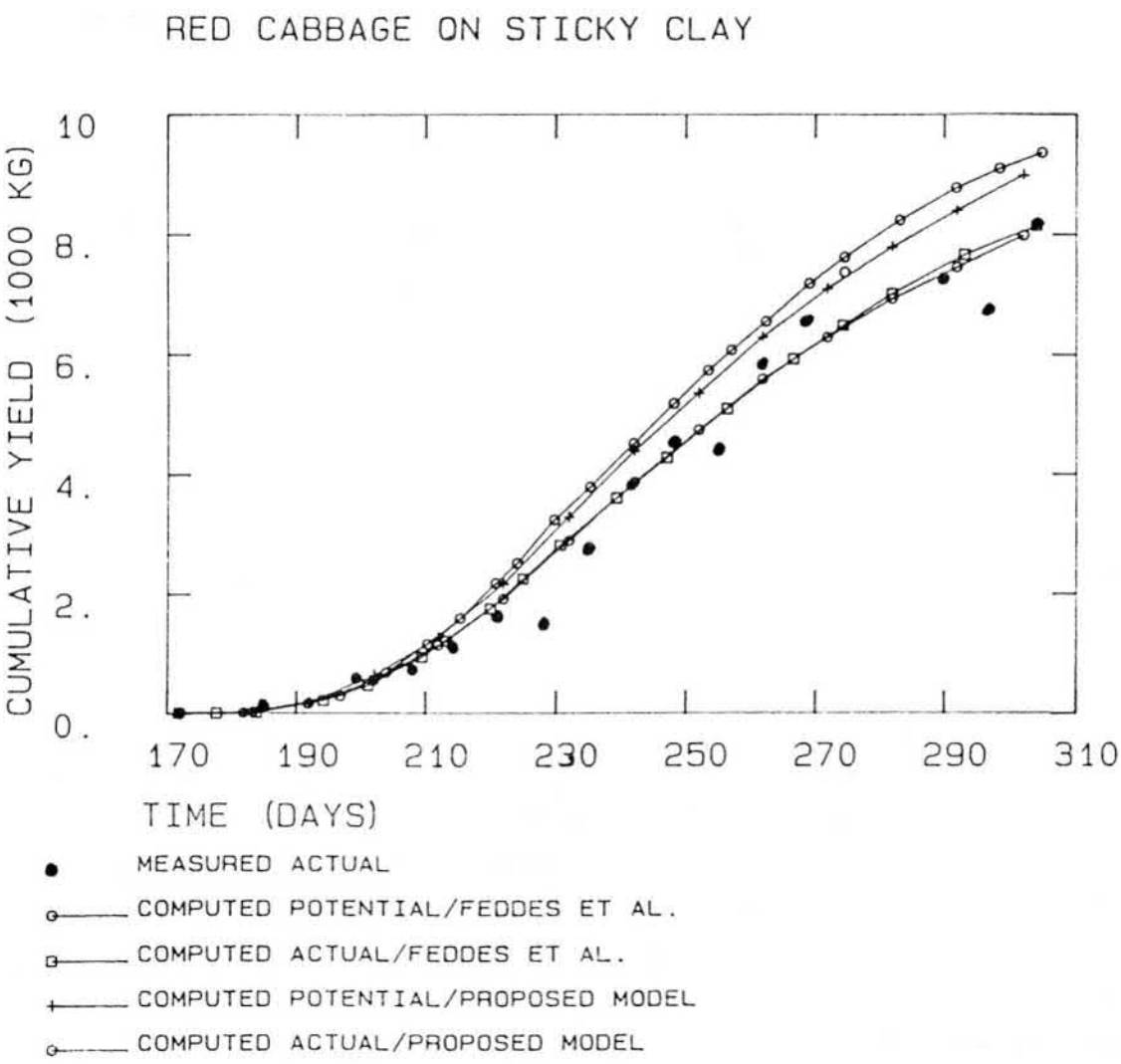

Fig. 5-12. Computed potential and computed actual cumulative crop yield as compared with measured data.

The small difference between the results of Feddes et al. (1978) and the proposed model is mainly attributable to the differences in the way the potential daily production was calculated. In the numerical simulations of Feddes et al. (1978) the potential daily production was calculated with equation (5-15). Later on Feddes (1985) has altered the computation of the potential daily production slightly (equation 5-7 with T_p substituted for T_a) and this latter version was used in the numerical simulations of the developed model.

6 TWO-DIMENSIONAL MODELS OF DRAINAGE AND SOIL WATER CONTENTS

6.1 Introduction

The objective of this Chapter is to present two-dimensional models of drainage and soil water movement. The field conditions have been clarified in section 6.2. Section 6.3 is devoted to strictly two-dimensional soil water model that uses the finite element solution of the Richard's equation. Finally, in section 6.4 the comparison of two-dimensional and quasi-two-dimensional solution methods has been carried out.

6.2 Field conditions

The aim of a two-dimensional soil water model is to characterize the response of the soil water regime to various combinations of subsurface and surface water management. The model can be used to predict the response of the water table and the soil moisture content above the phreatic surface to rainfall, evapotranspiration, given degrees of subsurface and surface drainage and irrigation. The system considered here is given in Fig. 6-1.

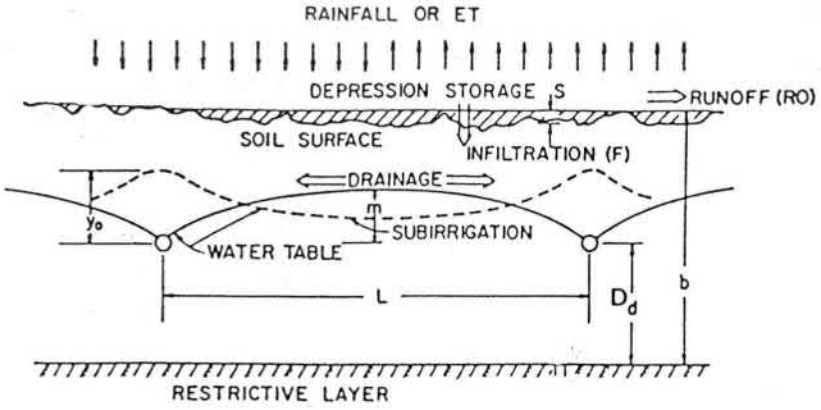

Fig. 6-1 Scheme of a system with subsurface drains that may be used for drainage or subirrigation (adapted from Skaggs, 1980).

The soil is almost flat and has an impermeable layer at a relatively shallow depth. Subsurface drainage is provided by drain tubes or parallel ditches spaced a distance L , and at a distance D_d above the impermeable layer. In the case of rainfall, water infiltrates at the surface and percolates through the profile raising the water table and increasing the subsurface drainage rate. If the rainfall is greater than the infiltration capacity of the soil, water begins to collect on the surface. When good surface drainage is provided, most of the surface water will be available for runoff. However, if the surface drainage is poor, a certain amount of water must be stored in depressions before runoff can begin. After rainfall ceases, infiltration continues until the water stored in surface depressions infiltrates the soil (Skaggs, 1980).

The rate of subsurface water movement into the drain tubes or ditches depends on the hydraulic conductivity of the soil, drain spacing and depth, profile depth and water table elevation. Water moves towards drains in both the saturated and unsaturated zones and can be quantified by solving the Richards equation for two-dimensional flow.

The computational and input requirements of the numerical solution of the two-dimensional Richards equation are considerably greater than the requirements of the quasi-two-dimensional model. The quasi-two-dimensional model uses one-dimensional solution in the vertical direction and the flux towards the drains is taken as a lower boundary condition. It would be beneficial to use the latter alternative for characterizing the effects of drainage on soil water contents if the accuracy of the quasi-two-dimensional solution method is good enough.

6.3 Two-dimensional solution of saturated-unsaturated flow to parallel drains

Efficient design of drainage systems requires the characterization of transient two-dimensional water movement. Methods have been presented in the literature involving the transient flow of water to a drain (open ditch or subsurface drain) in a saturated-unsaturated porous medium e.g. by Neuman et al. (1974, 1975), Skaggs and Tang (1976), Tang and Skaggs (1978), Zaradny and Feddes (1979), Zaradny (1986) and Fipps et al. (1986). Above the phreatic surface there is an unsaturated zone which controls the flow of water from the soil surface to the saturated zone. The drainage of this unsaturated slab is not instantaneous, and the flow in the unsaturated part is not completely vertical. However, the numerical solution of Richards' equation in two dimensions takes more computer time than the quasi two-dimensional solution outlined in section 4.2. It is frequently argued that the field variability of the soil hydraulic properties will mask the additional accuracy obtained from more precise methods.

6.3.1 Numerical solution with the finite element method

A schematic diagram of the drainage problem considered herein is shown in Fig. 6-2 for parallel subsurface drains. The soil is assumed to be slightly compressible and the governing relationship is taken to be Richards' equation, which may be written for two-dimensional cases as (Zaradny and Feddes 1979; Zaradny 1986):

$$[C(h)+ ß S_s]\frac{\partial h}{\partial t} = \frac{\partial}{\partial z}[K_V(h)\cdot(\frac{\partial h}{\partial z} + 1)] + \frac{\partial}{\partial x}[K_H(h)\frac{\partial h}{\partial x}]-S(h) \quad (6\text{-}1)$$

in which h is the soil-water potential (m), C(h) is the differential moisture capacity ($1\cdot m^{-1}$), ß is a factor ($0 \leq ß \leq 1$) and ß=1 at saturation, S_s is the specific storage which reflects the combined elastic properties of the medium, z and x are

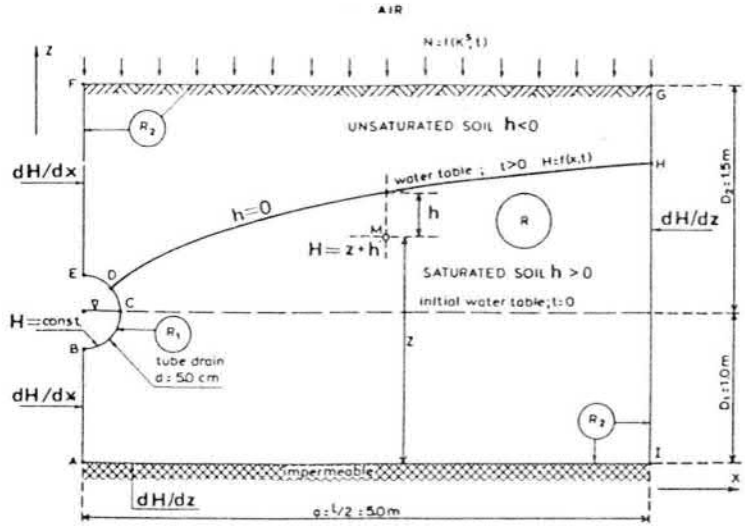

Fig. 6-2 Scheme of the drainage problem under consideration (adapted from Zaradny and Feddes (1979).

position coordinates (m), t is the time (d), $K_V(h)$ and $K_H(h)$ ($m \cdot d^{-1}$) are hydraulic conductivities in the vertical and horizontal directions, respectively (functions of soil-water pressure head) and S(h) represents the volume of water taken up by roots per unit bulk volume of the soil in unit time (the calculation of S(h) is described in Chapter 5).

To obtain a solution, equation (6-1) must be supplemented by the appropriate initial and boundary conditions. As the initial condition, the pressure heads are defined as a function of the x-coordinate, assuming that the total hydraulic head H (= h + z) is constant. The following can be applied as boundary conditions:

- flux boundary along FG, where the actual flux is obtained by maximizing the absolute value of the flux in a manner described in section 4.2.3.
- zero-flow boundary along AB, EF, AI and GHI
- two possibilities exist for the boundary condition along BCE : 1) constant hydraulic head along BCE and 2) constant pressure head along BC and region CDE acting as a surface of seepage (h constant along saturated zone CD and Q = 0

in the unsaturated zone DE)

The flow region is divided into a network of triangular elements for the numerical solution. The Galerkin method is used and the details of the numerical solution have been presented in Neuman et al. (1974, 1975) and Zaradny and Feddes (1979) and the resulting set of N_x quasilinear first-order differential equations is of the same type as shown in (4-9). The coefficient matrices and vectors have been defined in Neuman et al. (1975) and they are not shown here.

When the finite element method is used, the network of elements can be considered small in the neighbourhood of the drain where large hydraulic gradients are expected to occur, and proportionally larger at greater distances from the drain.

6.3.2 Testing of the two-dimensional model

The test example consists of calculation of flow towards a drain in a homogenous soil as shown in Fig. 6-2. The drain tube has a diameter of 5 cm, the spacing between the drains is 10 m, the depth of the soil layer below the drain is 1 m and above the drain 1.5 m. The rainfall intensity P applied to the system equals $0.01 \cdot K_S$, $0.05 \cdot K_S$ and $0.1 \cdot K_S$ respectively, where K_S represents the saturated hydraulic conductivity of the soil (= 12 $cm \cdot d^{-1}$). The problem is the same that has been calculated by Zaradny and Feddes (1979) and the results of the proposed numerical solution are compared with the results obtained by Zaradny and Feddes.

The moisture retention curve is presented in Fig. 6-3 and the hydraulic conductivity curve is shown in 6-4. A constant hydraulic head equal to 100 cm is taken as the initial condition. The boundary conditions are described in the previous section. A constant hydraulic head at the circumference of the drain is used as the boundary condition along the drain. This type of boundary condition was chosen since the paper of Zaradny and Feddes presents results from this type of case.

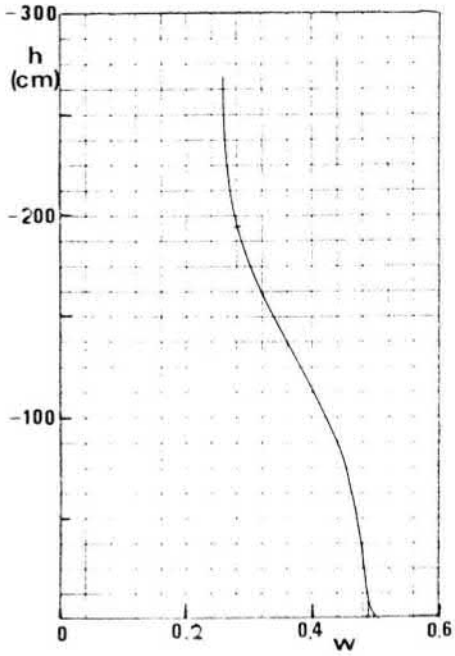

Fig. 6-3. Pressure head as a function of soil water content for fine sandy loam (adapted from Zaradny and Feddes, 1979).

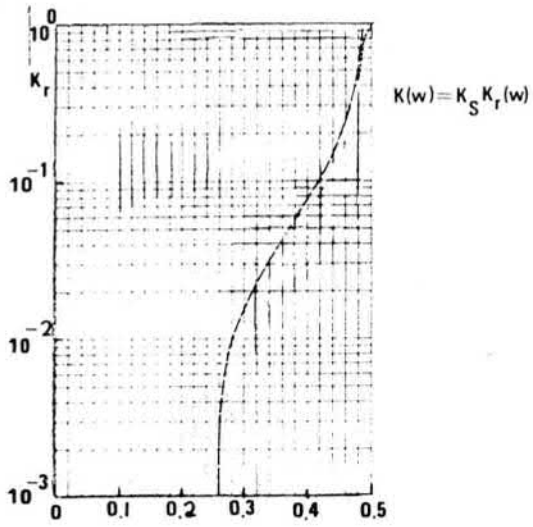

Fig. 6-4. Relative hydraulic conductivity versus soil water content (adapted from Zaradny and Feddes, 1979).

The finite element network is shown in Fig. 6-5 and it is the same as that used by Zaradny and Feddes (1979). The size of the elements was very small in the neighbourhood of the drain, where large hydraulic gradients are expected to occur, and larger elements away from the drain. The computation was started using the rainfall rate $P=0.01 \cdot K_s$ and was continued until a steady state was reached, i.e. the precipitation rate equals the calculated outflow to the drain. Thereafter, the rate was increased to $P=0.05 \cdot K_s$, and after the next steady state situation to $P=0.1 \cdot K_s$.

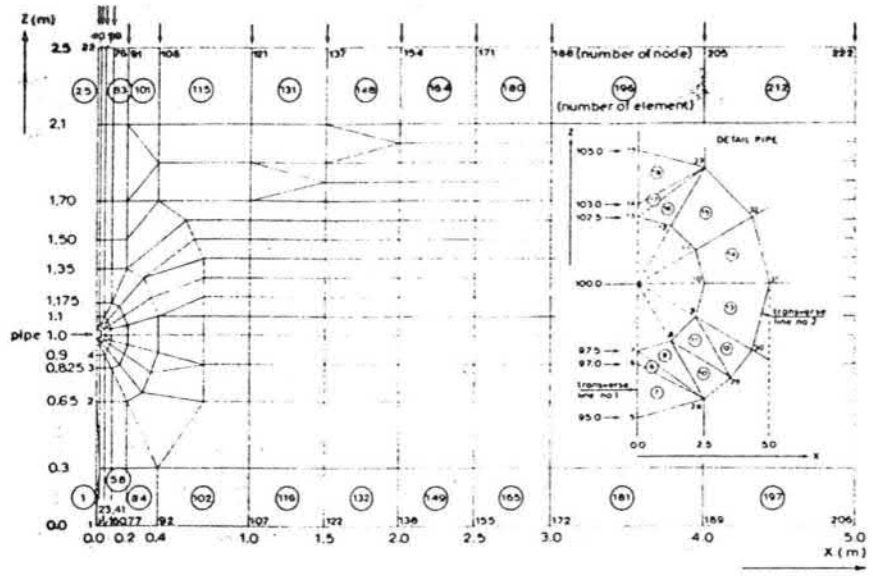

Fig. 6-5. Applied finite element network (adapted from Zaradny and Feddes, 1979).

The shapes of the calculated water table at these steady-state situations are presented in Fig. 6-6, which also shows the results obtained by Zaradny and Feddes. According to Fig. 6-6, there is very good agreement between the results obtained with the model of Zaradny and Feddes and the proposed model. The computed hydraulic heads for the steady-state situation $P=0.1 \cdot K_s$ are shown in shown in Fig. 6-7. In this case, there is a small discrepancy between the two numerical solutions. This is probably due to the different way of approximating the internodal hydraulic conductivity and the derivative of the

water retention curve. Moreover, in the calculations carried out with the proposed model, the approximation of the time derivative in equation (6-1) was a fully implicit one to guarantee the stability of the solution.

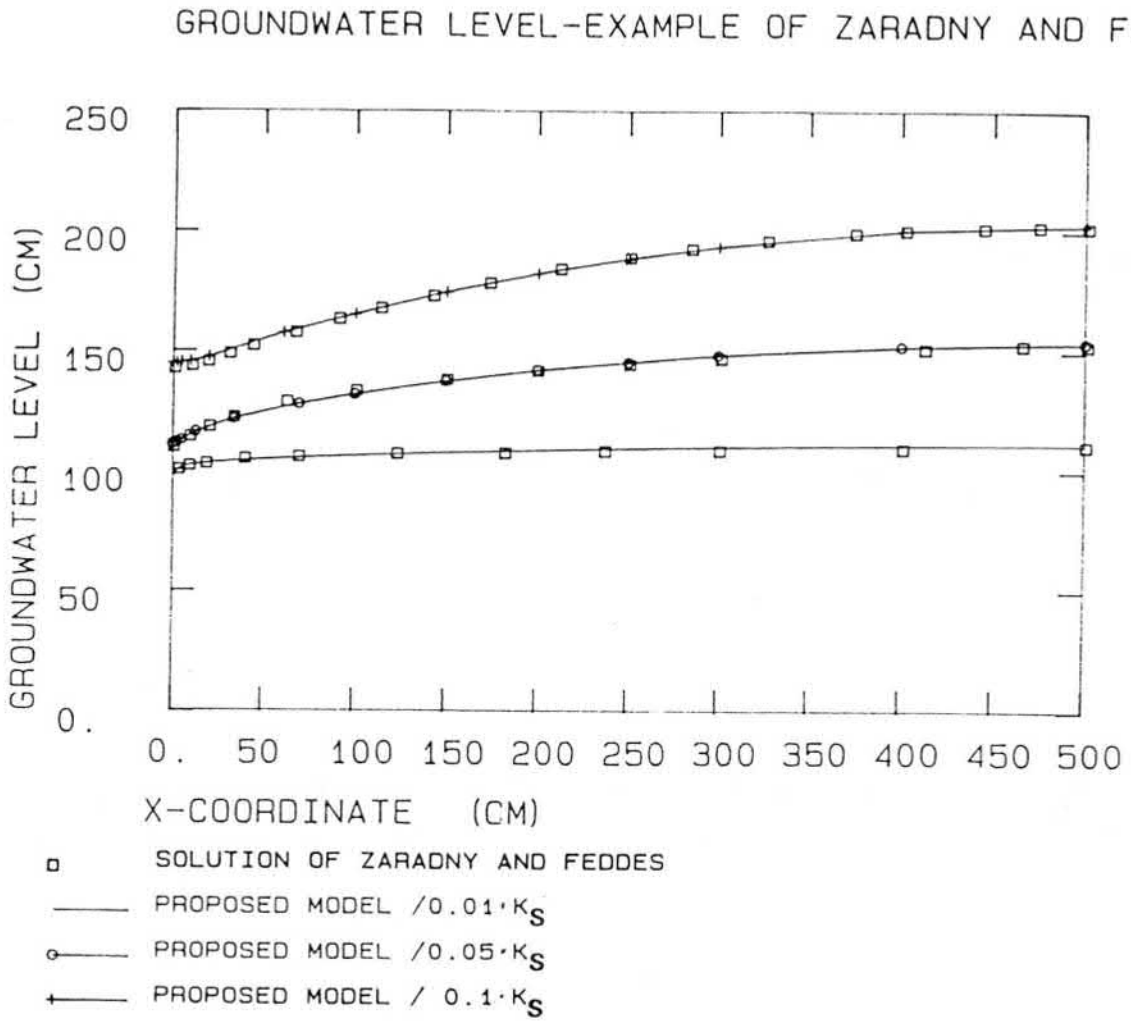

Fig. 6-6. Steady-state water table for rainfall rates $P=0.01K_S$, $0.05K_S$ and $0.1K_S$, respectively (constant head at the circumference of the drain was used as the boundary condition).

In the immediate vicinity of the drain, equipotential lines are almost circles and radial flow occurs at that region. The Thiem-Dupuit well formula can then be applied. For the case under consideration the analytical formula is written as

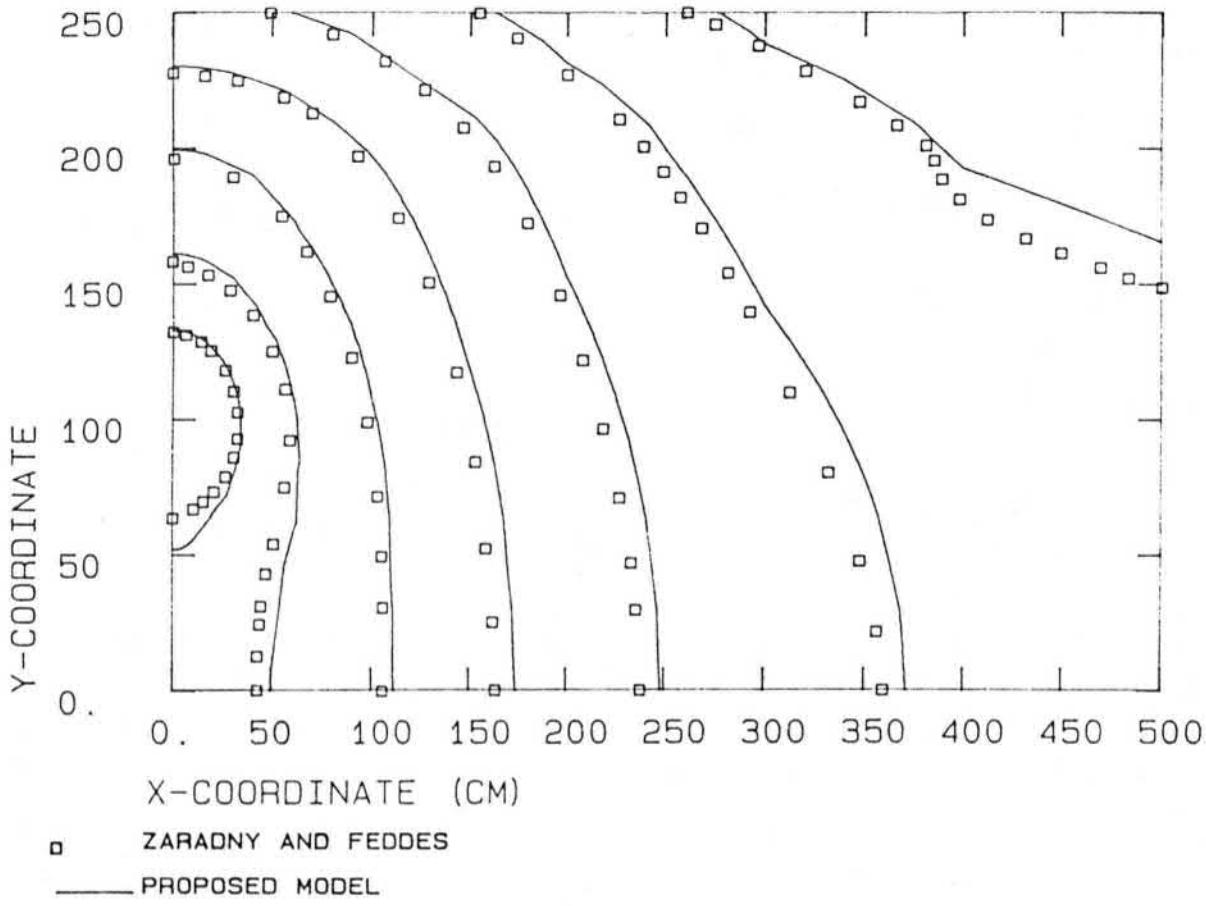

Fig. 6-7. Equipotential lines for the steady-state situation $P=0.1 \cdot K_S$, using a constant head as the boundary condition along the drain.

(Zaradny and Feddes, 1979):

$$H_R - H_{RD} = \Delta H_R = \frac{P \cdot L}{2 \cdot K_S} \ln\left[\frac{r}{r_D}\right] \qquad (6\text{-}2)$$

where H_R and H_{RD} are the average hydraulic heads at a distance r and the periphery of the drain, respectively, and L is the spacing between the drains. In this case the analytical solution for ΔH_R is 11.032 cm. From the numerical solution the average value of H for a distance of 5 cm from the middle of the

drain can be computed from the hydraulic heads in the neighbouring nodal points. According to the numerical solution the potential difference ΔH_5 is 10.521, i.e. the difference between the numerical and analytical solution is 4.6%, which is slightly greater than the error produced by the numerical solution of Zaradny and Feddes (4.1 %). The computed value is smaller than the analytical one, which is due to the tendency of the fully implicit solution to produce numerical diffusion (especially if the hydraulic gradients are steep).

A very important property of the numerical solution is its capability to preserve the mass balance. In this case the flow to the drain is calculated from (2-9) as a residual term since the boundary condition is of the Dirichlecht type in this example. The inflow to the system is also known, and the total water content of the system can be calculated as a function of the known pressure head values. Hence, it is possible to evaluate the accuracy of the water balance by calculating the net change in the total water content of the system and by comparing it with the net inflow of the system (rainfall minus flow to the drain). The error of the water balance was 0.5 % for $P=0.01 \cdot K_S$ and 2.0% for $P=0.1 \cdot K_S$ when time step 180 h was used in the calculations. The error was calculated by comparing the difference in the water balance with the net change of total water content in the system.

Two additional computer runs were carried out in order to reveal the sensitivity of the system to changes in saturated hydraulic conductivity. The change in the horizontal saturated conductivity was 10% in the first run and 20% in the second run. The effect of these changes on the computed shape of the water table can be seen in Fig. 6-8. According to Fig. 6-8, the effect of a 10% change in the horizontal hydraulic conductivity will easily mask the small difference observed between the numerical solution of Zaradny and Feddes (1979) and the proposed model.

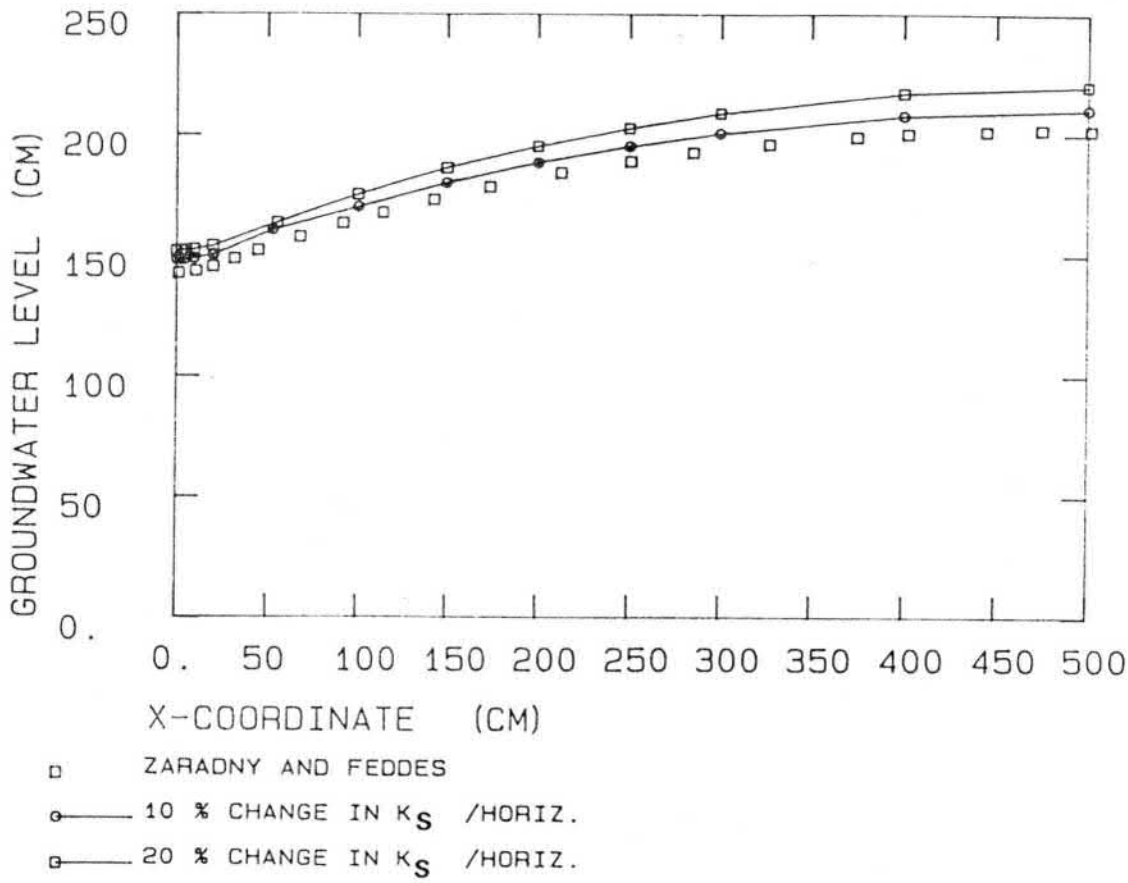

Fig. 6-8. The effect of 10 % and 20 % change, respectively, on the calculated shape of the water table.

6.3.3 Determination of hydraulic conductivity for two-dimensional drainage problem

The simplified Kalman filtering technique will be tested using the two-dimensional drainage problem discussed in previous sections. Here the measurements were generated using the known hydraulic conductivity values in the vertical and horizontal direction (= 12 $cm \cdot d^{-1}$ in both directions). The calculated shapes of the water table at five different distances from the drain (10 cm, 20 cm, 100 cm , 200 cm and 500 cm) were given as measurements. The measurement accuracy was assumed to be 1 cm. The period of 75 days was calculated and the measurement

interval was 7.5 days.

The initial values for the unknown hydraulic conductivity values were 2.4 $cm \cdot d^{-1}$ for both the vertical and the horizontal saturated conductivity (the true value being five times greater). With combined use of the two-dimensional model and the generated measurements of the shape of the water table, the simplified Kalman filtering technique should provide the correct parameter values. Here the measurements are accurate as should the parameter values be.

The results are shown in Fig. 6-9. In the beginning of the estimation procedure, the rise of the water table is very slow and therefore the parameter values are not substantially improved during the first 4-5 measurement intervals. However, after the 5th measurement, the water table begins to rise rapidly and the parameter estimates gradually become accurate as new measurements are used. After 10 time intervals, the errors in the parameter values are 0.4% and 0.9%, respectively.

6.4 Comparison of two-dimensional and quasi-two-dimensional solution of the drainage problem

A method for calculating the flow towards the drains is needed in the water management models. Many different types of solution methods could be used. The following are two of them:
1° Numerical solution of the two-dimensional Richards equation (see section 6.3).
2° One-dimensional solution of the Richards equation using the calculated flow towards the drains as a lower boundary condition (see section 4.2.3.2). This method is referred to as a quasi-two-dimensional solution of the drainage problem. In this case, calculation of the drainage rates can be based on the assumption that lateral movement occurs mainly in the saturated region. The effective horizontal saturated hydraulic conductivity is used and the flux is evaluated in terms of the water table elevation midway between the drains and the water level or hydraulic head in the drains.

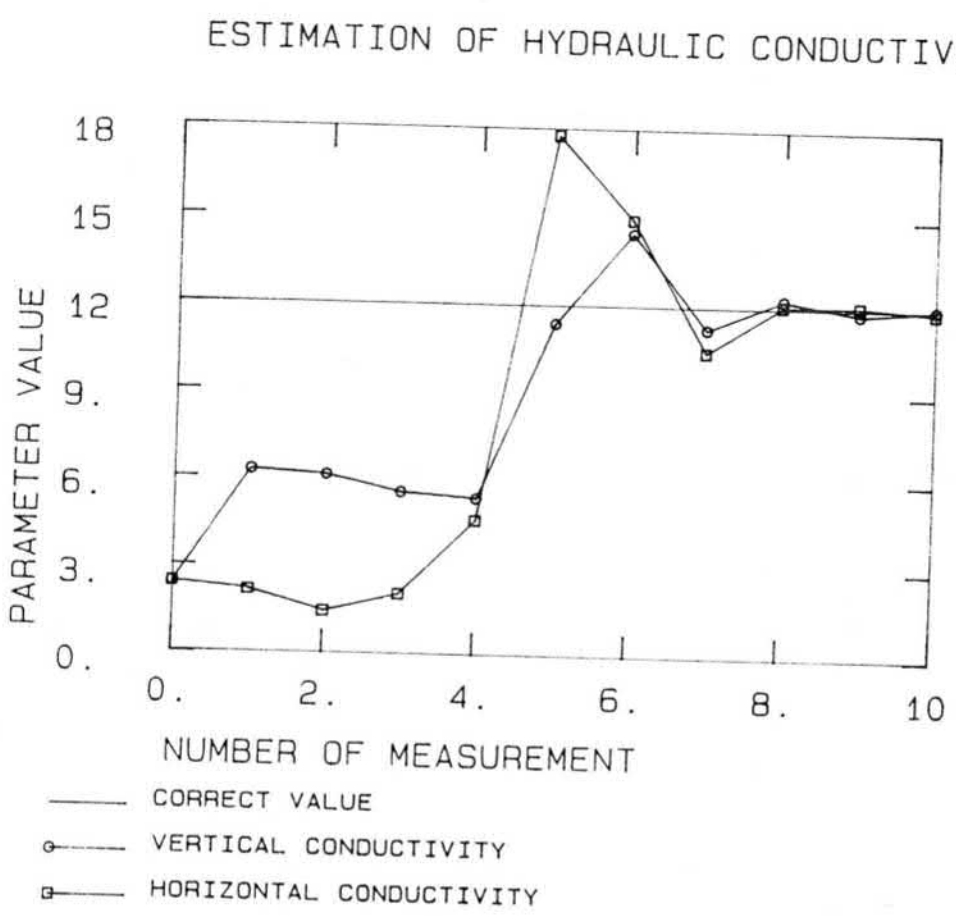

Fig. 6-9. The improvement in the parameter estimate.

There are two basic assumptions that produce difference in the two-dimensional and quasi-two-dimensional solution. First, the lateral movement of water in the unsaturated zone is neglected in the quasi-two-dimensional model. Second, the solution of the alternative 2° is based on the Dupuit-Forchheimer assumptions; the hydraulic gradient at any point is equal to the slope of the water table above that point, i.e. water flows horizontally because all the equipotentials are vertical planes. The error produced by these assumptions has to be compared with the error produced by inadequate field data in order to determine whether e.g. a small error in the saturated hydraulic conductivity will mask the additional sensitivity obtained with the more precise methods.

Skaggs and Tang (1976) have made a comparison between the solution of the two-dimensional Richards equation and the solution of the more approximate Boussinesq equation. According to Skaggs and Tang, there is little to be gained by solving the Richards equation instead of using simpler approximate methods for drawdown prediction unless enough measurements are made to define the field-effective values of both saturated and unsaturated field properties. In the comparison of Skaggs and Tang, the case of a continous fluctuation of the elevation of the water table was not included.

The comparison of these solutions (alternatives 1° and 2°) has to be carried out both in the steady-state situation and in the transient case. The variables that are of special importance are the elevation of the water table, cumulative flow to drains and cumulative transpiration rate. In the two-dimensional solution of the Richards equation, there are also numerous sources of error: field variability and uncertainty in the soil hydraulic properties, the entrance resistance of the drain, error in the depth of the restrictive layer and the representation of the drain tubes in the finite element method.

6.4.1 Comparison of steady-state flow rates

In order to compare solutions of the two-dimensional and quasi-two-dimensional model, it is necessary to select the method for calculating the flow towards the drains. Three different equations were tested:

1) Hooghoudt's steady-state equation, as used by van Schilfgaarde (1963, ref. Skaggs, 1980), which is also used in the DRAINMOD-model.

$$q_d = \frac{8 \cdot K_s \cdot D_e \cdot h_m + 4 \cdot K_s \cdot h_m^2}{L^2} \qquad (6\text{-}3)$$

2) The original form of the Hooghoudt's equation (Wesseling, 1973):

$$q_d = \frac{K_s \cdot h_m}{L} \cdot \left\{ \frac{(L - 0.5 \cdot D_d \cdot \sqrt{2})^2}{8\, D_d \cdot L} + \frac{1}{\pi} \ln \frac{D_d}{r_e \sqrt{2}} \right\}^{-1} \quad (6\text{-}4)$$

3) The Ernst equation (Wesseling, 1973):

$$q_d = \frac{K_s \cdot h_m}{L} \cdot \left\{ \frac{L}{8 \cdot D_d} + \frac{1}{\pi} \ln \frac{D_d}{r_e \cdot \pi} \right\}^{-1} \quad (6\text{-}5)$$

where q_d is the flux ($m \cdot d^{-1}$), h_m is the midpoint water table height above the drain (m), K_s is the equivalent lateral hydraulic conductivity ($m \cdot d^{-1}$), D_d is the depth from the drains to the impermeable layer (m), D_e is the equivalent depth from the drains to the impermeable layer (m), L is the spacing between the drains (m) and r_e is the effective drain tube radius (m). D_e can be calculated from (Skaggs, 1980):
For $0 < D_d/L < 0.3$

$$D_e = \frac{D_d}{1 + [D_d/L] \cdot \{(8/3.14)\ \ln[D_d/r_e] - a_{er}\}} \quad (6\text{-}6)$$

in which

$$a_{er} = 3.55 - \frac{1.6 \cdot D_d}{L} + 2 \cdot [D_d/L]^2 \quad (6\text{-}7)$$

and for $D_d/L > 0.3$

$$D_e = \frac{L}{8\ \{\ln [L \cdot r_e] - 1.15\}} \quad (6\text{-}8)$$

The entrance resistance of a drain tube may be defined as an additional loss of head caused by the partial permeability of its wall (Wesseling and Homma, 1967). In most of the drainage equations applied for calculating the flow to drains, an ideal drain is assumed and hence the entrance resistance is not taken

into account. However, in practical drainage situations this assumption is not always true. As a result, an extra potential loss due to the presence of an entrance resistance may manifest itself in a higher groundwater table with the possible consequence of inadequate drainage. Especially in soils with a relatively low hydraulic conductivity, the effect of entrance resistance is considerable. Especially thick envelopes are effective in reducing the entrance resistance (Sekendar, 1984).

6.4.1.1 Assumption of an ideal drain

Consider first the case in which the entrance resistance is assumed to be zero and it is necessary to calculate the steady-state flux to the drains. In the two-dimensional model, a constant hydraulic head was used as a boundary condition along the drain. The results are shown in Fig. 6-10 and 6-11 for four different drain spacings: 10 , 16, 24 and 40 m using a 'suitably' selected K_s value in order to prevent the profile from coming fully saturated. The K_s -values used were 0.12, 0.4, 1.0 and 2.0 $m \cdot d^{-1}$ for drain spacings 10, 16, 24 and 40 m, respectively. D_d was 1.0 m, r_e 0.025 m and h_m 0.7 - 1.0 m for different drain spacings.

In Fig. 6-10, the steady-state flow towards the drains is given for two different drain spacings - 10 and 40 m - as a function of water table elevation midway between the drains. In Fig. 6-11, the error introduced in the calculated flow rate is given as a function of drain spacing. According to Fig. 6-10, the quasi-two-dimensional method gives lower flow rates for all h_m values. There are two main reasons for the underestimation of the flow rates when equations (6-3) - (6-5) are used for predicting the effect of subsurface drains. First, the effect of the unsaturated slab is neglected in the quasi-two-dimensional models. Second, the effect of overpressure is not included in equations (6-3)-(6-5). i.e. the situation in which the drain is running full with back pressure (see Fig. 6-12).

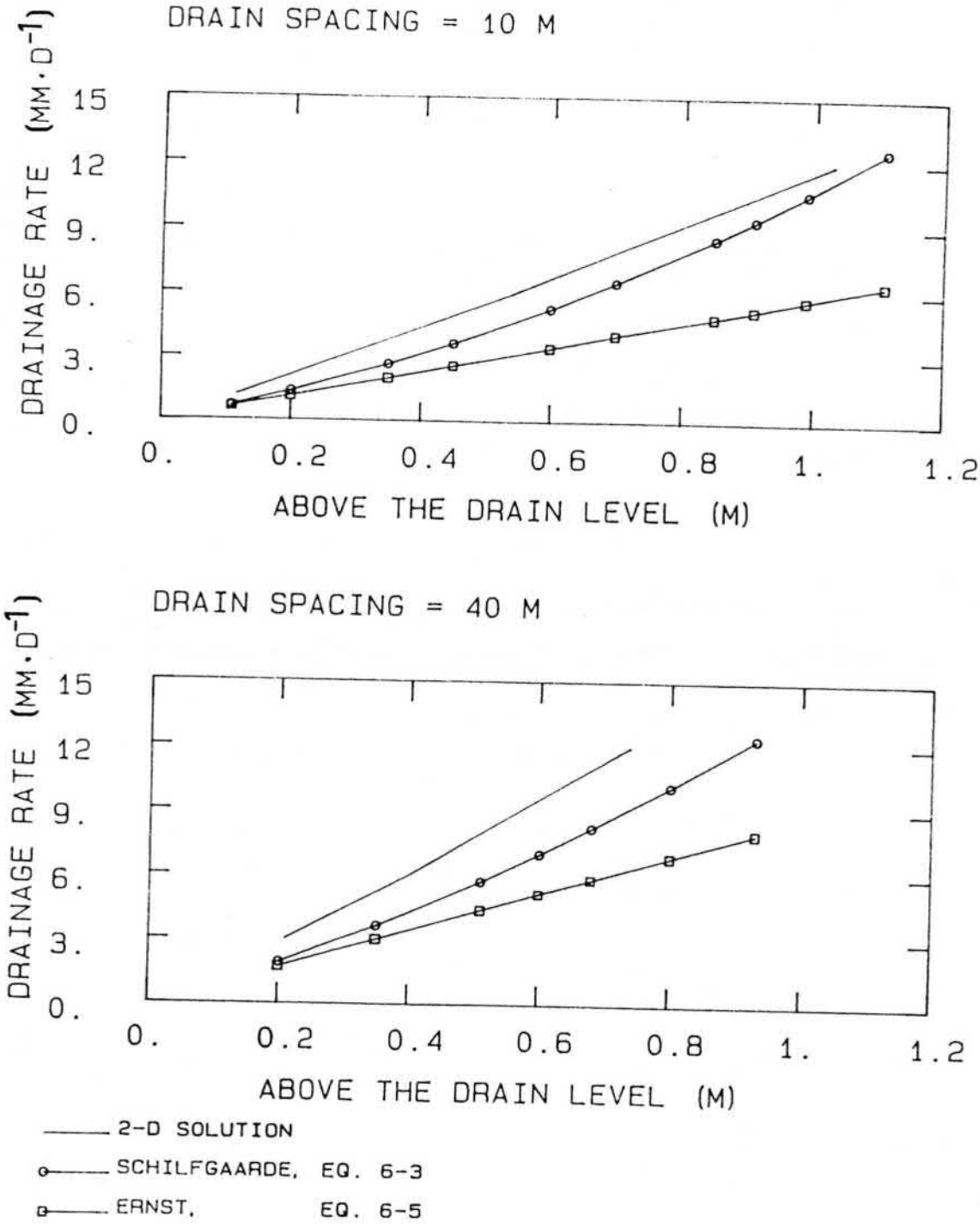

Fig. 6-10 Drainage rate as a function of water table elevation midway between the drains. a) L = 10 m, b) L = 40 m.

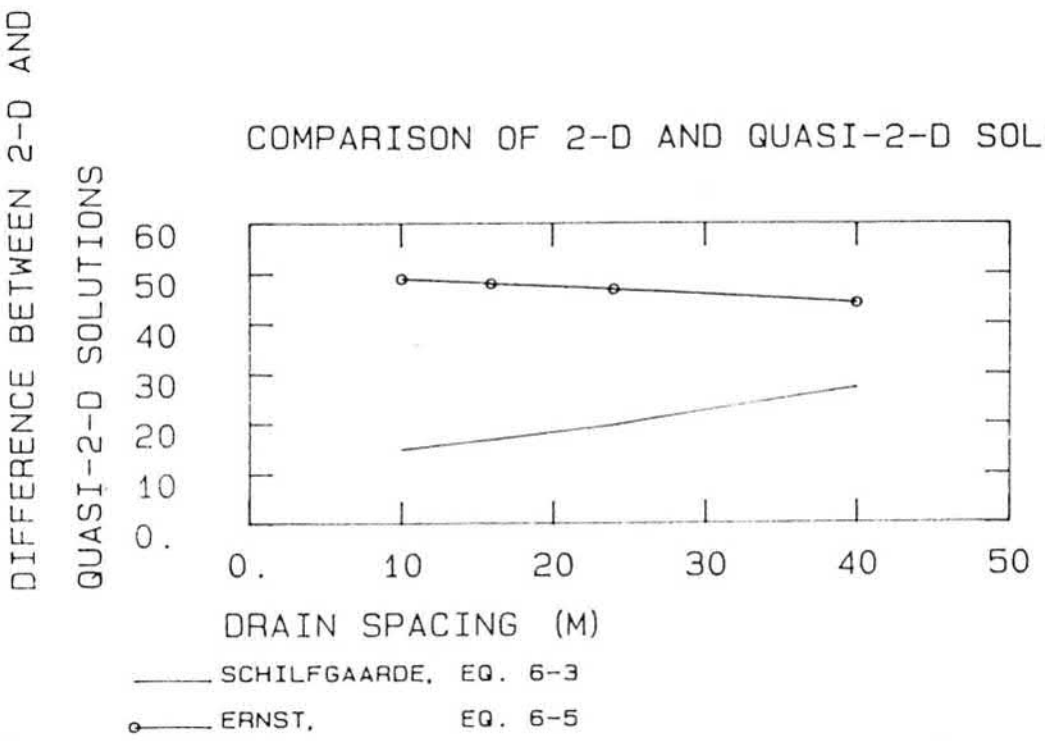

Fig. 6-11 The error of the quasi-two-dimensional solution compared to the solution of the two-dimensional Richards equation (steady-state situation with q_d equal to 8.64 $mm \cdot d^{-1}$).

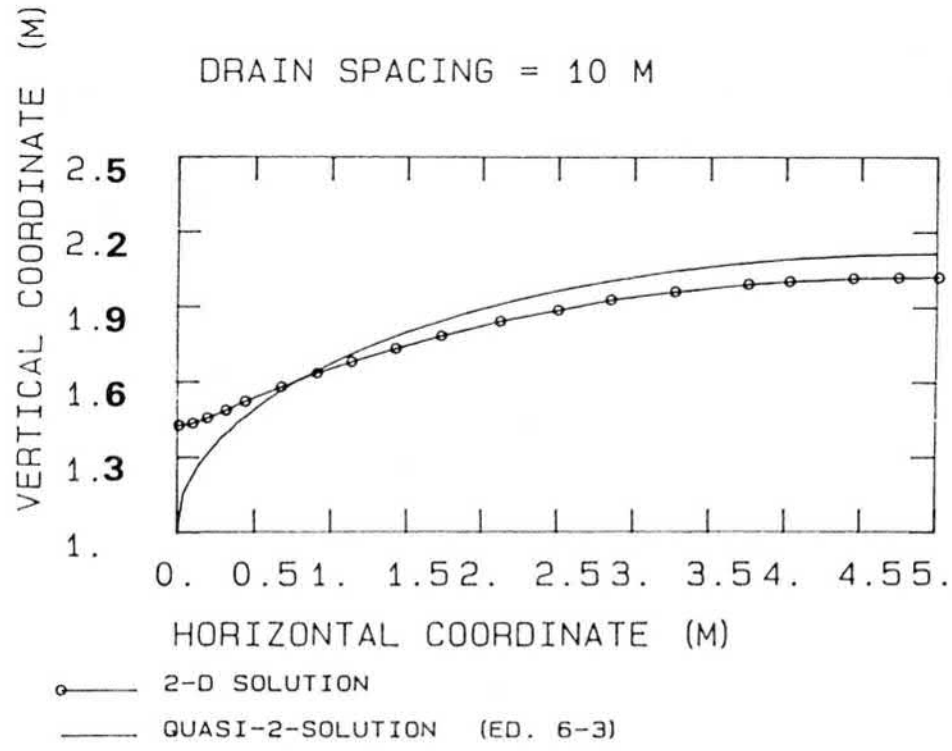

Fig. 6-12. The steady-state water table for drainage rate q_d=12 $mm \cdot d^{-1}$

According to Fig. 6-11, the error increases with decreasing drain spacing. The smaller the drain spacing, the greater the effect of the unsaturated slab. Moreover, the relative effect of the back pressure increases with decreasing drain spacing.

Equation (6-3) gave considerably better results compared with equations (6-4) and (6-5). This is due to the fact that the lateral flow above the drain level is included in equation (6-3) but not in the other equations used in testing. The underestimation of flow rate compared with the two-dimensional solution was about 50-60% for a flow rate 8.64 $mm \cdot d^{-1}$ (1.0 $l \cdot s^{-1} \cdot ha^{-1}$) which is the usual drainage coefficient used in Finland. When equation (6-3) was used, the underestimation was about 20%. Therefore, it is possible to recommend that an equation that takes into account the lateral flow above the drain level (e.g. the Hooghoudt equation equation (6-3), as used by Skaggs (1980) in the DRAINMOD model), should be used in the quasi- two-dimensional model.

6.4.1.2 Effect of inadequate field data on the flow rate

In the comparison presented in the previous section, it was implicitly assumed that the field data are completely accurate and the entrance resistance is equal to zero. This is not the case when a water management model is used for quantifying the effect of drainage on soil water regime. The effective horizontal hydraulic conductivity is difficult to measure accurately, especially in inhomogenous soils. The entrance resistance of a real tube can have a significant influence on the water table if envelope materials are not used. In practical design, it is always difficult to determine the depth of the impermeable layer accurately .

According to equations (6-3)-(6-5), the calculated flux is directly proportional to the effective horizontal hydraulic conductivity. An error of 20-25% in the effective K_S-value will mask the additional accuracy obtained from the two-dimensional solution (see Figs. 6-10 and 6-11), if the flow rate is calculated using equation (6-3). Rintanen (1986) has measured the saturated hydraulic conductivity of some Finnish soils with the falling head permeameter method. For homogenous sandy loam, the 50% and 90% confidence intervals were the mean value ±10% and the mean value ±25%, respectively. The total number of samples in this case was 57. For heterogenous sandy clay , the 50% confidence interval was the mean value ±60%. Consequently, it can be concluded that the uncertainty involved in the effective horizontal conductivity will mask the additional sensitivity obtained from the Richards equation unless accurate measurements of K_S-values are at disposal.

The depth of the restrictive layer also has a very pronounced effect on the calculated flow rates. A few computer runs were carried out using equation (6-3) to reveal the sensitivity of the q_d to small errors in D_d. The results are given in Fig. 6-13. The error introduced is a function of drain spacing and the actual depth of the restricting layer. E.g., an error of 0.3 m in D_d (0.7 m instead of 0.4 m for drain spacing equal to 40 m) produces flow rates that are overestimated by 35%. Another example is the case when the true value of D_d is 1.9 m and a value equal to 2.5 m is used in the calculations (drain spacing is 16 m). In this case the error in the flow rate is only 6%. In most cases, the depth to the restricting layer varies considerably in field conditions and the effect of the errors in the D_d values can be as big as the error introduced by the quasi- two-dimensional solution.

For real, rather than completely open drain tubes, the additional loss of hydraulic head due to entrance resistance should be taken into account. The total resistance W_{tot} of a real drain is the sum of the radial resistance W_r and the entrance resistace W_e, i.e. $W_{tot} = W_r + W_s$. Consider an ideal

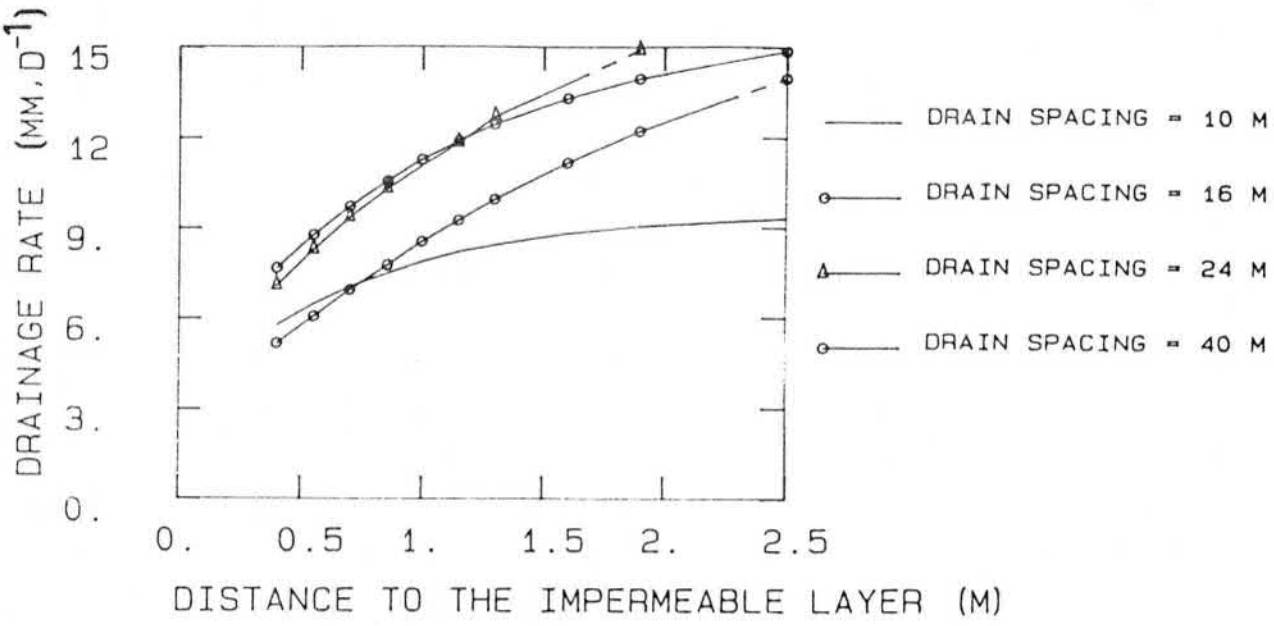

Fig. 6-13. Calculated drainage rate as a function of the depth from the drains to the impermeable layer(h_m=0.7 m, r_e=0.025 m, K_S according to the text).

drain of radius r_o and a homogenous surrounding soil of radius r_h. The radial resistance of such an ideal drain can be expressed as (e.g. Sekendar, 1984):

$$W_r = \frac{1}{2\pi K} \ln[r_h/r_o] \qquad (6\text{-}9)$$

The effect of entrance resistance can be approximated by defining an effective drain tube radius, r_e such that a completely open drain tube with radius r_e will offer the same resistance to inflow as a real tube with radius r_o. I.e., the entrance resistance can be thought of as an extra resistance between r_o and the imaginary effective radius, r_e. Hence:

$$W_e = \frac{1}{2\pi K_S} \ln[r_o/r_e] \qquad (6\text{-}10)$$

so that

$$r_e = r_o \cdot \exp[-2\pi K_S \cdot W_e] \qquad (6\text{-}11)$$

An entrance resistance parameter a_e, which is independent of the hydraulic conductivity of the soil, is defined as (Sekendar, 1984):

$$a_e = W_e \cdot K_S \qquad (6\text{-}12)$$

The loss of hydraulic head due to entrance resistance, h_e, can be calculated as follows (Wesseling and Homma, 1967):

$$h_e = q_d \cdot L \cdot W_e \qquad (6\text{-}13)$$

Wesseling and Homma (1967) and Sekendar (1984) have reported values for entrance parameter a_e for different types of envelopes. For a completely naked pipe, a_e values of 0.30 - 0.45 were obtained corresponding to an effective radius of 1.5 - 3.8 mm for a 50 mm diameter pipe, i.e. 6 - 15% from the radius of an ideal drain. The effective radius can be increased considerably by using e.g. a gravel envelope. According to Mohammad and Skaggs (1983), use of a 50 mm thick envelope resulted in an increase in the effective drain radius for a 100 mm diameter pipe from 5 mm to 55 mm by a 50 mm gravel thickness, i.e. to a value that is greater than the radius of an ideal drain. For the other envelope materials tested (fibre sheet, polyster sheet, coco fibre, synthetic fibre, glass wool) the effective radius increased considerably, so that the final values were 40 - 90% from the radius of an ideal drain.

As a general rule it can be stated that the lower the hydraulic conductivity of the soil, the greater the effect of the entrance resistance. In Fig. 6-14, the loss of hydraulic head due to entrance resistance is given for different K_S-values as a function of the effective radius r_e (50 mm pipe with q_d value equal to 8.64 $mm \cdot d^{-1}$). If the hydraulic conductivity of the surrounding soil is low, 0.1 $m \cdot d^{-1}$, the loss of hydraulic head with small r_e values can be very high, indicating that the envelope material is of special importance for poorly

impermeable soils. For soils with high hydraulic conductivity, the effect of entrance resistance is negligible even for naked pipes.

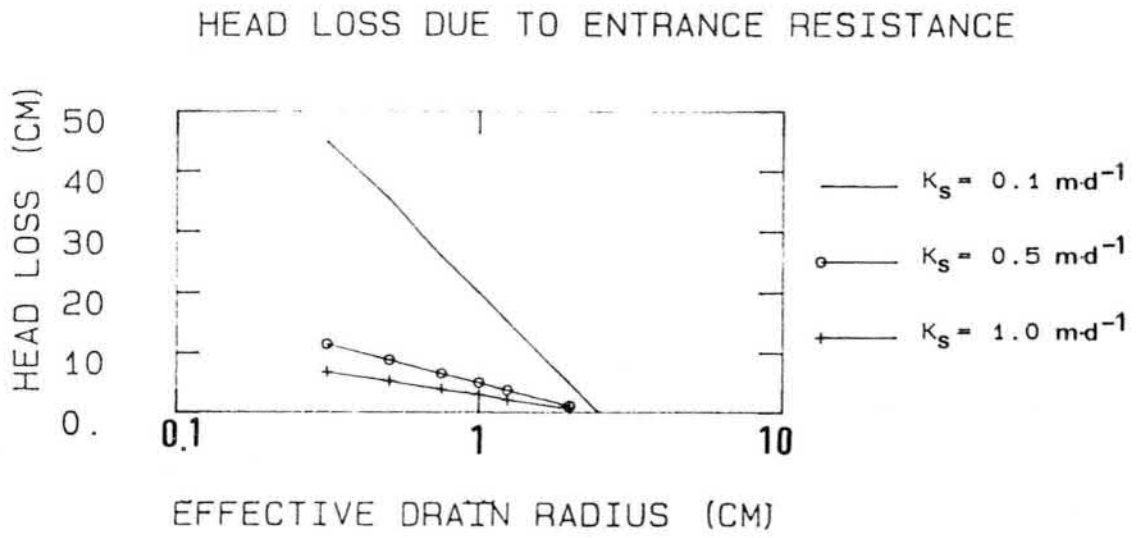

Fig. 6-14. Loss of hydraulic head due to entrance resistance as a function of effective radius for different K_S -values.

The effect of the entrance resistance should be taken into account in the two-dimensional solution of Richard's equation. It is not easy to determine the true value of the effective radius in practical calculations. Moreover, the use of a small drain produces difficulties in the numerical solution, e.g. requiring a very dense network of elements in the vicinity of the drain (see e.g. Fipps and Skaggs, 1986). Therefore, it seems preferable to use the quasi-two-dimensional solution to avoid the difficulties mentioned above.

As an overall summary of the results presented in this section, it can be recommended that in a water management model there is little to be gained by using the fully two-dimensional solution instead of approximate methods for calculation of the steady state flow rates and the elevation of water table. In the next section, the case of a fluctuating water table is considered.

6.4.2 Comparison of two-dimensional and quasi-two- dimensional models in transient state

Three different type of years - wet , normal and dry - were used in the comparison of two-dimensional and quasi-two-dimensional models of drainage. The soil water retention curve and hydraulic conductivity curve were the same that were used in the test example of Zaradny and Feddes (1979) (section 6.3.2).

Computed groundwater level for wet year (two months during the growing season) is given in Fig. 6-15. It can be seen that the computed groundwater level obtained by using the quasi-two-dimensional solution is almost all the time closer to the soil surface. However, the difference between these solutions is almost all the time less than 10 cm. The timing of the fluctuation of the groudwater level is almost exactly the same. There were observed no difference in the computed actual transpiration sum - in fact the transpiration rate was almost potential in both of the model versions.

During normal and dry years the computed groundwater level remained below the drain level and the computed actual transpiration rate differed from each other less than 3%. The small differencies are probably due to different numerical properties of the models.

The following conclusion can be drawn based on the three years of simulation: In the case that the groundwater level is not close to the soil surface during the growing season, two-dimensional and quasi-two- dimensional model give almost the same cumulative actual transpiration rate. However, a case where groundwater level is very near the soil surface for a long time during the growing season and the hydraulic parameters are very accurate, it may be advisable to use the two-dimensional solution.

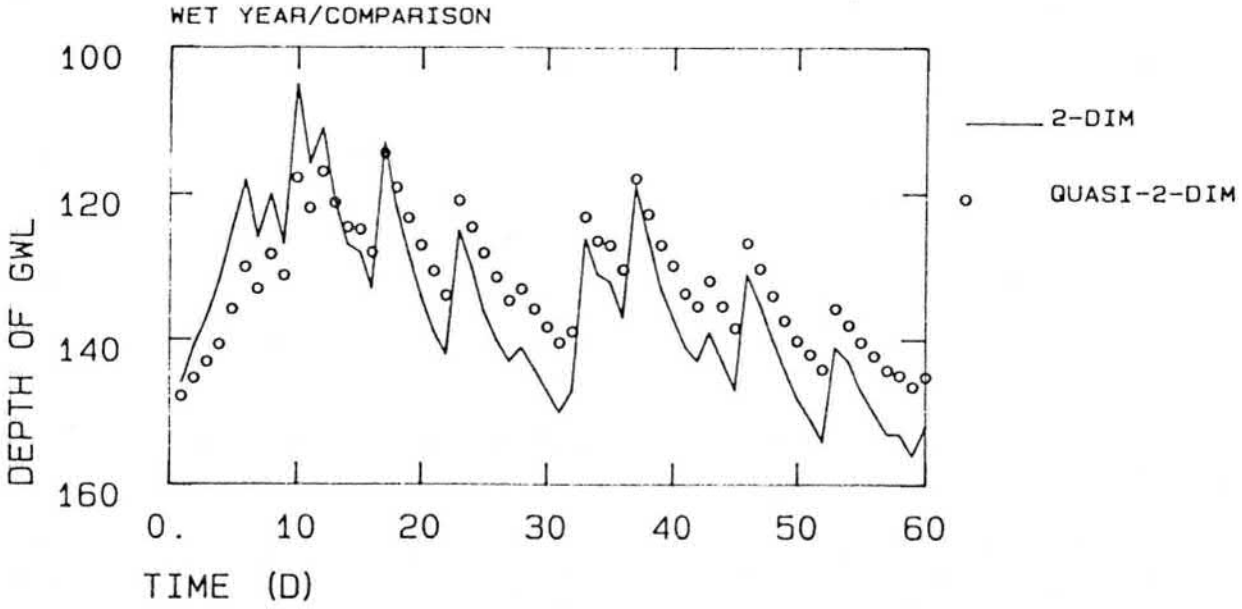

Fig. 6-15. Comparison of the depth of groundwater level when two-dimensional (Richards equation) and quasi-two- dimensional model are used (computation of a wet year).

7 VERIFICATION OF MODELS WITH FIELD EXPERIMENTS

7.1 Introduction

The models described in the previous Chapters have to be verified with data from field experiments. Unfortunately, a complete data set from one field experiment which would have included all the essential output variables, i.e. soil moisture, soil temperature and crop yield was not available. Hence, it was necessary to use the results obtained from Backas and Maasoja field experiments to verify the selected models.

Using the data measured at Backas experimental field it is possible to evaluate the capability of the model to simulate the winter and spring period - snow accumulation, snow melting and soil freezing and thawing phenomena. Testing with the data obtained at Backas was carried out with two primary objectives in mind. Firstly, to examine the capability of the simplified Kalman filter to produce reliable estimates of the soil thermal conductivity. Secondly, to test the accuracy of the soil temperature and soil moisture predictions when the upper boundary condition of the heat balance equation is calculated with the method given in section 4.4 (snow model).

The main aim of the Maasoja experiment was to test if the crop model can produce reasonably accurate results in the case that the field data is incomplete. Moreover, the objective was to try to find those crop parameters which are most uncertain and which should be measured more intensively in Finnish conditions.

7.2 Backas experimental field

7.2.1 pF-curve and hydraulic conductivity curve

The soil water retention curves and hydraulic conductivity values were not measured and it was necessary to estimate them based on the methods described in Chapter 3. The two estimated soil water retention curves are

shown in Fig. 7-1 and the relative unsaturated hydraulic conductivity functions determined by the method presented in section 3.3 is given in Fig. 7-2. The saturated hydraulic conductivity was estimated using the method of Bloemen (1980) which is based on soil texture. For topsoil, K_S-value 0.1 $cm \cdot d^{-1}$ was obtained and for subsoil, the corresponding value was 0.07 $cm \cdot d^{-1}$.

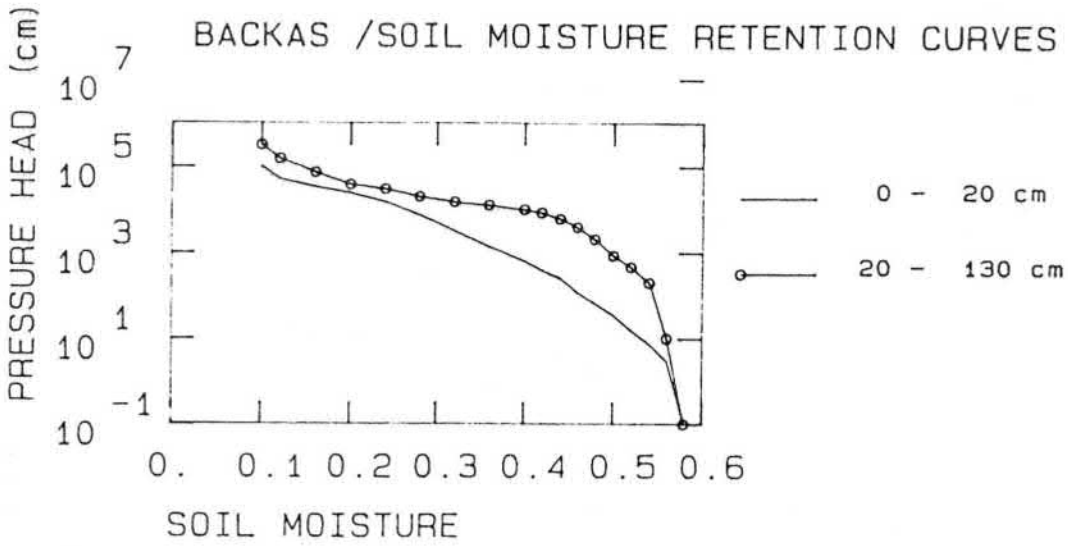

Fig. 7-1. Estimated soil water retention curves at the experimental field Backas.

7.2.2 Determination of soil thermal conductivity

The results obtained at the Backas are experimental field ideally suited for the verification of the heat balance model because the soil temperature was measured at different depths as a function of time. The estimation of the soil thermal conductivity was based on a short observation period in 14-15.5.1941 (24 hours) when the soil temperature was measured every second hour. The general idea behind the application of the simplified Kalman filter (see section 3.4) is to fully utilize an intensive measurement period.

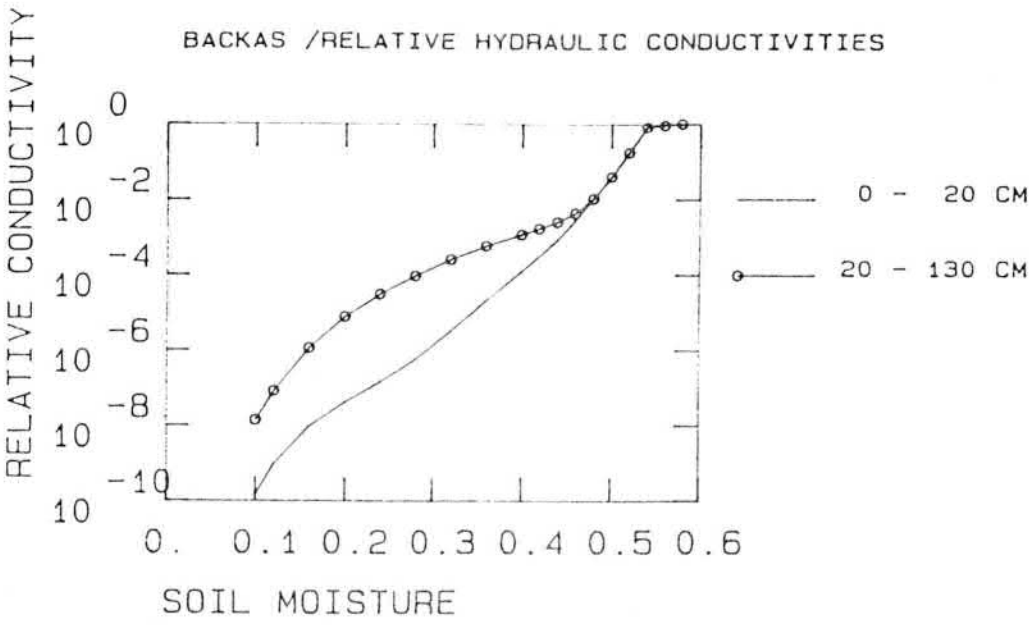

Fig. 7-2. Computed relative unsaturated hydraulic conductivity at the experimental field Backas.

The simplified Kalman filter was used to estimate the soil thermal conductivity using measured soil temperature (at point B) at 2.5 cm as an upper boundary condition and measured soil temperature at 125 cm as a lower boundary condition. The intermediate soil temperature measurements at depths 5, 10, 15, 20, 30, 40, 50, 60, 80 and 100 cm were given as the measurements. Soil moisture was assumed to be constant during the 24 hours. According to the estimation procedure, soil thermal conductivity can be represented by a function

$$K_T(w) = 0.56 + 0.57 \sqrt{w} \quad (W \cdot m^{-1} \cdot {}^{\circ}C^{-1}) \qquad (7\text{-}1)$$

The computed soil temperature values from the calibration period are given in Fig. 7-3. The results show a very good agreement between the measured and computed values, indicating that the simplified Kalman filter seems to be very well suited for the parameter estimation of the heat balance equation.

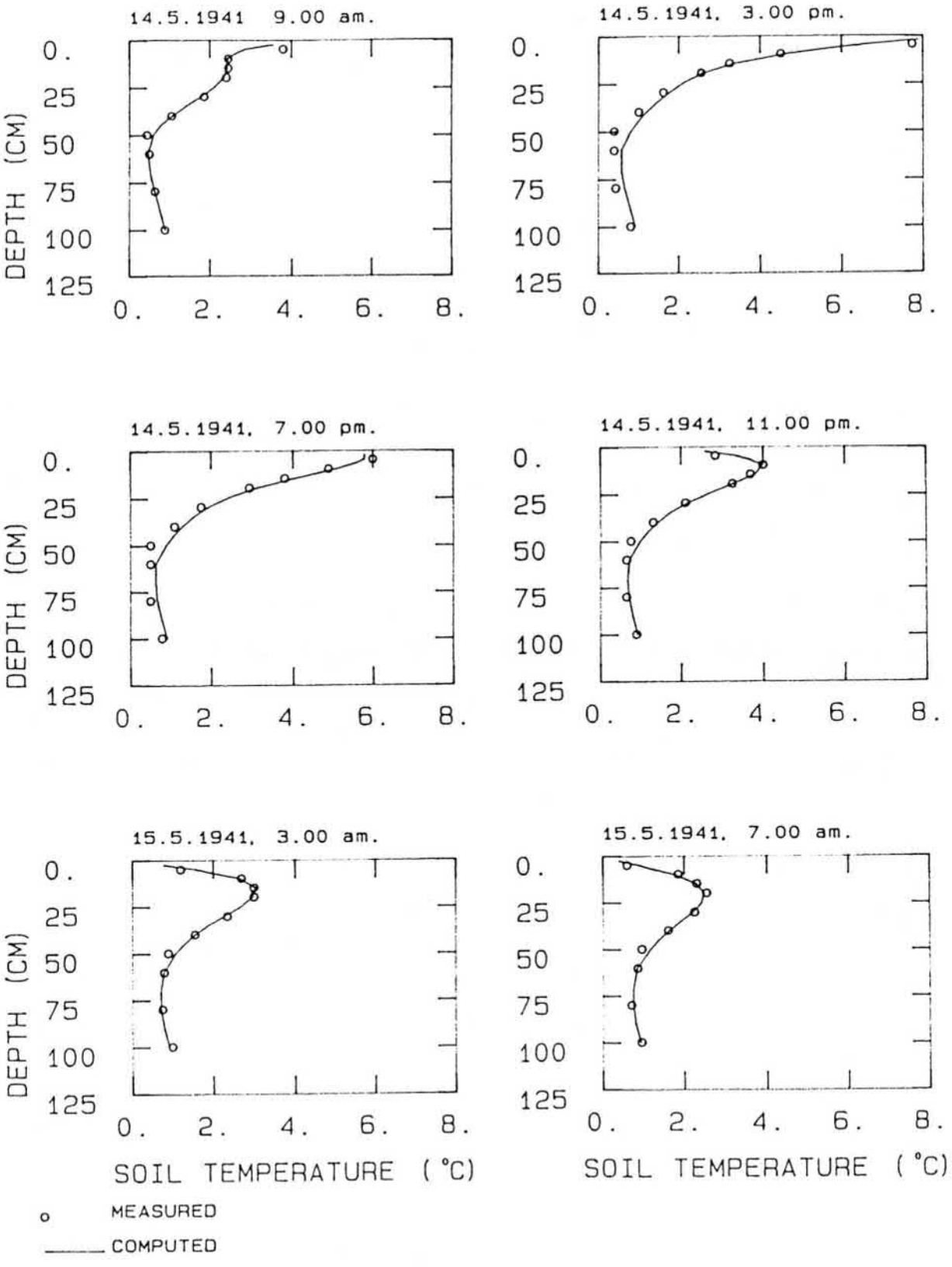

Fig. 7-3. Measured and computed soil temperature profiles during the calibration period.

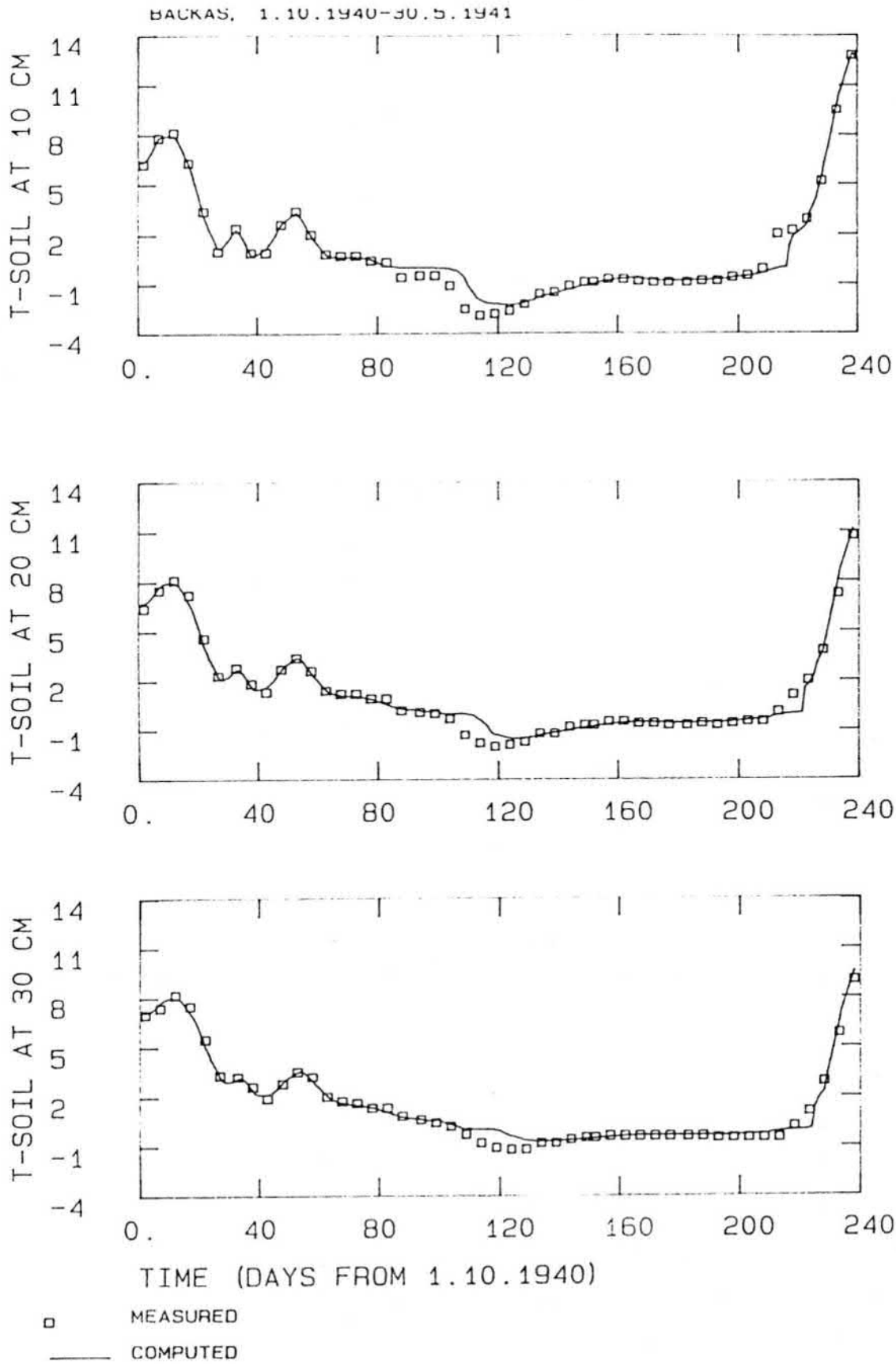

Fig. 7-4a-c. Measured and computed soil temperature during the verification period (1.10.1940 - 31.5.1941) at five different depths, a) 10 cm, b)20 cm and c) 30 cm.

The calibrated thermal conductivity curve was verified with a period of 8 months (1.10.1940 - 31.5.1941). The upper and lower boundary conditions were also given as measured input series. The results from the verification period are shown in Fig. 7-4 as a function of time at five different depths.

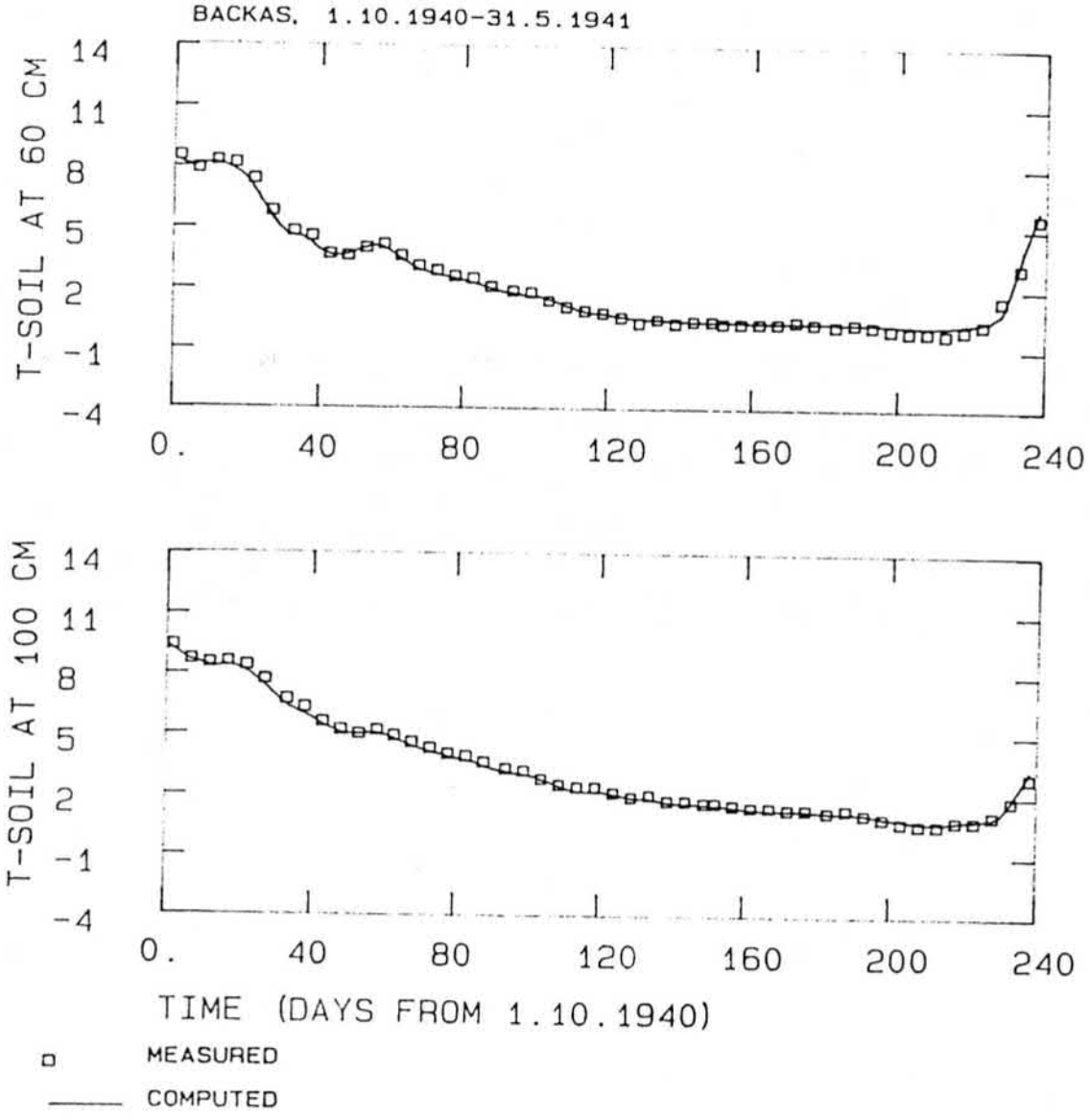

Fig. 7-4d-e. Measured and computed soil temperature during the verification period (1.10.1940 - 31.5.1941) at five different depths d) 60 cm and e) 100 cm.

The predicted and measured soil temperature values are very close to each other, indicating that the estimated soil thermal conductivity values are accurate. The only exception is the frozen period, since the energy released/stored as latent heat has a great influence on the soil temperature profile. For example, at a depth of 10 cm, the computed soil temperature is about 0.5 - 1 °C too high between time t=90 d and t=120 d. This is because during the freezing period the assumed unfrozen water content must have been too low, i.e. the amount of frozen water was too high, resulting in a slower advance of the frost depth. The opposite effect can be seen during the time period t = 210 and t=215, where the computed soil temperature is too low, indicating that more energy was needed to raise the temperature of the soil since the amount of frozen water was overestimated. This example shows very clearly that the estimation of the unfrozen water content is the most probable source of error in the prediction of soil temperatures. Even in a well-defined case like this, the error in the soil temperature can be of the order of 1 °C. The error tends to be higher in the actual prediction of soil temperatures when the upper and lower boundary conditions have to be approximated (see section 7.2.3).

7.2.3 Prediction of soil temperature, soil moisture and frost depth

In section 7.2.2, the soil temperature values were calculated assuming that the upper and lower boundary condition of the heat balance equation are known in advance. Generally this is not the case. For snowfree periods the air temperature must be used as the upper boundary condition. If the soil is covered with snow, the upper boundary condition must be approximated by the method described in section 4.4 (equation 4-41). In order to be able to predict the soil surface temperature, a snow model must be included since the snowcover effectively dampens large fluctuations in the air temperature.

The lower boundary condition of the heat balance equation also causes some problems. Here the profile is extended to the depth of 7 m, and it is assumed that the lower boundary is a no-flow boundary in the heat balance equation.

The lower boundary condition in the mass balance equation was a calculated flow rate towards the subsurface drains. The drain spacing was 16 m, the drain depth 1 m, the depth to the restricting layer was assumed to 2 m, the effective drain radius 0.025 m - pipe surrounded by gravel envelope - and the lateral hydraulic conductivity 0.01 $m \cdot d^{-1}$. The upper boundary was treated as an infiltration boundary according to the method in section 4.2.3.

The results from the numerical experiments have been presented in Fig. 7-5 for soil temperature at four depths, in Fig.7-6 for soil moisture at three different depths, in Fig. 7-7 for groundwater level depth and in Fig. 7-8 for frost depth and depth of snow.

The accuracy of the soil temperature prediction is not as high as in the previous section because the upper boundary condition was computed for periods with snow cover and for snow-free periods the measured air temperature was used as an upper boundary condition. For unfrozen periods the computed values are in good agreement with the measured values. When the soil is frozen, the computed values tend to be higher than the measured values. This is mainly due to an overestimated soil moisture content in the uppermost 40 cm (see Fig. 7-6). Moreover, the estimation of unfrozen water content as a function of soil temperature may contribute to errors in computed soil temperature.

Figs. 7-5a and 7-8 show that the computation of soil temperature is greatly affected by relatively small errors in the predicted depth of snow cover. Computed soil temperature is about 1- 2 °C too low for a period between t=83 d and t=100 (Fig. 7-5a). The main reason for the underestimation of the

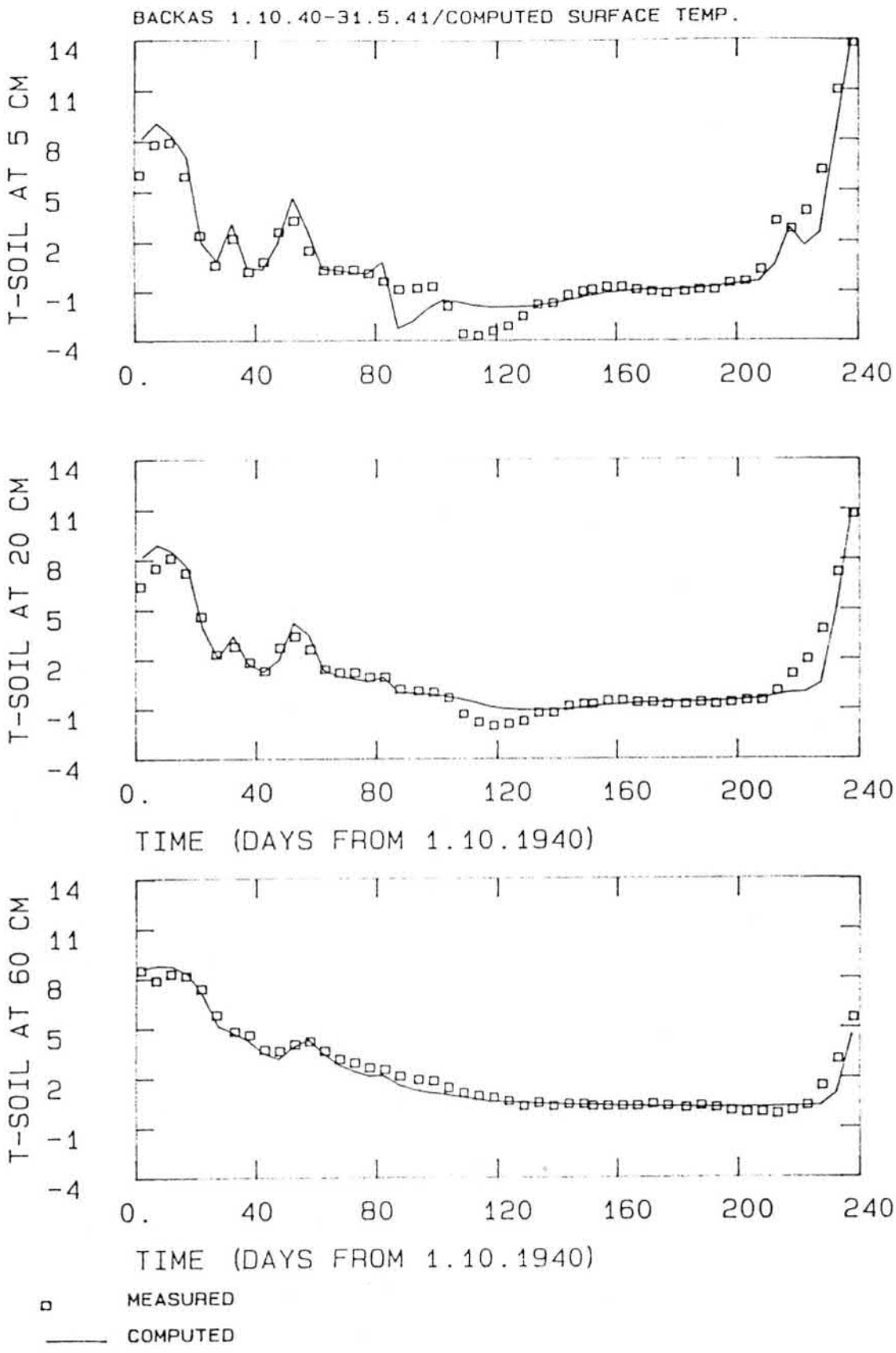

Fig. 7-5a-c. Measured and computed soil temperature at four different depths in the case that soil surface temperature was calculated, a) 5 cm, b) 20 cm and c) 60 cm.

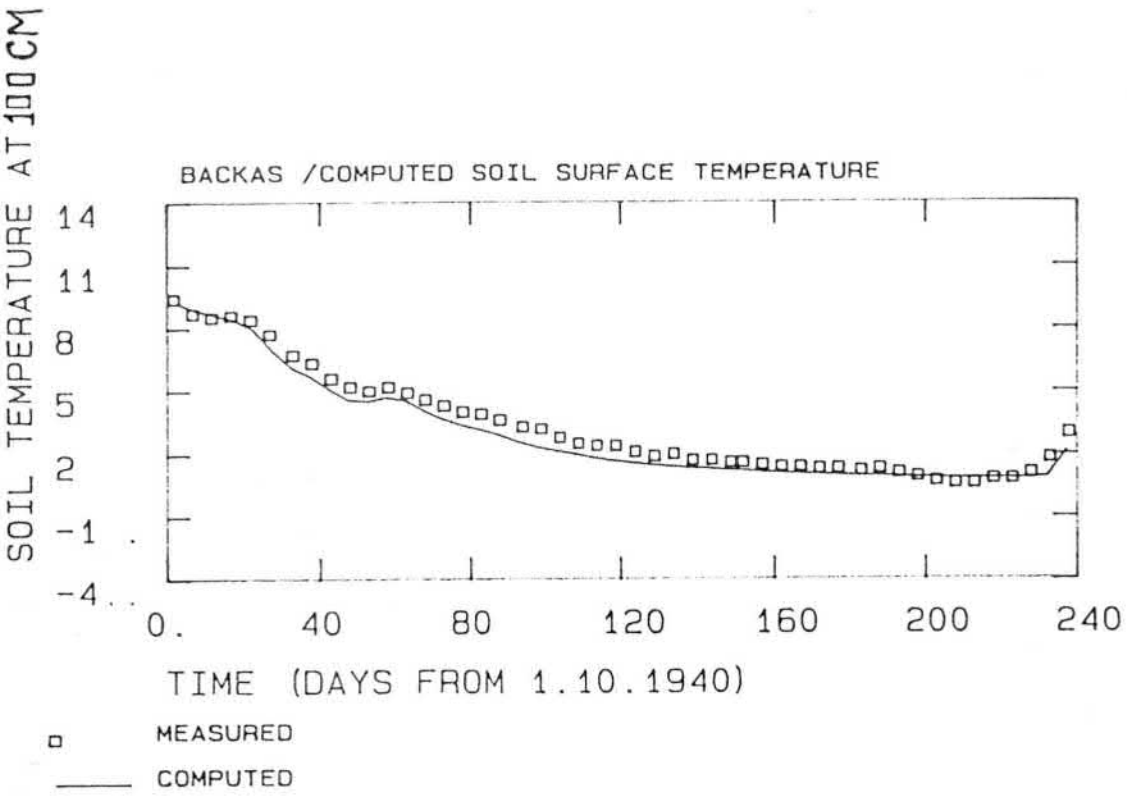

Fig. 7-5d. Measured and computed soil temperature at four different depths in the case that soil surface temperature was calculated, d) 100 cm.

soil temperature during that time is that the computed snow depth was equal to zero, whereas the measured snow depth was about 10 cm. The model assumed that the soil surface temperature was equal to the air temperature (about - 4 °C), but actually a higher boundary condition should have been used due to the existing snow cover.

The computed soil moisture content (Fig. 7-6) and predicted depth of the groundwater level (Fig. 7-7) are in relatively poor agreement with the measured values. By calibrating the saturated hydraulic conductivity values, it would be possible to obtain better simulation results. However, there was not a suitable period of intensive measurements which could have been used in the simplified Kalman filter and the first estimates based on the method of Bloemen (1980) were therefore accepted as final values for the saturated K_s-values.

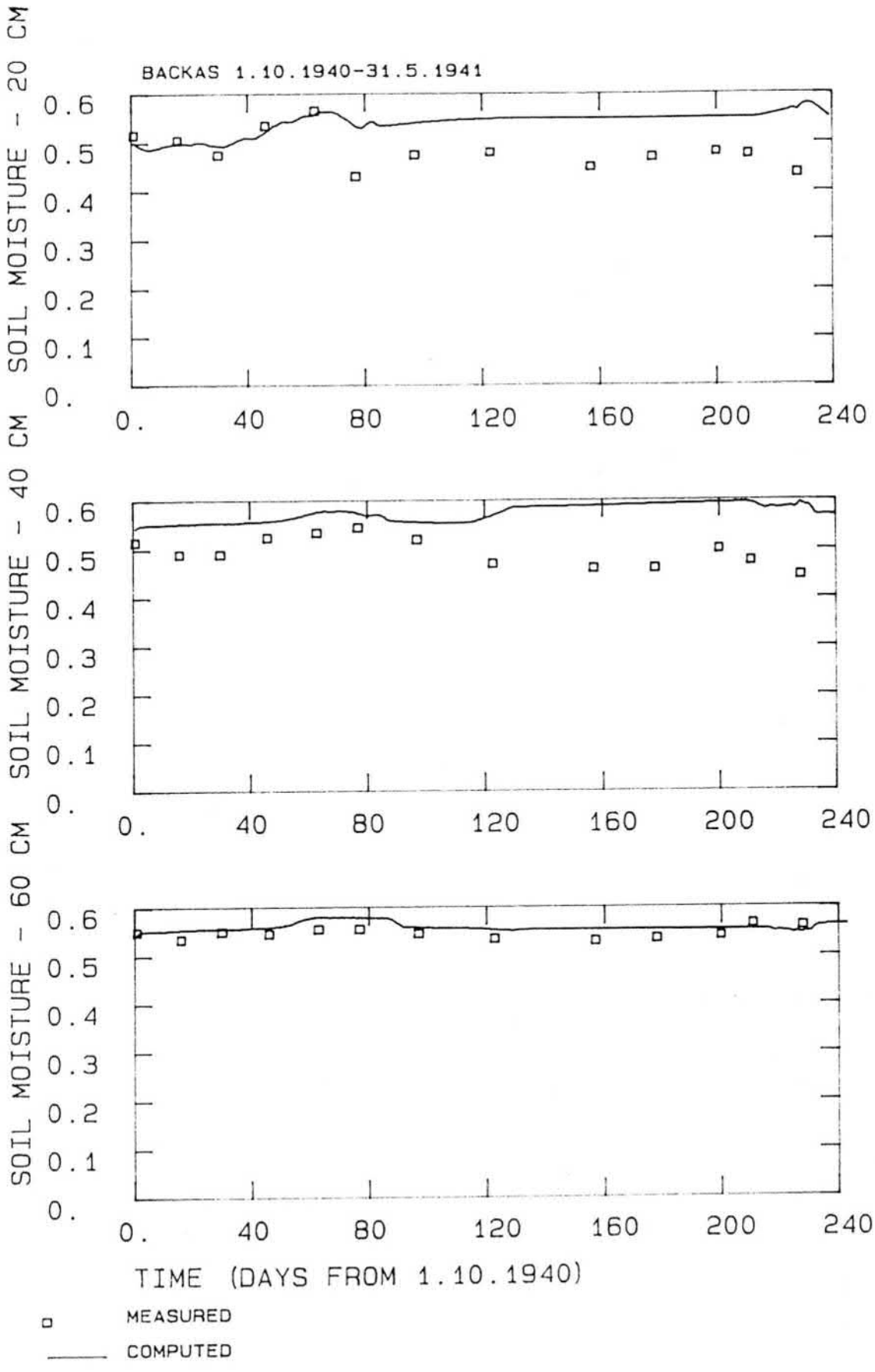

Fig. 7-6. Measured and computed soil moisture at three different depths (a) 20 cm, b) 40 cm and c) 60 cm).

It is useful to point out that the measured soil moisture content and observed depth of the groundwater level were not in agreement with each other. For example during the time t=40 d and t=60 d, the observed depth of the groundwater level was about 30-40 cm. The measured soil moisture content at a depth of 40 cm was 52-53% instead of the saturated value, which was 58%.

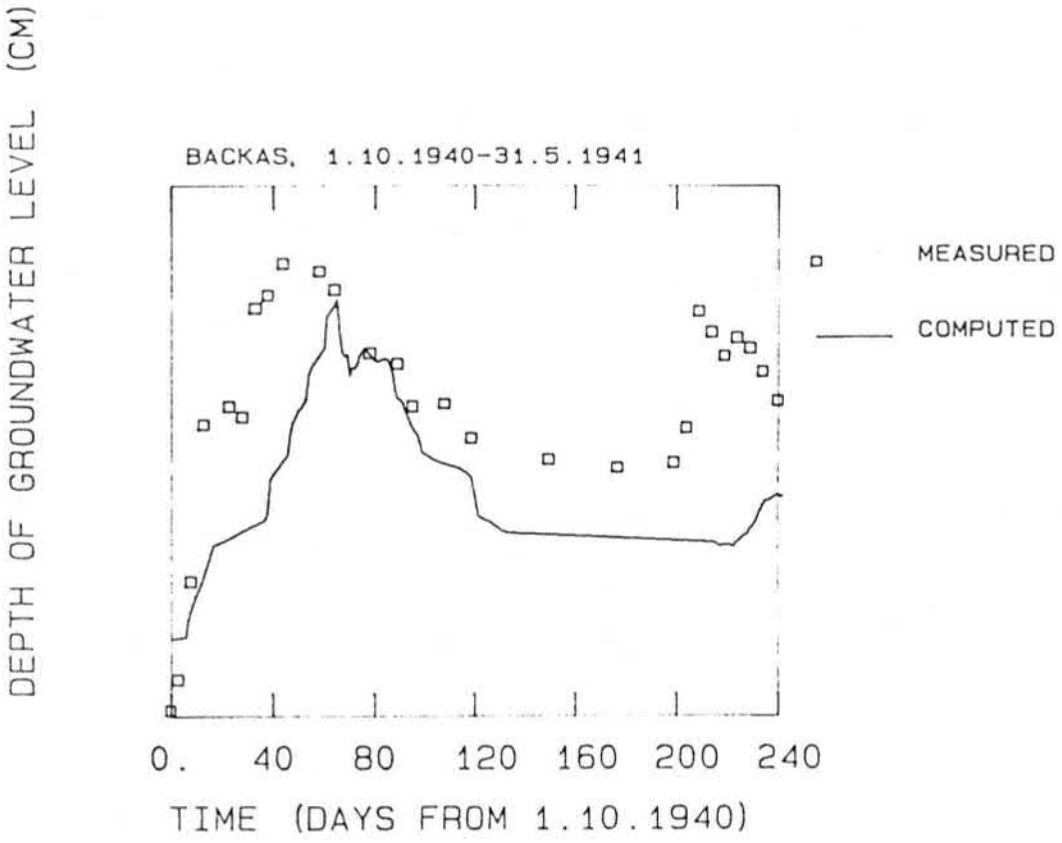

Fig. 7-7. Measured and computed depth of the groundwater level.

The predicted frost depth was slightly greater than the observed values almost all the time. This is partly because the frost depth in the model had to be estimated by locating the depth of the temperature value 0 °C, whereas the measured depth was defined as a boundary where the soil was truly frozen (at a point where the temperature is 0 °C, the soil is generally still unfrozen). There was a timing error of a few days in the predicted disappearence of soil frost. This is mainly due to

the excessively high frozen moisture content, which requires a considerable amount of latent energy during the thawing period.

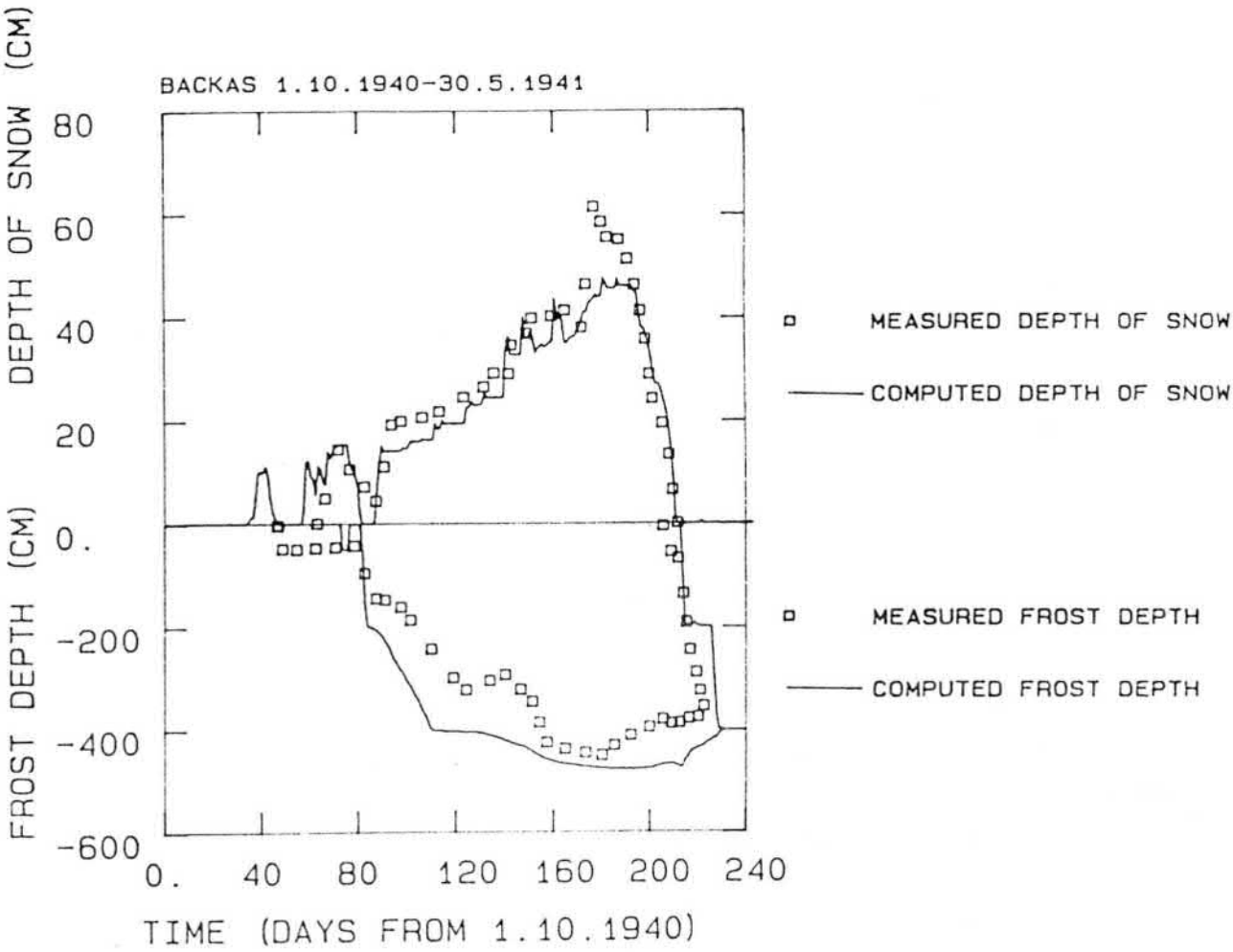

Fig. 7-8. Measured and computed frost depth and thickness of snow cover.

The calculated thickness of snow cover is in good agreement with the measured values with the exception of a period during time t=175 d and t= 185 when the computed values were 20-30% smaller than the measured values. The degree-day factor of equation (4-28) was assumed to be a constant value (2.7 $mm \cdot {}^{\circ}C^{-1} \cdot d^{-1}$) instead of being a function of snow density. The relatively simple snow model gave good results in this case. However, it was already mentioned previously in this section, that relatively small errors in the predicted snow depth during a period of thin snow cover can produce considerable error in the

predicted soil temperature values near the soil surface.

7.3 The Maasoja experimental field

7.3.1 Input data

7.3.1.1 Meteorological data

The meteorological data used in the computer simulations were daily values of precipitation, air temperature and cloudiness. The estimation of global radiation was based on equation 5-19a using the coefficients given in Table 5-3. The potential evapotranspiration rate was calculated with the Turc equation, i.e potential evapotranspiration was estimated from mean air temperature and global radiation. In the comparison made by Vakkilainen (1982), the equation of Turc gave the best results under Finnish conditions. Here it was not possible to use the Penman-Monteith equation because measurements of wind speed and vapour pressure deficit were not available. The potential evapotranspiration E_p was divided between potential soil evaporation E_s and potential transpiration T_p according to the expressions (Aslyng and Hansen, 1982):

$$E_s = E_p \cdot \exp(-K_e \cdot LAI) \qquad (7\text{-}2)$$

$$T_p = E_p \cdot [1 - \exp(-K_e \cdot LAI)] \qquad (7\text{-}3)$$

where K_e is the extinction coefficient and LAI is the leaf area index.

7.3.1.2 Soil parameters

The soil profile was divided into two layers with different soil parameters. The depth of the topsoil was 20 cm on average (Wäre 1947: Hooli 1971). The total depth of the profile used in the computations was 150 cm and the length of the elements were 5 cm between 0 and 30 cm and 10 cm below that level. The soil water retention curve for the topsoil was measured by Hooli (1971) and

for the subsoil the curve was estimated with the procedure described in section 3.2 (see Fig. 7-9).

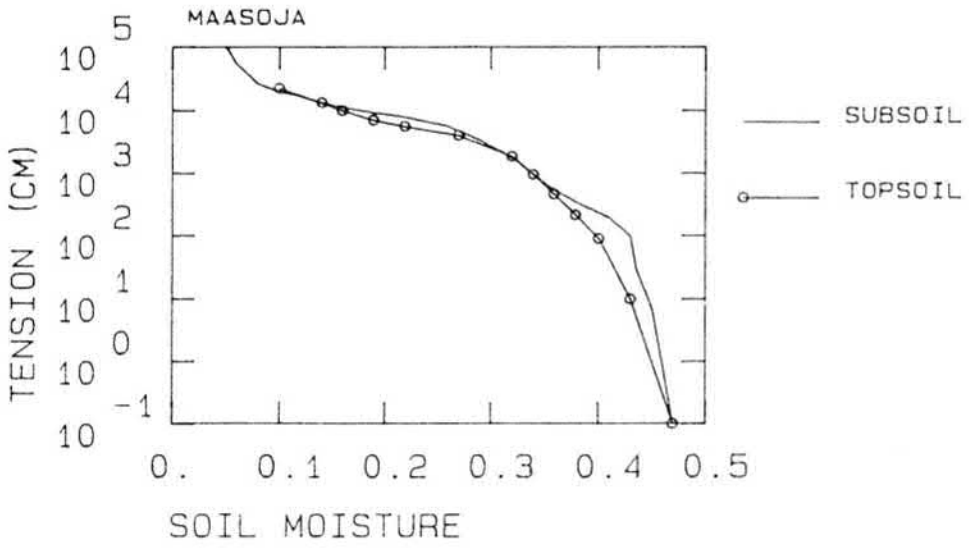

Fig. 7-9. Estimated soil water retention curves for topsoil and subsoil at the Maasoja experimental station.

The measured groundwater level was given as the lower boundary condition. The effective horizontal hydraulic conductivity was determined with the simplified Kalman filtering algorithm (section 3.4). The intensive measurement period needed in the Kalman filtering algorithm was obtained from the experiments made in test areas 3-5, where the water level in the surrounding ditches was maintained at a depth of 20 cm from the soil surface during June (test area 5), during June and July (test area 4) and during July (test area 3). The depth of the groundwater level was measured while the waterlevel in the surrounding ditches was raised or lowered. The average hydraulic conductivity was 0.96 $m \cdot d^{-1}$. Measured and computed water levels midway between the drains are given for four different cases in Fig. 7-10. The water level in the surrounding ditches is also given in Fig. 7-10. In the calculation of the groundwater level, equation (6-3) was used when the water level was lowered in the ditches corresponding to a case where water is flowing from the system. Equation (7-4) was used when the water level

in the ditches was raised and this corresponds to a situation where subirrigation is used to maintain the pressure head in the ditches above the level of the drain. The flow q_d towards the drains can be calculated with the equation (Skaggs 1980):

$$q_d = \frac{4 \cdot K_S \cdot m\{2 \cdot h_o + [h_o/D_o] \cdot m^2\}}{L^2} \qquad (7\text{-}4)$$

where $h_o = y_o + D_e$ is the equivalent water table elevation at the drain, m is defined as $h_m - h_o$ with h_m being the equivalent water table elevation midway between the drains, and $D_o = y_o + D_d$, and D_d is the distance from the drain to the impermeable layer, K_S is the effective lateral hydraulic conductivity and L is the drain spacing. Equation (7-4) can be used for quantifying the effect of poor basic drainage on the soil water regime and for estimation of the effect of subirrigation on soil moisture content and water table elevation.

The saturated vertical conductivity had to be estimated with the method of Bloemen (1980) that uses the measured grain-size distribution curve. According to the results, the vertical saturated conductivity was 0.08 $m \cdot d^{-1}$, which is considerably smaller than the lateral conductivity.

The unsaturated hydraulic conductivity functions for the topsoil and subsoil were estimated with the method given in section 3.3 (extension of the method of Andersson). The curves are given in Fig. 7-11.

7.3.1.3 Crop parameters

If the sowing date is known, the emergence date can be predicted with the method described in Chapter 5. The observations from test areas 9 and 10 were used to plot the mean air temperature versus the reciprocal of the time required for emergence of oats. The results are shown in Fig. 7-12. The temperature sum required for 50% of emergence was 97 dd and the minimum

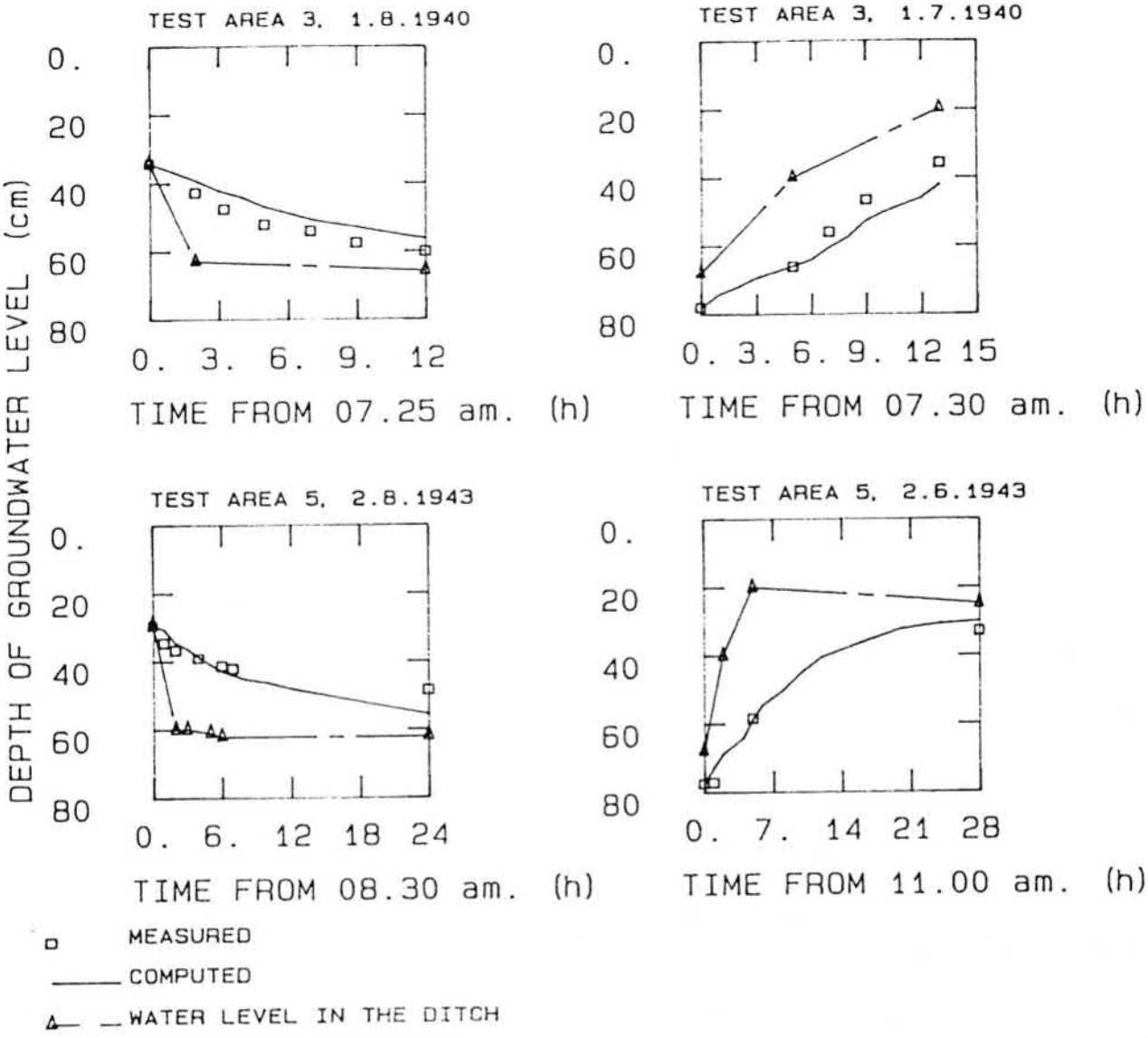

Fig. 7-10. Computed and measured elevation of the groundwater level at Maasoja test areas 3 and 4.

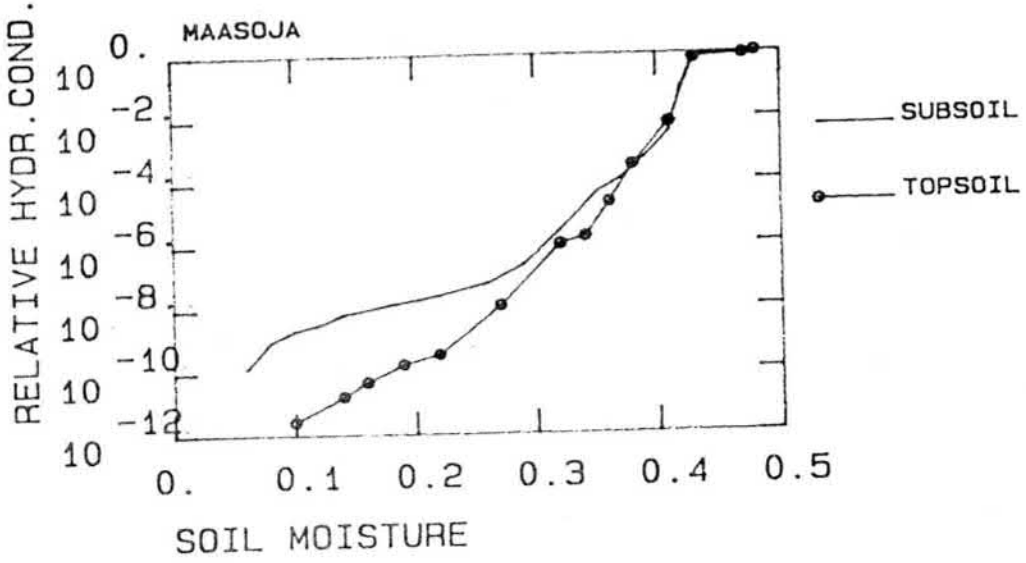

Fig. 7-11. Estimated unsaturated hydraulic conductivity relative values) at Maasoja.

temperature T_{mins} below which no germination occurs was 2.6 °C. The temperature sum

$$F_e = \sum [T_{air} - T_{mins}] \qquad (7-4)$$

is calculated starting from the known sowing date. The date of emergence is reached when F_e is greater than the required temperature sum 97 dd.

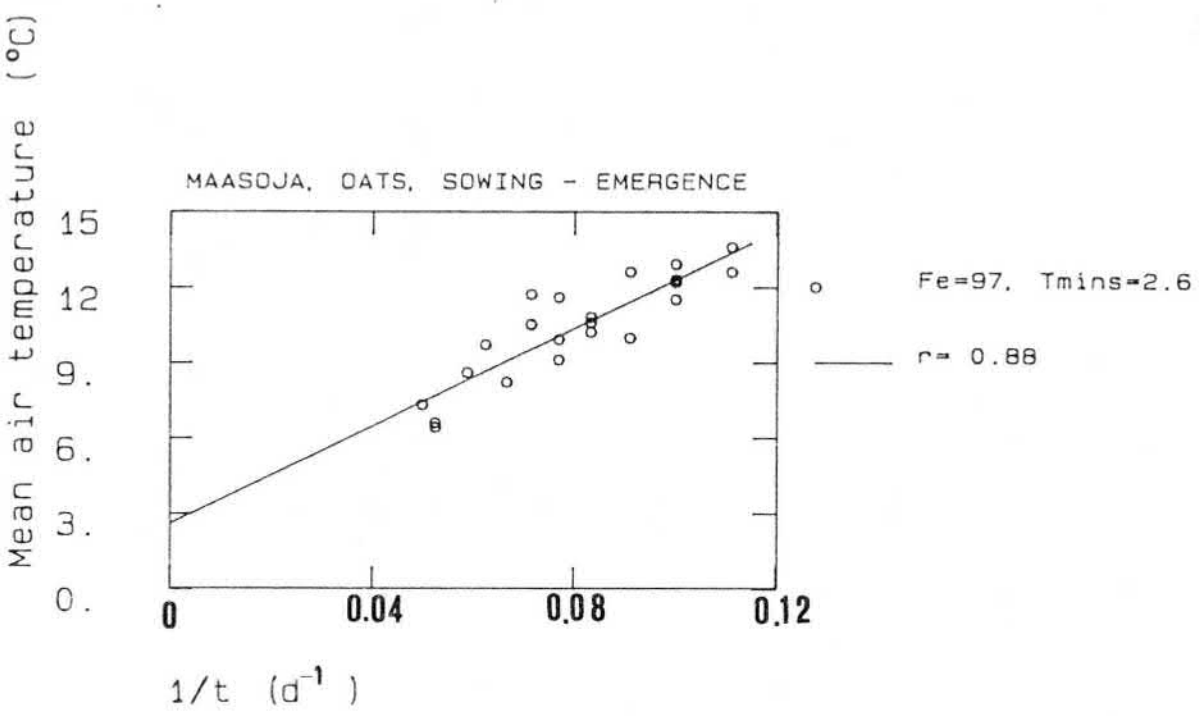

Fig. 7-12. Mean air temperature plotted versus the reciprocal of time required for emergence of oats in order to derive the heat sum F_e and the minimum temperature sum (T_{mins}) below which no germination occurs.

Based on the estimated date of emergence, the crop model starts to calculate the development stage (D_s). In this case D_s was 0 at emergence, 1 at flowering and 2 at harvest. The prediction of the date of flowering and ripening was based on effective temperature sums using 5 °C as the threshold value. Based on the observations, the effective sum required for flowering and ripening were calculated and the values obtained were 441 dd

from emergence to flowering and 367 dd from flowering to ripening, i.e. the effective temperature sum for the period between emergence and flowering was 808 dd. This value is almost the same that was obtained by Elomaa et al. (1986) for spring barley. According to Fig. 5-5, the effective temperature sum from emergence to ripening was 820 dd for spring barley at Jokioinen (assuming that the period between emergence and ripening equals the period when the green area index is above zero).

The model requires that the development of the leaf area index (LAI) must be given as a function of the development stage. Based on the above mentioned temperature sums, the curve measured by Elomaa et al. (1986) was modified so that LAI (GAI) can be given as a function of the development stage. The modified curve is given in Fig. 7-13. Unfortunately, no measured curves for oats were available.

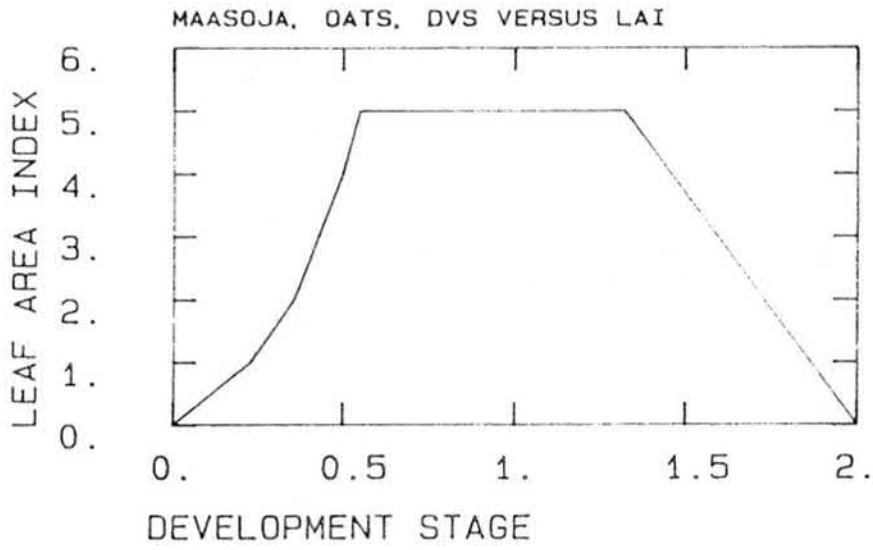

Fig. 7-13. Estimated leaf area index as a fuction of development stage for oats.

The rooting depth of oats at Maasoja experimental field had to be estimated from measurements carried out by Salonen (1949) for a similar type of soil. The maximum depth of the root zone was assumed to be 60 cm and the daily increase in the depth of the root zone was assumed to be 1.5 $cm \cdot d^{-1}$ (Aslyng and Hansen 1982).

In the computer model, the depth of the root zone starts to increase after emergence.

For growth respiration and maintenance respiration factor, values were selected on the basis of a literature review made by Aslyng and Hansen (1982). The following numerical values were taken: 0.70 for conversion factor r_{conv} (efficiency in converting carbohydrate into structural plant material) and 0.015 for the maintenance respiration factor.

The factor that takes into account the effect of temperature on production (see section 5.3.2) was adopted from Busoni et al. (1983): 0% for 0 °C, 80% for 5 °C and 100% for 10 °C or more.

The simulation model calculates the daily and cumulative actual production that include roots and shoots. The final aim is to predict the harvested part of the total biomass. At the Maasoja experimental station the biomass of grain and straw were available (only the final yield at the end of the growing season). In Fig. 7-14 the harvest index of oats (biomass of grains divided by the sum of grains + straw) is given for different years. According to Fig. 7-14 the harvest index varies considerably from year to year and the use of a constant value (the same value for all years) for this parameter produces significant errors in the prediction of the harvested yield.

The best way is to define the distribution of dry matter production over the harvested and non-harvested part as a function of the development stage. In this case measurements of the biomass allocation as a function of D_s were not available and hence simplified curves were adopted. It was implicitly assumed that before flowering (D_s between 0 and 1) the dry matter produced was allocated to roots,stem and leaves and after flowering (D_s increases from 1 to 2) all biomass was allocated to the harvested part (grain). In this way it was possible to calculate the cumulative biomass of roots+stems+leaves (non-harvested part) and cumulative biomass of grains (harvested part) for every year.

The calculated biomass of straw was obtained by subtracting the estimated biomass of roots (+ remains in the field) from the non-harvested yield calculated by the model. According to Ilola and Elomaa (1986) the biomass of roots varies from 1 500·kg ha^{-1} to 2 500 kg·ha^{-1} for spring barley and the average value of 2000 kg·ha^{-1} was selected to be subtracted from the non-harvested yield in order to obtain the calculated biomass of straw.

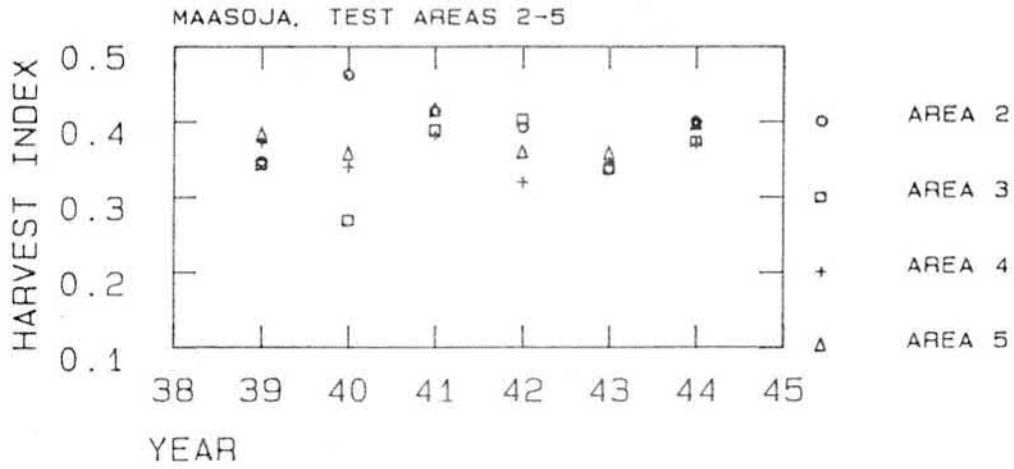

Fig. 7-14. The harvest index of oats at the Maasoja experimental station in 1939-1968 (biomass of grains divided by the biomass of grains plus straw).

7.3.2 Simulation of soil moisture content

The main objective of the Maasoja experiment was to estimate crop yield, and therefore the results of soil water content simulations will be presented very briefly. The computed and measured (gravimetric) soil water content for test area 9 are given in Figs. 7-15 for 1941, a relatively dry year, and in 7-16 for 1943, a wet year.

The soil water model presented in Chapter 4 is not capable of handling the cracking of clay, which speeds up infiltration considerably. From the results it can be seen that the computed soil profile tends to be too dry at a depth of 20 to 50 cm, and too wet at the soil surface, indicating that the computed infiltration capacity was generally too low because the effect of cracks was not included.

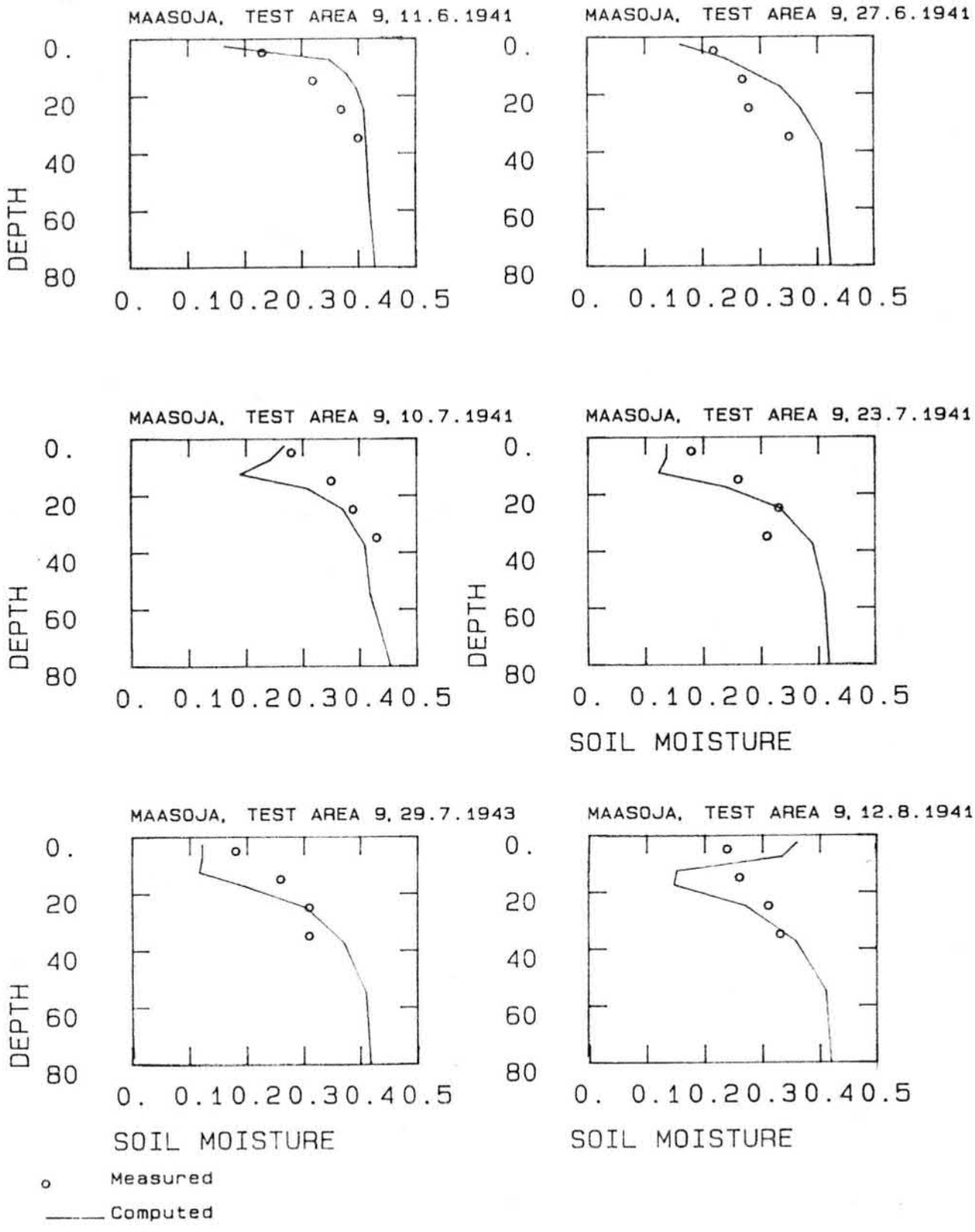

Fig. 7-15. Measured and computed soil water content at Maasoja (test area 9, dry year 1941).

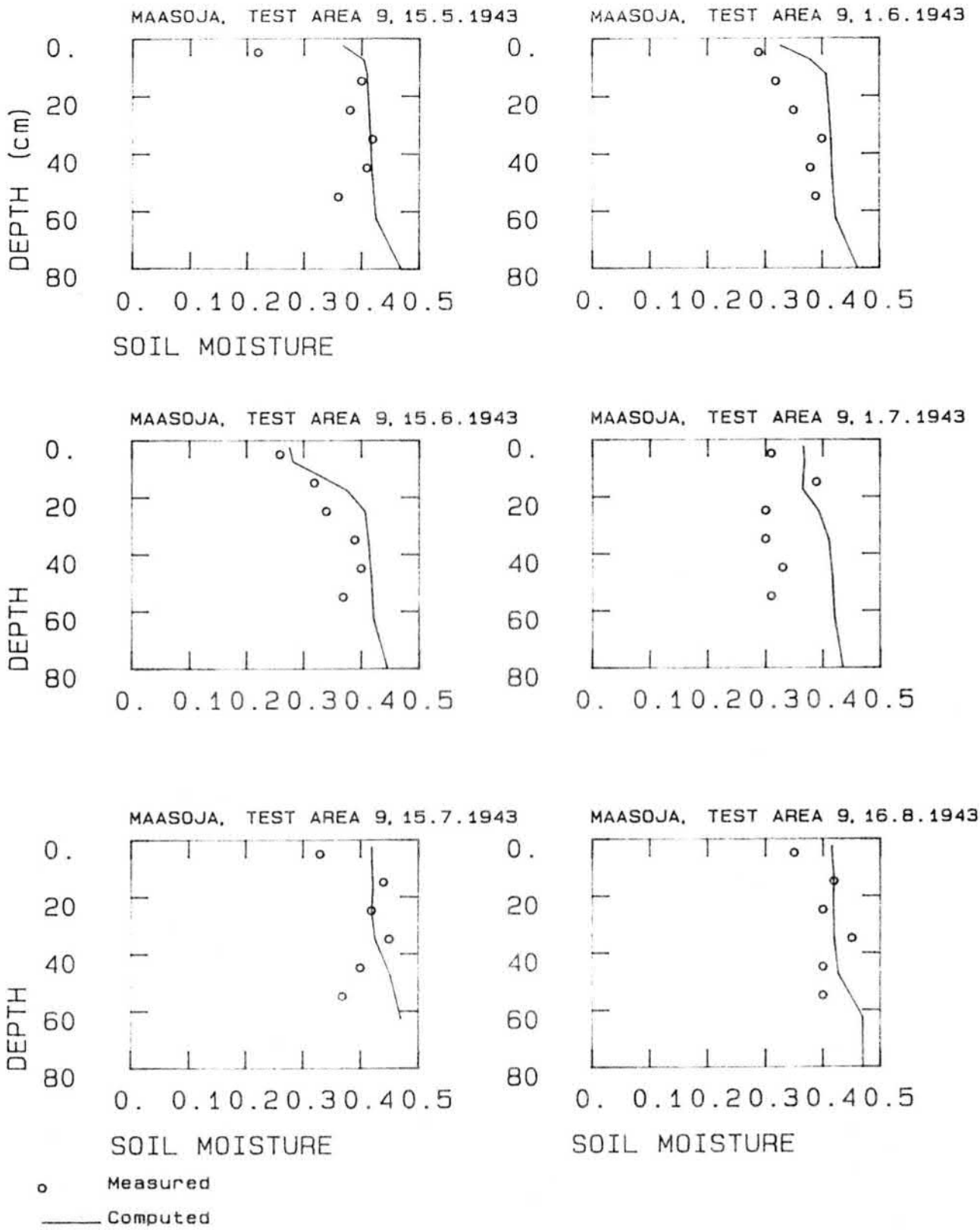

Fig. 7-16. Measured and computed soil water content at Maasoja (test area 9, wet year 1943).

7.3.3 Prediction of the length of the growing season

The predicted and observed dates of emergence with the temperature sum 97 dd and minimum temperature 2.6 °C are given in Table 7-1. The annual dates estimated by the model are in reasonably good agreement with the observed dates.

In Table 7-1 the estimated and observed annual dates of flowering and ripening are also given.

The estimated and observed length of the growing season is given in Fig. 7-17.

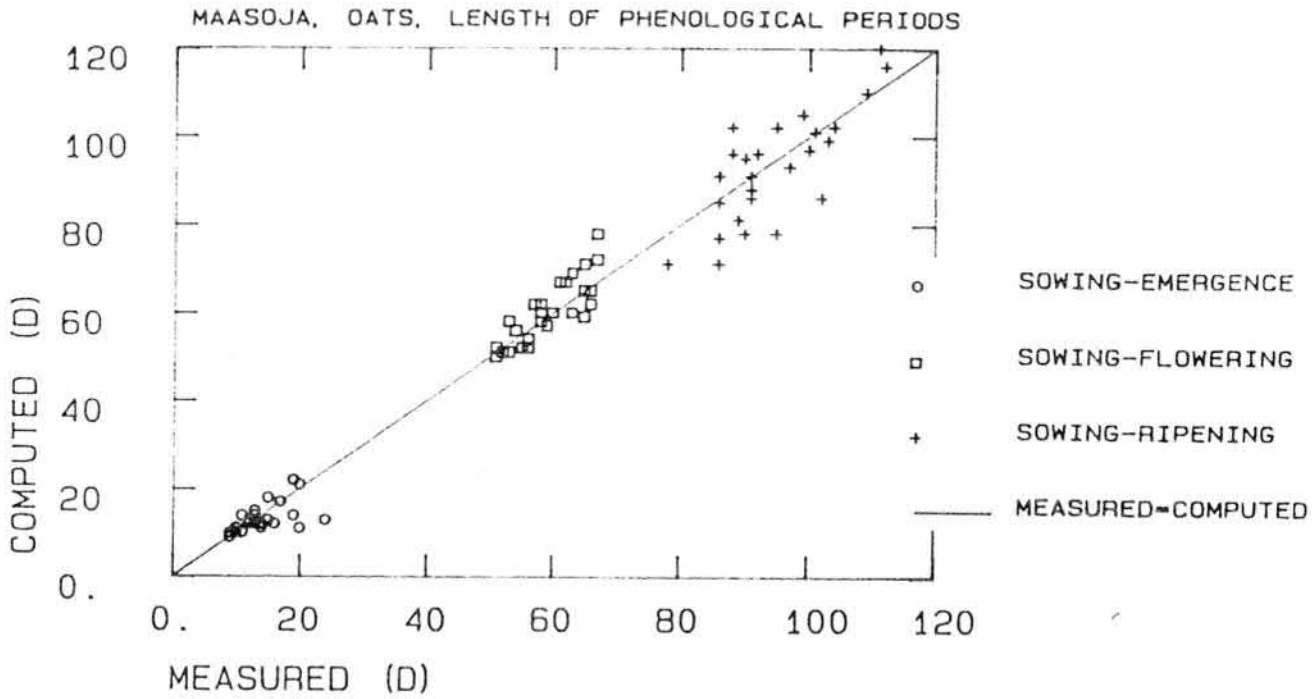

Fig. 7-17. Observed and estimated length of the growing period for oats at Maasoja experimental station in 1939-1968 (from sowing to emergence, from sowing to flowering and from sowing to ripening).

7.3.4 Calculation of potential and actual production rates

At the Maasoja experimental station the potential evapotranspiration rate had to be estimated with the Turc equation, and therefore the daily potential evapotranspiration rates are probably not very accurate. Here a simple version of

Table 7-1. Observed and predicted annual dates of emergence, flowering and ripening of oats at the Maasoja experimental field in 1939 - 1968 (Δd is the difference - days - between observed and estimated).

Year	Sowing	Emergence			Flowering			Ripening		
		Obs.	Est.	Δd	Obs.	Est.	Δd	Obs.	Est.	Δd
1939	16.5	25.5	26.5	+ 1	6.7	7.7	+ 1	10.8	1.8	- 9
1940	17.5	27.5	28.5	+ 1	8.7	7.7	- 1	3.8	27.7	- 8
1941	24.5	2.6	2.6	0	14.7	13.7	- 1	18.8	3.8	-15
1942	20.5	30.5	30.5	0	17.7	17.7	0	29.8	29.8	0
1943	16.5	27.5	30.5	+ 3	18.7	15.7	- 3	26.8	10.8	-16
1944	16.5	31.5	3.6	+ 3	21.7	17.7	- 4	24.8	21.8	- 3
1946	22.5	2.6	1.6	- 1	14.7	19.7	+ 5	16.8	21.8	+ 5
1947	16.5	29.5	30.5	+ 1	11.7	7.7	- 4	10.8	9.8	- 1
1948	7.5	21.5	19.5	- 2	3.7	8.7	+ 5	3.8	17.8	+14
1949	7.5	22.5	20.5	- 2	12.7	11.7	- 1	19.8	17.8	- 2
1952	10.5	30.5	31.5	+ 1	14.7	20.7	+ 6	21.8	17.8	- 4
1953	9.5	21.5	22.5	+ 1	7.7	5.7	- 2	9.8	13.8	+ 4
1954	13.5	27.5	25.5	- 2	12.7	12.7	0	18.8	24.8	+ 6
1955	18.5	4.6	4.6	0	19.7	24.7	+ 5	14.8	22.8	+ 8
1956	23.5	12.6	3.6	- 9	15.7	13.7	- 2	1.9	22.8	-10
1957	17.5	5.6	31.5	- 6	21.7	21.7	0	20.8	27.8	+ 7
1958	14.5	7.6	27.5	-11	16.7	22.7	+ 6	21.8	27.8	+ 6
1959	8.5	24.5	20.5	- 4	8.7	14.7	+ 8	2.8	7.8	+ 5
1960	11.5	23.5	23.5	0	6.7	2.7	- 4	9.8	28.7	-12
1961	12.5	25.5	27.5	+ 2	6.7	3.7	- 3	10.8	15.8	+ 5
1962	17.5	29.5	30.5	+ 1	23.7	3.8	+11	5.9	15.9	+10
1963	11.5	21.5	22.5	+ 1	4.7	6.7	+ 2	10.8	5.8	- 5
1964	19.5	29.5	30.5	+ 1	16.7	18.7	+ 2	22.8	5.8	-17
1965	11.5	30.5	2.6	+ 2	17.7	22.7	+ 5	7.9	5.9	- 2
1966	13.5	27.5	24.5	- 3	8.7	6.7	- 2	10.8	2.8	- 8
1967	16.5	29.5	28.5	- 1	13.7	17.7	+ 4	15.8	12.8	- 3
1968	9.5	28.5	31.5	+ 3	13.7	7.7	- 6	26.8	27.8	+ 1
Average				- 1			- 1			- 2

the crop model - equation (5-8) - was used and in this way the problem of determining the slope A (water use efficiency) of equation 5-7 was avoided. The daily crop production was calculated from the ratio of actual to potential transpiration. This ratio was multiplied by the maximum daily production rate q_m, which was determined with the method described in section 5.3.

Measured data from total above-ground production were available for 1939-1943. The results from test area 9 are given in Table 7-2. Computed and measured production rates are not in good agreement with each other. However, this was to be expected, as the estimation of the yield was based on fairly inaccurate data and most of the parameters needed had to be estimated from measurements which were not made at the Maasoja experimental field.

Table 7-2. Measured and computed dry matter production for oats at harvest and measured and estimated harvest index (Maasoja, test area 9).

Year	Total above-ground prodution ($kg \cdot ha^{-1}$)		Grain yield $kg \cdot ha^{-1}$		Straw yield $kg \cdot ha^{-1}$		Harvest index	
	Meas.	Comp.	Meas.	Comp.	Meas.	Comp.	Meas.	Comp
1939	7900	9300	2900	3500	5000	5800	0.37	0.38
1940	5000	7800	2000	3000	3000	4800	0.40	0.39
1941	8200	8900	3400	3200	4800	5700	0.41	0.36
1942	11100	10100	4300	3800	6800	6300	0.38	0.38
1943	11300	10200	3800	4200	7400	6100	0.34	0.41

The estimated production in very dry year 1940 was almost 3 000 $kg \cdot ha^{-1}$ too great for total above-ground production and the grain yield was overestimated by 1 000 $kg \cdot ha^{-1}$. The results of year 1940 reveal that the computed ratio of actual and potential transpiration during this year was too high and therefore the predicted yield was too high. One explanation for the overestimation of the relative yield is that the shape of soil water retention curve is not correct at high suction values (the amount of water available for plants was overestimated).

Computed and predicted values for the harvest index - grain yield divided by total above-ground production - are also given in Table 7-2. The computed harvest index values are in quite good agreement with the observed values. However, the variation of the computed values is smaller compared to measured values indicating that the allocation of biomass is not as straightforward as assumed in this case (assumption that production is allocated to root and straw between emergence and flowering and to grain between flowering and ripening).

Measured and computed grain yields for some years during the period 1939-1966 are given in Table 7-3. In the computation of the yields given in Table 7-3 the average ETS value 808 °C was used and therefore during some years the computed lentgh of the growing season was not correct. The result of too short estimated growing period is that the estimated leaf area index goes to zero too rapidly and the computed yield remains too low. However, in the evaluation of the effect of drainage on crop yield, the average effective temperature sum must be used and the relative yields are of greatest importance and therefore the yields of Table 7-3 were not computed with the actual ETS, but with the average value.

According to Table 7-3, the computed grain yield values are almost the same as the measured yield. Because a constant value for the effective temperature was used, the crop model was not capable of simulating the variation of grain yield very accurately.

Table 7-3. Measured and computed grain yields for oats at the Maasoja experimental station (test area 9):

Year	Grain yield		
	Measured	Computed	Computed-measured
	$kg \cdot ha^{-1}$		
1939	2800	3500	+ 700
1940	2000	3000	+1000
1941	3400	3200	- 200
1942	4300	3800	- 500
1943	3800	4200	+ 400
1946	3700	3000	- 700
1948	4200	4300	+ 100
1952	4600	3800	- 800
1954	3700	3400	- 400
1956	4400	5100	+ 700
1958	3600	4200	+ 600
1960	4900	3700	-1200
1962	3100	3400	+ 300
1964	4400	3600	- 800
1966	2500	4000	+1500
Average			+ 50

7.3.5 Simulation of irrigation experiments

The effect of irrigation on crop yield was studied at the Maasoja experimental station with computed results from three different years - 1940, 1941 and 1943. The measured precipitation values are given in Table 7-4. The amount of water irrigated was 20 + 20 mm (in the middle and at the end of June).

Table 7-4. Monthly precipitation values at the Maasoja experimental station (mm).

Year	May	June	July	August	May-Aug.
1940	23.7	21.0	20.3	86.2	151.2
1941	14.1	13.0	48.5	121.2	196.8
1943	30.1	69.8	142.8	125.0	367.7

The measured and computed values for total production above soil and for biomass of grain and straw yield are given in Table 7-5. The increase in dry matter production due to irrigation is also given in Table 7-5. The computed yield values were not in good agreement with the measured ones, but the calculated effect of irrigation was of the right magnitude with the exception of that for 1940. The reason for the underestimation of the effect of irrigation was that the soil surface was exceptionally dry at the time of irrigation and the model assumed that a great deal of irrigated water was lostin by surface runoff. Observations of the cracking of clay soil at Maasoja were not available, but it is reasonable to assume that during 1940 the irrigated water was infiltrated through the cracks. This explains the beneficial effect of irrigation on crop yield.

7.3.6 Simulation of subirrigation experiments

According to Wäre (1947) the subirrigation experiments were of greatest importance during 1939-1944. The average depth of the groundwater level during 1941 and 1943 in test areas 2-6 are given in Table 7-6. In test area 3 the groundwater level was raised to the depth of 20 cm from the soil surface at the beginning of July and lowered at the beginning of August. In test area 4 the average depth of the groundwater level was 20 cm during June and July and in test area 5 the depth of the groundwater level was 20 cm during June.

Table 7-5. Measured and computed dry matter production for oats at the Maasoja experimental station (test area 1). The lower line for each year shows the increase in yield.

Year	Total above-ground production kg·ha^{-1}		Grain yield kg·ha^{-1}		Straw yield kg·ha^{-1}	
	Meas.	Comp.	Meas.	Comp.	Meas.	Comp.
1940	6600	8300	2900	3200	3700	5100
	+1400	+ 500	+ 600	+ 200	+ 800	+ 300
1941	6700	9700	2900	3200	3800	6000
	+ 800	+ 800	+ 300	+ 300	+ 500	+ 500
1943	11000	10200	3200	4100	7800	6100
	+ 600	+ 0	+ 0	- 100	+ 600	+ 100

Table 7-6. Average depth of groundwater level (cm) at Maasoja in test areas 2 through 6 (adapted from Wäre 1947).

Year	Month	Test area				
		2	3	4	5	6
1941	V	61	58	56	56	54
	VI	80	62	17	18	54
	VII	61	19	16	60	77
	VIII	65	53	50	76	92
1943	V	62	60	61	60	59
	VI	73	70	20	21	59
	VII	48	19	20	42	45
	VIII	55	48	44	51	54

According to Wäre (1947), the effect of subirrigation on grain yield during 1939-1944 in test area 5 (subirrigation during June) was +3.7% on the average, and on straw yield +8.7%, respectively. The result of subirrigation was positive with the exception of the rainy years in 1943 and 1944. In test area 4 - subirrigation during June and July - the average grain yields were not lowered due to the high water table, but during the wet years of 1943 and 1944 grain yield was reduced by 7% and 27%, respectively. The effect of subirrigation on grain yield during July (test area 3) was -5.7% on average (Wäre 1947).

The simulation of subirrigation experiments showed that the crop model presented in Chapter 5 in these types of cases is very sensitive to two parameters: the development of rooting depth as a function of the development stage (or time) and the parameter that defines the negative pressure at which plants start to suffer from oxygen deficiency (h_1 in Fig. 5-7).

Wesseling and van Wijk (1957) suggested a tentative lower limit of 10% air porosity in soils for growth of plants. Stolzy and Letey (ref. Feddes et al. 1978) found that many plants do not grow in soils with an oxygen diffusion rate below $20 \cdot 10^{-8}$ g·cm^{-2}·min^{-1} . This value corresponds to critical gas porosities of about 4 to 25% for different soils.

At the Maasoja experimental field the critical value had to be estimated by trial-and-error,because the initial approximation of 10% for critical gas porosity gave a very low calculated yield from the period of subirrigation. This was because the groundwater level was at a shallow depth. Based on the simulations, a critical gas porosity of 5% seemed to produce realistic values. However, a reliable method to estimate the critical gas porosity based on some easily measured variables would be needed.

Another uncertain parameter in the simulation of subirrigation experiments was the depth of the root zone. In test area 9 (section 7.3.4) the maximum rooting depth was assumed to be 60 cm. In experiments where subirrigation was started at the beginning of June, this assumption of maximum rooting depth proved to be overestimated. This was because the depth of the rooting zone was less than 20 cm at the beginning of the subirrigation experiment (average date of emergence at the end of May). Hence, the rooting depth of the crop was not increased during the subirrigation and the straw yields in particular were increased.

In test area 3 the subirrigation was started at the beginning of July. It can be assumed in these experiments that the rooting depth had already reached its maximum before the experiment was started, and therefore the 5.7% average decrease in grain yield can be explained. The lowest part of the rooting zone (between depth 20 and 60 cm) was in anaerobic conditions and the dry matter production was lowered. However, the decrease in yield was not very different, indicating that the crop can partly adapt to situations where the groundwater level is very close to the soil surface in the middle of the growing season.

The results of the subirrigation experiments - the measured and computed values for 1941 and 1943 - are given in Table 7-7. The magnitude of the effect of subirrigation was predicted reasonably well after calibration of the critical gas porosity. However, the results of the following experiments listed below show that more research is needed before completely reliable results can be obtained when the groundwater level is near the soil surface for a long period during the growing season. For the test area 5 in 1941 the effect of subirrigation on grain yield was underestimated and straw yield overestimated, but for test areas 4 and 5 in 1943 the change in grain yield due to subirrigation was clearly overestimated.

Table 7-7. Measured and computed yield of oats at the Maasoja experimental station.

Test areas 2 and 6 = no subirrigation
Test area 3 = subirrigation during July
Test area 4 = subirrigation during June and July
Test area 5 = subirrigation during June

1941

	Total above-ground production kg·ha^{-1}		Grain yield kg·ha^{-1}		Straw yield kg·ha^{-1}	
	Meas.	Comp.	Meas.	Comp.	Meas.	Comp.
2,6	8200	7800	3400	3000	4800	4800
3	9700	8000	3800	3200	5900	4800
4	11500	9700	4400	4300	7100	5400
5	10100	8700	4200	3200	5900	5500

1943

	Total above-ground production kg·ha^{-1}		Grain yield kg·ha^{-1}		Straw yield kg·ha^{-1}	
	Meas.	Comp.	Meas.	Comp.	Meas.	Comp.
2,6	11100	10200	3700	4000	7400	6200
3	10200	9100	3400	3200	6800	5900
4	9900	9600	3400	3700	6500	5800
5	9700	9800	3400	3800	6300	6000

7.4 Conclusions

7.4.1 Calculation of soil moisture and soil temperature

Based on the results obtained from simulations in the Backas and Maasoja experiments the following conclusions can be drawn:

1° The cracking of heavy clay soils should be included in the model if an accurate prediction of the soil moisture profile is of special importance.

2° The estimation of soil thermal conductivity based on an intensive measurement period proved very successful.

3° Accurate prediction of the soil temperature profile can be obtained if the soil surface temperature is given as an upper boundary condition.

4° If the soil surface temperature under the snow cover is computed, the results are very sensitive to the calculated density of the snow pack (relatively small errors in the calculated snow depth during a period of thin snow cover can produce considerable error in the estimated soil temperature values near the soil surface).

5° The new method used for alleviating the numerical problems in the calculation of combined heat and mass flow in frozen soil (see section 4.3) seems to produce reasonably good results.

7.4.2 Estimation of crop yield

The following conclusions can be drawn:

1° Most of the parameters needed in the simulation of grain yield of oats had to be estimated from data of poor quality and therefore it was not possible to verify completely the crop model based on the data collected at Maasoja. It would have been very important to have measurements of dry matter production as a function of time, and not only the final yield which was the case at Maasoja.

2° A method based on calculating the development stage of a plant as a function of the effective temperature sum seems to be suitable for Finnish conditions (date of harvest need not be given as a prescribed value). Hence, the measured values of the leaf area index as a function of the effective temperature sum should be available for different species.

3° Methods for the estimation of the critical gas porosity and anaerobic point should be developed if the prediction of the

effect of high groundwater level on crop yield is needed.

4° In the future, it will be necessary to develop models that can adapt to changes in soil moisture content , i.e. to develop models that need as few prescribed parameter values as possible.

8. APPLICATION OF MODELS IN DESIGNING DRAINAGE SYSTEMS

8.1 Introduction

The main purpose of this study was to develop a methodology that links climatological data, crop drainage requirements and drainage theory into a design method called the water management model. The objective of this Chapter is to discuss the prospects for using this type of approach in designing drainage systems in Finland.

The decision parameters regarding drainage are the only components in a water management model that can be affected by the planning of a drainage project. These parameters include drain spacing and depth and drainage coefficient (the design flow that the system must be capable of conveying when it is running full). A diagram of the effect of the decision parameters is given in Fig. 8-1. The choice of drainage parameters affects the soil moisture and soil temperature of a drained field. Soil moisture and soil temperature are related to each other by freezing and thawing phenomena. The effect of soil moisture and on crop yield must also be computed. As a final step, the effect of the decision parameters on yield, cost and profit has to be estimated.

Subsurface drainage systems for an area of 30,000-35,000 ha are built yearly. The average size of a plan is about 6 ha, i.e. the number of projects is approximately 5,000- 6,000 every year. It would be impractical to apply a water management model to all these projects. It is necessary to find the particular applications where the water management model can help in designing the planning principles used in Finland.

Section 8.2, discusses the use of the proposed methods in selecting the drainage coefficient. This analysis is based on data measured at the Nurmijärvi experimental station (Virtanen 1987). Section 8.3 gives the application of the quasi-two-dimensional model for predicting the starting date of

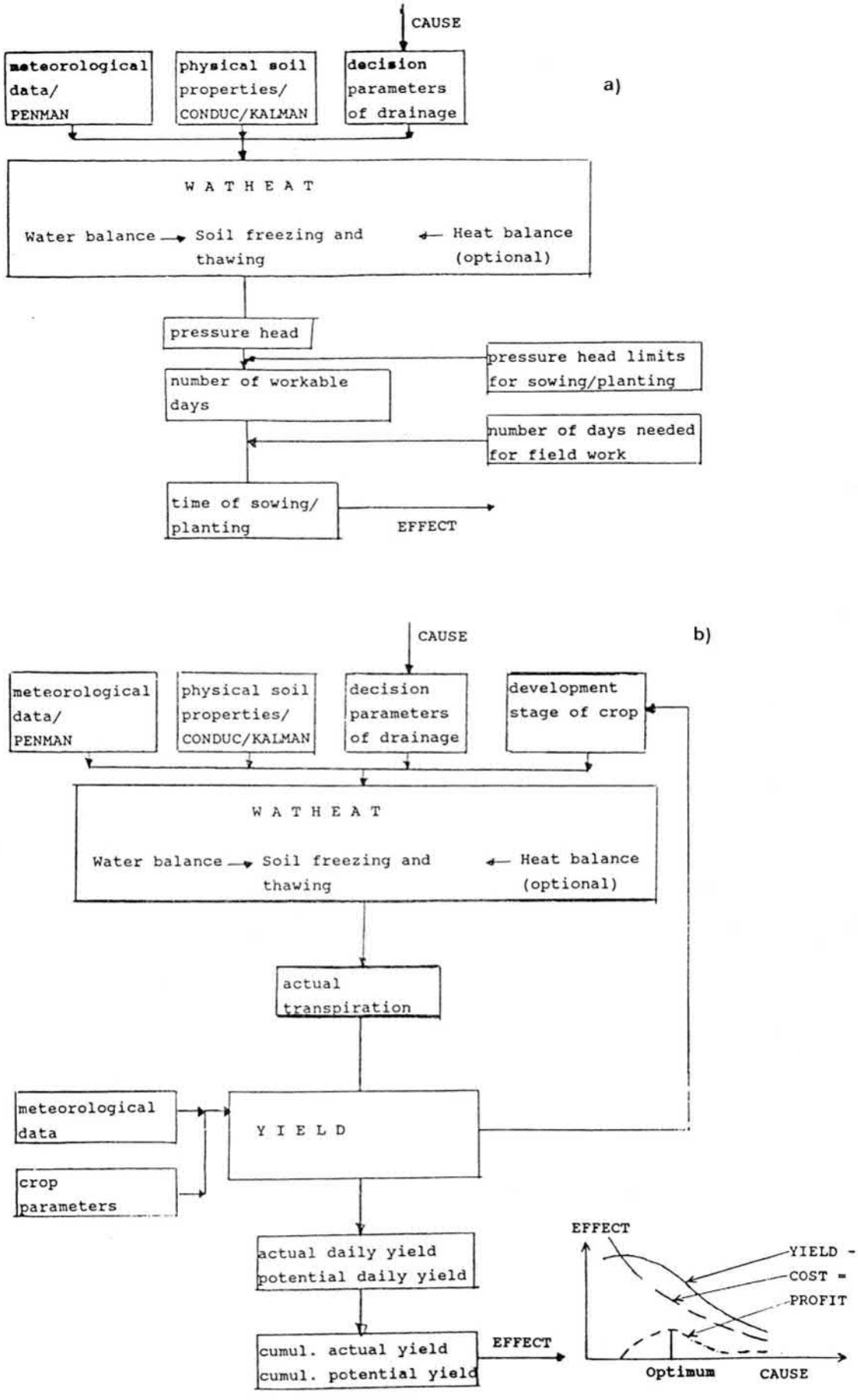

Fig. 8-1. A simplified flowchart of the water management model for computation of the effect of drainage on soil moisture, soil temperature and crop yield.
a) Before the growing season, b) During the growing season.

sowing and for estimating the harvest date, and section 8.4 gives an example of the calculation of the optimum drain spacing.

8.2 Selection of the drainage coefficient

In this context the drainage coefficient is defined as follows: the amount of water (in units $l \cdot s^{-1} \cdot ha^{-1}$ or $mm \cdot d^{-1}$) that the pipe system must be capable of conveying when it is running full, without back pressure. The drainage coefficient presently in use in Finland is 1.0 $l \cdot s^{-1} \cdot ha^{-1}$ (=8.64 $mm \cdot d^{-1}$) for most cases. If a smaller drainage coefficient could be used the size of the collectors could be reduced, and this would also reduce the total cost of the subsurface drainage system. As a rough approximation it can be stated that a reduction of the drainage coefficient from 1.0 $l \cdot s^{-1} \cdot ha^{-1}$ to 0.5 $l \cdot s^{-1} \cdot ha^{-1}$ would lower the total cost of a subsurface project by about 1-5%, which corresponds to a total sum of 2.7 - 13.5 million Finnish marks every year (on average 9 000 $FIM \cdot ha^{-1}$ and 30 000 $ha \cdot year^{-1}$) or on average 550 - 2700 FIM for a farmer (based on the assumption of 6 ha for a project).

In 1984 an experimental field was established by the Finnish Field Drainage Centre in order to study the amount of water flowing from the subsurface outlets. The experimental field is situated at Nurmijärvi in Southern Finland (about 40 km north of Helsinki). A description of the experimental field has been given by Virtanen (1987). The soil type in Nurmijärvi is silty clay with a saturated hydraulic conductivity of 2.8 $cm \cdot h^{-1}$ as a mean value (Vakkilainen and Virtanen 1986).

According to measurements made by Virtanen (1987), the highest measured outflow rate due to melting of snow has been 3.9 $l \cdot s^{-1} \cdot ha^{-1}$, i.e. almost four times greater than the drainage coefficient. An average outflow rate of 1.5 $l \cdot s^{-1} \cdot ha^{-1}$ during a period of 8 days was measured in spring 1986. The highest outflow rates caused by rainfall were 2.8 $l \cdot s^{-1} \cdot ha^{-1}$ (in October) and 2.4 $l \cdot s^{-1} \cdot ha^{-1}$ (in August). Should these results

be interpreted in such a way that the drainage coefficient must be increased? The answer to this question is given in the next two sections.

8.2.1 Summer period 25.8-26.8.1986

The highest outflow rate measured during the growing season was 2.41 $l \cdot s^{-1} \cdot ha^{-1}$ (25-26.8.1986). The measured rainfall during the 24 hours (25.8. 09.00 am - 26.8. 09.00 am) was 15.8 mm, but unfortunately hourly values were not available. The measured outflow rate as a function of time is given in Fig. 8-2. The outflow rate increases very rapidly from 0.06 $l \cdot s^{-1} \cdot ha^{-1}$ to 2.41 $l \cdot s^{-1} \cdot ha^{-1}$ during a period of four hours and decreases from 2.41 to 1.0 $l \cdot s^{-1} \cdot ha^{-1}$ in four hours and then from 1.0 to 0.27 $l \cdot s^{-1} \cdot ha^{-1}$ in 9 hours.

The calculated values of outflow rate for two different assumptions of rainfall distribution are also given in Fig. 8-2. In the first assumption the rainfall rate was assumed to be 1.8 mm for one hour and 7 $mm \cdot h^{-1}$ for two hours and in the second assumption 5.3 mm for three hours. The calculated shape of the outflow rate does not completely coincide with the measured one, but the model seems to give realistic values for the outflow rate, which is more important in the present analysis than the exact matching. Without accurate knowledge of rainfall distribution, it is not possible to obtain exactly the measured values.

Since the model gives reasonably good results, it can be used to analyze the effect of the drainage coefficient on the duration of high groundwater level caused by the above mentioned rainfall. The use of a smaller drainage coefficient implies that the hydraulic capacity of the drain tubes is lowered. The effect of the drainage coefficient is taken into account with the method suggested by Skaggs (1980): If the calculated flow rate to the drains exceeds the drainage coefficient, the flux is set equal to the drainage coefficient.

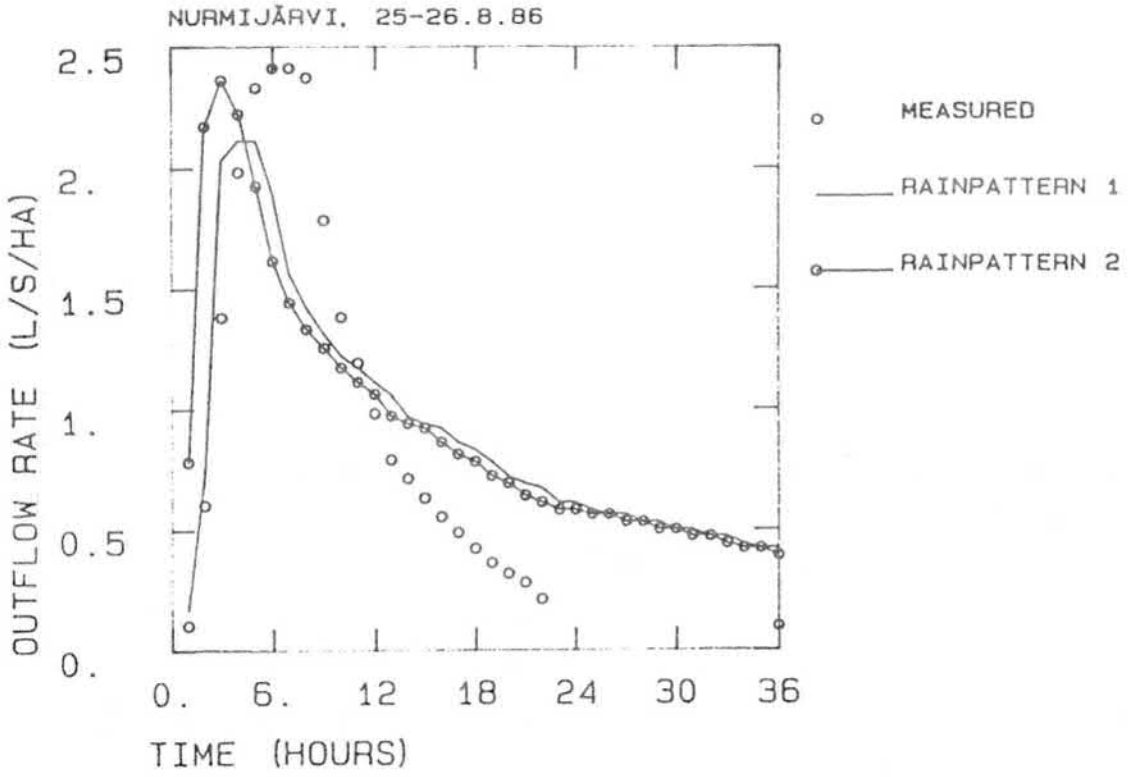

Fig. 8-2. Measured and computed outflow rate from subsurface drains at Nurmijärvi during 25-26.8.1986. Rain pattern 1 = 1.8 $mm \cdot h^{-1}$ + 2x7 $mm \cdot h^{-1}$, Rain pattern 2 = 3x5.3 $mm \cdot h^{-1}$.

Three different cases are discussed: 1) the computed peak flow, assuming that the hydraulic capacity of the drains is not a limiting factor, 2) the drainage coefficient is equal to 1.0 $l \cdot s^{-1} \cdot ha^{-1}$ and 3) the drainage coefficient is 0.5 $l \cdot s^{-1} \cdot ha^{-1}$, i.e. if the calculated outflow rate exceeds 0.5 $l \cdot s^{-1} \cdot ha^{-1}$ in the third case, the outflow rate is set equal to 0.5 $l \cdot s^{-1} \cdot ha^{-1}$.

The results from calculations are given in Fig. 8-3. The calculated outflow rates are given in Fig. 8-3a and the computed groundwater level in Fig. 8-3b. From Fig. 8-3 it can be seen that the rise of the groundwater level is very rapid in all cases 1) to 3). In case 1) (corresponds to the situation at the experimental field) the groundwater level falls very rapidly, but it is interesting to note that even when the drainage coefficient 0.5 $l \cdot s^{-1} \cdot ha^{-1}$ is used, the groundwater level drops relatively soon after the rainfall ceases. At least in this example, a reduction of the drainage coefficient to a

value of 0.5 $l \cdot s^{-1} \cdot ha^{-1}$ would not cause a significant delay in the lowering of the groundwater level during the growing season, as compared with the case when the peak flow is 2.4 $l \cdot s^{-1} \cdot ha^{-1}$ for a short period of time. A more thorough analysis of the effect of the drainage coefficient on the groundwater level falls outside the scope of this study but e.g. different soil types and various types of rainfall patterns affect the determination of the lowest possible drainage coefficient that can be used in Finnish conditions. However, it is encouraging that the models presented in Chapters 4 and 6 can be used in estimating the proper drainage coefficient.

In is necessary to point out that according to the design nomogram (the nomogram used in Finland in determining the pipe dimensions), the Nurmijärvi drainage system should convey only about 2.0 $l \cdot s^{-1} \cdot ha^{-1}$ (80 mm pipes with a slope equal to 3.08 %) which is 50 % from the highest measured outflow rate (=3.9 $l \cdot s^{-1} \cdot ha^{-1}$). The high hydraulic capacity is due to two factors: 1) the pressure in the pipe system is not included in the nomogram and 2) the nomogram includes extra safety. In the calculations of Figs. 8-2 and 8-3, the extra safety included in the nomogram is not taken into account.

8.2.2 Effect of drainage coefficient during the melting of snow

In the previous section (8.2.1) it was shown that for one particular summer storm the reduction of the drainage coefficient to 0.5 $l \cdot s^{-1} \cdot ha^{-1}$ did not have a significant effect on the lowering of the groundwater level because the period of high rainfall rate was short. This is not the situation during the snow melt period in Finland (e.g. the average outflow rate equal to 1.5 $l \cdot s^{-1} \cdot ha^{-1}$ for a period of 8 days at the Nurmijärvi experimental station in 1986).

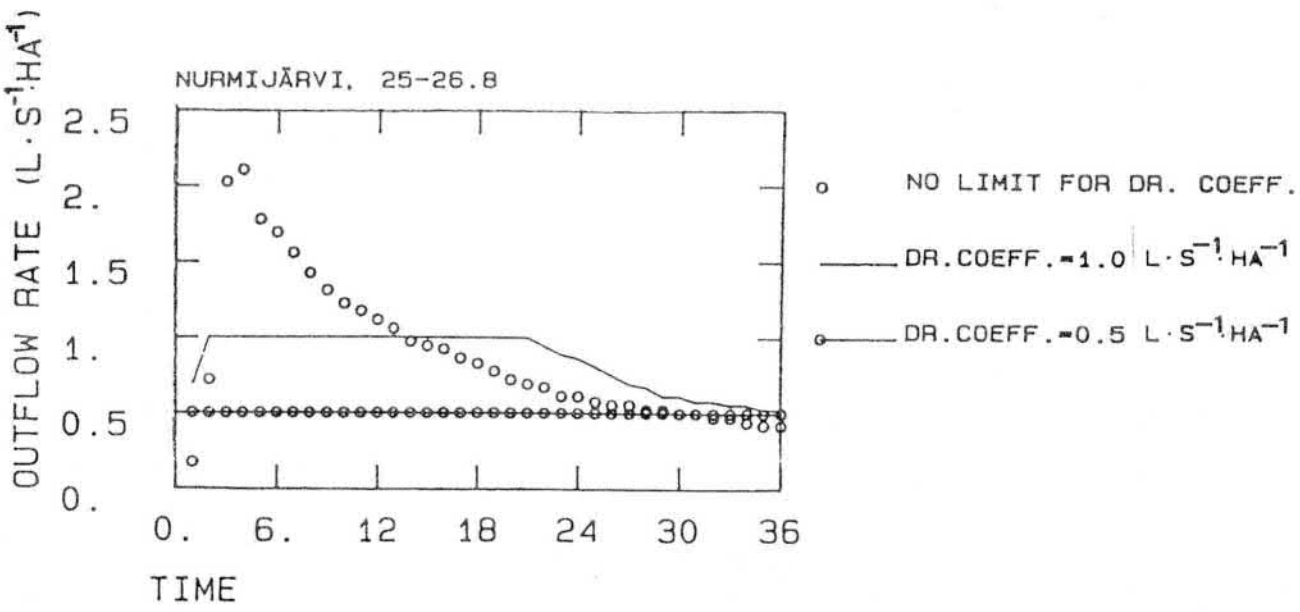

Fig. 8-3a. Computed outflow rates for three different cases at Nurmijärvi, 25-26.8.1986. (1=no limit for drainage coefficient,2= drainage coefficient equal to 1.0 $l \cdot s^{-1} \cdot ha^{-1}$ and 3=0.5 $l \cdot s^{-1} \cdot ha^{-1}$, respectively).

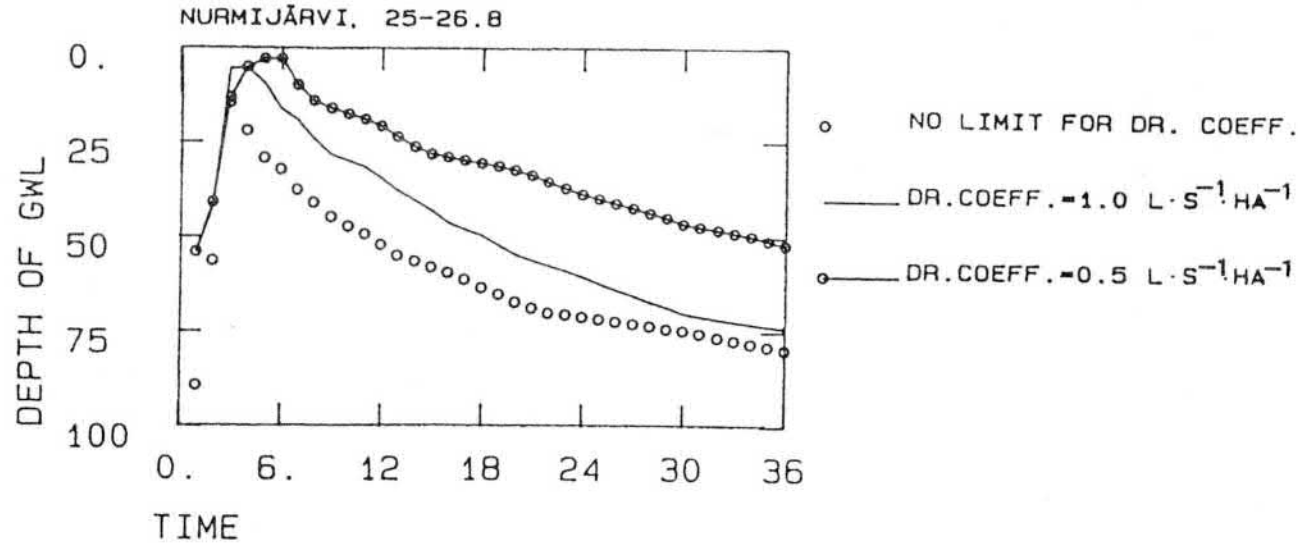

Fig. 8-3b. Computed depth of groundwater level for three different cases at Nurmijärvi, 25-26.8.1986. (1=no limit for drainage coefficient, 2=drainage coefficient equal to 1.0 $l \cdot s^{-1} \cdot ha^{-1}$ and 3=0.5 $l \cdot s^{-1} \cdot ha^{-1}$, respectively).

The average measured and computed outflow rates during the most intensive melting period (20.4-11.5.1986) are given in Fig. 8-4. The computed values are based on the assumption that the hydraulic capacity of the drains is not a limiting factor. The computed values are of realistic magnitude, and the model can be used to estimate the effect of the drainage coefficient on the earliest possible time of sowing.

In the analysis it is necessary to have a method for predicting the earliest possible day of sowing as a function of the soil water pressure head or soil water content, i.e. one has to be able to predict the number of workable days. A day is defined as a working day if the soil water pressure at a depth of e.g. 5 cm, is less than a given limiting value which is dependent on soil type and crop. The pressure head limits for sowing spring cereals, sugar beet and planting potatoes for four soil groups are given by van Wijk and Feddes (1986) and these values are given in Table 8-1. The workability index suggested by Buitendijk (1985) are in complete agreement with the results proposed by van Wijk and Feddes. Unfortunately, measured values from Finland were not available.

Table 8-1. Soil water pressure head (at 5 cm depth) at which spring cereals and sugar beets can be sowed and potatoes planted without deterioration of soil sructure (van Wijk and Feddes 1986).

Soil type	Soil water pressure head (cm)		
	Spring cereals	Sugar beet	Potatoes
Sandy soils	-50	- 70	- 70
Silt/sandy loam (8-20% particles<2μm)	-80	-100	-100
Loam/silty clay loam (20-40 % particles < 2μm)	-60	-100	-120
Silty clay (< 40 % particles < 2μm)	-40	- 60	- 80

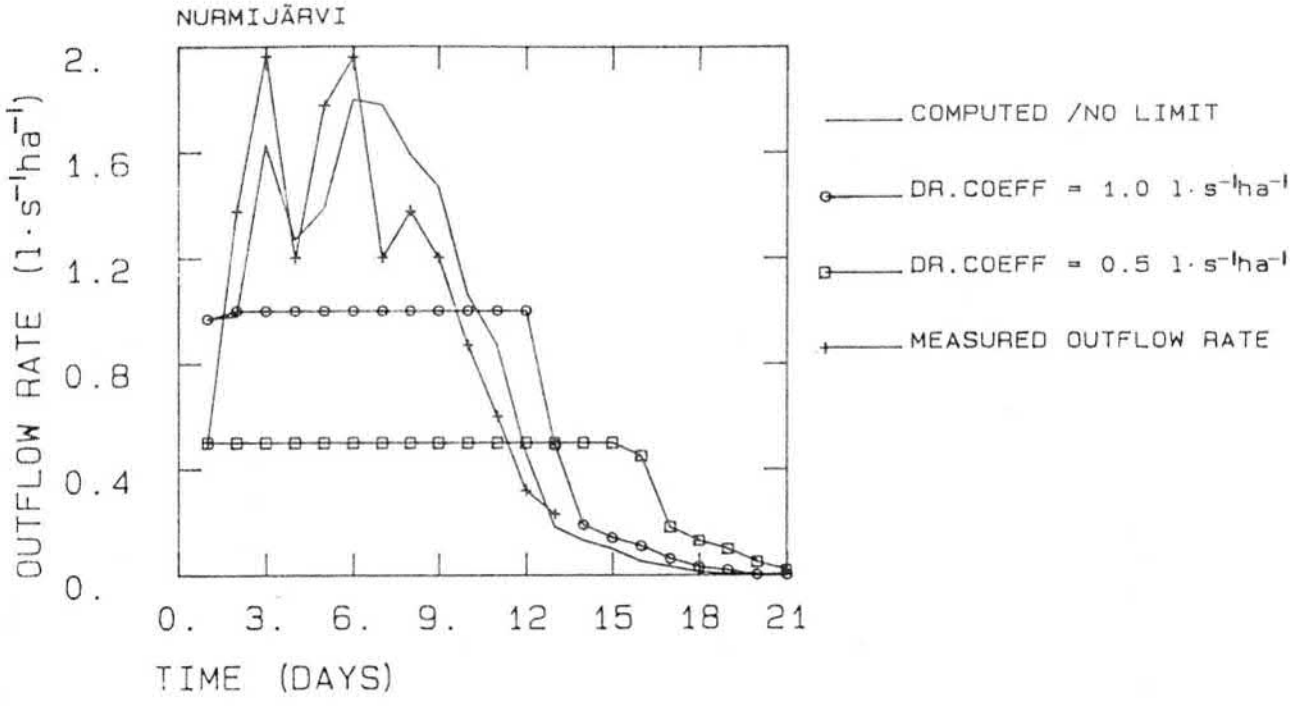

Fig. 8-4a. The measured and computed outflow rate during the 1986 spring flood (1=no limit for drainage coefficient, 2=drainage coefficient equal to 1.0 $l \cdot s^{-1} ha^{-1}$ and 3=0.5 $l \cdot s^{-1} \cdot ha^{-1}$, respectively).

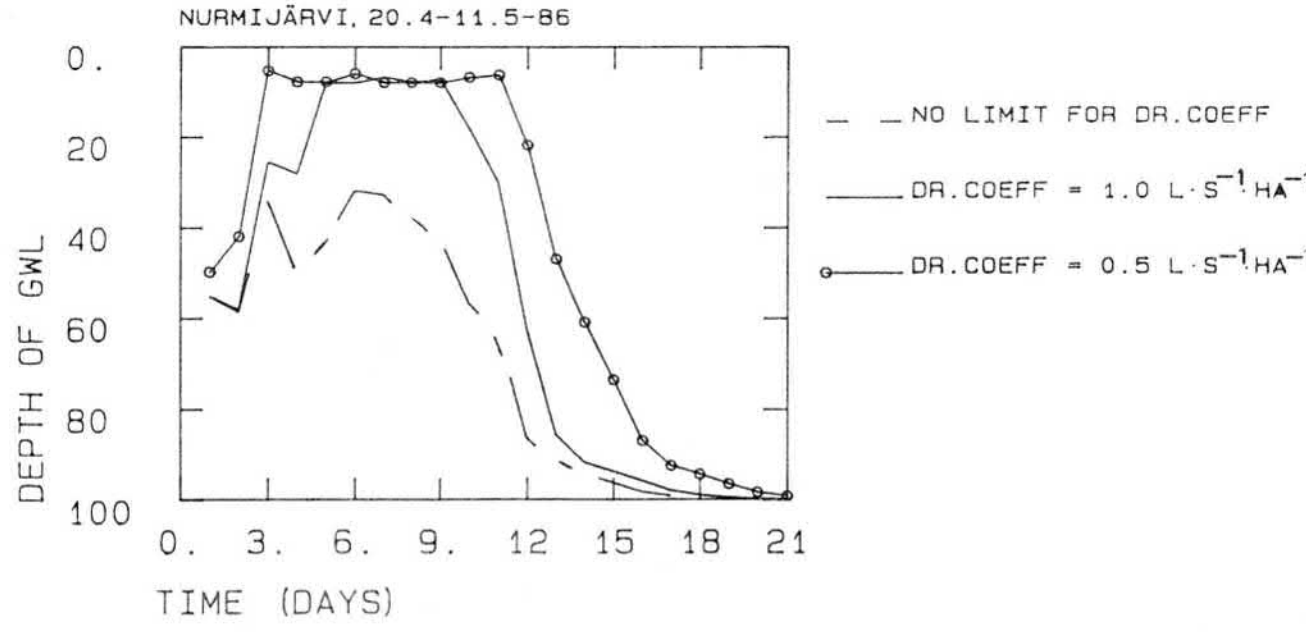

Fig. 8-4b. The computed depth of groundwater level during the 1986 spring flood (1=no limit for drainage coefficient, 2=drainage coefficient equal to 1.0 $l \cdot s^{-1} \cdot ha^{-1}$ and 3=0.5 $l \cdot s^{-1} \cdot ha^{-1}$, respectively).

Using the methods described in Chapter 4, it is possible to predict the daily course of the soil water pressure head at a depth of 5 cm. With the aid of the workability limits in Table 8-1, the number of working days in spring can be predicted. If the number of days required for field works is known, one can predict the time for sowing or planting.

The analysis of the effect of the drainage coefficient is simplified in such a way that only the computed pressure head at a depth of 5 cm is shown in Fig. 8-5 for three cases : 1) the hydraulic capacity of the drains is high enough, 2) the drainage coefficient is equal to 1.0 $l \cdot s^{-1} \cdot ha^{-1}$ and 3) the drainage coefficient is 0.5 $l \cdot s^{-1} \cdot ha^{-1}$. The effect of the reduction of the drainage coefficient on the pressure head at a depth of 5 cm can be seen from Fig. 8-5. According to Table 8-1, it is assumed that if the value of the pressure head is less than -80 cm, it is possible to start sowing. According to Fig. 8-5, if no limit is set for the drainage coefficient, the earliest possible time for sowing is on day 12 corresponds to the 1st of May (the starting date of calculations was on the 20th of April). If a drainage coefficient of 1.0 $l \cdot s^{-1} \cdot ha^{-1}$ is used, the earliest time is delayed by approximately one day. If the drainage coefficient is equal to 0.5 $l \cdot s^{-1} \cdot ha^{-1}$, the delay is four days. However, the earliest possible starting date for the field work is the 5th of May even if the drainage coefficient is as low as 0.5 $l \cdot s^{-1} \cdot ha^{-1}$.

A complete analysis of the effect of the drainage coefficient should be made by estimating the effect of the drainage coefficient on longterm average yields. However, based on the two examples presented in sections 8.2.1 and 8.2.2 , it seems that there is no need to increase the drainage coefficient from the present value 1.0 $l \cdot s^{-1} \cdot ha^{-1}$, and it may even be possible to reduce it.

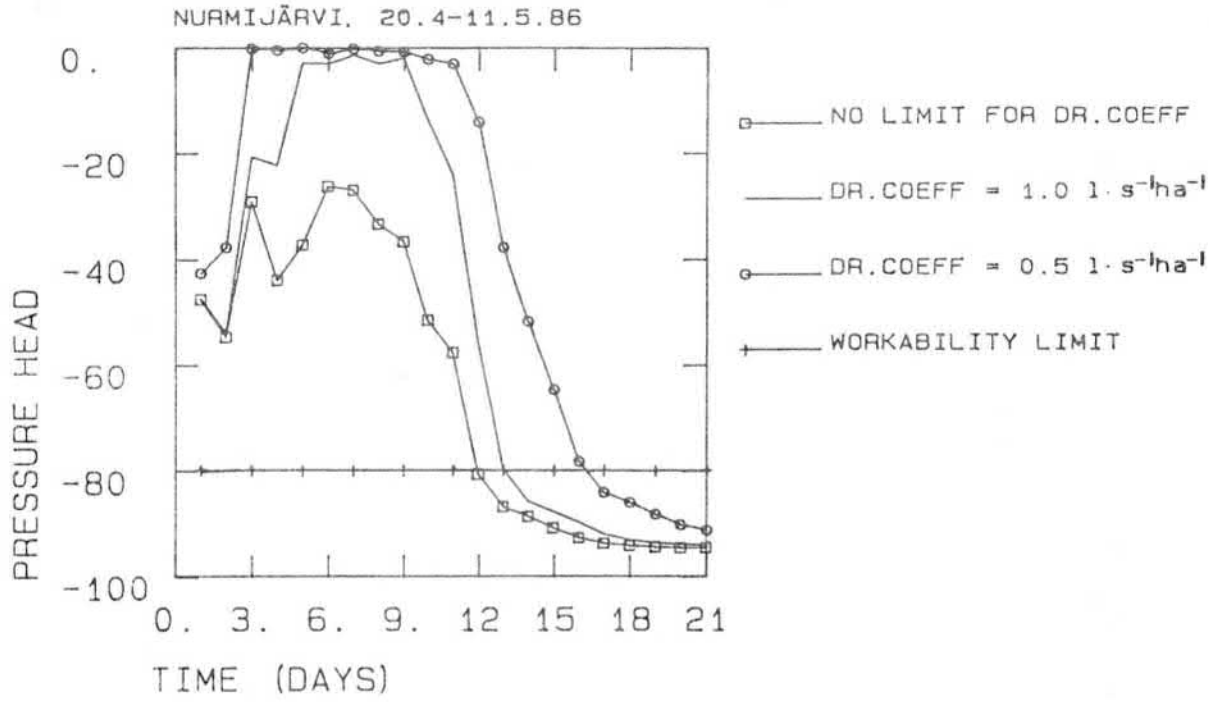

Fig. 8-5. The computed pressure head at a depth of 5 cm at Nurmijärvi in spring 1986. (1=no limit for drainage coefficient, 2=drainage coefficient equal to 1.0 $l \cdot s^{-1} \cdot ha^{-1}$ and 3=0.5 $l \cdot s^{-1} \cdot ha^{-1}$, respectively).

8.3 Estimation of the effect of drain spacing on the time for sowing and harvesting of oats

Based on the workability limits presented in Table 8-1 and on the calculated daily course of the pressure head, it is possible to estimate the starting date for sowing as a function of the drain spacing. This type of analysis was carried out for a light clay soil with relatively low saturated hydraulic conductivity (=0.1 $m \cdot d^{-1}$). The results are given in Fig. 8-6. 15 years of meteorological data were taken from the Maasoja experimental station and the starting date of sowing was calculated for eight different drain spacings, i.e. 6, 8, 10, 12, 15, 20, 25 and 30 m. According to Fig. 8-6, the average starting date for sowing would be delayed almost three weeks when drain spacings of 30 m was used instead of the 6 m spacing that gives the earliest starting date.

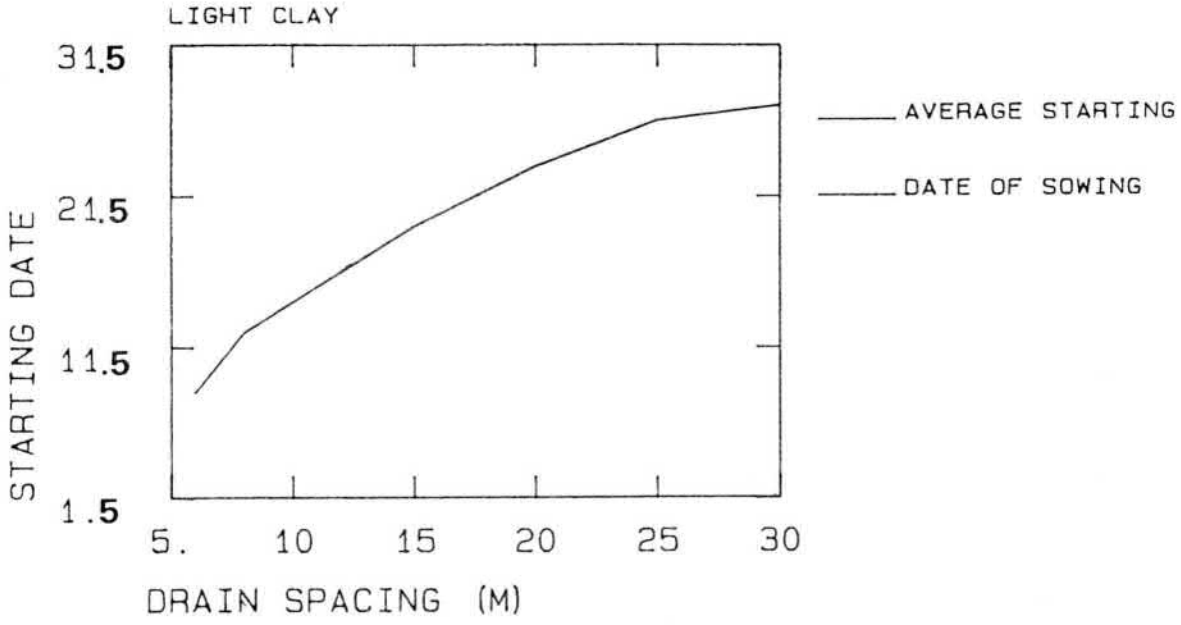

Fig. 8-6. Effect of drain spacing on the average starting date for sowing (data from 15 years) in light clay.

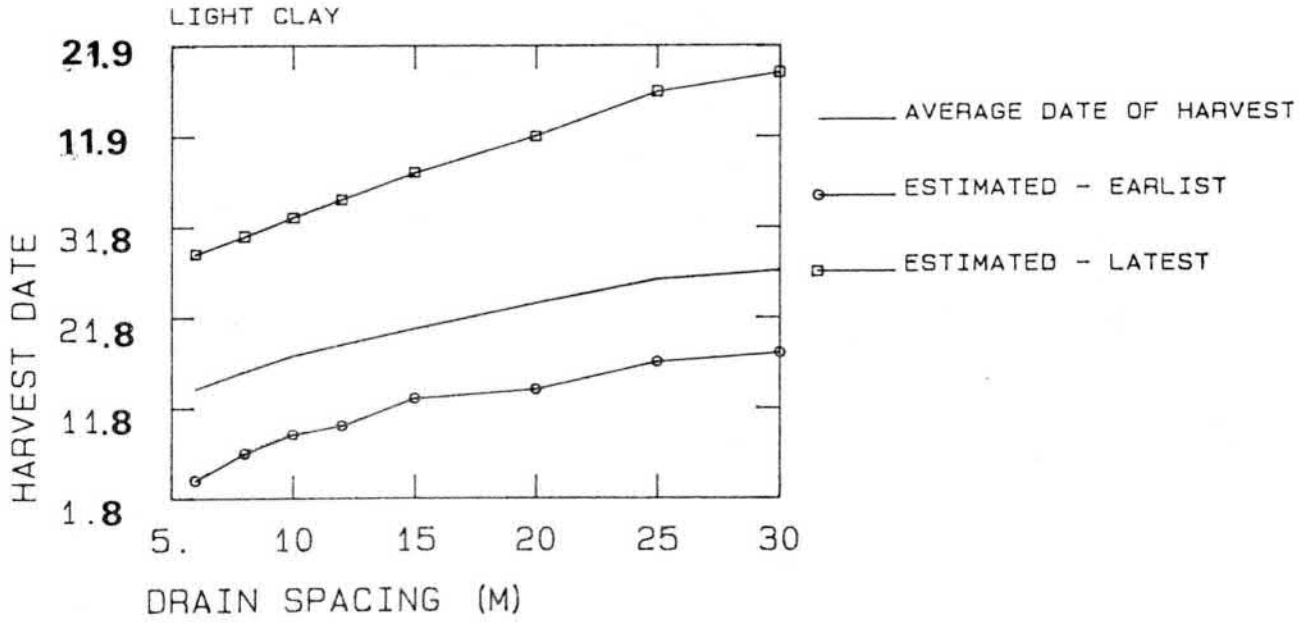

Fig. 8-7. Effect of drain spacing on the average date of harvest, and on the earliest and latest possible, respectively (data from 15 year) in light clay.

The average duration of the growing season for cereals can be estimated fairly accurately from the effective temperature sum. Moreover, a certain temperature sum is needed from emergence to sowing (e.g. 97 dd with a treshold value 2.7 °C for oats at Maasoja, see section 7.3). Based on the above mentioned temperature sums and on the estimated date of sowing, the average time of harvest can be predicted as a function of the drain spacing. The results of these calculations are given in Fig. 8-7. The average estimated date of harvest for all drain spacings was before September, but the scatter of estimated dates was very high as can be seen from Fig. 8-7, where the earliest and latest estimated dates of harvest, respectively, are given as a function of the drain spacing. In Fig. 8-7, the most exceptional year (1962) is not included. Using the meteorological data of year 1962, the model estimated that with drain spacings of 15, 20, 25 and 30, the yield could not be harvested at all due to very cold weather which delayed the growing season considerably.

8.4 Effect of drain spacing on profit

In Finland subsurface drainage projects are usually carried out in order to replace open ditches with subsurface drains. In the determination of the optimum drain spacing, the yields before and after the subsurface drainage have to be compared with the estimated cost of the subsurface drainage amortized over its useful life (about 30 years) or its economic life (generally about 10 years).

It is possible to use the proposed models to search for the optimum drain spacing of subsurface drainage , considering that optimality is achieved when the profit is maximized. Taking into account that the water management model is not an optimization technique, the search for the optimum value can only be achieved by calculating the profit obtained with various drain spacings.

Yield

The quasi-two-dimensional drainage model presented in Chapter 6 can be used in the evaluation of the effect of drain spacing on the soil moisture regime of the drained field. The relative yield can be calculated as a function of the drain spacing using the crop growth models of Chapter 5. This type of analysis has been carried out using the same meteorological data and soil parameters as in section 8.3. The crop parameters were taken from the Maasoja experiment.

Here the relative yield was calculated by the model, and the actual yield used in the estimation of the profit was obtained by multiplying the relative yield with two assumed maximum yields - a high value of 5000 $kg \cdot ha^{-1}$ and a relatively low value of 3000 $kg \cdot ha^{-1}$. The profit was calculated using these two maximum yields. Based on simulations, the relative yield of the field drained with open ditches (the spacing between ditches was assumed to be 14 m and the depth of the ditches 0.7 m) was only 75% of the maximum relative yield obtained with a drain spacing of 8 m (depth 1.0 m).

Costs

The total cost of the subsurface drainage can be estimated from the amount of drains needed for one hectare, and on the average cost of drainage, which is approximately 13 $FIM \cdot m^{-1}$. For example with a drain spacing of 15 m, 667 $m \cdot ha^{-1}$ is needed on average, corresponding to a total cost of 8700 $mk \cdot ha^{-1}$. The initial cost of the drainage system must be amortized over its useful life or economic life. The useful life can be considered to be at least 30 years, whereas the economic life depends e.g. on the repayment period of the loan needed to cover the costs of the drainage system. If economic life is used in estimating the profitability, subsurface drainage is considered to be an investment which has to cover the costs of the implementation while the loan is being repaid.

Income

Profit is dependent on the increase in yield due to subsurface drainage compared with the situation where the field was drained by open ditches, and on the amortized cost of the drainage system. Here the productivity value of the crop (oats) was calculated using a unit price that takes into account the production costs for oats (seed, lime, fertilizer, tractor fuel, labour, etc.). These data for different crops is published annually in Finland by the Central Association of Agricultural Centres. For oats the following net price was used:

$$YP = 2300 + 1.54 \cdot (YIELD - 2600) \quad (FIM \cdot ha^{-1}) \quad (8\text{-}1)$$

where YP is the net price ($FIM \cdot ha^{-1}$) and YIELD is the estimated yield of oats ($kg \cdot ha^{-1}$). The net price is dependent on the total crop yield because the production costs are almost independent of the crop yield. The total income can be obtained by first calculating the net price of the yield for different drain spacings and for maximum crop yields of 3000 and 5000 $kg \cdot ha^{-1}$ and by subtracting from these values the net price of the crop, assuming that the field were drained by open ditches, i.e. the increase in yield due to the subsurface drainage must be calculated.

Profit

Finally, the profit must be estimated as a function of drain spacing, for different maximum yield levels and for two time periods (10 and 30 years). The results have been given in Fig. 8-8. In Figs. 8-8a...8-8d, income (increase compared to the situation before the subsurface drainage), amortized costs of drainage system and the profit (income - costs).

In estimating the profit, the other benefial effects of subsurface drainage compared with fields drained by open ditches, are not included. The economic value of these effects (e.g. the decrease in the amount labour needed for field work,

decrease in machinery fuel and lube oil, reduced seed, lime and fertilizer costs) is difficult to evaluate, but an approximate value of a few hundred FIM $\cdot ha^{-1} \cdot year^{-1}$ can be considered a reasonable value. The exclusion of the above mentioned effects does not change the optimum drain spacing, but may in some cases give a negative profit for a project which is profitable if all the effects of subsurface drainage are taken into account.

In Figs. 8-8a and 8-8b, the profit is given for the higher maximum yield (5000 kg $\cdot ha^{-1}$). If an economic life of 10 years at interest rate of 10% is used to calculate the amortized costs (Fig. 8-8a), the optimal drain spacing is about 12 m. If the useful life of 30 years with interest rate of 8% is used in the calculations, the maximum profit can be obtained with a drain spacing of 10 m (Fig. 8-8b). The use of a low interest rate corresponds to the case in which the subsurface drainage is subsidized by the Finnish state.

The results when the lower maximum yield (3000 kg $\cdot ha^{-1}$) is used, are given in Figs. 8-8c and 8-8d. The maximum profit can be obtained with a drain spacing of 15 m. Here even the maximum profit is negative, indicating that at a low yield level, the increase in yield is not large enough to cover the costs of the subsurface drainage if an economic life of 10 years is used in the calculations.

The profit (due to the increase in yield) is also negative when the useful life is 30 years and the interest rate 8%. However, if all the beneficial effect of drainage are included, the drainage system is profitable if the useful life is the basis for calculations.

A very interesting conclusion can be drawn from the results of Fig. 8-8: the optimum drain spacing is not only dependent on the soil type and on the crop grown, but the choice of optimum drain spacing is also influenced by the overall maximum crop yield and by the time period used in the economic analysis. If high yields are desired (efficient cultivation technique,

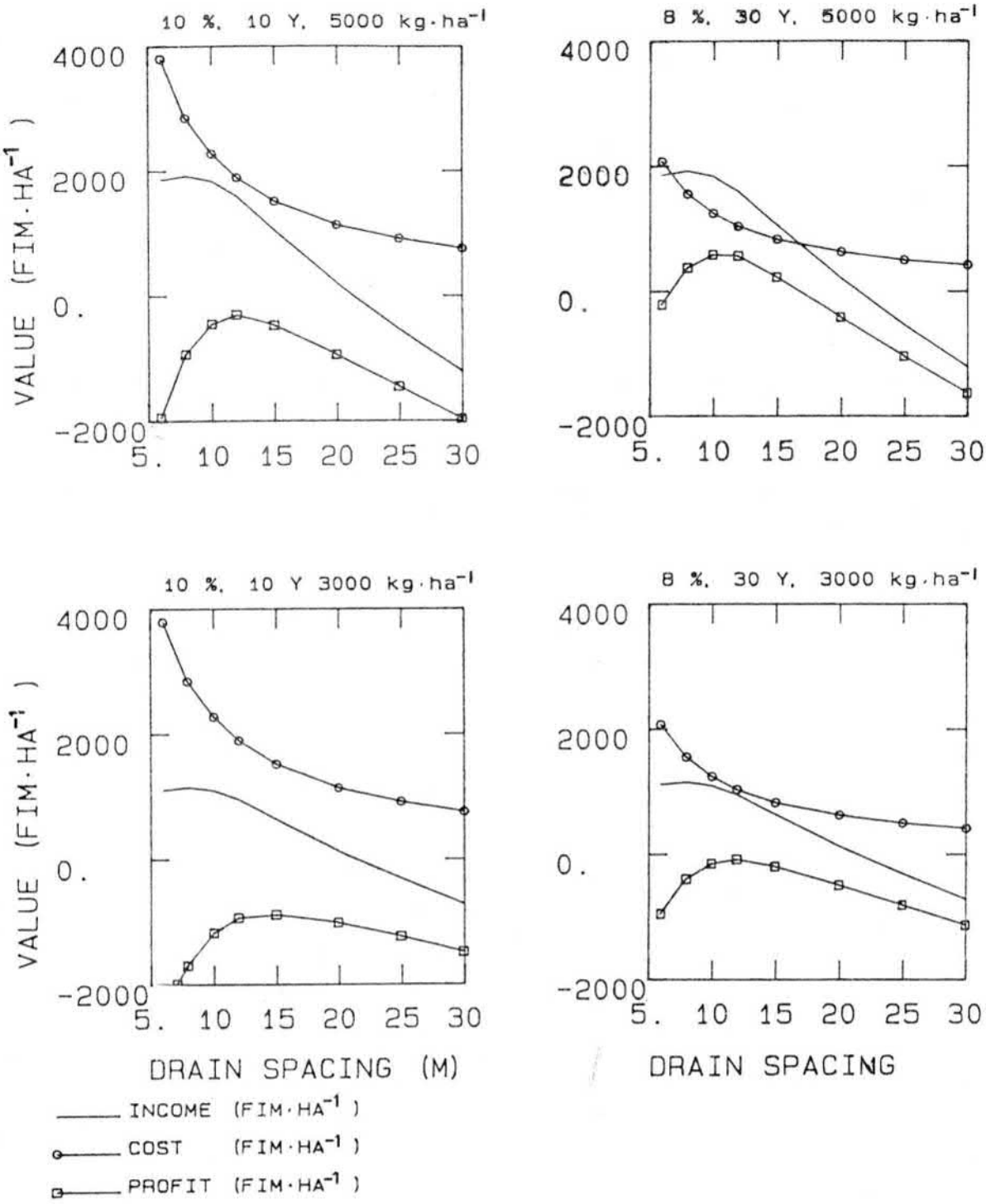

Fig. 8-8. Effect of drain spacing on income (increase in yield due to subsurface drainage), amortized cost and profit.

a) Maximum yield MY = 5000 kg·ha^{-1}, economic life EL=10 years, interest rate IR=10%,

b) MY=5000 kg·ha^{-1}, EL=30 years, IR=8%,

c) MY=3000 kg·ha^{-1}, EL=10 years, IR=10%,

d) MY=3000 kg·ha^{-1}, EL=30 years, IR=8%.

powerful tractors), it is desirable to use smaller drain spacings compared with the case when a "softer" cultivation technique is used. If the farmer is not willing to extend the investment over the approximated useful life of the drainage system, it is preferable to use larger drain spacings to compensate for the increase in the amortized cost due to the short calculation period.

8.5 Conclusions

Section 8.2 shows that for the two particular cases considered, the drainage coefficient characterizing the hydraulic capacity of the drains could be reduced to a value of 0.5 $l \cdot s^{-1} \cdot ha^{-1}$ from the value 1.0 $l \cdot s^{-1} \cdot ha^{-1}$ without a significant effect on the groundwater level. By applying the same type of analysis (as given in section 8.2) for different type of soils, it would be possible to evaluate whether the drainage coefficient of 0.5 $l \cdot s^{-1} \cdot ha^{-1}$ can be used for all drainage systems planned in Finland. If this is the case, it would imply that the total cost of the subsurface drainage could be reduced by approximately 1-5% depending on the amount of collectors required for the project.

The purpose of sections 8.3 and 8.4 was to illustrate the applicability of the water management model in designing subsurface drainage systems. A practical result was obtained, indicating that the optimum choice of drain spacing is dependent on the time period used in the economic calculations and on the overall yield level of the farm.

CHAPTER 9 DISCUSSION

9.1 Introduction

The mathematical models presented in this study are aimed at quantifying the effect of drainage on soil moisture, soil temperature and crop yield. Therefore, the underlying theory covers a very wide field of research. It has been necessary to develop both the numerical solution methods for the combined heat and mass transfer in saturated-unsaturated and seasonally frozen soil, and to present methods for the determination of the parameters of these equations.A brief evaluation of the applicability of the presented models is given in Sections 9.2 -9.5. Moreover, future development and research is also a topic of these sections.

9.2 Determination of the physical soil properties

The estimation procedures presented in Chapter 3 gave reasonably good results for most cases. However, in the application of the water management model, it would be useful to have estimation methods in which the final results - the soil water retention curve and the hydraulic conductivity curve - are functions, not tabulated values. The intention of the author is to pursue this line of research.

The most practical way to estimate the physical soil properties would probably be based on an intensive measurement period in the field. The simplified Kalman filtering algorithm presented in section 3.4 grants an oppurtunity to analyse the results of this type of measurement period.

9.3 Soil water and heat balance model

The mathematical model presented was subjected to numerous tests to verify its performance. Comparison of the model results with analytical and numerical solutions of soil-water flow problems, laboratory and field tests, showed that the results are

sufficiently accurate, and the agreement with the reported data is generally good.

In future, it necessary to extend the soil water model in such a way that the cracking of heavy clay soil can be analysed to some extent. More data is needed to verify the combined heat and mass balance in seasonally frozen soil.

The model can be extended in future research to include osmotic forces which result from the presence of solutes. The primary objective of extending the model in this fashion would be to try to estimate the accumulation of solutes in the root zone. This would enable assessment of the leaching effects.

9.4 Crop yield model

The model presented in Chapter 5 grants an opportunity to estimate the effect of soil water conditions on actual and potential crop yield. In future, several improvements are needed to produce more reliable estimate of the effect of drainage on crop yield.

The crop parameters needed in the model should be values measured in Finland. These include e.g. the development stage as a function of effective temperature sum, the leaf area index as a function of the development stage and the development of the rooting depth.

It is preferable to develop models that need as few prescribed parameter values as possible. Once the sowing/planting date is given/computed, the model should be capable of generating the development stage of the crop, the rooting depth, the leaf area index, the crop height and the allocation of the biomass produced.

9.5 Application of the model in designing drainage systems in Finland

The applicability of the water management model in designing drainage systems was discussed briefly in Chapter 8. The possibilities to utilize this type of technique are numerous:

a) The effect of soil type on optimum drain spacing and drain depth.
b) The effect of crop grown on drain spacing.
c) A detailed analysis of the effect of drainage coefficient on the earliest possible time of sowing/planting.
d) The effect of drainage coefficient on crop yield.
e) The effect of the water level of the main canal on the earliest possible time of sowing/planting.
f) The effect of surface drainage on crop yield.

9.6 The model in practice

The present version of the water management model can prove difficult to use due to the amount of data required. A number of features should be added to the computer algorithms developed here, to eliminate the above mentioned problems and make the use of the model both practical and economically viable. These are:

a) Develop computer programs for easy input of the data required in the models.
b) Provide more options for using the model depending on the quality and quantity of data available.
c) Provide special routines to interpret the results interactively on a graphic terminal.
d) Develop micro computer based versions of the water management model.

CHAPTER 10 SUMMARY

This study was undertaken with the primary objective of developing a methodology that combines climatological data, soil properties, crop drainage requirements and drainage theory into a design method called a water management model. This type of methodology is intended for designing subsurface drainage systems in Finland. The final result of the application of the methods presented in this study is a decision on optimum drainage parameters, i.e. drain spacing and depth, and drainage coefficient.

The main aim of this study was to present methods that quantitatively describe the physical relations in a drained fields. Detailed practical applications of the methodology fall outside the scope of this research, and only a few practical examples are treated.

The first stage in the application of the water management model is the determination of the physical soil parameters needed in the models. Chapter 3 presents methods for the estimation of the soil water retention curve from the soil texture, for the calculation of the unsaturated hydraulic conductivity function from the soil water retention curves, and for the determination of soil thermal conductivity based on an intensive measurement period of soil temperatures at several depths. The extension of the theory originally presented by Sigvard Andersson (1969) for calculating the unsaturated hydraulic conductivity function proved to give good results compared with the existing models of Mualem (1976), Averjanov (1950), Van Genuchten (1978) and Brooks and Corey (1966).

Chapter 4 describes methods for calculating the soil moisture content and soil temperature of a saturated- unsaturated soil. The Chapter presents a new method for the solution of combined mass and heat flow in a porous media. The models were subjected to numerous tests to verify their performance, test the accuracy of the numerical results and examine the reliability of the

predictions. Comparison of the results of the models with analytical and numerical solutions of soil-water flow problems, and laboratory and field tests which have been published in the recent literature, showed that the results are sufficiently accurate and the agreement with the reported data is quite good.

Chapter 5 is devoted to the mathematical description of the crop growth model that accounts for the growth factor water and the potential growth rate. Methods for calculating the potential evapotranspiration rate are given in this Chapter. This Chapter presents a new method that combines the effective temperature sum (cumulative sum of air temperature values above 5 °C) with the calculation of the development stage of a plant. In this chapter the crop growth model was tested against the experimental data collected at the Geestmerambacht experimental station in the Netherlands. The models presented gave a realistic estimation of the cumulative biomass as a function of time.

The methodology developed is planned mainly for quantification of the effect of subsurface drainage on soil moisture, soil temperature and crop yield. Mathematical models of drainage are presented in Chapter 6. In short, the results of this Chapter suggest that in a water management model there is little to be gained by using a fully two-dimensional solutions to the drainage problem; approximate methods for the calculation of the flow rates and the elevation of the water table should be used instead. However, in a case where the groundwater level is near the soil surface for a long time during the growing season and the hydraulic parameters are very accurate, it may be advisable to use the fully two-dimensional solution.

Chapter 7 discusses the simulation results of the Backas and Maasoja field experiments. In most cases the models presented produced realistic results. However, the cracking of heavy clay soil should be included in the model if an accurate prediction of the soil moisture profile is of special importance. The estimation of the soil thermal conductivity function based on an

intensive measurement period proved to be very succesfull. If the soil surface temperature can be given as a boundary condition, an accurate prediction of soil temperature can be obtained. If the soil surface temperature under the snow cover is computed by the model, the results are very sensitive to the calculated density of the snow pack.

In the calculation of the crop growth for oats at the Maasoja experimental station it was concluded that the method based on calculating the development stage of a plant as a function of effective temperature sum seems to be very suitable for Finnish conditions. In this way, the date of harvest need not be given as a prescribed value since the model is capable of predicting it. Measured values of the leaf area index as a function of the effective temperature sum should be available for different species. If a prediction of the effect of high groundwater level is needed, methods should be available for estimation of the critical gas porosity and anaerobic point.

Finally, the simulation results for Maasoja suggest that it is necessary to develop crop growth models that can adapt to changes in soil moisture content and soil temperature, i.e to develop models that need as few prescribed parameter values as possible since the model is capable of generating e.g. the depth of the rooting zone.

Chapter 8 discusses the prospects for use of the methodology presented in designing subdrainage systems in Finland. It was shown that the methods can be used in estimating the proper drainage coefficient, i.e. the design flow that the pipe system must be capable of conveying. The methodology was tested against the data collected at the Nurmijärvi experimental field. A detailed analysis was not made, but two cases show that there is no need to increase the drainage coefficient from the present value of 1.0 $l \cdot s^{-1} \cdot ha^{-1}$ even though the measured peak flows were 200-250% greater than the design flow. It also seems realistic to decrease the design flow; this would reduce the total costs of the drainage system.

Chapter 8 presents the application of the suggested methodology in estimating the optimum drain spacing for a light clay soil. It was found that the optimum spacing is not only dependent on the soil type and crop grown; the choice is also affected by the time period used in the economic analysis and by the overall maximum yield level, which is an indication of the efficiency of the cultivation techniques used on the farm.

REFERENCES

Abbott, M.B., Kastberg, J., Havnø, K., Høgh Jensen, K., Kroszynski, U.I. and Warren, I.R. (1982). Research and development for the unsaturated zone component of the European Hydrologic System - Système Hydrologique Europèen (SHE). In "Engineering applications of computational hydraulics, Volume I" (ed. M.B. Abbott and J.A. Cunge). Pitman, pp 40 - 70.

Al-Soufi, R.W. (1983). Unsaturated hydraulic conductivity, "Evaluation research study". Thesis for the degree of licenciate in technology, Helsinki University of Technology, Laboratory of Hydrology and Water Resources Engineering, Otaniemi, Finland.

Andersson, S. (1962). Some theoretical relationships between soil water retention curves, drainage equilibrium and pore-size distribution (in Swedish). Grundförbättring, 15(1-2), 51-107.

Andersson, S. (1969). Theoretical relationships in capillary systems between capillary conductivity, pore-size distribution, tension, and water content(in Swedish). Grundförbättring, 22(4), 143-154.

Andersson, S. and Wiklert, P. (1972). The water-holding properties of the Swedish soil types (in Swedish). Grundförbättring 25: 53-143.

Arya, L.M., Farrell, D.A. and Blake, G.R. (1975). Determination of hydraulic properties of the soil. Soil Sci. Soc. Amer. Proc., 39, 424-430.

Aslyng, H.C. and Hansen, S. (1982). Water balance and crop production simulation. Model WATCROS for local and regional application. Hydrotechnical Laboratory. The Royal Vet. and Agric. Univ., Copenhagen. 200 pp.

Averjanov, S.F. (1950). About permeability of subsurface soils in case of incomplete saturation. Eng. Collect. 7.

Axelsson, B. and Ågren, G. (1976). Tree growth model (PT 1) - a development paper. Swed. Conif. For. Proj. Int. Rep. 41, 79 pp.

Belmans, C., Wesseling, J.G. and Feddes, R.A. (1983). Simulation model of the water balance of a cropped soil: SWATRE. J. of Hydrology 63,3/4: 271-286.

Bierhuizen J.F. and Slatyer, R.O. (1965). Effect of atmospheric concentration of water vapour and CO2 in determining transpiration - photosynthesis relationships of cotton leaves. Agric. Meteor. 2, pp. 259-270.

Black, T.A., Gardner, W.R. and Thurtell, G.W. (1969). The prediction of evaporation, drainage, and soil water storage of a bare soil. Soil Sci. Soc. Amer. Proc., 33, 655-660.

Bloemen, G.W. (1980). Calculation of hydraulic conductivities of soils from texture and organic matter content. Z. Pflanzenernaehr. Bodenkd. 143, 581-605.

Box, G.E.P. and Jenkins, G.M. (1970). Time series analysis, forecasting and control. Holden - Day Inc.

Brooks, R.H. and Corey, A.T. (1966). Properties of porous media affecting fluid flow. J. Irrig. Drain. Div., 92(IR2), 61-88.

Buitendijk, J. (1985). Effect of workability index, degree of mechanization and degree of certainty on the yield of sugar-beet. Soil&Tillage Research, 5(1985), pp. 247-257.

Burdine, N,T. (1953). Relative permeability calculation from size distribution data. Am. Soc. Agri. Eng. 10, 400-404.

Busoni, E., Kowalik, P. and Sanesi, G. (1983). Effect of different natural drainage conditions on whinter wheat production. Agric. Water Management, 7:425,438.

Campbell, G.S. (1974). A simple method for determining unsaturated conductivity from moisture retention data. Soil Sci., 117, 311-314.

Carslaw, H.S. and Jaeger, J.C. (1959). Conduction of heat in solids. 2nd ed. Oxford University Press, London. 509 p.

Corps of Engineers 81956). Snow hydrology. Summary report of the snow investigations. Portland, Oregon: U.S. Army, North Pacific Division, 437 pp.

Curry, R.B., Baker. C.H. and Streeter, J.G. (1975). SOYMOD I: A dynamic simulator of soybean growth and development. TRANSACTIONS of the ASAE, pp. 963-969.

Desai, C.S. (1979). Elementary finite element method. Prentice Hall, Inc.

Elomaa, E. and Pulli, S. (1985). Variationer i global-strålning, effektiva temperatursumma, nederbörd, potentiella

evapotranspiration och nederbördsunderskott i relation till växtproduktion i södra Finland. NJF-seminarium, Nr 77, Uppsala 23-24 September 1985. pp. 19-28.

Elrick, D.E. and Bowman, D.H. (1964). Note on an improved apparatus for soil moisture measurements. Soil Sci. Soc. Amer. Proc., 28, 450-453.

Engelmark, H. (1984). Infiltration in unsaturated frozen soil. Nordic Hydrology, 15 : 243-252.

Engelmark, H. (1986). Infiltration and run-off during the period of snow melt. Field observations and numerical simulations (in Swedish, English summary). Division of Water Resources Engineering, Serie A, nr 145, Luleå, Sweden.

Feddes, R.A. (1971). Water, heat and crop growth. Thesis for the degree of Doctor of Technology. H. Veenman&Zonen N. V., Wageningen. 184 pp.

Feddes, R.A. (1984). Crop water use and dry matter production: state of the art. Conference Internationale de la CIID sur les Besoins en eau des Cultures, Parias, 11-14 septembre 1984.

Feddes, R.A. (1985). Modeling and simulation in hydrologic systems related to agricultural development: state of the art. 15 pp.

Feddes, R.A., Bresler, E. and Neuman, S.P. (1974). Field test of a modified numerical model for water uptake by root systems.

Feddes, R.A., Kowalik, P.J. and Zaradny, H. (1978). Simulation of field water use and crop yield. Wageningen. 189 p.

Fipps, G., Skaggs, R.W. and Nieber, J.L. (1986). Drains as a boundary condition in finite elements. Water Res. Res. 22:1613-1621.

Fukuda, M. (1983). Experimental studies of coupled heat and moisture transfer in soils during freezing. Contribution No. 2528 from the Institute of Low Temperature Science. pp. 37-85.

Gardner, W.R. (1958). Some steady state solutions of the unsaturated moisture flow equation with application to evaporation from a water table. Soil Sci. 85: 228-232.

Ghali Sami Ghali (1986). Mathematical modeling of soil moisture dynamics in trickle irrigated fields. Ph.D. dissertation, University of Southampton, Civil Engineering Department,

Institute of Irrigation Studies. 322 p.

Gilpin, R.R. (1980). A model for the prediction of ice lensing and frost heave in soils. Water Resources Res., 16(5): 918-930.

Green, R.E. and Corey, J.C. (1971). Calculation of hydraulic conductivity. A further evaluation of some predictive methods. Soil. Sci. Soc. Amer. Proc. 35, 3-7.

Guymon, G.L. and Luthin, J.N. (1974). A coupled heat and moisture transport model for arctic soils. Water Resources Res., 10(5) : 995-1001.

Guymon, G.L., Hromadka, T.V. and Berg, R.L. (1980). A one-dimensional frost heave model based upon simultaneous heat and water flux. Cold Regions Sci. Techol., 3: 253-262.

Halldin, S., Grip, H., Jansson, P.E. and Lindgren, Å. (1980). Micrometeorology and hydrology of pine forest eco- systems. II. Theory and models. Ecol. Bull. 32: 463-503.

Hanks, R.J., Klute, A. and Bresler, E. (1969). A numerical method for estimating infiltration, redistribution, drainage and evaporation of water from soil. Water Res. Res. 5: 1064-1069.

Hanks, R.J., Austin, D.D. and Ondrechen, W.T. (1971). Soil temperature estimation by a numerical method.

Hardjoamidjojo, S. and Skaggs, R.W. (1982). Predicting the effects of drainage systems on corn yield. Agricultural Water Management, Vol. 5: 127-144.

Harlan, R.L. (1973). Analysis of coupled heat-fluid transport in partially frozen soil. Water Resources Res., 9(5): 1314-1323.

Heldal, B. (1970). Estimating the global radiation at Ås.Meldingar fra Norges Lantbrukshøgskole, Vol. 49, Nr. 11.

Hooli, J. (1971). Säätekijöiden vaikutuksesta viljelykasvien satoihin ja vesitalouteen. (English summary: Effect of weather on water economy and crop yields). Helsingin teknillinen korkeakoulu, Tieteellisiä julkaisuja 35, Otaniemi.

Hornberger, G.M. and Remson, I. (1970). A moving boundary model of a one-dimensional saturated-unsaturated, transient porous flow system. Water Res. Research, Vol. 6, No. 3, 898-905.

Hromadka, T.V, Guymon, G.L. and Berg, R.L. (1981). Some approaches to modeling phase change if freezing soils. Cold Regions Sci. Technol., 4: 137-145.

Hundal, S.S. and De Datta, S.K. (1984). In situ water transmission characteristics of a tropical soil under rice- based cropping systems. Agric. Water Manage., Vol. 8, No. 4, 387-396.

Ilola, A., Elomaa, E. and Pulli, S. (1986). Klimafaktorers innvirkning på planters vegst og produksjon, Slutrapport, Vedlegg 2, Nordisk kontaktorgan för jordbruksforskning (manuscript, in English). 11+3 pp.

Jackson, R.D. (1972). On the calculation of the hydraulic conductivity and diffusivity of unsaturated soils. Soil Sci., Vol. 113, No. 4, 264-275.

Jansson, P-E. and Halldin, S. (1980). Soil water and heat model. Technical description. Technical Report 26, Swedish Coniferous Forest Project, Uppsala, Sweden.

Jazwinski, A.H. (1970). Stochastic processes and filtering theory. Academic Press, New York. 376 p.

Jensen, K.H. (1983). Simulation of water flow in the unsaturated zone including the root zone. Institute of Hydrodynamics and Hydraulic Engineering, Technical University of Denmark, Series Paper No. 33, Lungby.

Jensen, M.E. and Hanks, R.J. (1967). Nonsteady state drainage from porous media. J. Irrig. Drain. Div., 93(IR3), 209-231.

Juusela, T. (1945). Untersuchungen über den Einfluss des Entwässerungsverfahrens auf den Wassergehalt bes Bodens, den Bodenfrost und die Bodentemperatur. Acta Agr. Fenn. 59:1-212.

Kaitera, P. (1940a). Peltojemme vesitysmahdollisuuksista (in Finnish). Karjatalous 16: 471-477.

Kaitera, P. (1940b). Sadonlisäyksistä sadetuskokeissa. Referat: Über die Mehrerträge bei Beregnungsversuchen in den Jahren 1938-1940. Maanvilj. ins. yhd. vuosik. 1940: 101-144.

Kalyuzhnyi, I.L., Pavlova, K.K. and Lavrov, S.A. (1984). Physical simulation of water migration in soil freezing. Meteorologiya i Gidrologiya, 1: 77-85.

Kersten, M.S. (1949). Thermal properties of soils. Inst. of

Technology, Engineering Exp. Station, Bull. No. 28, Minneapolis, Univ. Minnesota.

Kettunen, J. and Varis, O. (1986). A recursive Gauss-Newton algorithm for nonlinear parameter estimation. Research Report 1986:2, Helsinki University of Technology, Laboratory of Hydrology and Water Resources Engineering, Otaniemi, Finland. 15 p.

Kinosita, S. and Ishizaki, T. (1980). Freezing point depression in moist soils. The 2nd International Symposium on Ground Freezing, June 24-26., 1980., Trondheim, Norway.

Kowalik, P.J. and Sanesi, G. (1980). Simulazione della produttivita reale del suolo; alcuni esempi per i suoli idromorfi del Mugello (Firenze). CNR Pubbl. 46 P.F. Conservazione del Suolo, Firenze, 75 pp.

Kowalik, P.J. (1981). Program of yield prognosis in soil information system BIGLEB. Roczniki Gleboznawcze (Warsaw, Poland), 32, 251-261.

Kunze, R.J., Uehara, G. and Graham, K. (1968). Factors important in the calculation of hydraulic conductivity. Soil Sci. Soc. Amer. Proc., 32, 760-765.

Kuusisto, E. (1984). Snow accumulation and snowmelt in Finland. Publications of the Water Research Institute 55, Helsinki.

Maasilta, A. (1961). Pohjaveden korkeus ja kevätviljojen sadot (in Finnish). Koetoim. ja Käyt. 11.

Maybeck, P.S. (1979). Stochastic models, estimation and control. Volume I. Academic Press, New York. 423 p.

McKinion, J.M., Jones, J.W. and Hesketh, J.D. (1975). A system of growth equations for the continuous simulation of plant growth. TRANSACTIONS of the ASAE, pp. 975-979, 984.

Miller, R.D. (1978). Frost heaving in non-colloidal soils, 4rd, Int'l Conf. Permafrost, op. cit., 707-713.

Millington R.J. and Quirk, J.P. (1961). Permeability of porous solids. Trans. Faraday Soc. 57, 1200-1206.

Molz, F.J. and Remson, I. (1970). Extraction term models of soil moisture use by transpiring plants. Water Res. Res. 6:1346-1356.

Motovilov, YU.G. (1977). Numerical modeling the process of

water infiltration in frozen soils (in Russian). Meteorologiya i Gidrologiya, 9: 67-75.

Motovilov, YU.G. (1978). Mathematical model of water infiltration into frozen soil. Soviet Hydrology, 17(1): 62-66.

Motovilov, YU.G. (1979). Simulation of meltwater losses through infiltration into Soil. Soviet Hydrology, 18(3): 217-221.

Mualem, Y. (1976). A new model for predicting the hydraulic conductivity of unsaturated porous media. Water Res. Research, Vol. 12, No. 3, 513-522.

Mustonen, S.E. (1964). Potentiaalisen evapotranspiraation määrittämisestä (English Summary: Estimating potential evapotranspiration). Suomen Maataloustieteellisen Seuran Julkaisuja 102,2, 24 pp.

Neuman, S.P. (1972). Finite element computer programs for flow in saturated- unsaturated porous media. Technion, Israel.

Neuman, S.P. (1973). Saturated-unsaturated seepage by finite elements. Journal of the Hydr. Div. 99(HY12), 2233- 2250.

Neuman, S.P., Feddes, R.A. and Bresler, E. (1974). Finite element simulation of flow in saturated - unsaturated soils considering water uptake by plants. Technion, Israel.

Neuman, S.P., Feddes, R.A. and Bresler, E. (1975). Finite element analysis of two-dimensional flow in soils considering water uptake by roots:I. Theory. Soil Sci. Soc. Amer. Proc. 39:224-230.

Nimah, M.N. and Hanks, R.J. (1973). Model for estimating soil water, plant and atmospheric interrelations. I. Description and sensitivity. Soil Sci. Soc. Amer. Proc. 37:522-527.

Mohammad, F.S. and Skaggs, R.W. (1983). Drain tube opening effects on drain inflow. J. of Irr. and Drain. Eng. Vol. 109, No. 4, pp. 393-403.

O'Neill, K. and Miller, R.D. (1982). Numerical solutions for a rigid-ice model of secondary frost heave. CCREL Report 82-13.

Penman, H.L. and Schofield, R.K. (1951). Some physical aspects of assimilation and transpiration. Proc. Symp. nr. V, Soc. Exp. Biol, pp. 115-129.

Philip, J.R. (1957a). The theory of infiltration: 1. The infiltration equation and its solution. Soil Sci., Vol. 83,

pp. 345-357.

Philip, J.R. (1957b). The theory of infiltration:2. The profile at infinity. Soil Sci., Vol. 83, No. 6, pp. 435-448.

Pinder, G.F. and Gray, W.G.G.(1977). Finite element simulation in surface and subsurface hydrology. Academic Press, London.

Pingoud, K. (1982). A lumper-parameter model for infiltration, Journal of Hydrology, Vol. 57,pp. 175-185.

Pingoud, K. (1984). Sensitivity analysis of a lumped-parameter model for infiltration. Journal of Hydrology, Vol. 67, pp. 97-113.

Pingoud, K. and Orava, P. (1980). A dynamic model for the vertical infiltration of water into the soil. International Journal of Systems Science, Vol. 11, No. 12, pp. 1491-1498.

Poulovassilis, A. (1970). Hysteresis of pore water in granular porous bodies. Soil Sci., 109, 5-12.

Prasad, R. (1986). A linear root water uptake model (prov. title). Submitted to J. of Hydrology.

Remson, I., Hornberger, G.M. and Molz, J.F. (1971). Numerical methods in sussurface hydrology. Wiley Intersci., New York, pp. 1 - 240.

Ritchie, J.T. (1972). A model for predicting evaporation from a row crop with incomplete cover. Water Res. Res. 8(5) , pp. 1204-1213.

Rintanen, S. (1986). Hydraulisen johtavuuden mittaaminen, vaihtelu ja hyväksikäyttö salaojituksen mitoituksessa. Ms.Sci. Thesis, Helsinki University of Technology, Otaniemi.

Rubin, J. and Steinhardt, R. (1963). Soil water relations during rain infiltration. I. Theory. Soil Sci. Soc. Proc., 27: 246-251.

Saarinen, J., Pulli, S. and Elomaa, E. (1986). Sääkentän käyttö kasvin potentiaalisen sadon määrittämisessä. Maataloustieteen päivät 1986.

Salonen, M. (1949). Tutkimuksia viljelyskasvien juurten sijainnista Suomessa (English summary: Investigations of the root positions of field crops in the soils of Finland). Maataloustieteellisen Seuran julkaisuja 70,1. 91 pp.

Sekendar, M.A. (1984). Entrance resistance of enveloped drainage pipes. Agric. Water Management, 8:351-360.

Sibma, L. (1977). Maximization of arable crop yields in the Netherlands. Neth. J. Agric. Sci. 25, pp. 278-287.

Skaggs, R.W.(1980). A water management model for artificially drained soils. North Carolina Agricultural Research Service, Tech. Bul. No. 267. 54 p.

Skaggs, R.W., Monke, E.J. and Huggins, L.F. (1971). An approximate method for defining the hydraulic conductivity-pressure potential relationship for soils. Transactions of the ASAE, p. 130-133.

Skaggs, R.W. and Nassehzadeh-Tabrizi, A. (1983). Optimum drainage for corn production. Tech. Bull. 274, N.C. Agr. Res. Service, N.C.S.U., Raleigh, N.C. 41 pp.

Skaggs, R.W. and Tang, Y. (1976). Saturated and unsaturated flow to parallel drains. J. Irrig. Drain. Div., 102 (IR2), 221-237.

Smithsonian Meteorological Tables. Washington.

Stephens, D.B. and Rehfelt, K.R. (1985). Evaluation of closed- form analytical models to calculate conductivity in a fine sand. Soil. Sci. Soc. Amer. Proc., 49, 12-19.

Tang, Y.K. and Skaggs, R.W. (1978). Subsurface drainage in soils with high hydraulic conductivity layers. Transactions of the ASAE, Vol. 21(3):515-521.

Talsma, T. (1970). Hysteresis in two sands and the independent domain model. Water Res. Research, Vol. 6, No.3, 964-970.

Taylor, G.S. and Luthin, J.N.(1978). A model for coupled heat and moisture transfer during soil freezing. Canadian Geotech. J., 15: 548-555.

Thornley, J.M.H. (1976). Mathematical models in plant physiology. Academic Press, London.

Topp, G.C. and Miller, E.E. (1966). Hysteresis moisture characteristics and hydraulic conductivities for glass- bead media. Soil Sci. Soc. Amer. Proc., 30, 156-162.

Vachaud, G. and Vauchlin, M. (1975). Comments on 'A numerical model based on coupled one-dimensional Richards and Boussinesq equations'. Water. Res. Research, Vol. 11, No.3, 506 - 509.

Vakkilainen, P. (1982). Maa-alueelta tapahtuvan haihdunnan arvioinnista (English summary: On the estimation of actual evapotranspiration). Acta Universitas Ouluensis, Series C, No.

20, Oulu.

Vakkilainen, P. and Virtanen, S. (1986). Applicability of drainage design equations to Finnish conditions. Proceedings of International Seminar on Land Drainage (ed. J. Saavalainen and P. Vakkilainen), Helsinki University of Technology, Department of Civil Engineering, Water Engineering, Otaniemi, Finland. pp. 27-35.

Van Genuchten, M.Th. (1978). Calculating the unsaturated hydraulic conductivity with a new closed-form analytical model. Princeton Univ. Research Report no: 78-WR-08.

Van Schilfgaarde J. (1963). Design of tile drainage for falling watertables. Proc. ASCE 89(IR2), pp. 1-11.

Wang, H.F. and Anderson, M.P. (1982). Introduction to groundwater modeling. Finite difference and finite element methods. W.H. Freeman and Company, San Fransisco.

Watson, K.K. (1967). Numerical and experimental study of column drainage. J. Hydraul. Div., 93(HY2), 1-15.

Watson, K.K. (1974). Some applications of unsaturated flow theory. In J. van Shilfgaarde (ed.) Drainage for agriculture. Agronomy 17: 359-401. Amer. Soc. Agron., Madison, Wis.,USA.

Wells, L.G. and Skaggs, R.W. (1976). Upward water movement in field cores. Transactions of the ASAE, 275-283.

Wesseling J. (1973). Theories of field drainage. ILRI Publ. 16, Wageningen, The Netherlands, 30 pp.

Wesseling, J. and Homma, F. (1967). Entrance resistance of plastic drain tubes. Neth. J. Agric. Sci. 15.3, pp. 170-182.

Wiebe, H.J. (1975). Zur Übertragung von Ergebnissen aus Klimakammern auf Freilandbedingungen mit Hilfe eines Simulationsmodells bei Blumenkohl-Gartenbauwissenschaft 2, pp. 70-74.

Wierenga, P.J., Nielsen, D.R. and Hagan, R.M. (1969). Thermal properties of Yolo silt loam. Soil Sci. Soc. Amer. Proc., Vol. 33, pp 354 - 359.

Wijk, A.L.M. Van and Feddes, R.A. (1982). A model approach to the evaluation of drainage effects. In 'Land Drainage' (ed. M.J. Gardiner). A seminar in the EC programme of Coordination of Research on Land Use and Rural Resources, Cambridge, UK,

27-31 July 1981. A.A. Balkema, Rotterdam: 131-149.

Wijk, A.L.M. Van and Feddes, R.A. (1986). Simulating effects of soil type and drainage on arable crop yield. Proceedings of International Seminar on Land Drainage (ed. J. Saavalainen and P. Vakkilainen), Helsinki University of Technology, Department of Civil Engineering, Water Engineering, Otaniemi, Finland. pp. 127-142.

Winkler, E. (1961). Assimilationsvermögen, Atmung und Erträge der Kartoffel-sorten Oberambacher Frühe, Planet, Lori und Agnes im Tal 8610 m) und an der Waldgrenze bei Innsbruck und vent (1880 m bzw. 2014 m). Flora Jena 151: 621 -662.

Virtanen, S. (1987). Unpublished manuscript (in Finnish). Finnish Field Drainage Center.

Wit de , C.T. (1965). Photosynthesis of leaf canopies. Agric. Res. Rep. 663. Pudoc, Wageningen. 57 pp.

Wit de, C.T. et al. (1978). Simulation of assimilation, respiration and transpiration of crops. Simul. Mon., Pudoc, Wageningen, 141 pp.

Wäre, M. (1947). Maan vesisuhteista ja viljelyskasvien sadoista Maasojan vesitaloudellisella koekentällä vuosina 1939-44. Referat: Über die Wasserverhältnisse des Bodens und die Erträge von Kulturpflanzen auf dem wasserwirtschaftlichen Versuchsfeld Maasoja in den Jahren 1939-44. Maa- ja Vesitekn. Tutk. 15, 240 pp., Helsinki.

Wäre, M. (1955). Pohjavedenkorkeuden vaikutusta selvittäviä kokeita nurmikasveilla vuosina 1939-54 (English summary: Experiments on the effect of the ground water level on grasslands in 1939-54. Maatal. ja Koetoim. 9: 17-22.

Wäre, M. (1956). Peruna ja pohjavesi (in Finnish). Koetoim. ja Kđyt. 9, 7 pp.

Zaradny, H. and Feddes, R.A. (1979). Calculation of non-steady flow towards a drain in saturated- unsaturated soil by finite elements. Agricultural Water Management, 2: 37-53.

Zaradny, H. (1986). A method for dimensioning of subsurface drainage in heavy soils considering the reduction in potential transpiration. Proceedings of International Seminar on Land Drainage (ed. J. Saavalainen and P. Vakkilainen), Helsinki University of Technology, Department of Civil Engineering, Water Engineering, Otaniemi, Finland. pp. 258-266.